UNIVERSITY OF LONDON THESIS

Degree PHD Year 2008 Name of Author THIRLWELL, CHRISTINA.

MECHANISMS OF COLORECTAL TUMORIGENESIS ASSOCIATED WITH MUT-Y (*MYH*) DEFICIENCY AND IDENTIFICATION OF NOVEL PREDISPOSITION GENES IN THE MULTIPLE ADENOMA PHENOTYPE

Christina Thirlwell

Thesis submitted for the degree of
Doctor of Philosophy
in the
University of London

Cancer Research UK
July 2008

ProQuest LLC
789 East Eisenhower Parkway
P.O. Box 1346
Ann Arbor, MI 48106-1346

The work presented in this thesis is my own.
All collaborators are named in relevant chapters.

Christina Thirlwell 31st July 2008

Abstract

The main subjects of my thesis can be divided into three related areas.

Firstly, determination of the mechanisms of tumoriogenesis associated with a recently identified, recessively inherited syndrome, *MYH*-associated polyposis (MAP). MAP results from defective base excision repair (BER) caused by bi-allelic germline mutations in the human Mut-Y homologue (*MUTYH, MYH*) and leads to the development of colorectal adenomas and cancer. My work includes: further characterisation of the MAP phenotype; completion of screening for mutations in other BER enzymes (*OGG1* and *MTH1*) in individuals with multiple colorectal adenomas; determination of the genetic pathway(s) involved in MAP tumorigenesis through studying loss of heterozygosity (LOH) and chromosomal abnormalities with array comparitive genomic hybridisation. A mouse model of MAP was developed as part of this thesis in order to study the development of intestinal adenomas from their earliest stages, and to evaluate the impact of environmental modification and chemopreventative therapies.

Secondly, I determined to identify novel predisposition genes for the multiple adenoma phenotype. Up to fifty percent of individuals with multiple (5-100) colorectal adenomas (MCRAs) have no germline mutation in known predisposition genes (*APC* and *MYH*), but probably have a genetic origin. In these cases I determined to identify novel predisposition genes for the MCRA phenotype utilising various techniques. These included somatic screening of the adenomas for mutational signatures, expression array analysis of lymphoblastoid cell lines from these individuals and candidate gene approaches.

Finally, I investigated the clonal origins of colorectal adenomas through studying adenomas from familial adenomatous polyposis (FAP), attenuated FAP (AFAP) and sporadic cases. In this thesis I developed a novel technique which utilises somatic *APC* mutations as clonal markers. This approach found 100% of FAP adenomas to be polyclonal and 100% of AFAP adenomas to be clonal in their origin.

Acknowledgements

I would like to thank my supervisor Ian Tomlinson for his enormous support, inspiration and encouragement during the course of my thesis. Daniel Hochhauser my second supervisor provided continuous encouragement and stimulating discussion. My thanks also go to all of my colleagues in the Molecular and Population Genetics Laboratory, in particular Andrew Rowan, Kimberley Howarth, Emma Jaeger, Angela Jones, Luis Carjaval, Zoe Kemp and Stefania Segditsas. Also thanks to all the staff in the Equipment park at Cancer Research UK for their support in my practical work.

I have had the pleasure of collaborating with Oliver Sieber, Simon Leedham and Kevin Monahan and would like to thank them for their intellectual and practical contribution to my thesis.

None of my work would be possible without the patients who agree to take part in research studies, the support of my colleagues at the Cancer Research UK Family Cancer Centre and Polyposis Regsitry at St Mark's Hospital. I am also very grateful for the funding I received from the Medical Research Council supporting my thesis.

Finally, I would like to thank my family and friends for their unerring support and encouragement. In particular, Paul Mulholland for introducing me to Ian and the MPG lab, and to Rob Deakin for vociferous support in all of my endeavours.

Abbreviations

aa	amino acid
AAPC	attenuated polyposis coli
Alb	albumin
ALK3	activin receptor-like kinase 3
APC	adenomatous polyposis coli
BER	base excision repair
BMP	bone morphogenic protein
BMPR1A	bone morphogenic protein receptor type 1A
CCND1	G1/S-specific cyclin-D1
CDC4	cell division control protein 4
CDH1	cadherin 1
cDNA	complementary DNA
CGH	comparative genomic hybridisation
CHEK2	Serine/threonine-protein kinase Chk2
CIN	chromosomal instability
Co-SMAD	common-mediator SMAD
COX1/2	cyclo-oxygenase-1/2
CPK1-α	casein kinase 1-α
CRC	colorectal cancer
CXCR4	C-X-C chemokine receptor type 4
dH_2O	distilled water
DI	DNA index
DNA	deoxyribonucleic acid

Dsh	dishevelled
DSS	dextran sodium sulphate
DUT	deoxyuridine 5'-triphosphate nucleotidohydrolase
ES cell	embryonic stem cell
FAP	familial adenomatous polyposis
GSK3β	glycogen synthase kinase 3-β
HMPS	hereditary mixed polyposis syndrome
HMG-CoA	hydroxymethylglutaryl-CoA
HNPCC	hereditary nonpolyposis colorectal cancer
HRAS1	Ras association domain-containing protein 7
JPS	juvenile polyposis syndrome
kb	kilo basepairs
LOH	loss of heterozygosity
LRP	low density lipoprotein receptor-related protein
MAP	*MYH* associated polyposis
mb	mega base pairs
MCR	mutation cluster region
MCRA	multiple colorectal adenomas
Min	multiple intestinal neoplasia
MLH1	human homologue of *E.coli* MutL
MLPA	multiplex ligation-dependent probe amplification
MMR	mismatch repair
Mom1	modifier of Min 1
MSH2	human homologue of *E. coli* MutS
MSI	microsatellite instability

MTH1	human homologue of *E. coli* MutT
MTHF	methyl tetrahydrofolate
MYH	human homologue of *E. coli* MutY
NAT2	N-acetyltransferase 2
nm	nanometer
NSAID	nonsteroidal anti-inflammatory drug
nt	nucleotides
OGG1	human homologue of *E. coli* MutM
8-oxo-G	8-oxo-7,8-dihydroxyguanosine
PCR	polymerase chain reaction
PJS	Peutz-Jeghers syndrome
PMS2	postmeiotic segregation increased 2
POLE2	DNA polymerase epsilon subunit 2
PPAR	peroxisome proliferators-activated receptor
PTEN	phosphatase and tensin homologue deleted on chromosome 10
PTT	protein truncation test
RNA	ribonucleic acid
ROS	reactive oxidative species
rpm	rotations per minute
R-SMAD	receptor-regulated SMAD
SMAD	human homologue of Drosophila small mothers against decapentaplegic
SSCP	single strand conformation polymorphism
TCF	T cell factor
TDG	thymine-DNA glycosylase

TGF-β	transforming growth factor-β
UC	ulcerative colitis
UDG	uracil-DNA glycosylase
Wif1	Wnt inhibitory factor 1

All genes have been italicised throughout the text, whereas proteins are shown in plain text.

Table of Contents

Table of Figures

Table of Tables

Introduction

1.1 Colorectal Cancer

1.1.1 Incidence and Aetiology

Colorectal cancer (CRC) is diagnosed in 35,000 people per year (approximately 100 people per day) in the United Kingdom. CRC is a common form of malignancy in developed countries but is much less common in developing countries. Worldwide, one million cases are diagnosed per annum. In the UK it is the second most common cause of cancer-related death with a mortality of 17,000 people per year. CRC accounts for 13% of all cancers in the UK and is the second most commonly diagnosed cancer in women following breast cancer and the third most common cancer in men following prostate and lung cancer (Cancer Research UK statistics, http://info.cancerresearchuk.org/cancerstats/).

Eighty three percent of CRC occurs in people who are 60 years of age or older [(Office for National Statistics. Cancer statistics registrations: Registrations for cancer diagnosed in 2002, England vol. Series MB1 no 33. London; National Statistics, 2005), (Welsh Cancer Intelligence and Surveillance unit. 2005. www.wcisu.wales.nhs.uk) (ISD Online. Cancer incidence and mortality data. 2005 www.isdscotland.org) (Northern Ireland Cancer Registry. Cancer statistics. 2005. www.qub.ac.uk/nicr), (Cancer Research UK. Information Resource Centre, 2006 info.cancerresearchuk.org)]. The male:female ratio is 1.2:1.0, the lifetime risk for men is 1:18 and women 1:20.

Ninety percent of CRC cases are adenocarcinomas, the vast majority of which arise from adenomas. Adenomas are benign, relatively common lesions occurring in approximately one third of the European and American populations (Midgley & Kerr, 1999). It is thought that up to 10% of adenomas progress to invasive cancer (Scholefield, 2000). Adenomas which are most likely to progress to adenocarcinoma are of larger size with villous histology and exhibit severe dysplasia (Terry et al., 2002).

In general terms, there is no association between socio-economic deprivation and CRC risk in the UK. Within the UK there is no associated geographical distribution of CRC cases as seen with lung and stomach cancer (Quinn MWH, 2005).

Interestingly, epidemiological studies have demonstrated a rapid increase in CRC risk in migrants moving from low to high risk countries (Boyle & Langman, 2000). The risk for second generation migrants is double that of the first, most likely due to the "Westernisation of the diet" (Flood et al., 2000). When considering these studies, other factors need to be taken into consideration such as differences in CRC reporting between countries, availability and provision of local heath care and variation in life expectancy between developed and developing countries.

1.1.2 CRC Risk Factors

Over the last thirty years significant progress has been made in determining risk factors not only for CRC but for cancer in general in terms of inherited predisposition, lifestyle and attitudes towards health. Poor diet, obesity, lack of physical exercise and alcohol and tobacco use are known to contribute to many cancers (Doll, 2003). It has been predicted that two thirds of CRC could be prevented by changes to diet and lifestyle (Doll & Peto, 1981).

I will discuss the following in relation to CRC.

Diet

The incidence of CRC is higher in populations with a "westernised diet", who also have higher incidence of obesity and sedentary life style.

An observation by Burkitt in 1969 (Burkitt, 1969) suggested a link between dietary fibre intake and CRC, in that CRC appeared to have a similar geographical distribution to diverticular disease – which is associated with low dietary fibre intake. Since then it has been determined that it is the insoluble as opposed to the soluble dietary fibres which promote bacterial fermentation in the large bowel and increased stool bulk – and hence protection against CRC. Cummings et al (Cummings & Englyst, 1987; Englyst et al., 1987) demonstrated a role of starched resistant to digestion in the small bowel which then promotes fermentation in the large bowel (in a similar way to fibre) with

production of fatty acids. Of these fatty acids it is thought butyrate confers the most protection as it has been shown to reduce the liability of epithelial cells to malignant change.

Specific studies in to the amount of red meat, fibre, fat, vitamin and micronutrients have determined that a diet high in fibre, fish, dairy fat, fruit and vegetables and low in red and processed meat is the healthiest diet in terms of CRC prevention. The European Prospective Investigation Into Cancer and Nutrition (EPIC) study demonstrated a significantly increased CRC risk of 55% in those with 100g/day increased intake of red and processed meat (Norat et al., 2005). This study also demonstrated the protective effect of a high fibre diet – particularly if the fibre is sourced from fresh fruit and vegetables. At the present time in the UK, 75% of the population are failing to eat the recommended five portions of fruit and vegetables per day (National Statistics Health Survey for England 2004 and 2005).

Obesity

It is predicted that up to 11% of CRC in developed countries is associated with being overweight or obese. CRC risk increases by 15% in overweight and 33% in obese individuals (Bergstrom et al., 2001). This relationship is most obvious in men and pre-menopausal women (Murphy et al., 2000). A worrying statistic is that of the increasing incidence of obesity in both men and women in the UK, between 1995 and 2004 the percentage of obese men rose from 15% to 24% and women from 18% to 24% (2005) (National Statistics Health Survey for England 2004, 2005).

Physical exercise

Few studies have specifically addressed CRC in relation to exercise. In studies looking at risk factors in the broader context, men with higher levels of activity throughout their lives are at lower risk of colon cancer but this risk reduction has not been statistically associated with rectal cancer (Wei et al., 2004); (Slattery et al., 2003); (Viano H, 2002).

Alcohol and tobacco

A meta-analysis of eight cohort studies has demonstrated an increased CRC risk of 16% in people who drink 30-45g alcohol/day and 41% in those

drinking >45g alcohol/day (Cho et al., 2004). Alcohol is likely to have a stronger effect in those with poor dietary folate in take.

Inflammatory disease of the large bowel

Inflammatory syndromes affecting the large bowel namely Crohn's disease and Ulcerative colitis (UC) predispose to CRC. In UC the lifetime CRC risk is 40% (Gillen et al., 1994) (Levin, 1992) (Sugita et al., 1991). There is also some evidence to suggest that there is a genetic element in CRC development in UC as there is a higher sibling relative risk of CRC when compared to the general population (Satsangi et al., 1998). A potential linkage locus on chromosome 12 has been identified for UC (Parkes et al., 2001). UC-related CRCs have several distinct features when compared to sporadic CRC, namely there is a predominance of left sided, multiple, mucinous cancers which often arise from flat adenomas rather than polypoid adenomas (Colliver et al., 2006) (Crawford et al., 2005).

The incidence of precursor areas of dysplasia is as common in the right side of the colon as the left - which suggests there are other factors present in the transition from dysplasia to neoplasia. A "field effect" has been suggested by Rutter (Rutter et al., 2004). More recently a mechanism has been suggested by Castellone et al (Castellone et al., 2005) whereby increased levels of inflammatory cyclooxygenases inhibit the degradation of β–catenin through the binding of prostaglandin E2 to its receptor. This activates a G-protein coupled receptor (Gαs) which in turn binds axin. Axin complexed with *APC* and *GSK3β* phosphorylate β-catenin leading to accumulation and nuclear entry whereby target genes are transcribed resulting in an increased rate of cellular proliferation.

Pharmaceutical agents affecting CRC risk

Non-steroidal anti-inflammatory drugs (NSAIDs)

There is strong evidence to support a protective effect of non-steroidal anti-inflammatory drugs (NSAID) use in adenoma development and progression to CRC. This effect was first observed in large population based studies where NSAIDs were ingested for other medical indications and followed up as a

result of astute clinical observation (reviewed in(DuBois et al., 1996)). Aspirin has been in longest use with a recent study including 10 years of follow up data demonstrating a reduced risk of 40-50% (Chan et al., 2005). Two randomised controlled trials have also supported the finding that aspirin use reduces adenoma formation (Baron et al., 2003) (Sandler et al., 2003).

The protective mechanism of NSAIDs is through the inhibition of *COX-2,* which in turn slows adenoma development and growth (Ricchi et al., 2003). *COX-2* is an inducible enzyme which regulates prostaglandin synthesis. Prostaglandins promote many varied biological effects including immunological induction of inflammatory processes, vascular endothelial integrity, reproductive regulation, nerve growth production and development, bone metabolism and activation of nuclear hormone receptors (via it's metabolites) (Dubois et al., 1998). *COX-2* is over-expressed in 50% of adenomas and 85% of CRCs. In the same samples, *COX-1* expression remained unchanged between normal mucosa and CRC (Eberhart et al., 1994). *COX-2* has been demonstrated to promote tumour-associated angiogenesis, although the mechanism of this remains unclear (Dormond et al., 2001).

Other members of the NSAID family, sulindac (both *COX-1* and *2* inhibitor) and celecoxib (a selective *COX-2* inhibitor), have been used in the prevention and treatment of individuals with familial adenomatous polyposis (FAP) (Nugent et al., 1993) (Phillips et al., 2002) (Giardiello, 1994) (Debinski et al., 1995).

The Colorectal Adenoma/carcinoma Prevention Programme (CAPP (formerly Concerted Action Polyp Prevention)) studies set out to prospectively address the preventative impact of NSAIDs and diet in patients with FAP (CAPP 1 study) and more recently HNPCC (CAPP 2 study). The CAPP studies are international, multi-centre randomised controlled trials. CAPP 1 investigated the effects of aspirin (600mg/d) and/or resistant starch (30g/d) in 206 FAP carriers. One year follow up found that although there was not a significant decrease in polyp number, the mean largest polyp size was reduced in the aspirin only group. Intestinal crypt length was also affected in that those individuals treated with starch had significantly shorter crypts, and those on aspirin had longer crypts and 37% increased crypt cell proliferation rate. It was suggested that both interventions have a protective effect but with

differing mechanisms (Burn et al., 1998) (Mathers et al., 2003). CAPP 2 is investigating the impact of aspirin and resistant starch (at the same dose as CAPP 1) in 1000 individuals with HNPCC. Recruitment was completed in March 2007 and results awaited.

The impact of NSAIDs on adenoma and CRC development have been confirmed in animal models. The $Apc^{Min+/-}$ mouse, the $Apc^{\Delta 716}$ mouse (both models of FAP), azoxymethane (AOM) treated rat and the nude mouse xenograft assay have all demonstrated that either non-selective inhibition of *COX-1* and *-2* or *COX-2* inhibition alone suppress adenoma multiplicity and CRC cell growth. Polyp multiplicity was reduced in the FAP mouse models using celecoxib and rofecoxib respectively (Jacoby et al., 2000) (Oshima et al., 2001). Celecoxib use led to decreased tumour incidence, multiplicity and growth in AOM treated rats (Reddy et al., 2000); (Kawamori et al., 1998). In the nude mouse celecoxib caused reduced colon carcinoma cell growth and also demonstrated the absence of toxicity to normal gut mucosa whilst using *COX-2* selective inhibitors (Williams et al., 2000). This evidence is further supported by crossing Apc^{Min} mice with *COX-2* knockout mice and mice lacking the prostaglandin E2 receptor (Oshima & Taketo, 2002). These animals develop fewer adenomas therefore demonstrating the significance of both *COX-2* and prostaglandin E2 and inflammatory processes *per se* in the development of adenomas.

Statins

Statin (*HMG-CoA* reductase inhibitor) use has been shown to reduce CRC risk by 47% when taken over a five year period in a large case-control study (Poynter et al., 2005). Statins are used to treat hypercholesterolaemia, ishaemic heart disease and inflammatory bowel disease. This study included 1953 CRC cases and 2015 controls, the observed association remained significant when other factors such as concurrent aspirin use, physical activity, hypercholesterolaemia, family history of CRC and ethnic group were taken in to consideration. However, a recent population-based study with 1809 CRC cases and controls (Coogan et al., 2007) found no evidence of a decreased incidence of CRC when statins were used for longer than 3 months – with no

consistent trend across dose taken or duration of use. A significant reduction in the incidence of Stage IV disease was observed (OR 0.49, 95% CI 0.26-0.91) in the individuals taking statins. As it has been shown that statins have anticancer activity in various cancer cell lines (including CRC cell lines) these observations warrant further study.

Hormonal manipulation – HRT and OCP

Women who have ever used Hormone replacement therapy (HRT) have a 20% reduction in CRC risk and current users have a 30% risk reduction. A large meta-analysis found the risk of all bowel cancers to be reduced by 50% within 5-10 years of use (Grodstein et al., 1999). However, these results were muddied as further case-control studies demonstrated further reduced risk in women taking oestrogen only and trans-dermal HRT preparations (Csizmadi et al., 2004). These results are not entirely reproducible in randomised controlled trials with a 44% reduced risk of CRC seen in women taking combined oestrogen and progestogen preparations (Chlebowski et al., 2004), but another further study found no reduced risk in women taking oestrogen only HRT (Anderson et al., 2004).

In pre-menopausal women, oral contraceptive (OCP) use has been found to result in a reduced risk of CRC of up to 18% in a meta-analysis undertaken in 2001 (Fernandez et al., 2001). A more recent case-control study in 2005 found a non-significant CRC risk reduction of 11% for women who had ever used OCP's and a significant reduction in rectal cancer of 50% in women who had taken OCP's in the preceding 14 months (Nichols et al., 2005).

Inherited risk factors

Up to 6% of CRC is caused by known inherited genetic syndromes, although it is likely there is a hereditary component in up to 35% (Lichtenstein et al., 2000). Inherited genetic factors affect not only a predisposition to CRC but also concurrent illness, handling of pharmaceutical agents and overall outcome. The genetic make-up of any individual tumour affects the grade, response and overall outcome for any individual with CRC. The known inherited CRC predisposition syndromes will be dealt with in detail in a later section of this chapter.

1.1.3 Natural History, Staging, Treatment and Current CRC Outcome

1.1.3.1 The Natural history of CRC

The natural history of a cancer can be described as the histological progression from normal tissue through tumour initiation to distant metastases. In CRC this progression is well characterised and has been called the adenoma – carcinoma sequence whereby adenomas form from normal colonic mucosa and then progress to carcinoma.

Specific mutations have since been identified and associated with different steps in the adenoma – carcinoma sequence, the "stepwise model of colorectal carcinogenesis" was suggested by Fearon and Volgestein in 1988 (Vogelstein et al., 1988) see Figure 1–1. This is explained in detail in section 1.1.3.3

Figure 1–1 **The stepwise model of CRC (Vogelstein et al., 1988)**

The study of CRC from its earliest stages is facilitated by access to tissue for study – through colonoscopy and surgery. This can further the understanding of sequential development of CRC from normal gut mucosa through adenomatous polyp formation to invasive carcinoma with metastatic spread.

The colorectum has nine anatomical regions, the caecum, appendix, ascending colon, transverse colon, descending colon, sigmoid colon and rectum see Figure 1-2.

Figure 1–2 **Anatomy of the colon, sites of CRC by incidence England 1997-2000 (CRUK Statistics)**

The normal colonic mucosa comprises invaginated crypts lined with a single layer of absorptive cells. These are interspersed with mucin-secreting goblet cells, neuroepithelial and paneth cells. The mucosa rests on a basement membrane (muscularis mucosa), lamina propria and muscularis propria. Cell division is thought to occur in the lower third of the crypt, termed the "proliferative compartment". It is here that stem cells reside. As cells migrate up the crypts the mature and develop differentiating and finally undergoing programmed cell death – apoptosis. At this point the cells are sloughed off in to the gut lumen.

Cell turnover in crypts takes approximately 3-6 days (Cotran R, 1999).

1.1.3.2 Clonal origins of colorectal tumours

Current theories of clonality in colonic tumorigenesis

The Unitarian theory of the origin of the four epithelial cell types suggests that differentiated cell lineages found within the intestinal epithelium arise from a single stem population (Cheng & Leblond, 1974). Stem cells, due to their longevity and capacity for self-renewal, are considered by some to be the original targets for the mutation(s) required to initiate a neoplasm (Bach et al., 2000) (Wong & Wright, 1999). The subsequent question is whether such a cell acts alone or in co-operation with other mutated stem cells. Proponents of an interaction theory suggest that tumours are not initially clonal and that any later apparent clonality is the consequence of outgrowth of a dominant clone (Alexander, 1985) (Rubin, 1985).

Clonality studies of neoplasms are therefore of great relevance to our understanding of tumourigenesis. To date the study of clonality in human tissue has relied on utilising natural mutations or polymorphisms which can be used as "markers" of clonality.

The clonality of colonic adenomas and tumours is a source of some debate. Early X-chromosome inactivation studies examining the status of tumours from female patients mosaic for various X-linked genes were conflicting. Beutler reported a polyclonal colorectal carcinoma (Beutler et al., 1967) and Hsu described polyclonal adenomas (Hsu et al., 1983) based on gel electrophoresis analysis of X-inactivation mosaicism of G6PD isoenzymes. Fearon *et al* used DNA rather than protein polymorphisms and examined X-inactivation patterns of the phosphoglycerate kinase (PGK) gene, using restriction fragment length polymorphisms. They found that adenomas and carcinomas taken from female patients with sporadic and familial adenomatous polyposis (FAP) associated lesions, had a consistently monoclonal pattern of X-chromosome inactivation (Fearon et al., 1987). It should be noted however that patch size was overlooked in these studies, and it is possible that tumours were covertly polyclonal but appeared monotypic as they arose within a large X linked patch. Following this, Novelli *et al* (Novelli et al., 2003) studied Sardinian females heterozygous for the glucose-

6-phosphatase (G6PD) Mediterranean mutation (563 C→T) and heat deactivated the defective gene followed by enzyme histochemistry to demonstrate glucose-6-phosphate activity. Crypts were arranged in hexagonal arrays in large patches, with irregular patch borders, containing up to 450 individual crypts with only 8% of crypts situated on patch borders. For a polyclonal tumour to appear heterotypic for an X-inactivated gene it has to occur on a patch border and thus the large patch size in the colon means that X-inactivation studies are heavily biased toward showing colorectal tumour monoclonality.

Direct observation, rather than the indirect methods previously utilised led to some confounding results. Novelli and colleagues (Novelli et al., 1996) studied a highly unusual individual who had a diagnosis of FAP and was also a sex chromosome mixoploid chimera (presumably as a consequence of a dicentric Y chromosome). Thus his tissues were a mosaic with the majority – some 80% of cells, being XY and the remaining 20%, XO. The detection of the Y chromosome in the excised colonic tissues provided an excellent binary marker for lineage analysis. Of the 263 adenomas analysed, 246 were wholly XY, 4 were entirely XO, while 13 were of mixed XO/XY genotype. When considering only the tumours containing the XO lineage, 13/(13 + 4), or 76% of all adenomas appeared to be polyclonal. A very similar result was produced in a study using mice heterozygous for the multiple intestinal neoplasia (Min) allele of the adenomatous polyposis coli (*Apc*) gene and chimaeric for the lineage reporter gene ROSA 26 expressing lacZ. 22 of 251 adenomas were heterotypic for the blue (ROSA 26) and white (non-ROSA 26) lineages. Applying the same ratio as Novelli et al, gave an adenoma polyclonal fraction of 79% (Merritt et al., 1997).

Three hypotheses have been proposed to explain tumour polyclonality.

1. Adenoma "pseudo" mosaicism caused by focal loss of the lineage marker in otherwise clonal dysplastic tissue.

2. Random / regional collision between independently arising neoplasms as a consequence of high tumour multiplicity in FAP patients (Novelli et al., 1996) and chimeric Min mice (Merritt et al., 1997).

To test this hypothesis Thliveris et al reduced tumour multiplicity in the chimaeric mouse model described above by introducing homozygosity for the

tumour resistance allele of Mom1. Overall tumour multiplicity was reduced 8-fold but the percentage of mixed tumours ranged from 8-63%, with a mean of 22% (Thliveris et al., 2005). This is higher than would be expected if heterotypic tumours are indeed formed through random collision.

3. Active interaction between adjacent crypts. Possible mechanisms include microheterogeneity of tumour susceptibility where local stroma promotes somatic mutation in adjacent crypts - the so-called landscaper effect or stem cell interaction between neighbouring intiated crypts.

To date no firm conclusion has been drawn as to which of these theories holds true.

Niche succession

Several theories have been put forward to suggest how a single mutated stem cell in normal intestinal crypt can then proliferate to dominate the whole crypt (a monocryptal clone) – this has been termed "niche succession". Possible mechanisms resulting in niche succession include genetic drift, selective advantage or "hitchhiking". Genetic drift can occur through an imbalance in symmetric and asymmetric division (or death) of stem cells, therefore altering the balance of the number of clones within a normal intestinal crypt. Selective advantage or "natural selection" is only possible in a population demonstrating three characterstics i) variation within the population ii) variation which is heritable and iii) variation which affects the progeny. Therefore when considering mutagenesis in the intestinal crypt, genetic instability results in the production of many heritable genetic variants which are then selected for the growth advantage they confer to the cell. It is equally possible that the heritable variants confer a selective disadvantage in that they may trigger apoptosis and cell death. A malignant cell population therefore fulfils the criteria for natural selection – resulting in the selection of cells harbouring mutations which confer a growth advantage (Nowell, 1976). Maley *et al* suggested that certain mutations found within malignant cells are evolutionarily "neutral" in that they confer no selective advantage or disadvantage to the cell. When such mutations are present in cells which also contain a selectively advantageous allele these "neutral" mutations hitch-hike alongside the strongly selected advantageous allele (Maley et al., 2004).

Crypt fission and clonal expansion

Following niche succession and formation of a monocryptal clone the next step in the development of a microadenoma is the expansion of this clone in to the surrounding tissue.

Studies in human and mouse tissue have demonstrated clusters of phenotypically similar crypts found together in patches in the intestinal mucosa (Taylor et al., 2003) (Greaves et al., 2006) (Park et al., 1995). It has been suggested that a process of "crypt fission" whereby crypts bifurcate and divide through longitudinal division is responsible for this. Crypt fission is certainly the mechanism by which intestinal crypts multiply in the post-natal period (Maskens & Dujardin-Loits, 1981) and also during regeneration of gut mucosa following radiation (Cairnie & Millen, 1975). It has been calculated that the crypt fission cycle (the time taken for a single crypt grow and then produce two daughter crypts by crypt fission) is 108 days in the mouse jejunum and anything from 9-18 years in the human (Bjerknes, 1986; Totafurno et al., 1987). In pathological conditions such as inflammatory bowel disease, FAP, sporadic and hyperplastic adenomas, the rate of crypt fission increases (Cheng et al., 1986) (Bjerknes et al., 1997) (Wasan et al., 1998; Wong et al., 2002).

The mutator phenotype hypothesis is based on the observation that malignant cells accrue genomic alterations (mutations) at a higher rate than normal somatic cells. It is estimated that a malignant cell has up to 10^{12} genomic alterations (Tomlinson et al., 2002). This hypothesis suggests that early mutations which allow the maintenance of genetic stability result in an increased mutation rate in that cell and overall may be one of the main mechanisms driving tumorigenesis (Loeb, 2001). A increased mutation rate *per se* may not be sufficient to initate tumourigenesis - in that individuals with HNPCC with MMR defects develop the same number of bowel tumours as the general population. In HNPCC however a higher number of these tumours become malignant. Additionally, a raised mutation rate may in fact be detrimental if it results in the activation of apoptotic mechanisms. Therefore it may be that the mutator phenotype simply enables the progression to cancer to occur at an increased rate (Tomlinson & Bodmer, 1999).

There remains much to be determined as to the mechanisms underlying the expansion of a few dysplastic crypts (microadenoma) to an adenoma and potentially a carcinoma and whether adenomas are truly monoclonal or polyclonal in their origin.

1.1.3.3 The stepwise model of colorectal carcinogenesis

The adenoma-carcinoma sequence describes a series of (epi)genetic and pathological changes which occur in stepwise progression from normal bowel mucosa through to carcinoma (Vogelstein et al., 1988). It is thought that the progression from adenoma to carcinoma takes anything from 10 to 40 years (Ilyas et al., 1999).

In sporadic CRC (accounting for ~ 90% of cases), the adenoma-carcinoma sequence is usually initiated by bi-allelic mutation of the adenomatous polyposis coli (*APC*) tumour suppressor gene. It is therefore described as a gatekeeper gene in this context as it appears *APC* mutation must occur before subsequent genetic changes (Levy et al., 1994). The bi-allelic loss of *APC* follows Knudsons two-hit hypothesis for tumour suppressor genes (Knudson, 1971). In normal circumstances, tumour suppressor genes inhibit cellular turnover and growth, and therefore growth inhibition is lost when both alleles of the tumour suppressor gene are either mutated or lost through chromosomal changes. Oncogenes, in contrast, exert their effect through stimulation of cellular proliferation and growth. Proto-oncogenes are the non-mutated (wild type) version of oncogenes. Mutations in proto-oncogenes lead to inappropriate or excessive expression of their protein resulting in accelerated cellular proliferation. This occurs when only one allele is mutated.

Up to 80% of sporadic adenomas and CRC's harbour somatic *APC* mutations (Cottrell et al., 1992) (Powell et al., 1992) (Nakamura et al., 1992). *APC* mutations have also been found in microadenoma pre-cursor lesions (Smith et al., 1994) (Otori et al., 1998).

It therefore follows that bi-allelic *APC* mutations are the initiating step in adenoma development and subsequent genetic and epigenetic changes are required for adenoma growth and progression.

1.1.3.4 The Wnt signalling pathway

Bi-allelic inhibition of *APC* leads to Wnt signalling dysregulation. Wnt signalling is responsible for driving epithelial proliferation in the bowel epithelium.

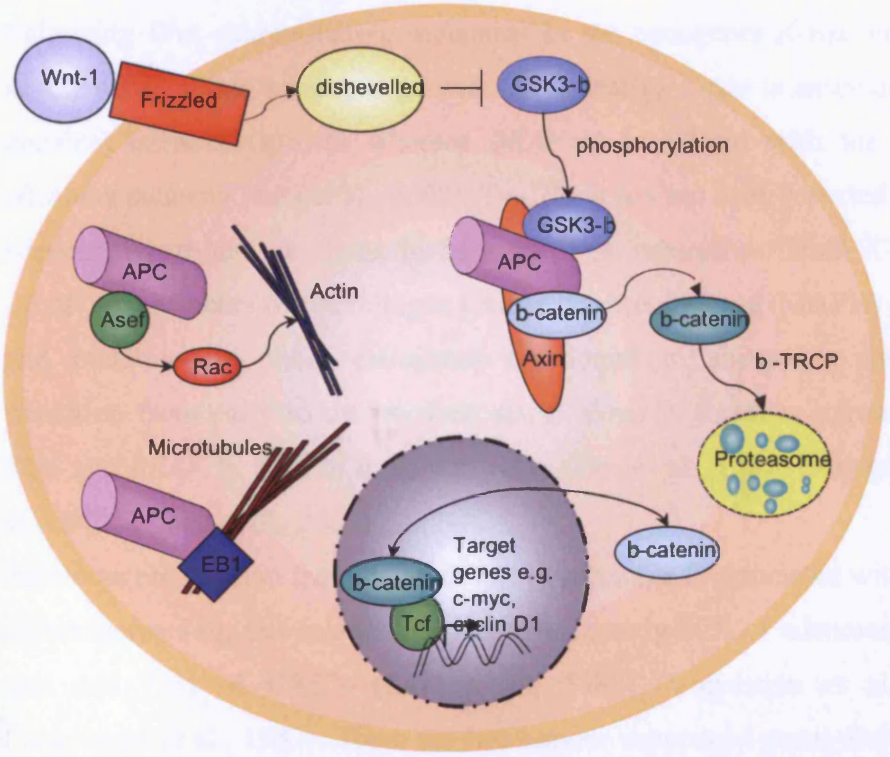

Figure 1–3 **Schematic overview of the Wnt signalling pathway**

One of the key elements of the Wnt signalling pathway is *β-catenin* which is found both cytoplasmically and in the cell nucleus where it triggers target gene transcription and cellular proliferation. *β-catenin* levels and activity are therefore tightly controlled. Wnt signalling is initiated by extracellular binding of the Wnt ligand to a co-receptor comprised of the transmembrane receptor frizzled and a low density lipoprotein receptor related proten (LRP). This triggers translocation of axin, a scaffold protein, from the cytoplasm to the membrane, where it binds to the intracellular tail of the LRP co-receptor. This results in destabilisation of the *β-catenin* degradation complex. (Pinson et al., 2000) (Mao et al., 2001). *β-catenin* degradation is further inhibited via the inhibition of GSK3-β through hyperphosphorylation of dishevelled (Dsh) (Yanagawa et al., 1995). This leads to nuclear and cytoplasmic accumulation

of *β-catenin* resulting in up-regulation of many genes, through stimulation of transcription factors (T cell factor/lymphoid enhancer factor), resulting in over production of the proto-oncogenes cyclin D1 and c-myc. (Parker et al., 2002) (Thompson et al., 2002). Therefore, when the Wnt pathway is dysregulated high levels of cytoplasmic and nuclear *β-catenin* are found, leading to over-transcription of target genes and uncontrolled cellular proliferation.

Following Wnt dysregulation, mutations in the oncogenes *K-ras* and *BRAF* appear to facilitate adenoma growth. Historically, *K-ras* is associated with classical adenoma growth whereas *BRAF* is associated with the serrated adenoma pathway (Jass et al., 2002). To date, it has not been reported that any adenomas harbour mutations in both of these oncogenes. Both *K-ras* and *BRAF* are members of the mitogen activated protein kinase (MAPK) pathway and mutations in these oncogenes are found in adenomas undergoing transition from early to intermediate stage. *K-ras* is found in approximately 50% and *BRAF* in 10% of these adenomas (Bos et al., 1987) (Rajagopalan et al., 2002) (Yuen et al., 2002).

Adenoma progression from intermediate to late stage is associated with loss of chromosome 18q, this is observed in approximately 80% of adenomas >5mm size and 75% of CRC's (Law et al., 1988) (Vogelstein et al., 1988) (Vogelstein et al., 1989). There are two tumour suppressor genes *SMAD2* and *SMAD4* (small mothers against decapentaplegic) which are thought to be associated with this loss. They both belong to the transforming growth factor-β/bone morphogenic pathway (*TGF*-β/BMP) signalling pathway. Point mutations have been reported in *SMAD2* and *SMAD4* in CRC's (Eppert et al., 1996) (Thiagalingam et al., 1996).

Transition from late adenoma to carcinoma is associated with loss of chromosome 17q – where the tumour suppressor gene p53 resides (Fearon et al., 1987) (Vogelstein et al., 1988). Missense and truncating mutations in p53 correlating with 17q loss of heterozygosity (LOH) have been reported (Baker et al., 1989) (Baker et al., 1990).

In addition to the adenoma-carcinoma sequence, two other genetic and epigenetic changes are observed in CRC resulting in genomic instability which is partly responsible for accumulation of mutations in tumour

suppressor genes and oncogenes. Chromosomal instability and microsatellite instability appear to occur early in tumorigenesis (Jacoby et al., 1995) (Nowak et al., 2002). Chromosomal instability, demonstrated by whole and partial chromosomal losses and gains is observed in tumours of FAP patients and although not completely understood, it is thought that mutations in *APC* may be the underlying cause of chromosomal instability (Fodde et al., 2001). Karyotypic changes namely polyploidy have been observed in in-vitro studies of cells with mutant *APC* suggesting that it has a role in chromosomal segregation. However, there is little evidence to support this finding in vivo (Fodde et al., 2001) (Kaplan et al., 2001).

Microsatellites are numerous mono, di, tri, or tetra nucleotide repeats in DNA sequences, both intronic and extronic. They occur throughout the genome. During DNA replication, mutations can occur in the microsatellite regions causing misalignment of the daughter strands – this is termed microsatellite instability. Therefore MSI is associated with underlying germline mutation in mismatch repair enzymes which are the cause of HNPCC cancers (Aaltonen et al., 1993) (Aaltonen et al., 1994; Boland et al., 1998).

1.1.3.5 Characteristics of adenomatous polyps

Adenomatous polyps develop when the homeostatic balance between cell proliferation and apoptosis is disrupted in the bowel epithelium. Adenomatous polyps are discrete lesions comprising dysplastic or neoplastic tissue bounded by an intact basement membrane. On histological examination, dysplastic epithelium is characterised by cellular crowding, nuclear abnormalities (enlargement, elongation and hyperchromatism) and cellular abnormalities (loss of polarity and loss of stratification). As nuclear size increases, so the cytoplasmic volume decreases. The proliferative compartment of dysplastic crypts enlarges from its usual third, and in some cases extends to the crypt surface. It is thought that adenomas arise from unicryptal lesions which enlarge and multiply by crypt fission (Chang & Whitener, 1989) (Wasan et al., 1998) {Wong, 1999 #647, forming microadenomas (clusters of up to 20 abnormal crypts). As the microadenoma continues to grow in, there is further

evidence that dysplastic epthelium may also contribute to growth in adjacent crypts through "top down" growth (Preston et al., 2003). The clonality of microadenoma/adenoma development and progression is addressed in the work described in chapter 9.

Adenomatous polyps can be morphologically classified into three distinct groups, tubular, tubulovillous and villous. Tubular adenomas have a villous component which makes up less than 25% of the whole adenoma. Villous components are areas of non-dyplastic fronds which are up to twice the height of normal crypts. Villous adenomas have a villous component of 75% or higher whereas tubulo-villous adenomas have a villous component somewhere between 25 and 75%. As adenoma size increases, so the grade of dysplasia generally worsens and the villous component enlarges (O'Brien et al., 1990). Large adenomas with severe dysplasia, but with an intact basement membrane are termed carcinoma *in situ*.

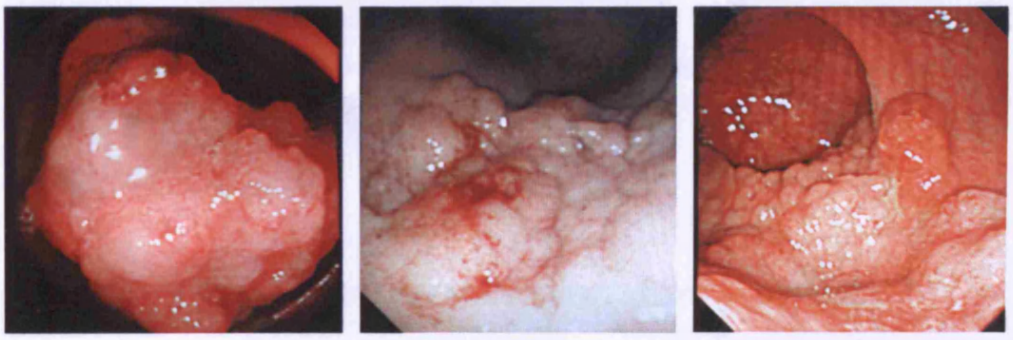

Tubular adenoma Tubulo-villous adenoma Villous adenoma

Figure 1–4 **Endoscopic view of tubular, tubulo-villous and villous adenomas**

1.1.3.6 Characteristics of hamartomatous polyps

Hamartomatous polyps arise in two inherited syndromes, juvenile polyposis and Peutz-Jeghers syndrome. They do not normally exhibit any of the classical signs of dysplasia, but can contain areas of adenomatous dysplasia and invasive carcinoma. Hamartomatous polyps associated with Juvenile Polyposis are characterised by stromal, mucin-filled cysts which are lined by

flattened epithelium. In Peutz-Jeghers syndrome, the polyps are characterised by normal epithelial mucosa and a tree-like branching smooth muscle core.

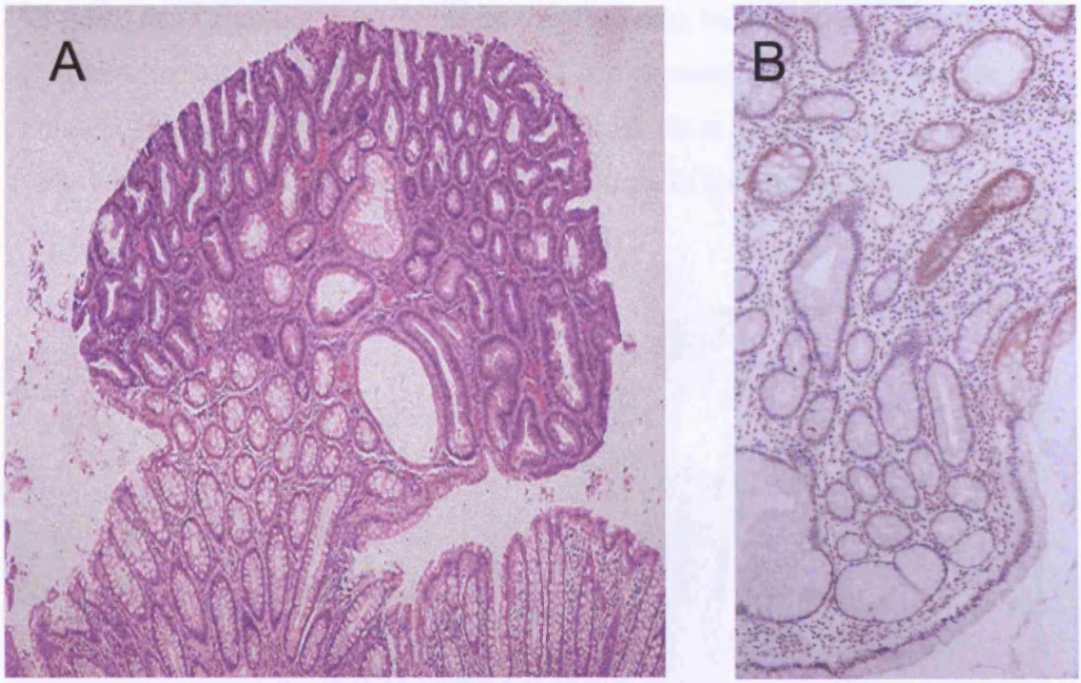

Figure 1–5 **H&E stained tubuloadenoma x200 (A) and hamartomatous juvenile polyposis polyp x200 (B) characterised by mucinous cysts**

1.1.3.7 CRC symptoms and presentation

Symptoms and presentation of CRC may vary considerably depending on the site and size of the primary tumour. Symptoms may in fact be absent in early disease or non-specific such as weight loss and anaemia secondary to occult blood loss. Tumours arising in the distal colon and rectum can present with rectal bleeding, a change in bowel habit and in late and extreme cases show symptoms of bowel obstruction and perforation (up to one fifth of patients present with bowel obstruction or peritonitis secondary to bowel perforation).

1.1.3.8 Staging of CRC

CRC staging involves a combination of Dukes staging for CRC (introduced in 1932) and the T (tumour size), N (nodal involvement), M (presence or absence of distant metastases) system. This combined system gives more precise clinico/pathological information than either used alone (see Figure 1-6 and Table 1-1 for TNM staging with the approximations of Dukes staging).

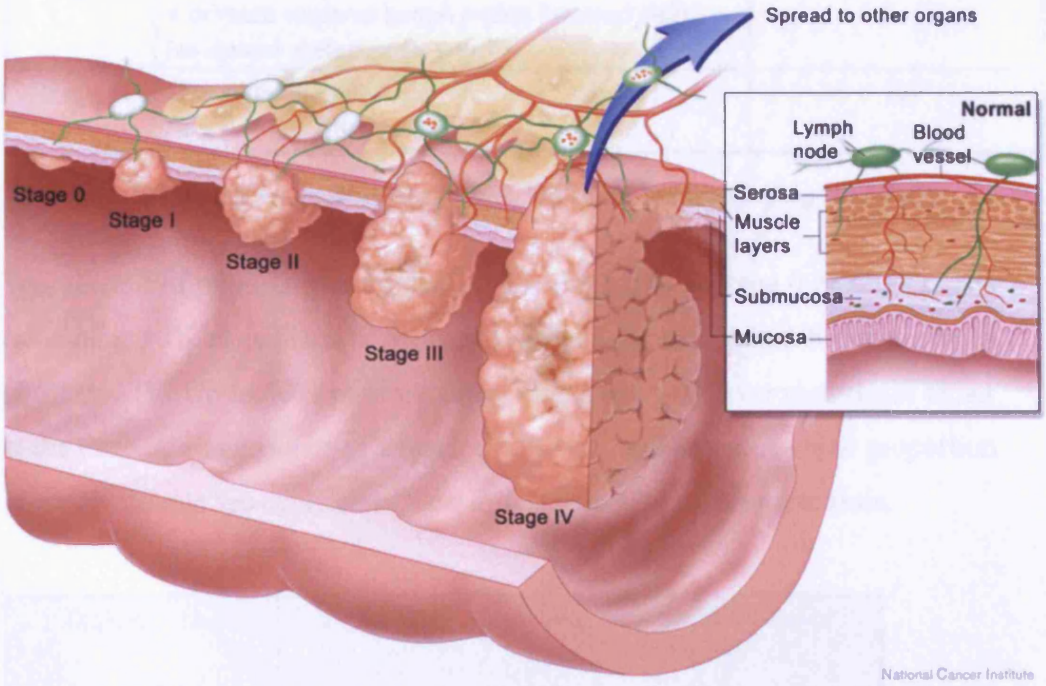

Figure 1–6 **Staging of CRC – (National Cancer Institute, USA)**

TNM		Modified Dukes'
Stage 0	Carcinoma *in situ*	A
Stage I	Tumour invades submucosa (T1) Tumour invades muscularis propria (T2) No nodal involvement, no distant metastases	A
Stage II	Tumour invades beyond muscularis propria (T3) Tumour invades into other organs (T4) No nodal involvement, no distant metastases	B
Stage III	1-3 regional lymph nodes involved - any T (N1) 4 or more regional lymph nodes involved (N2) No distant metastases, any T	C
Stage IV	Distant metastases Any T stage, any N stage	D

Table 1–1 **TNM staging with approximate Modified Dukes staging for CRC**

Ten percent of patients at presentation are diagnosed as stage 0 or stage I. The remaining 90% of patients at diagnosis are equally distributed between stages II, III and IV. Up to 50% of patients are diagnosed with liver metastases either at the time of diagnosis or as a result of disease recurrence. A small proportion of these patients are candidates for surgical resection of the metastasis.

Dukes' stage	Freq. at diagnosis	Approx. 5-year survival
A	11%	83%
B	35%	64%
C	26%	38%
D	29%	3%

Table 1–2 **Frequency of CRC diagnoses by Dukes stage with 5 year survival (England and Wales 1996-1999)**

At this time early diagnosis of CRC is uncommon (unless an individual is screened due to an affected family member(s)). This may be for many reasons including the insidious onset, vague, non-specific symptoms and the fact that

the average General Practitioner in the UK will see one case of CRC per year (Hobbs, 2000). A nation-wide screening programme is in progress involving the use of faecal occult blood tests and colonoscopy in individuals aged 60-69 years of age. It is expected that the whole of the UK will be actively involved in CRC screening by 2009.

1.1.3.9 Current treatment strategies

Current treatment incorporates surgery, +/- chemotherapy, +/- radiotherapy, +/- molecularly targeted treatments depending on the CRC stage at diagnosis.

Surgery

Standard surgical treatment for CRC patients is open resection of the primary tumour with regional lymph node dissection. Eighty percent of CRC patients undergo surgery with curative intent (NICE. Improving outcomes in CRC, updated manual Sept 2003). However up to 50% of all patients with > Stage II disease recur by two years of follow up. Variation in recurrence rate has been observed in different treatment centres with surgeons of varying experience (Dorrance et al., 2000). Therefore it is vital that CRC patients are cared for and treated in designated cancer centres with multidisciplinary team management.

Chemotherapy and Radiotherapy

The most commonly used chemotherapy regimes use 5-fluoruracil (5-FU, a nucleoside analogue), leucovorin and more recently oxaliplatin (a DNA chelator) and irinotecan (a topoisomerase inhibitor).

Neo-adjuvant therapy – The role of neo-adjuvant therapy is to reduce the size of the primary tumour before surgical resection, it would also incorporate the "adjuvant" treatment up-front should this be required.

Adjuvant therapy – Adjuvant therapy is used following surgery – allowing sufficient time for healing. The aim is to treat "micro-metstases" systemically and is currently offered to patients with stage III disease where there is an improved overall survival benefit of 12% when compared to patients who undergo surgery alone (Laurie et al., 1989). The most commonly used

adjuvant treatment is the De-Gremont regime which incorporates infusional 5-FU with leucovorin, There is some debate as to whether adjuvant chemotherapy should be offered to patients with stage II disease, particularly those with higher risk clinical features such as tumour adherence to adjacent tissue or higher risk molecular features such as aneuploidy or deletion of chromosome 18q (Lanza et al., 1998) (Jen et al., 1994). There are currently trials addressing the use of adjuvant therapy in stage IIb disease. Currently stage II patients are candidates for clinical trials in which either surgery alone or 5-FU-leucovorin remain the standard treatment (Poplin et al., 2005).

Post-operative radiotherapy is indicated in higher risk patients, T3 or 4 primary tumour, tumour location in immobile sites, local perforation, obstruction and residual disease post resection.

Chemotherapy for advanced disease, recurrent disease and palliative therapy – Treatment options at this stage include the use of oxaliplatin, irinotecan (a topo-isomerase inhibitor) and capecitabine (an oral pre-metabolite of 5-FU) alongside surgical resection and radio-ablation of liver metastses, should they be amenable to that approach.

Molecularly targeted treatments

Since 2003 molecularly targeted treatments have been approved for use in CRC following the results of two randomised controlled trials.

Bevacizumab – a monoclonal antibody directed against vascular endothelial growth factor (VEGF) demonstrated improved progression free survival and overall survival in patients with advanced disease (Kabbinavar et al., 2003).

Cetuximab – a monoclonal antibody directed against epidermal growth factor receptor, was used either alone or in combination with irinotecan in patients with irinotecan resistant CRC. An improved response rate and progression free survival was seen in the cetuximab treated group, but no improvement in median survival was observed (Cunningham et al., 2004). Current studies are assessing the use of cetuximab in higher risk patients in the adjuvant setting.

1.1.3.10 CRC outcome in the UK

Individuals with stage I and II disease have an 83% and 64% 5 year overall survival rates respectively. When considering stage III patients, 50% are cured by surgery alone, 7% are cured by surgery and adjuvant chemotherapy and 43% relapse in spite of surgery and adjuvant chemotherapy. See Table 1-2 for survival rates per stage. One of the most important prognostic factors is lymph node status (Berger et al., 2005). A study of predictive molecular factors with 11 years post-operative follow up in stage III patients who received adjuvant chemotherapy found that those tumours with no chromosome 18q loss, microsatellite stable (MSS) tumours without chromosome 18q loss compared to MSS tumours with 18q loss, tumours with microsatellite instability (MSI) compared to MSS tumours and MSI tumours with *TGF*β1 mutation compared to MSI without the *TGF*β1 mutation all had improved overall survival (Watanabe et al., 2001). MSI status itself can be used as a predictive factor for response to treatment with 5-FU, MSI high tumours have an increased overall survival but do not respond as well to 5-FU treatment (Ribic et al., 2003). Tumour markers measured in the serum – carcinoembryonic antigen (CEA) and carbohydrate antigen 19.9 (CA 19.9) are also indicative of poor prognosis or recurrence of disease (Reiter et al., 2000).

Therefore it is imperative that further understanding of the CRC risk factors, inherited genetic predisposition, molecular markers and natural history of the disease continue alongside improved primary prevention and screening programmes if we are to improve on the current incidence, survival and mortality statistics.

1.2 Hereditary Colorectal Cancer Syndromes

Germline mutations can be identified in approximately 2-6% of CRC cases, the majority of which occur in families showing Mendelian inheritance (Kinzler & Vogelstein, 1996). Until recently, the known inherited CRC

syndromes were solely the result of autosomal dominant, highly-penetrant high risk alleles which facilitated early recognition of the underlying genetic diagnosis (Cannon-Albright et al., 1988), (Houlston et al., 1992), (Esteller et al., 2001). These syndromes are well characterised and include Hereditary Non-Polyposis CRC (HNPCC) with germline mutations in *MLH1, MSH2, PMS2* and *MSH6* genes, Familial Adenomatous Polyposis (FAP) with mutations in the *APC* tumour suppressor gene. The most recently identified inherited CRC predispositon syndrome is *MYH*-associated polyposis (MAP) which is caused by mutations in the base excision repair gene *MYH*. MAP was first described in 2002 (Al-Tassan et al., 2002) (Crabtree et al., 2003), and is inherited in an autosomal recessive manner. MAP will be described in more detail in a following section of this chapter. Other inherited polyposis syndromes include Peutz-Jeghers syndrome (*LKB1* gene) and juvenile polyposis (*SMAD4* and *ALK3* genes). See Table 1-3 for overview of inherited CRC syndromes and mode of discovery.

Syndrome	Gene	Location	Inheritance	Function	Method of discovery
FAP	*APC*	5q	AD	Inhibition of wnt signalling	Linkage analysis
HNPCC	*MLH1*	3p	AD	DNA mismatch repair	Linkage analysis
	MSH2	2p	AD	DNA mismatch repair	Linkage analysis
	MSH6	2p	AD	DNA mismatch repair	Candidate gene
	PMS2	7p	AD	DNA mismatch repair	Candidate gene
MAP	*MYH*	1p	AR	Base excision repair	Somatic mutation screening
Peutz-Jeghers	*LKB1*	19p	AD	Serine threonine kinase	CGH and linkage analysis
Juvenile polyposis	*SMAD4*	18q	AD	TGF-beta signalling	Candidate linkage analysis
	ALK3	10q	AD	TGF-beta signalling	Linkage analysis
Cowden's	*PTEN*	10q	AD	Phosphatase, inhibition of AKT signalling	Somatic screening, Linkage

Table 1–3 **Summary of inherited CRC syndromes, inheritance and method of discovery (AD – autosomal dominant; AR – autosomal recessive; BER – base excision repair; CGH – comparative genomic hybridisation)**

At this time defects in the known predisposition genes account for up to 6% of all CRC. However, twin studies suggest that up to 35% of colorectal cancers have a genetic component (Lichtenstein et al., 2000), and the relative risk in siblings is 2-3 fold for adenomas and CRC (Cannon-Albright et al., 1988; Houlston et al., 1992). Some of these cases may be due to as yet undiscovered moderate or high penetrance genes, but the remainder are likely to involve changes in genes conferring a lower level of risk and also highly probable that they are harder to identify.

Hereditary colorectal cancer predisposition syndromes can be divided into two main categories depending on the presence or absence of multiple benign precursor lesions.

1.2.1 Hereditary Non-Polyposis Colorectal Cancer (Lynch syndrome).

Hereditary non-polyposis colorectal cancer (HNPCC) is an autosomal dominant disorder characterised by few colonic adenomas, early onset of predominantly right sided CRC, and specific extra-colonic tumours including cancer of the ovary, endometrial, stomach, small bowel and uro-epithelial tract (although there is a lower risk of developing these tumours than CRC). A diagnosis of HNPCC is made if the affected individual and family members fulfill the Amsterdam criteria (Vasen et al., 1999), see table Table 1-4 for Amsterdam criteria. The disease accounts for approximately 1-6% of colorectal cancer cases when the Amsterdam and Bethesda criteria are used for diagnosis.

Table 1–4 **Amsterdam criteria (Vasen et al., 1999)**

Mutations in the DNA mismatch repair (MMR) genes *MLH1* and *MSH2* account for 90% of cases and *MSH6* and *PMS2* for the remaining 10% of

cases (Miyaki et al., 1997). Up to 29% of *MLH1* and 16% of *MSH2* mutations are missense making it difficult to determine the potential pathogenicity (Thibodeau et al., 1998) (nonsense mutations often lead to either a stop codon or a frameshift). A database of germline mutations in HNPCC has been developed by the International Collaborative Group on Hereditary Nonpolyposis Colorectal Cancer and can be found at http://www.nfdht.nl. If left without screening there is an 80% lifetime chance of developing CRC when carrying a heterozygous mutation in one of these MMR genes. The average age at CRC diagnosis is 45 years.

When compared to sporadic cancers HNPCC cancers are more poorly differentiated and there is a higher incidence of synchronous cancers (occurring within six months of diagnosis) and metachronous cancers (occurring greater than six months from diagnosis). Histologically, an excess of mucoid and signet cells occur along with a Crohn's like picture of inflammatory infiltrate.

Adenoma development in HNPCC has previously been reported to range from between 17 and 49%, the largest study to date of 695 patients with proven MMR mutations found 10.6% of HNPCC patients to have at least one adenoma at first colonoscopy (Liljegren et al., 2008). Interestingly, the same study found 5.3% of HNPCC patients to have at least one hyperplastic polyp. When present, adenomas progress more rapidly to carcinoma in HNPCC, in 2-3 years compared to 8-10 years in the general population (Lynch & de la Chapelle, 2003).

Microsatellite instability occurs due to the loss of function of MMR genes and immunohistochemistry can be performed on tumour tissue to demonstrate the absence or weak expression of the MMR protein (Thibodeau et al., 1998).

Individuals with HNPCC (with either known germline MMR mutations or strong clinical evidence) are screened from the age of 20-25 onwards with annual colonoscopy. In women, screening for endometrial and ovarian cancer is undertaken with annual trans-vaginal ultrasonography which is performed from the age of 30 onwards. Serum Ca-125 levels are also measured as a sign of ovarian malignancy. However the sensitivity and specificity of both of these is limited in ovarian cancer diagnosis.

There is a relatively high incidence of CRC (albeit non-fatal cases) in those patients who are screened (study of 15 year follow up of 3-year and annual screening) due to the accelerated pathogenesis of HNPCC and in light of this, subtotal colectomy and total abdominal hysterectomy with bilateral salpingo-oopherectomy are offered to selective high risk patients.

1.2.2 Familial Adenomatous Polyposis.

Familial Adenomatous Polyposis (FAP) is a highly penetrant autosomal dominant disorder accounting for ~1% of CRC diagnoses. Its incidence is approximately 1:13,500 (Bisgaard et al., 1994). Affected individuals develop hundreds to thousands of adenomatous polyps during the second and third decades of life, one or more of which progress to cancer in nearly 100% of cases. The selective disadvantage associated with such a highly penetrant disease (with in certain cases an extreme phenotype) is overcome by the fact that there is a high incidence of *de novo* germline mutations which account for up to 25% of cases (Bisgaard et al., 1994) (Bulow, 1986). Diagnosis is made clinically in individuals with >100 adenomas (fewer in younger patients) (Vasen et al., 1993).

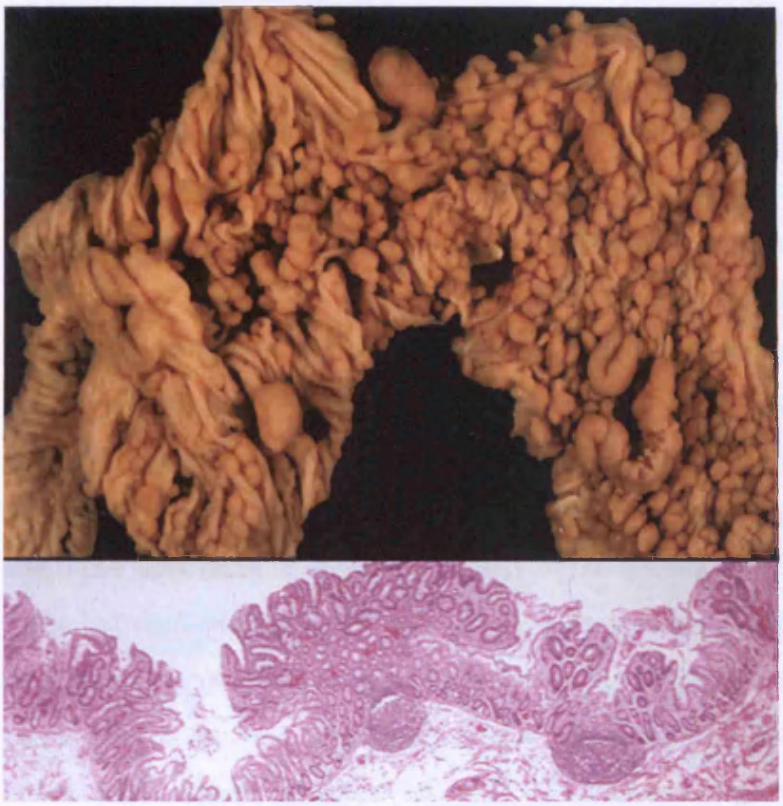

Figure 1–7 **Colectomy specimen and H&E stained adnenoma (x20) from an FAP patient**

Each individual adenoma has a low likelihood of progressing to carcinoma but the sheer number results in a lifetime risk of 100% with most affected individuals developing CRC in their forties if left untreated.

Extracolonic features include desmoids, osteomas, congenital hypertrophy of the retinal epithelium (CHRPE), sebaceous cysts and abnormal dentition (Blair & Trempe, 1980) (Heiskanen & Jarvinen, 1996). Associated cancers include sarcomas, papillary cancer of the thyroid, hepatoblastomas, pancreatic cancer and medulloblastoma (Turcot's syndrome type 1) (Hamilton et al., 1995) (Van Meir, 1998).

1.2.2.1 The *APC* tumour suppressor gene.

The *APC* gene is located on chromosome 5q21. It consists of 15 translated exons with its most common isoform encoding a 2843 amino acid protein (Groden et al., 1993). Exon 9 may undergo alternative splicing which adds an additional 18 amino acids to the transcribed protein (Sulekova & Ballhausen,

1995). *APC* is expressed in a variety of tissues including epithelial and mesenchymal cells of both foetal and adult tissue (Midgley et al., 1997) and has a number of functional domains.

The 5' amino-terminal domain contains a series of heptad repeats which are thought to be involved in *APC* homo-dimer formation (Groden et al., 1991) (Joslyn et al., 1993). Amino acids 453-767 share some homology with the central repeat region of the Drosophila segment polarity protein armadillo which through binding Asef controls cell adhesion and motility through the actin cytoskeleton (Kawasaki et al., 2000). The following two motifs – an imperfect repeat of 15 amino acids occurring three times between codons 1020 and 1169 and another imperfect repeat of 20 amino acids occurring seven times between residues 1262 and 2033 are involved in *β-catenin* binding and degradation (Rubinfeld et al., 1993) (Su et al., 1993). *β-catenin* is a central component of the Wnt signalling pathway (see section 1.1.3.4). Each of the 20 amino acid repeats contains an SXXXS consensus site which acts as a substrate for *GSK3β* phosphorylation (Munemitsu et al., 1995) (Rubinfeld et al., 1996). Three SAMP repeats occur between the 20 amino acid repeats, these mediate the binding of axin (Kishida et al., 1998). Several signalling motifs exist which are thought to mediate nuclear import and export of *APC* (Rosin-Arbesfeld et al., 2000). Interaction with microtubules occurs through a region located between codons 2200 and 2400 (Deka et al., 1998) and also at the carboxyl terminal (codons 2560 – 2843) where the microtubule associated protein EB1 binds (Su et al., 1995). A role in chromosomal segregation has been suggested by Fodde and Kaplan in that *APC* and EB1 co-localise at the ends of microtubules attached to kinetochores at mitosis (Fodde et al., 2001) (Kaplan et al., 2001).

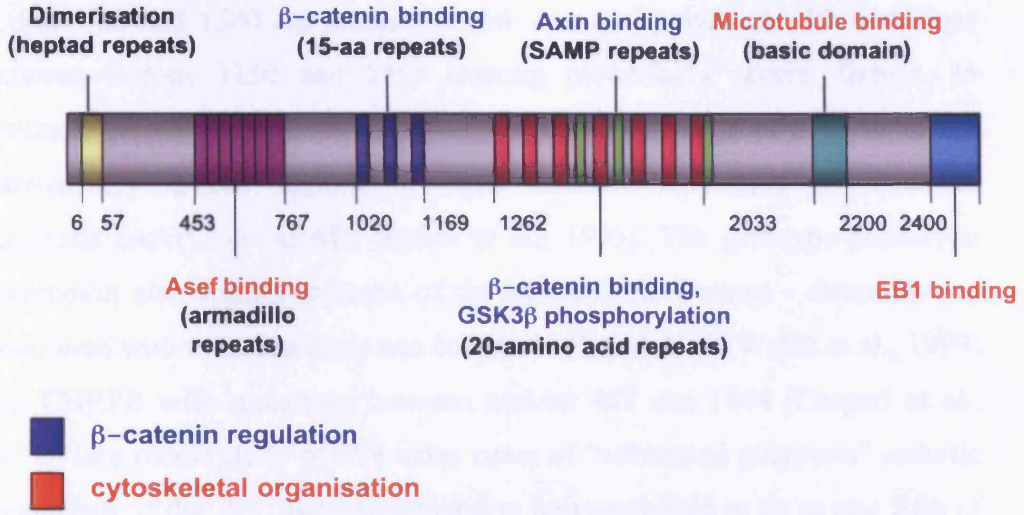

Figure 1–8 **The *APC* gene with functional domains annotated**

Due to the diversity of its function, *APC* has been implicated in a variety of cellular processes including cell migration, cytoskeletal organisiation, cell cycle control and apotosis (Sieber et al., 2000). In terms of its role as a tumour suppressor gene in CRC, it appears that it is the impact it has on Wnt signalling through controlling levels of *β-catenin* that is most important. Mutant *APC* is unable to down-regulate *β-catenin,* therefore resulting in clonal expansion of mutant cells. This is supported by studies demonstrating that colorectal tumours without *APC* mutations can harbour mutations in *β-catenin* which prevent the degradation of the protein and resulting in similar dysregulation of cell cycle control (Ilyas et al., 1997) (Sparks et al., 1998). There also appears to be an "optimal level" of Wnt signalling through which there is a relationship between the underlying germline mutation in *APC* and the somatic "second hit" mutation (Lamlum et al., 1999). The role that *APC* may play in chromosomal segregation suggests a mechanism by which it may cause chromosomal instability observed in FAP tumours.

APC harbours detectable germline mutations in approximately 85% of cases of FAP. The vast majority of these are insertions, deletions and nonsense mutations resulting in frameshifts and premature stop codons. Ten percent of FAP patients have a deletion of AAAAG at codon 1309. Initiation of tumour growth occurs following a second somatic event through either mutation, allelic loss or silencing leading to inactivation of the wild type *APC* allele. There is a distinct genotype-phenotype correlation in FAP. Mutations between

codons 450 and 1580 are associated with classical polyposis with mutations between codons 1250 and 1464 causing particularly severe disease. In contrast, germline mutations in the extreme 5' or 3' ends of *APC* or in the alternatively spliced regions of exon 9 cause attenuated adenomatous polyposis (AAPC or AFAP) (Spirio et al., 1993). The genotype-phenotype correlation also applies to some of the extracolonic features - desmoids are associated with mutations between codons 1395 and 2000 (Wallis et al., 1999) and CHRPE with mutations between codons 457 and 1444 (Caspari et al., 1995). In a recent study of 599 index cases of "attenuated polyposis" somatic mosaicism of the *APC* gene was found to be responsible in up to one fifth of cases (Hes et al., 2007). At this time there are no other studies to support this finding.

There is also some evidence suggesting that other environmental and genetic factors play a role in disease severity, as some individuals with identical germline *APC* mutations have differing polyp burden (Paul et al., 1993).

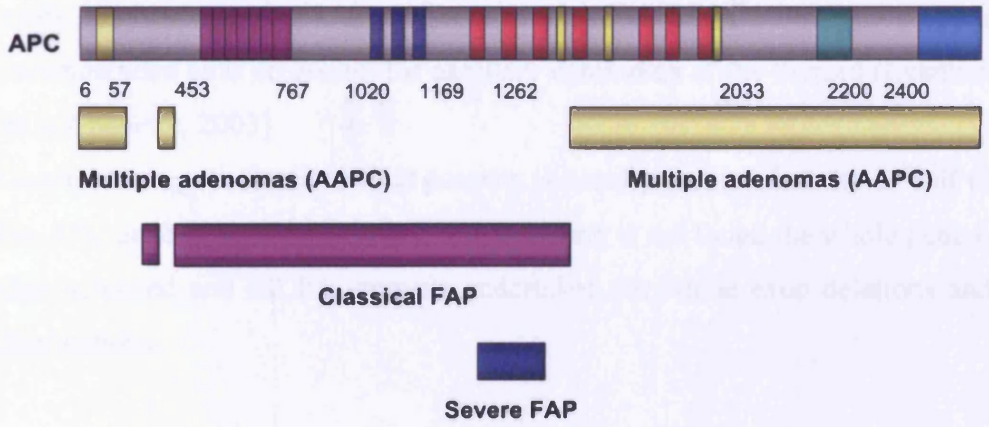

Figure 1–9 **Genotype/phenotype correlation associated with germline *APC* mutations**

1.2.2.2 Somatic mutations at *APC* – the mutation cluster region

In the majority of FAP tumours the second allele of *APC* is disrupted through either a truncating mutation or through allelic loss. In patients with germline mutations at codon 1309 (5bp deletion) the second allele is lost (LOH) in up to 85% of tumours studied (Crabtree et al., 2003). Through studying tumours of

individuals with FAP alot has been learned to improve the understanding of tumorigenesis in sporadic cases. In both FAP and sporadic cases the majority of somatic mutations occur in the 5' region of the *APC* gene. There is a region between codons 1284 and 1580 where 80% of somatic mutations occur. This was termed the mutation cluster region by Miyoshi *et al*, there are three "hotspots" at codons 1309, 1450 and 1554 which account for 20% of all somatic mutations (Miyoshi et al., 1992).

1.2.2.3 Clinical management of FAP patients.

Following clinical and molecular diagnosis – through genetic counselling and testing, strict surveillance is the key with annual colonoscopy and elective sub-total colectomy when adenoma burden deems it necessary. This is usually by the mid 20's. Colonoscopic surveillance usually commences in the teenage years. Regular endoscopic surveillance of the upper GI tract with endoscopy is recommended as is screening for papillary carcinoma of the thyroid (Lynch & de la Chapelle, 2003).

Genetic testing in classical FAP patients is usually restricted to the 5' half of the *APC* gene in the first instance, if a mutation is not found the whole gene is then screened and MLPA analysis undertaken for whole exon deletions and duplications.

1.2.3 Hamartomatous Polyposis Syndromes.

The hamartomatous polyposis syndromes comprise familial juvenile polyposis, Peutz-Jehgers syndrome, Cowdens disease and Bannyan-Ruvalcaba-Riley syndrome.

Juvenile polyposis

Juvenile polyposis syndrome (JPS) is a rare autosomal dominant syndrome caused by germline mutations in *SMAD4/DPC4* (Howe et al., 1998b), *BMPR1A/ALK3* (bone morphogenic protein receptor 1A/activin receptor-like kinase 3) (Howe et al., 2001) (Sayed et al., 2002). Both *SMAD4* and *BMPR1A*

are members of the *TGFβ/BMP* signalling pathway which is a target in CRC carcinogenesis.

The phenotype is that of multiple colonic hamartomatous polyps and sometimes polyps in the small intestine and stomach (Hofting et al., 1993) (Veale et al., 1966). Associated clinical manifestations and can include mental retardation, macrocephaly, heart defects (aortic valve malformations) and polydactyly. Diagnosis is usually made before the age of 10 years due to rectal bleeding, diarrhoea and abdominal pain (Heiss et al., 1993). There is an associated CRC risk despite there being fewer benign colonic polyps (Giardiello et al., 2000). Clinical management of JPS depends on the severity of the polyp burden whereby prophylactic surgery is sometimes indicated (Heiss et al., 1993) (Scott-Conner et al., 1995), or colonoscopic surveillance (Howe et al., 1998a).

Peutz-Jehgers Syndrome

Peutz-Jehgers syndrome is an autosomal dominant condition characterised by hamartomatous polyps of the small intestine and less commonly the colon. Other clinical features include peri-oral pigmentation, pigmentation if the fingers and sex cord tumours with annular tubules of the ovary (Giardiello et al., 1987). The syndrome is caused by germline mutations in serine threonine kinase *LKB1/STK11* (Hemminki et al., 1998). The highest cancer risk is in the GI tract (both small intestine and colon), but tumours also occur in the breast, ovary, pancreas and endometrium (Boardman et al., 1998) (Giardiello et al., 2000). Diagnosis is often made in adolescence due to gastrointestinal bleeding, abdominal pain or intestinal obstruction. The characteristic peri-oral and finger freckling aid clinical diagnosis. Germline mutation of *LKB1* is found in 50% of PJS families and between 30–60% of sporadic cases resulting in truncation or loss of the protein (Hemminki et al., 1998) (Jenne et al., 1998).

LKB1 appears to play a role in apoptosis and foetal development. It is found in apoptotic intestinal cells (Karuman et al., 2001) and has also been found to regulate p53 dependent apoptosis and control of cellular proliferation (Yoo et al., 2002).

Cowdens syndrome and Bannyan-Riley-Ruvalcaba Syndrome

Cowdens syndrome is an autosomal dominant disorder characterised by multiple muco-cutaneous lesions including multiple trichilemmomas, acral keratoses and oral mucosal papillomatosis (Brownstein et al., 1979) (Starink et al., 1986). 40% of patients develop multiple hamartomatous polyps involving the whole of the GI tract (Hizawa et al., 1994) (Waite & Eng, 2002). Hamartomatous polyps demonstrate excessive smooth muscle in the core of the polyps which are also often inflamed or fibrotic (Oberhuber & Stolte, 2000). In Cowdens syndrome there is an increased risk of developing thyroid, breast and genito-urinary cancers (Salem & Steck, 1983) (Starink et al., 1986). Bannayan-Riley-Ruvalcaba syndrome is characterised by macrocephaly, lipomatosis, haemangiomatosis and speckling of the penis. Patients may also develop hamartomatous polyps (Gorlin et al., 1992).

The presence of hamartomatous polyps in both of theses syndromes suggests an increased risk of CRC but a firm association is yet to be made.

Germline mutations in *PTEN* (phosphatase and tensin homologue deleted on chromosome 10) tumour suppressor gene cause both of these syndromes (Liaw et al., 1997) (Marsh et al., 1997). *PTEN* is a dual specificity phosphatase which has a number of pro-apoptotic functions including negative regulation of *PI3K/AKT* and MAPK signalling pathways (Waite & Eng, 2002).

1.2.4 The Hereditary Mixed Polyposis Syndrome

Hereditary mixed polyposis syndrome (HMPS) is an autosomal dominant condition characterised by the development of multiple tumours within the colon. These include atypical juvenile polyps, hyperplastic polyps, serrated adenomas, classical adenomas and carcinoma (Whitelaw et al., 1997). The locus for HMPS (*CRAC1*) has been mapped to chromosome 15q13-14 in Ashkenazi families and has been found to correlate with the Ashkenazi susceptibility locus *CRAC1* (Jaeger et al., 2003). Some Asheknazi families with the HMPS/*CRAC1* locus only develop multiple classical adenomas and CRC (Jaeger et al., 2003).

More recently, (single nucleotide polymorphism) SNP genotyping of a panel of SNPs associated with the *CRAC1* locus in CRC cases and controls found 2 SNPs associated with *GREM1* and *SCG5* (both found within the *CRAC1* locus) to be strongly associated with CRC risk (P=4.44x10^{14})(Jaeger et al., 2008).

1.2.5 Hyperplastic Polyposis Syndrome

Hyperplastic polyps (HPPs) are common bowel tumours usually found in individuals aged 60 and over. The great majority of HPPs do not have malignant potential but there is increasing evidence to suggest that some may progress to CRC (Church et al., 1988) (Jass et al., 2002). This risk is highest

when polyps exhibit dysplastic features as in cases of mixed HPP/adenomatous polyps and serrated adenomas. The age at presentation, size, number and anatomical location (ascending colon) all contribute to the CRC risk (Goldstein et al., 2003). The diagnostic criteria of HPPS and the real CRC risk associated with it are still evolving, Burt and Jass defined HPPS as any individual with >5 HPP's proximal to the sigmoid colon two of which >1cm in diameter or any individual with >30 HPP's anywhere in the colon (Burt, 2000). Rashid et al have devised a different classification for HPPS whereby any individual with >20 HPP's anywhere in the colon may be diagnosed. Further classification based on size (>1cm) or "multiple" HPP's (5-10) was also suggested (Rashid et al., 2000).

The proposed "serrated pathway" of colorectal neoplasia suggests HPP's to be the initiating lesion prior to development in to mixed polyposis (hyperplastic/adenomatous polyps), serrated adenomas and finally CRC. *BRAF* mutations are found commonly in serrated adenomas (Jass et al., 2002) (Goldstein et al., 2003).

A recent study of somatic mutations in 245 HPP's found mutations in *BRAF* and *KRAS*2 in 75% of polyps, the frequency of *BRAF* mutations was higher individuals with >10 polyps (Carvajal-Carmona et al., 2007). Patients would have either *BRAF* or *KRAS*2 mutations in any one polyp, none were found to have both. MSI was not observed and the epithelium of the polyps was found to be monoclonal (which is also the case for JPS).

There is mounting evidence to suggest a genetic predispostion to HPPS in young onset patients with multiple HPP's but to date a locus or candidate gene is yet to be determined (Niv et al., 2003) (Jeevaratnam et al., 1996) (Lage et al., 2004).

1.2.6 *MYH*-associated Polyposis and CRC

The role of *MYH* as a polyposis and CRC predisposition gene was discovered in 2002 through somatic screening of adenomas found in an interesting family with multiple adenomas and CRC which harboured a germline *APC* mutation

E1317Q of questionable pathogenicity (Sampson et al., 2003). *MYH* associated polyposis (MAP) has an autosomal recessive inheritance.

Al Tassan *et al* found that analysis of the somatic mutation spectrum of *APC* in tumour samples from a single family who had none of the known germline *APC* or MMR mutations revealed 18 somatic inactivating mutations in *APC*, 15 of which were G:C -> T:A transversions - a significantly higher proportion than that found in sporadic or FAP tumours (Sampson et al., 2003). This mutational signature suggested faulty DNA repair of 7,8-dihydro-8-oxo-2'deoxyguanosine (8-oxo-G), which led to screening for germline mutations in *MYH* and other BER enzymes, *MTH1* (Mut-T Homologue) and *OGG1*. Mutations in *MYH* were identified in both maternal and paternal alleles in affected individuals. *MYH* associated polyposis (MAP) is the first human cancer predisposition disorder to be linked to BER.

MYH is a DNA glycosylase involved in the repair of oxidative damage of DNA by base excision repair (BER). *MYH* maps to the short arm of chromosome 1, between p32.1-p34.3. It is 7.1 kb long, and contains 16 exons. It encodes a 535 amino acid protein with 41% identity to the shorter *E coli* protein (Slupska et al., 1996).

1.2.6.1 DNA base excision repair glycosylases and the function of *MYH*

Genomic integrity is maintained through several DNA repair mechanisms which continuously identify and rectify damaged and mispaired bases. Base excision repair involves a family of DNA glycosylases working alongside apyrimidine/apurine (AP) lyases, structure specific nuclease, repair polymerase, DNA ligase and PCNA tethering complexes. The overall mechanism is that of a simple cut and patch process removing DNA bases which have undergone oxidative damage. Damage specific excision is initiated by the recognition of oxidatively damaged bases either in the mother or daughter strand of replicating DNA or in the nucleotide pool itself. Once the commitment to excision is made this is followed by protection of the abasic site – in particular avoidance of deleterious double-stranded breaks in DNA, insertion of the correct base by a repair DNA polymerase and finally

sealing of the nicked DNA backbone by DNA ligase. As base damage is the most common form of cellular DNA damage, BER is one of the major mechanisms for dealing with the majority of DNA damage (Lindahl & Wood, 1999) (Wood, 1996).

Reactive oxygen species are generated through normal cellular oxygen metabolism and through external oxidative stress. They have been implicated in aging and carcinogenesis (Marnett, 2000).
The mutagenic effects of 8-oxo-G are opposed by the synergistic action of *MYH*, *MTH1* and *OGG1*. *MTH1* is a nucleotide phosphatase which catalyses the hydrolysis of 8-oxoGTP to 8-oxo-GMP, preventing its incorporation opposite adenine during replication. *OGG1* detects and then removes 8-oxo-G mispaired with adenine. *MYH* acts as "belt and braces" by detecting and removing adenine preventing it mis-pairing with thymine in subsequent rounds of replication. See Figure 1-10 for site of action of BER enzymes.

The frequency of oxidative damage to DNA is estimated at 10^4 lesions/cell/day in humans (Lu et al., 2001). This is most commonly caused endogenously as a by-product of cellular metabolism (Demple & Harrison, 1994) (Izumi et al., 2003). External factors such as radiation and cigarette smoke also contribute to oxidative damage. 8-oxo-7,8-dihydro2'deoxyguanosine (8-oxodG) is one of the most stable deleterious products of oxidative DNA damage. It readily mispairs with adenine (A) residues leading to G:C > T:A transversion mutations in the daughter strand. Levels of 8-oxydG are high in breast, lung and kidney cancers (Malins & Haimanot, 1991) (Jaruga et al., 1994; Olinski et al., 1992) (Okamoto et al., 1994). The incorporation of 8-oxoG into DNA is either through the direct oxidation of guanine (G) residues in the template strand or via the incorporation of an 8-oxodGTP from the nucleotide pool (Hayashi et al., 2002). The resultant G:C > T:A transversions after the next round of DNA replication occur because polymerases incorporate adenine opposite 8oxodG at a rate between 5 fold and 200 fold more frequently than they incorporate cytosine opposite the 8-oxoG lesions. (Shibutani et al., 1991).

When compared to other DNA repair mechanisms, such as nucleotide excision repair, BER is vertically well conserved from bacteria to humans in terms of the core components of BER machinery. This is very useful for studying the functional implications of BER enzyme mutations *in vitro*. In E.coli, three enzymes protect the cell against damage from ROS, their homologues *MTH1*, *OGG1* and *MYH* have similar functions in human cells. *MTH1* hydrolyses the oxidised triphosphate 8-oxo-dGTP to monophosphate 8-oxo-dGMP, thus eliminating mutagenic substrates from the cell's nucleotide pool (Nakabeppu, 2001). *OGG1* provides a second level of defence by detecting and removing 8-oxodG from the DNA leaving an abasic site (Slupska et al., 1996). *MYH*, provides the third level of defence by scanning the daughter strand after replication, removing A mispaired with G or 8-oxoG (Slupska et al., 1996) (Slupska et al., 1999) (Lu et al., 2001).

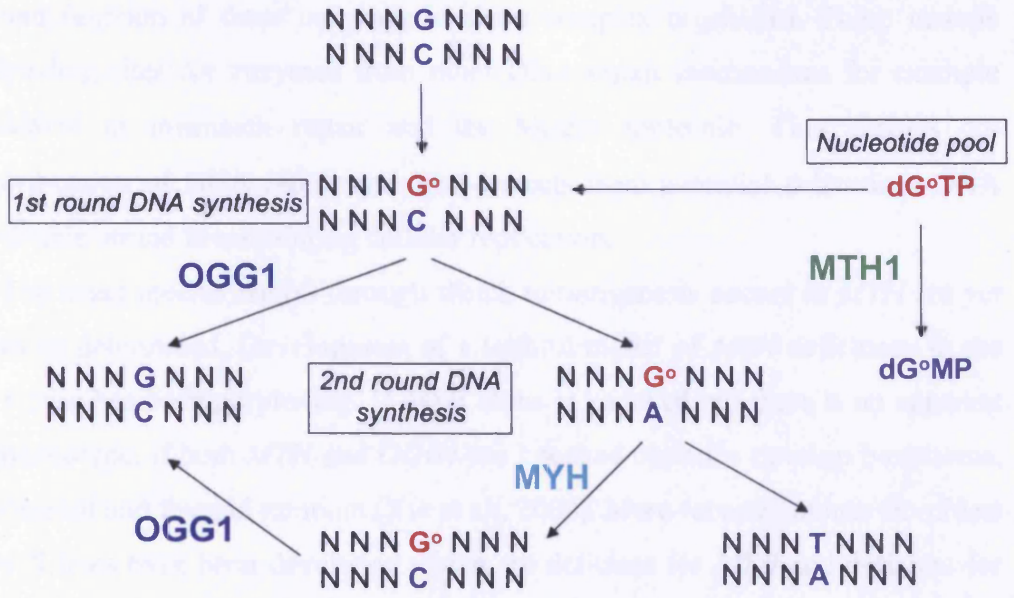

Figure 1–10 **Schematic overview of the sites of action of the BER repair genes *MYH*, *OGG1* and *MTH1*. Oxidised guanine is shown in red**

MutY and it's homologues have a catalytic core domain with an [4Fe-4S] iron sulphur cluster in the N terminus (Guan et al., 1998) and a C-terminal MutT like domain (Volk et al., 2000) (Fromme et al., 2004). It is the C-terminal domain that is thought to be responsible for recognition of 8-oxoG, as when this domain is truncated discrimination between 8-oxoG:A and G:A mispairs is lost (Gogos et al., 1996) (Noll et al., 1999). In 2004, the full-length structure of MutY interacting with DNA was determined (Fromme et al., 2004). This has enabled further understanding of how 8-oxoG and adenine are recognised. The [4Fe-4S] catalytic core domain is very similar to that of Endonuclease III which excises oxidised pyrimidines (Kuo et al., 1992) (Guan et al., 1998). The C-terminal domain is very similar to MutT. Both the catalytic core domain and MutT domains encircle oxidatively damaged DNA making contact with the appropriate DNA strands. Adenine is then flipped out in to a deep pocket (similar to other Hairpin-helix-Hairpin DNA glycosylases) the 8-oxoG remains in position and undergoes removal and repair by other members of the BER family.

Eukaryotic BER enzymes have additional termini which elaborate the activites and function of these enzymes in more complex organisms. These include binding sites for enzymes from other DNA repair mechanisms for example *MSH6* in mismatch repair and the MutSα molecule. This enables co-ordination of DNA repair and also protects from potential deleterious DNA double-strand breaks during cellular replication.

The exact mechanism(s) through which tumorigenesis occurs in *MYH* are yet to be determined. Development of a faithful model of *MYH* deficiency in the mouse has been perplexing. If *MYH* alone is knocked out there is no apparent phenotype, if both *MYH* and *OGG1* are knocked out mice develop lymphoma, ovarian and thyroid tumours (Xie et al., 2004). More recently mouse fibroblast cell lines have been developed which are deficient for *MYH* and deficient for both *MYH* and *OGG1*. When these cell lines were exposed to low dosage oxidative stress a reduction of S phase and increase of G2/M phase in *Myh* $^{-/-}$ *Ogg1*$^{-/-}$ cells was observed than in wild type cells. A similar level of cell death was observed in both cell lines. The oxidants also induced a greater number of multinucleated cells in *Myh* $^{-/-}$*Ogg1*$^{-/-}$ cells than in wild type, centrosome amplification and multi-polar spindle formation was also seen (Xie et al., 2008).

It was concluded from this study that when under oxidative stress, *MYH* and *OGG1* are likely required for normal cell cycle progression and nuclear division, suggesting multiple roles of *MYH* and *OGG1* in the maintenance of genome stability and tumor prevention.

Despite *MTH1* and *OGG1*s known roles in the base excision repair pathway, numerous studies of patients with multiple adenoma phenotype or FAP and with no known *APC* mutations failed to show any definite pathogenic changes in *OGG1* and *MTH1*. (Al-Tassan et al., 2002) (Jones et al., 2002) (Sieber et al., 2003).

1.2.6.2 Clinico-pathological features of MAP

Common pathogenic variants occur in *MYH* amongst different ethnic groups. Northern European populations have a predominance of Y165C and G382D mutations (Jones et al., 2002). Other pathogenic variants include Y90X in

patients of Pakistani origin and E466X which has been found solely in patients of Indian origin. An in frame deletion nt1395delGGA has been identified in patients of Mediterranean origin (Gismondi et al., 2004).

The phenotype of affected individuals is that of 10's to 1000's of adenomatous polyps and CRC. It is thought to account for approximately 1% of CRC (Farrington et al., 2005) (Webb et al., 2006) and to also account for up to 30% of patients with 15-100 adenomas (Sieber et al., 2003).

Affected individuals generally present in their fifth or sixth decade although there have been exceptional cases presenting in their late teens (Y165C/G382D) and thirties (E466X/E466X) – unpublished data. A handful of extracolonic features have been found in the small number of patient cohorts described to date such as congenital hypertrophy of the retinal pigment epithelium (CHRPE) – (4 cases), duodenal polyps – (3 cases), osteomas –(2 cases), gastric cancer – (1 case), desmoids – (1 case) and dental cysts – (1 case) (Enholm et al., 2003; Gismondi et al., 2004; Sampson et al., 2003; Sieber et al., 2003). To date no definite genotype-phenotype correlation has been identified.

The prevalence of CRC associated with MAP at presentation varies between populations studied; one group has reported a prevalence nearing that of FAP of 78% (Gismondi et al., 2004), whereas others have reported a lower frequencies of 48% (Sampson et al., 2003) and 50% (Sieber et al., 2003). MAP cancers are predominantly left sided (71%). Metachronous or synchronous CRCs occur in a substantial number (27%) of bi-allelic mutation carriers (Lipton et al., 2003b). In homozygous individuals, the cancer penetrance is 100% at 60 years (Farrington et al., 2005), that is, similar to FAP (albeit at an older age).

1.2.6.3 Mutation spectrum associated with MAP

Molecular analysis of adenomas and cancers from MAP patients has demonstrated that *APC* is targeted and a higher frequency of G:C>T:A transversions are seen at TGAA/AGAA motifs, creating nonsense mutaitons. Somatic screening for *APC* mutations in adenomas and cancers did not find a

"mutation cluster region" as observed in FAP. Mutations in *K-ras* have only been found at codon 12, all are G:C>T:A transversions. MAP cancers are near diploid (using flow cytometry) and microsatellite stable (Lipton et al., 2003b). A recent study examining micro-dissected MAP adenomas with comparitive genomic hybridisation has suggested that chromosomal instability is present in MAP adenomas (Cardoso et al., 2006).

1.2.6.4 Significance of the heterozygous state in *MYH*

To date there has been some debate as to the significance in terms of polyposis and CRC risk in heterozygote *MYH* carriers. Farrington et al (Farrington et al., 2005) suggested an increased relative risk of 1.68 (95% CI 1.07-2.95) in simple heterozygote patients with either Y165C or G382D mutations, arbitrarily over the age of 55 in a large population based study of 2239 cases and 1845 controls. This compared all patients with CRC irrespective of the presence of adenomas with age and sex matched controls in Scotland. Webb et al (Webb et al., 2006) published a series of 2561 cases and 2695 controls finding no significant increase in CRC risk in mono-allelic carriers of the same common Caucasian mutations.

The first *MYH* mouse model described in this thesis (*ApcMin*$^{+/-}$ / *Myh*$^{+/-}$) did not demonstrate an increased number of intestinal adenomas in the *MYH* heterozygote group when compared to wt controls (Sieber et al., 2004).

Heterozygous status in the general population has been found to be 1% in a sample of 1845 individuals (Farrington et al., 2005). Common polymorphisms of as yet unknown pathological significance have also been identified. In Caucasian northern European populations Q324H is observed in 20%, V22M in 10% and S521F in 2% of the population, predominantly as heterozygote carriers. These polymorphisms may have implications if they form compound heterozygotes with known pathogenic mutations or in the presence of external or environmental factors such as cigarette smoking or radiation.

In the clinic, testing for *MYH* mutations is available for individuals and at risk relatives in whom no known *APC* mutation has been found or who appear to have recessively inherited multiple adenomas or CRC. For individuals who have homozygous deletions the follow up would be identical to those who

have *APC* mutations, that is annual colonoscopy. However, to date a firm follow up programme for heterozygous carriers is yet to be published.

1.3 The Multiple Adenoma Phenotype

Individuals who develop multiple colorectal adenomas (MCRAs) are a genetically and clinically heterogeneous group who are at increased risk of CRC. The MCRA phenotype can usefully, but arbitrarily, be defined as the development of 5-100 adenomas during an individual's lifetime. Germline mutations in the *APC* gene account for about 15% of cases with an MCRA phenotype, these patients have AFAP (Spirio et al., 1999). An additional ~35% of such patients have bi-allelic germline mutations in the *MYH* gene and are classified as having MAP (Sieber et al., 2003) (Sampson et al., 2003). As mentioned previously, *MYH* deficiency leads to adenoma formation through somatic hypermutation of the *APC* and *K-ras* genes. The remaining MCRA patients have no known underlying genetic cause for their phenotype.

To date, the most widely used strategy for identifying candidate predisposition genes for polyposis syndromes and CRC has been through genetic linkage analysis. This approach has been particularly successful for the dominantly inherited syndromes FAP and HNPCC. Its ability to disclose moderate and low penetrance genes is more questionable. No susceptibility gene for a complex cancer has yet been identified using this approach.

The frequency of low penetrance genes may be much higher than the frequency of high penetrance genes in the general population due to the low selective disadvantage associated with these changes. Identification of these novel predisposition genes is important, enabling clinical geneticists to identify individuals at risk and raises the possibility of setting up reliable, cost effective population screening.

However, detection of low penetrance genes using linkage analysis requires prohibitively large numbers of multi-generational families in order to yield results. For example, a dominant model with a gene frequency of 0.1 and risk ratio of 6 would require 473 affected sib pairs, 205 three affected sibs, 145 four affected sibs, 545 cousin pairs or 550 avuncular pairs to give a lod score of 3.3. (Houlston & Tomlinson, 2000). Therefore alternative approaches need to be utilised.

It is likely that there may still be highly penetrant CRC predisposition genes as yet undiscovered, but the majority of remaining are genes most likely to be of moderate and low penetrance. The possibility of the remainder of the genetic influence of CRC being inherited as a polygenic trait or through the inheritance of multiple low penetrance alleles at several genetic loci is becoming more accepted (reviewed in (Kemp et al., 2004)).

Rodent studies have led to the identification of modifier genes loci associated with murine FAP models. The identification of the (Modifier of Min 1) Mom1 and Mom2 alleles being one such example in mice (Dietrich et al., 1993). Mom1 maps to the phospholipase 2 (*Plga2*) gene in humans. However, to date no mutation or evidence to suggest this is a modifier gene in humans has been found. The search for modifier genes which affect the severity of Mendelian cancer syndromes is of importance as these genes may act as a low-penetrance pre-disposition genes in their own right.

In order to identify these remaining genes, different strategies need to be used in tandem for the highest chance of success. Linkage analysis should not be disregarded however, with the development of array technology traditional linkage analysis can be superseded with tagged single nucleotide polymorphism (SNP) arrays. This approach allows linkage to be undertaken with a higher resolution across the genome. Traditional linkage analysis utilises up to 400 microsatellite markers across the genome whereas the first SNP arrays (Affymetrix®) contained 10 000 SNPs (Risch, 2001). This approach led to the identification of an area of interest on chromosome 3q21-q24 when germline DNA from 69 families (with a family history of CRC but no mutations in the known predisposition genes) were analysed (Kemp et al., 2006).

Array comparative genomic hybridisation (CGH) followed by linkage analysis identified the locus (19p) and then pre-disposition gene *LKB1* for Peutz-Jegher's syndrome in 1998 (Hemminki et al., 1998).

Mutation screening of potential candidate genes may help to identify future pre-disposition genes and sub-polymorphic variants. Selection of candidate genes for screening is guided by preliminary studies – such as linkage analysis and more recently association studies and through knowledge of the underlying pathological mechanisms involved in polyposis and CRC.

Therefore genes involved in the Wnt signalling pathway and DNA repair mechanisms are obvious first line candidates, with cell cycle checkpoint genes and modulators of apoptosis being of significance in any cancer pre-disposition syndrome.

1.3.1.1 *APC* Missense variants and the Multiple Colorectal Adenoma Phenotype

The APC missense variant E1317Q

The germline missense variant *APC* E1317Q was first reported in 1996 by White et al (White et al., 1996) as an incidental finding when screening for somatic, protein-truncating *APC* mutations in sporadic colorectal cancers. Further studies in a set of 164 individuals with multiple (3-100) colorectal adenomas screened for germline *APC* mutations (Lamlum et al., 2000) found a small number of these patients carried protein-truncating mutations in exon 9 and the 3' part of exon 15 of *APC*, seven patients carried E1317Q, compared with only two of 503 UK controls. These data suggested E1317Q to be a low-frequency (or sub-polymorphic) risk allele for colorectal adenomas (in this sample set, odds ratio=11.2, 95%CI=2.30-54.3, $p<0.001$). At this time it was not possible to provide a convincing mechanism for the effects of the 1317Q allele, since the amino acid change (glutamine>glutamic acid) is a relatively conserved one. It was hypothesised, however, that since the polymorphism lay within a critical region of the *APC* protein, between repeat sequences involved in *β-catenin* binding and degradation, subtly increased *β-catenin* levels and hence activated Wnt signalling were a plausible mechanism of increased tumour susceptibility.

Several subsequent studies have examined the possible association between the *APC* 1317Q allele and colorectal adenomas and/or carcinoma. Popat et al (Popat et al., 2000) found E1317Q in 2 of 364 early-onset colorectal cancer patients and 2 of 290 controls. Gismondi et al (Gismondi et al., 2002) found E1317Q in 2/182 patients with single or multiple colorectal adenomas and in 2/135 controls (OR=1.29, 95% CI=0.09-18.0). Hahnloser et al (Hahnloser et al., 2003) found no excess of E1317Q in colorectal adenoma patients (5/231)

or cancer cases (9/377) compared with spouse controls (10/362), but did find an excess compared with individuals who had had a normal screening colonoscopy (1/317), thus providing an odds ratio of 1.164 for 1-3 adenomas, 0.523 for 4-100 adenomas and 0.838 for cancer in the latter case (95% CIs 0.28-4.78, 0.10-2.68 and 0.31-2.26 respectively). These studies involve patients with different inclusion criteria and controls from differing sources. Overall, they suggest that *APC* E1317Q has at most a small effect on the risk of colorectal tumours and it is possible that it is simply a non-functional rare polymorphism (Evertsson et al., 2001) (Popat et al., 2000).

How studying E1317Q led to the discovery of MYH

Researchers were attempting to find some clues as to possible functional effects of the 1317Q allele. One strategy was to determine whether or not colorectal tumours from these patients had acquired an independent somatic *APC* mutation on the 1317Q allele and, if so, whether that mutation lay 5' or 3' of codon 1317; if mutations were found which truncated the *APC* protein before codon 1317, for example, a functional effect of the Q allele would be much less likely. In colorectal adenomas from one family which carried 1317Q, not only did the somatic mutations appear to target both the 1317E and 1317Q alleles equally, but also the mutation spectrum was grossly atypical for *APC*. Allelic loss and frameshift mutations – the most common types of change - were almost absent and nearly all point mutations were G:C>T:A transversions, typical of oxidative damage or defective base excision repair. The identification of pathogenic bi-allelic mutations in the 8-oxo-guanine DNA glycosylase *MYH* followed soon afterwards (Al-Tassan et al., 2002).

The APC germline missense variant I1307K

The I1307K *APC* variant occurs in roughly 6-9% of Ashkenazi Jews (Redston et al., 1998) and is very rarely found in any other ethnic groups. This variant leads to the appearance of an A_8 tract which is hypermutatble resulting in somatic slippage and frameshift mutations (Laken et al., 1997). Similarly to the E1317Q variant there are differing reports as to the relative risk of developing colorectal adenomas and CRC. Frayling et al (Frayling et al.,

1998) and Gryfe et al (Gryfe et al., 1999) found an associated relative risk of 1.5-2.0 when studying a solely Ashkenazim population, whereas Figer and Woodage (Figer et al., 2001) (Redston et al., 1998) found no increased risk in unselected Israelis and Ashkenazim. Interestingly only 50% of CRC tumours from I1307K carriers demonstrate slippage of the A_8 tract (Gryfe et al., 1998) (Laken et al., 1997) (Zauber et al., 2003). It appears that other oligonucleotide tracts within *APC* are not hypermutable. As I1307K lies within a region of *APC* associated with severe FAP phenotype it may simply have a direct functional effect as well as predisposing to hypermutability.

1.3.1.2 Non-*APC* related rare low risk alleles and their CRC risk

The current situation as regards rare low-risk alleles and colorectal tumour risk is intriguing. Whilst *CHEK2* alleles are convincingly associated with increased breast cancer risk, the evidence for an effect on colorectal cancer is mixed. Meijers-Heijboer et al (Meijers-Heijboer et al., 2002) found no association between *CHEK2* and colorectal cancer: the 1100delC allele was present in 3 index cases from 107 colorectal cancer families of otherwise unknown genetic origins, compared with 18/1620 controls of mixed origins (OR=2.34, 95%CI=0.95-5.79). 1100delC was, however, over-represented in breast cancer families which also contained members with evidence of hereditary colon cancer, compared with breast cancer families without such evidence (OR=5.41, 95%CI=2.29-12.8). Meijers-Heijboer et al (Meijers-Heijboer et al., 2002) have interpreted these data as showing evidence for the hypothesised distinct hereditary breast-colon cancer phenotype, but they found no mirroring evidence to show that colorectal cancer families with evidence of hereditary breast cancer had an excess of the 1100delC allele. Lipton et al (Lipton et al., 2003a) studied 149 patients with 3-100 colorectal adenomas and found no excess of 1100delC. Cybulski et al (Cybulski et al., 2004) typed 1100delC in 300 Polish colorectal cancer cases and 4,000 controls, but found no significant excess in the former, although the missense *CHEK2* I157T variant was over-represented in cases. Kilpivaara et al (Kilpivaara et al., 2003)

evaluated the frequency of 1100delC in 662 familial and sporadic colorectal cancer cases, including some putative hereditary breast-colon cancer kindreds, and found no increased frequency compared with population controls.

It is likely that definitive answers about alleles such as *APC* E1317Q and *CHEK2* 1100delC will only come from large international studies and/or from meta-analyses, which have the associated risks of imperfect matching of cases and controls and population-specific effects on risk.

Other variants in candidate genes conferring increased CRC risk have also been described, these include cyclin D1 (*CCND1*) (Porter et al., 2002), E-cadherin (*CDH-1*) (Kim et al., 2000) and a member of the transforming growth factor β family (*BMPR1A*) (Lipton et al., 2003c). One study including analysis of beta-catenin (*CTNBB1*), axin (*AXIN1*), *MLH1* and *MSH2* in 124 MCRA patients and 483 controls found significant odds ratios in *AXIN1* (6 missense variants in total) and MSH2 (3 missense variants in total) (p=0.012 and p=0.001 respectively) (Fearnhead et al., 2004). In this case the *AXIN1* P312T missense variant substituted a polar threonine with a neutral proline in a region where axin binds with *APC* and *GSK3β*

Two variants in Methylene tetrahydrofolate reductase (*MTHF*) (C677T and A1298C), rapid acetylator alleles in N-acetyl transferase 2 (*NAT2*) and *VNTR* rare alleles in Harvey rat sarcoma virus 1 (*HRAS1*) have also been reported as low risk alleles (Houlston & Tomlinson, 2001) (de Jong et al., 2002).

The careful use of strategies such the analysis of familial cases and the study of negative, rather than population, controls may enhance the power of studies, but the accumulation of overwhelming evidence on variants such as *APC E1317Q, I1307K* and *CHEK2* 1100delC may take many years.

1.4 Common disease variants and CRC risk

It is becoming increasingly apparent that many of the remaining polyposis and CRC pre-disposition genes may be common, less penetrant disease variants with small effects on risk.

Genome-wide approaches are currently being undertaken with the hope of identifying common, low-risk alleles but historically their discovery to date has relied on candidate gene analysis followed by determining allele frequencies in large case-control cohorts (Meijers-Heijboer et al., 2002).

Association studies enable an unbiased approach for searching for disease associations without prior knowledge of function or presumptive involvement of any gene in disease causation. This has been made possible by utilising second generation SNP arrays (550 000 SNPs) allowing genome-wide case-control association studies to be performed. In principle it is possible to identify the real disease-associated variant by scanning nearby genes for variants that could plausibly have a real effect in the pathogenesis of the disease being studied.

This approach using 550K SNP arrays has recently led to the identification of a series of regions of interest in CRC development on chromosomes 8q24, 10p14, 11q23 and 18q21, (Tomlinson et al., 2007; Zanke et al., 2007), (Haiman et al., 2007) (Tomlinson et al., 2008) (Tenesa et al., 2008).

Second stage analysis (3 replication sample sets totalling 7,473 CRC cases and 5,948 controls) of the top 5% of polymorphic SNPs identified from Tomlinson *et als* first genome wide association study of 940 CRC cases and 965 controls (Tomlinson et al., 2007) identified 3 SNPs in *SMAD7* to be significantly associated with development of CRC (P_{trend}=1.0x10^{12})(Broderick et al., 2007).

1.5 Aims of this Thesis

The main objectives of this thesis can be divided into three main areas -

1: Determination of the mechanisms of carcinogenesis associated with *MYH*-associated polyposis (MAP).
This includes –
i) further characterisation of the MAP phenotype
ii) search for any genotype/phenotype correlation in MAP
iii) completion of germline screening for mutations in enzymes of the same family (*OGG1* and *MTH1*) in individuals with the multiple adenoma phenotype
iv) looking for evidence and mechanisms of genomic instability in the development of MAP through comparative genomic hybridisation
v) development of a mouse model of MAP

2: Identification of novel predisposition genes for the multiple adenoma phenotype was undertaken utilising various techniques, including somatic screening for mutational signatures, expression microarray analysis of lymphoblastoid cell lines from MCRA cases and subsequent candidate gene screening.

3: Investigation of the clonal origins of colorectal adenomas and CRC

2 Materials and Methods

Solutions and media which are shown in **bold** have their recipes given at the end of this chapter.

2.1 DNA Extraction

2.1.1 DNA extraction from blood

DNA extraction from fresh frozen blood taken via peripheral venesection was performed using either the ammonium acetate method described below or latterly with the automated Chemagen system.

The ammonium acetate method involves three key steps. Cell lysis by hypotonic shock, nuclei lysis (and further cell lysis) by detergent action and proteinase K digestion, and finally precipitation of DNA with ammonium acetate and ethanol.

Nine ml of fresh frozen, EDTA preserved venous blood were thawed and transferred in to a 50ml polypropylene tube (Corning). Cells were lysed by adding ice-cold distilled water (dH_2O) to a final volume of 50ml. This was mixed by inversion, and cells separated by centrifugation at 2300 rpm for 20 minutes at 4°C in a swing out rotor centrifuge (CR412 Jouan). Following discarding of the supernatant, the cell pellet was washed in 25ml of **0.1% NP-40** at 4°C. Nuclei were lysed by the addition of 3ml of **nuclei lysis buffer**, 200µl **10% SDS,** and 600µl **proteinase K solution**. The sample was then vortexed until the pellet was completely resuspended and incubated for 2 hours at 60°C. One ml of saturated ammonium acetate was added to the tube which was then vortexed for 15 seconds. The sample was then incubated at room temperature for 10-20 minutes and centrifuged at 2300 rpm fro 20 minutes at room temperature. The supernatant was then transferred to a clean 50ml polypropylene tube and two volumes of ice-cold 100% ethanol (BDH) were added. The DNA was precipitated by gentle inversion of the tube several times and then spooled out using a plastic inoculating loop. The spooled DNA

was dipped in to an Eppendorf tube containing **70% ethanol** to remove excess salt, and transferred to a labelled screw-capped Eppendorf tube. Following air drying, the DNA was re-suspended and stored in 1ml dH_2O. Quantification of the DNA extracted was performed with spectrophotometry at 260 and 280nm.

2.1.2 DNA extraction from cell lines

DNA extraction from lymphoblastoid or colorectal cell lines was performed using a high salt method. This method avoids the use of toxic phenol which is used conventionally to separate DNA from protein debris. The high salt method involves four key steps. Cell lysis by detergent action and proteinase K digestion, degradation of ribonucleic acids (RNAs) as these can interfere with downstream applications, separation of DNA from protein debris using sodium chloride and chloroform, and precipitation of DNA with isopropanol. Approximately $5x10^7$ cells were transferred to a 50ml polypropylene tube (Corning) and then centrifuged for 10 minutes at 1500 rpm at room temperature (CR412 Jouan centrifuge). The supernatant was discarded and the remaining cell pellet washed twice in **PBS** before resuspending in 15ml **SE buffer**. RNA's were degraded by adding 50µl of **10mg/ml RNAseA** to the mixture followed by incubation for 1 hour at 37°C. Proteinase K (BDH) was added to a final concentration of 200µg/ml and cells lysed by overnight incubation at 55°C. Separation of DNA from protein debris was performed by the addition of 4.5ml of **5M sodium chloride** (final concentration 1.5M) and 20ml of chloroform (BDH). The tube was mixed by rotation for 30 minutes and then centrifuged at 2000rpm for 10 minutes at room temperature. The DNA-containing aqueous layer was transferred to a new 50ml tube, and an equal volume of isopropanol (BDH) was mixed together for 5 minutes to precipitate the DNA. Extracted DNA was spooled out using a plastic inoculation loop and washed in **70% ethanol** for 1 hour to remove excess salt. Following air drying, the DNA was re-suspended and stored in 1ml dH_2O. Quantification of the DNA extracted was performed with spectrophotometry at 260 and 280nm.

2.1.3 DNA extraction from fresh frozen tissue

DNA extraction from fresh frozen tissue was performed using the QIAamp DNA mini kit (Qiagen) according to the manufacturers instructions. This method allows the isolation of up to 40μg of DNA from 25mg of tissue.

Tissue was cut in to small pieces and digested with proteinase K overnight. Following digestion, **RNaseA 10mg/ml** was added to degrade RNAs, DNA was precipitated by adding ethanol which was then collected by binding on a spin column. Following a series of washes to remove protein debris, the DNA was eluted from the column with dH_2O. Quantification of the DNA extracted was performed with spectrophotometry at 260 and 280nm.

2.1.4 DNA extraction from formalin fixed paraffin embedded tissue

DNA extraction from formalin fixed paraffin embedded tissue involved two key steps – manual dissection of dewaxed tissue from unstained slides followed by cell lysis and proteinase K digestion.

Formalin fixation of tissue causes cross-linkage and breakage of DNA, therefore DNA extracted with this method is generally fragmented and of relatively poor quality. In light of this, when using this DNA for PCR, primers should be designed to amplify small amplicons of approximately 1-200 base pairs. This method does however allow the investigation of historical samples which may be up to 40 years old.

Depending on the size of the sample tissue, between 5 and 8 10μm sections were cut from each paraffin block on to non-coated glass slides using a microtome (Reichert-Jung). The tissue was then dewaxed in xylene (BDH) for 10 minutes, and washed twice in 100% ethanol (BDH) for 10 minutes. One section was stained with haematoxylin and eosin (Merck) according to manufacturers instructions, and inspected using an Eclipse 400 light microscope (Nikon). Haematoxylin, a dye obtained from the heartwood of the *Haematoxylon campechianum* tree stains cell nuclei purple whilst eosin, a halogenated derivative of fluoroscein, stains cell cytoplasm red. Following

identification of areas of interest, tissue was micro-dissected using sterile needles under microscope guidance. Extracted tissue was digested in a small volume (50-100µl) of proteinase K buffer [500µl 10x Mg^{2+}-free PCR buffer (Promega), 50µl 20mg/ml proteinase K (BDH), 4.45ml d H_2O]. The tissue and proteinase K buffer were transferred to a screw top Eppendorf tube and digested for 24-48 hours at 55°C. The proteinase K was then denatured and inactivated by heating to 95°C for 10 minutes. The sample was then centrifuged at 1300rpm for 15 minutes in a 5415C bench-top centrifuge (Eppendorf). The supernatant containing DNA was then removed with a pipette and transferred into a fresh Eppendorf tube. Spectrophotometry of DNA extracted via this method is often inaccurate due to fragmentation of the DNA.

2.1.5 DNA extraction from laser micro-dissected single crypts

DNA extraction from single large bowel epithelial crypts involves three key steps. Isolation of crypts, digestion with proteinase K solution and inactivation of proteinase K.

Up to six crypts were cut and isolated in to a 50µl capped tube (see Laser-microdissection method for details of slide preparation and micro-dissection). These were digested overnight in 10µl of proteinase K solution at 60°C in PicoPure DNA extraction proteinase K (PicoPure DNA Extraction kit (Kit:0103), Molecular Devices Corporation, CA94089-1136, USA) as per manufacturers directions. Each tube was sealed with Parafilm (Parafilm M sealing film, Pechiney Plastic Packaging, WI 54952, USA) to prevent sample evaporation. Proteinase K was then denatured and inactivated by heating to 90°C for 10 minutes. Samples were then centrifuged at 13000 rpm for 10 minutes in a 5415C bench-top centrifuge (Eppendorf) before use.

2.1.6 DNA extraction from mouse tail and ear clips

DNA extraction from mouse tail and ear clips involves four key steps. Digestion of tissue in proteinase K solution, DNA extraction using the high salt method, precipitation and washing of DNA.

Mouse tail and ear snips were received in screw topped Eppendorf tubes on dry ice. To each tail snip tube 400µl of **tail lysis buffer** and 5µl of proteinase K (BDH) stock solution (20mg/ml) were added. This was followed by incubation for 3 hours minimum or overnight at 55°C. 160µl of 5M NaCl was added and vortexed well, tubes were returned to 55 °C for a few minutes to allow any precipitate to dissolve. Samples were vortexed and centrifuged at 13000 rpm for 10 minutes (5415C bench-top centrifuge (Eppendorf)) at room temperature. 500µl of the supernatant was pipetted into a new 1.5ml Eppendorf tube and DNA was precipitated by the addition of 300µl of isopropanol (BDH). The samples were mixed gently by inversion to aid the precipitation of DNA and then centrifuged at 13000 rpm for 10 minutes (5415C bench-top centrifuge (Eppendorf)) at room temperature. The resulting supernatant was aspirated with a pipette and the sample washed with 300µl of **70% ethanol**. Samples were then vortexed and centrifuged at 13000 rpm for 10 minutes (5415C bench-top centrifuge (Eppendorf)) at room temperature. The resulting supernatant was aspirated with a pipette and the extracted DNA resuspended in 100µl dH_2O (tail snip) or 30µl dH_2O (ear snip) as there is less starting material with ear snips. Quantification of the DNA extracted was performed with spectrophotometry at 260 and 280nm.

2.2 RNA Extraction

2.2.1 RNA extraction from cell lines

RNA extraction from lymphoblastoid cell lines was undertaken using the trizol (Invitrogen) / chloroform method. Trizol is a monophasic solution of phenol and guanidine isothiocyanate. During RNA extraction, trizol maintains

RNA integrity whilst disrupting the cell membrane and dissolving cellular components. Centrifugation following the addition of chloroform separates the solution in to an aqueous phase (containing the extracted RNA) and an organic phase. The RNA is then recovered following precipitation with isopropyl alcohol.

Lymphoblastoid cells in culture were washed with **phosphate buffered saline** and pelleted prior to RNA extraction.

Fifty mls of lymphoblastoid cells in culture medium were pelleted in a 50ml polypropylene tube (Corning) and centrifuged for 4 minutes at 300 g in a swing out rotor centrifuge (CR412 Jouan) at room temperature. These cells were re-suspended and washed and pelleted twice in 50 ml of **phosphate buffered saline**. 1.5 ml of Trizol was added to the pelleted cells, mixed gently and left for 5 minutes at room temperature. 300µl of chloroform (BDH) was added, mixed gently and left to stand for 5 minutes at room temperature. Samples were then transferred and split between two screw top Eppendorf tubes and centrifuged (5415C bench-top centrifuge (Eppendorf)) at 12000 g at 4°C for 15 minutes. The upper aqueous phase containing the RNA was removed via pipette and placed in a new screw top Eppendorf tube. 750µl of isopropyl alcohol (BDH) was added, gently mixed with a pipette and left to stand at room temperature for 5 minutes. Samples were then centrifuged (5415C bench-top centrifuge (Eppendorf)) at 12000 g at 4°C for 10 minutes. The pelleted RNA was then washed with 1 ml of **75% ethanol** and centrifuged (5415C bench-top centrifuge (Eppendorf)) at 7500 g at 4°C for 5 minutes. The resulting RNA was re-suspended in 200µl RNAse free dH_2O and immediately placed on wet ice. Samples were further cleaned prior to use in expression array work on a Qiagen column (details of kit). Quality and quantity of RNA extracted was assessed using the Agilent platform and by running 10µl of the final RNA product on a 1% agarose gel at 100V for 45 minutes.

2.2.2 RNA extraction from tissue

RNA extraction from mammalian tissue was undertaken using the Sigma GenElute mammalian total RNA mini-prep kit (RTN-70) following

manufacturers instructions. A total of up to 150μg of total RNA can be extracted from up to 40mg (10^7 cells) of starting material.

2.3 Spectrophotometry

DNA quantity and quality was assessed with spectrophotometry at 260nm and 280nm using the Nanodrop (supplier) spectrophotometer. An optical density (OD) of 1 at 260nm corresponds to approximately 50μg/ml double stranded DNA. Therefore DNA sample concentrations in μg/ml were calculated as "dilution factor x 50 x OD_{260}". DNA quality was assessed by calculation of OD_{260}/OD_{280} ratios with 1.8 being the ratio found in a pure sample of DNA. Contamination with protein decreases the ratio towards 1.4 and RNA contamination increases the ratio towards 2.0.

RNA samples (on wet ice) were assessed for quantity and quality using the Nanodrop spectrophotometer following the same principles as outlined above and also using the Agilent (supplier) system following manufacturers instructions.

2.4 Polymerase Chain Reaction

The polymerase chain reaction (PCR) is an *in vitro* technique used for selective amplification of a specific DNA sequence.

The DNA region of interest is amplified using two complementary oligonucleotide primers which hybridise to the selected region of the template DNA on opposing strands.

A typical PCR reaction consists of 35 cycles, each made up of three steps: (i) denaturation of the DNA template through heating to 94°C, (ii) annealing of the primers to the separated template strands through heating to 55-60°C (varies between primer sets) and (iii) extension of the primers by DNA polymerase at 72°C. The reaction requires addition of the four deoxyribonucleoside triphosphates dATP, dTTP, dGTP, dCTP and thermostable DNA polymerase.

The first cycle produces two new strands of DNA template of variable length, which can then be a target for the second cycle. The third cycle results in the

production of double stranded DNA product which includes the target region. The following cycles produce an exponential doubling of the target sequence which becomes the predominant reaction product. PCR amplification can saturate with the desired target sequence gradually failing to accumulate. Factors affecting when this point occurs include utlisation of the reaction substrates – dNTP's or primers, the stability of DNA polymerases and finally competition for substrates by non-specific products or primer dimers.

Primers for use in PCR were designed using the Primer3 programme designed by the Whitehead institute of Biomedical Research (http://www-genome.wi.mit.edu/cgi-bin/primer/primer3_www.cgi).

Typically a 25µl PCR reaction contains 30-50ng of template DNA, 0.4pmols of each primer, 1 x Mg^{2+} - free PCR buffer (Promega), 1-2mM $MgCl_2$ (Promega). 0.2mM of each dNTP (Amersham) and 1 unit of PIC *Taq* polymerase (Cancer Research UK). PCR reactions were undertaken in 96 well plates (ABgene). DNA samples were aliquoted in to the plate and the PCR master mix then added after vortexing. The plate was sealed with Thermowell sealers (Corning) and immediately run on a Tetrad PCR machine (MJ Research). The PCR reaction programme typically consisted of initial denaturation at 94°C for 5 minutes followed by 35 cycles of 94°C for 1 minute, 55 °C for 1 minute, 72 °C for 1 minute with a final extension at 72 °C for 10 minutes. Various parameters were altered such as Mg^{2+} concentration, annealing temperature, extension time and other additives were altered depending on which conditions suited the selected primer pairs and target DNA size. Primer sequence details and required PCR conditions are listed in Appendix 1.

Resultant PCR products were analysed by agarose gel electrophoresis with ethidium bromide staining.

2.4.1 Purification of PCR products

PCR products were cleaned up prior to sequencing using either of the two methods below.

2.4.1.1 Qiagen clean up

QIAquick PCR purification kit (Qiagen) can be used to purify single or double stranded PCR products ranging from 100bp to 10kb from primers, polymerases and salts. All solutions were supplied by Qiagen and manufacturer's protocol followed.

Briefly, this method utilises a spin column with a membrane whereby the PCR product (DNA) is first bound to the membrane, undergoes two washes whilst bound to the membrane with buffer to remove impurities and finally eluted with either **TE buffer** or dH_2O.

2.4.1.2 ExoSAP-IT®

ExoSAP-IT (USB Corporation, Cleveland, Ohio, USA, product no. 78201) is an alternative method for PCR product purification which utilises the action of recombinant exonuclease I and shrimp alkaline phosphatase (*Pandalus borealis*) in a buffered solution. Manufacturer's instructions were followed.

Briefly, 5µl of PCR product was mixed with 2µl of ExoSAP-IT in a PCR plate (ABgene) and underwent the following programme on a tetrad PCR machine. Heating to 37 °C for 15 minutes followed by heating to 80 °C for 15 minutes, samples were then left at 8°C until used for sequencing reactions. Cleaned up PCR products were then diluted with dH_2O depending on their strength as determined on a 2% agarose gel.

2.5 Agarose Gel Electrophoresis

Agarose gel electrophoresis is a tool which separates DNA molecules by their size. When in solution DNA molecules carry a negative charge and therefore migrate towards the anode of an electrical field. Agarose gel is a 3D matrix which enables DNA to migrate according to its size, larger molecules migrate at a slower rate than smaller ones. Ethidium bromide dye staining is used to visualise DNA. The ethidium bromide intercalates between DNA base pairs and fluoresces when exposed to UV light of 302nm.

Agarose gel electrophoresis was performed using either 1 or 2% agarose depending on the size of the DNA PCR products to be analysed. Either 10g (1%) or 20g (2%) of agarose powder (Invitrogen) was dissolved in **1x TBE** buffer and boiled. The molten agarose was allowed to cool to 60°C at which it was then stored for use. **Ethidium bromide** was added at a final concentration of 0.25μg/ml. Molten agarose was poured in to a gel casting tray (Bio-rad) with well combs in position and left to set. Following removal of the comb the gel was covered with **1x TBE buffer**. For standard PCR products, 10μl of DNA was combined with 2μl of 5 x Orange G Loading Dye (Trevigen) and loaded in to a gel well. 10μl of 1kb ladder (Gibco BRL) – prepared as per manufacturers instructions was added to the outermost well as a guide for the size of the DNA products under analysis. The gel was then connected to a DC power pack (Bio-rad PowerPac 300), and run at 120V for 20 -30 minutes. After removal from the tank the DNA was visualised under UV light at 302nm in a White / 2UV box transilluminator (UV products). Photographs for record keeping were taken with a UV products recording camera.

2.6 Mutation Detection

2.6.1 Single-strand Conformation Polymorphism Analysis

Single strand conformation polymorphism (SSCP) analysis enables detection of mutations in DNA target regions amplified by PCR. This method allows the detection of nucleotide insertions, deletions, substitutions and inversions in DNA fragments ranging from 100-500 base pairs in size.

SSCP analysis has three main steps – amplification of the DNA target region, denaturation of the double-stranded PCR product by heating with a denaturing chemical and finally separation of the resultant single strands by electrophoresis on a non-denaturing gel matrix. The conditions of the non-denaturing gel allows single stranded DNA fragments to form unique secondary structures which are determined by their primary sequence and stabilised by hydrogen-bonding. As the complementary strands of DNA have different primary sequences they form different conformations in the non-denaturing gel. The same single-stranded fragment may adopt more than one

secondary structure. Subsequent mutation detection relies on the different conformations of DNA migrating at differing speeds through the electrophoresis gel than wild-type strands under analysis. The formation of secondary structures is affected by variables such as temperature and ionic strength, each sample is run at two temperatures as certain mutations will only be detected under certain running conditions.

SSCP analysis PCR amplification is undertaken using fluorescently labelled forward and reverse primers (FAM, HEX and less commonly TET). Resultant PCR products were diluted with dH_2O and multiplexed for analysis depending on the product size and the fluorescent labelling of the PCR primers. 4μl aliquots were transferred in to a 96 well optical reaction plate (PE-Applied Biosystems), and 0.5μl of **0.3M sodium hydroxide**, 0.5μl TAMRA-350 size standard (PE-Applied Biosystems), and 10μl formamide (BDH) were added. Samples were then denatured at 95°C for 5 minutes, placed on ice and then run on the ABI3100 sequencer (PE-Applied Biosystems). The ABI3100 sequencer is a high throughput mutation analysis system which runs on a capillary based system rather than a less sensitive gel-based systems. All samples were run at 18 °C and 24 °C on 36cm capillaries containing 5% native polymer (PE-Applied Biosystems), 10% glycerol (BDH) and **1x TBE** running buffer containing 10% glycerol. GENESCAN and GENOTYPER software (PE-Applied Biosystems) were used for sample analysis. Mutant strands were identified, reamplified and sequenced in both forward and reverse orientation (see section 2.1.8 for sequencing analysis method).

2.6.2 Denaturing High Performance Liquid Chromatography using the WAVE platform.

Denaturing High Performance Liquid Chromatography (DHPLC) is a mutation detection tool dependent on temperature sensitive separation of DNA containing mismatched base pairs from a pool of PCR amplified DNA fragments. Mutation detection with DHPLC is reliant on formation and subsequent separation on double-stranded DNA fragments which contain

mismatched base pairs termed heteroduplex DNA. Heteroduplex DNA is generated by denaturing and re-annealing both reference "wild type" DNA and "mutant" sample DNA. These heteroduplex fragments form as a result of complementary pairing between single stranded mutated DNA and single stranded wild type DNA. These strands do not form hydrogen bonds at the mutation site due to mis-pairing therefore giving the "mutant" heteroduplex different melting properties to the "wild type" homoduplexes. The WAVE system separtes heteroduplexes from homoduplexes over pre-selected temperature gradients calculated from the sequence of the DNA fragment amplified by PCR. At a critical temperature (partially denaturing conditions), the mismatched bases in the heteroduplexes begin to separate, while the matched bases in the homoduplex remain intact. Heteroduplexes elute from the HPLC column earlier than homoduplexes. The "mutant" samples – either containing a polymorphism or pathological mutation are detected on the chromatogram by additional "peaks", "shoulders" or by having a different conformation when compared to the "wild type" chromatogram.

DHPLC was performed on the 3500HT WAVE nucleic acid fragment analysis system (Transgenomic, Crewe, UK). Mutation detection is possible for larger amplicons of target DNA than with SSCP analysis (250 to 500+ base pairs). Unlabelled primer sets were designed accordingly using Primer3 software as described previously. To enhance formation of heteroduplexes prior to DHPLC, the PCR products were heated to 94°C and then re-annealed by cooling gradually to a temperature of 50 °C at a rate of 1 °C per minute. DHPLC was then performed at temperatures calculated by Wavemaker (version 4.0) software (Transgenomic) with a 12% acetonitrile gradient over 2.5 minutes. Samples demonstrating abnormalities on the chromatogram were sequenced directly as described later in this chapter.

2.6.3 Lightscanner Analysis

Lightscanner analysis subjects PCR-amplified products to a high-precision denaturation process in the presence of a double-strand DNA binding dye (LCGreen® Plus) on the Idaho Technology LightScanner® Instrument (Herrmann, Durtschi et al. 2006). High-resolution melting analysis of the PCR

products amplified in the presence of LCGreen Plus can identify both Mutation detection analysis using the LightScanner® is most successful when analysing products of 120-220bp with a low GC content, but has been shown to have near 100% sensitivity and specificity when used on products of up to 400 bp in length (Liew, Seipp et al. 2007).

Nucleic acid melting is tracked by monitoring the fluorescence of the mixture across a defined temperature range, generating melting profiles that can be used to identify the presence of sequence variation within the amplicon. PCR reactions were performed in duplicate and with positive and negative sequence controls. The reaction is optimised by testing these sequence controls with varying concentrations of Q® (Qiagen), $MgCl_2$ and different annealing temperatures (as described in PCR methods). 1µl of the LCGreen dye is added to the reaction mix. The total reaction volume of 12.5µl is overlaid with mineral oil which is a necessary step for analysis by the LightScanner. Melting curves are produced which differentiate sequence variants. The advantage of this technique over SSCP is that it is cheaper and has a higher throughput as up to 144 samples (288 PCR products) may be analysed per hour. Another benefit is that following analysis on the LightScanner the PCR products may be processed directly for sequencing.

2.6.4 Loss of Heterozygosity Analysis

Loss of heterozygosity (LOH) analysis is one method by which chromosomal instability can be assessed in tumour samples. Tumour suppressor genes have a negative effect on cell growth and division. If one tumour suppressor gene allele is left intact this is generally enough to control cell growth and division. Tumour growth occurs when both alleles are disrupted either by mutation or epigenetic change. The first genetic change on one allele is usually a small inactivating mutation within the tumour suppressor gene itself. The second genetic change may be a small genetic change, an epigenetic change or allelic loss due to partial or whole chromosomal abnormalities. It is thought that possible mechanisms leading to loss of heterozygosity include non-disjunction of homologues during mitosis, mitotic recombination or *de-novo* interstitial mutations.

For LOH analysis to be undertaken, matched germline (peripheral venous blood) DNA and tumour tissue DNA were genotyped at a set of microsatellite markers lying close to the tumour suppressor gene under investigation. Microsatellite markers are short mono-, di-, tri- or tetra-nucleotides which are frequently polymorphic in the general population. PCR was performed for each of the microsatellite markers using a fluorescently labelled forward primer (FAM, HEX or less commonly TET) and unlabelled reverse primer. The resulting PCR products were run on a semi-automated ABI Prism 377XL DNA sequncer (PE-Applied Biosystems) together with the GENESCAN-350 TAMRA size marker (PE-Applied Biosystems). Results analysis for LOH was performed using the GENESCAN and GENOTYPER software (PE-Applied Biosystems). Heterozygous samples could be analysed for LOH. The area under each allele peak was calculated and the ratio of the peak areas calculated. The LOH value was determined by dividing the allelic ration of normal tissue by the allelic ration of the tumour tissue. LOH values smaller or equal to 0.5, or larger or equal to 2.0 were scored as having allelic loss on the assumption that the tumour contained more than 50% neoplastic starting material as confirmed by histological analysis.

2.6.5 MLPA analysis for whole exon deletion or duplication

Multiplex ligation-dependent probe amplification (MLPA) analysis was undertaken using an MLPA kit designed specifically to screen for whole exon deletions or duplications in the *APC* gene (MRC-Holland, Amsterdam, The Netherlands. Probe kit P043 APC). Manufacturer's instructions were followed. This kit contains a probe mix for each of the 15 coding regions of *APC*. Three probes were also included for the promoter region of the *APC* gene according to Esteller et al (Esteller, Sparks et al. 2000) and Lambertz et al (Lambertz and Ballhausen 1993). As exon 15 has a coding region of more than 8kb, 5 probes are used for this exon. As a control, 13 probes for other human genes located on different chromosomes are included for each experiment. Details of the probe ligation sites for *APC* used in this kit can be found at http://www.mrc-holland.com

Briefly, MLPA is used to detect deletions and duplications in one or more exons of the gene of interest. Deletions of probe recognition sequences are apparent by a 35-50% reduction in the relative peak area of the amplification product of that probe. Mutations and polymorphisms occurring close to the probe ligation site may result in a reduced relative peak area and therefore any apparent exon deletion is always confirmed with further investigation.

MLPA analysis consists of four main steps.

1. DNA denaturation and hybridisation of the SALSA-probes

Between 20-500ng of starting template DNA is required and diluted with **TE buffer** to 5µl. This is heated for 5 minutes at 98°C in a tetrad PCR thermal cycler, then cooled to 25oC. 1.5µl of the SALSA-probe mix is added along with 1.5µl MLPA buffer. Samples were incubated at 95°C for 1 minute and then 60°C for 16 hours.

2. Ligation reaction

Samples were reduced from 60°C to 54°C and 32µl of Ligase-65 mix was added to each sample and mixed with a pipette. Samples were then incubated at 54°C for 15 minutes and then 98°C for 5 minutes.

3. PCR reaction

4µl of 10xSALSA PCR buffer was added to 26µl of dH_2O and 10µl of the MLPA ligation reaction. The samples were placed in a thermal cycler at 60°C and then 10µl of polymerase was added to each sample and the PCR reaction started. PCR cycling conditions were as follows – 35 cycles of 30 seconds at 95°C, 30 seconds at 60°C, 30 seconds at 72°C followed by a final incubation at 72°C for 20 minutes.

Samples were then run on the ABI-3100 genescan (PE-Applied Biosystems) and data analysed with Genotyper® v.2.5 software. The area under each peak for each probe was calculated and compared with that of the control samples. The size and peak areas are imported in to an Excel (Microsoft office) file for further analysis. Non-specific amplification products, primer dimer peaks, and the peaks produced by the MLPA control mix can be removed at this stage.

When only the peak areas of the expected MLPA products remain, all peak areas are normalised by dividing each peak area by the combined peak area of all peaks in that lane. These normalised peak areas are then compared to the

average results obtained on all samples. A deletion of one copy of a probe target sequence will usually result in a reduction of the relative peak size of 35-50%. A gain in copy number for two or three copies / diploid genome usually results in an increase in peak area of 35-50%.

2.7 Fluorescence cycle-sequencing of PCR products

Fluorescence cycle sequencing is an automated method of DNA sequencing which uses double stranded DNA as a template. The original technique developed by Sanger in 1977 (Sanger, Nicklen et al. 1977) is based on the dideoxy procedure. This procedure depends on the ability of DNA polymerase to synthesise complementary copies of single stranded target DNA. Therefore DNA synthesis is undertaken in the presence of one specific primer for the target sequence, the four dNTP's and a low concentration of their dideoxy analogues each of which is labelled with a different fluorophore. The standard sequencing reaction involves 34 cycles of heat denaturation, primer annealing and extension. As dideoxy nucleotides lack the 3'-hydroxyl group necessary for extension, chain termination occurs whenever one of these nucleotides is incorporated. As they are present at low concentration, chain termination occurs at each nucleotide along the target DNA sequence. The resultant strands therefore have a common 5' end defined by the primers but vary in length depending on their base specific 3' ends. The different resultant strands are then separated by PAGE. As the chain terminating events have a specifically attached fluorophore identifier (one for each base) the sequence can be read as the strands pass a fluorescence detector.

PCR products selected for DNA sequencing were first purified – removing unincorporated primers and nucleotides using the QIAquick PCR purification kit (Qiagen) according to manufacturer's instructions. Proteins and oligonucleotides smaller than 100bp's were removed by washing through a silica-gel membrane under different salt conditions. The resultant purified PCR products were then sequenced in the forward and reverse orientation using the same primer as for the original PCR reaction. Each 20μl reaction contained 8μl of Big Dye Terminator Ready Reaction mix (PE-Applied Biosystems), 2μl primer (2μM; forward or reverse), 2μl of purified product

and 8µl of dH_2O. Sequencing cycle conditions for the Tetrad PCR machine (MJ Research) consisted of an initial denaturation at 94°C for 4 minutes, 25 cycles of 94 °C for 30 seconds, 50 °C for 10 seconds and 60 °C for 4 minutes with a final extension step at 60 °C for 7 minutes. The resultant sequencing products were finally purified from excess dye-labelled dideoxy nucleotides using the QIAquick PCR purification Kit with a final elution in 8µl of microSTOP loading buffer (PE-Applied Biosystems). Sequencing samples were then denatured at 94 °C for 4 minutes and run on a 5% polyacrylamide gel on a semi-automated ABI prism 377XL DNA sequencer (PE-Applied Biosystems). Sequence analysis was perfomed using the Semi-adaptive Base Calling option of the Sequencing Analysis Programme Version 2.1 (PE-Applied Biosystems). The NCBI BLAST database was then searched with the resultant sequence to ensure correct origin of the target DNA sequence (http://www.ncbi.nlm.nih.gov/blast). All sequences were also analysed by eye for mutations.

2.8 Cloning of PCR products

Cloning allows the amplification of a single DNA fragment such as a PCR product. The techniques involves ligation of the DNA fragment into an appropriate vector which, following transformation, can be propagated in a suitable bacterial host. Recombinant clones are selected based on vector-encoded genes, grown up to a high density, and the recombinant vector is then purified.

Cloning of PCR products was undertaken using the pGEM®-T Easy vector system (Promega). This system utilises a high copy number vector which carries a gene conferring resistance to the antibiotic ampicillin. The vector is provided ready for ligation, having been prepared by cutting with the restriction endonuclease *Eco*RV. The *Eco*RV restriction site is located with an open reading frame encoding the α–peptide of β-galactosidase (*lacZ'*). When intact, this enzyme can convert the colourless substrate X-gal into a blue product upon induction with IPTG. This vector has a 3' thymidine overhang which allows insertion of PCR products which have a 3' overhang of

adenines. PCR products are ligated to the vector then incubated with competent cells following heat shock at a temperature specific to the vector. Transformation is undertaken and the transformation culture then plated out on to LB/ampicillin/IPTG/X-Gal plates. The culture plates are incubated at 37°C overnight (whilst shaken at 150 rpm). White colonies are then selected (containing successful PCR product inserts) for subsequent sequencing. All solutions were supplied by Promega unless otherwise stated.

1. Ligation:

PCR products were purified and cleaned up using the Qiagen QIAquick kit following manufacturers instructions.

Additional adenine bases were attached to the 3' end of the PCR product by firstly denaturing at 95°C for 20 minutes, 25µl of the denatured product was then incubated with 7µl of 100µM dATP (AR stock check) and 5U of Taq polymerase (CRUK) at 70°C for 15 minutes.

Ligation to the pGEM®-T Easy vector was performed by incubating 2µl of PCR product (with poly-A tail), 1µl pGEM®-T Easy vector, 1µl T4 DNA ligase and 5µl of rapid ligation buffer at 4°C overnight.

2. Transformation:

LB/ampicillin/IPTG/X-Gal plates were set up by adding 400µl of ampicillin (100mg/ml), 2000µl of IPTG (100mM stock AR) and 640µl of X-gal to 400ml of LB agar (at 55°C). 15-20ml of this solution was poured in to bacteriological plates under sterile conditions and left to set for 20 minutes. Plates could then be stored at 4°C prior to use. All of the following steps for transformation were undertaken in sterile conditions.

Transformation of JM109 high efficiency competent cells was undertaken by adding 50µl of the thawed competent cells to 2µl of the ligation reaction in a sterile 1.5ml tube (source) on ice, the solution was mixed by gentle flicking of the tube and then left on ice for 20 minutes. A control tube was also prepared containing 0.1ng of uncut plasmid. The cells were heat shocked by placing in a water bath at exactly 42°C for 45-50 seconds. The tube was then immediately placed on ice for 2 minutes. 950µl of SOC at room temperature was added to the tubes and incubated at 37 °C for 1 ½ hours whilst being shaken at 150 rpm. 100µl of each transformation culture was plated in

duplicate on to the pre-prepared LB/ampicillin/IPTG/X-gal plates and incubated overnight at 37 °C. White cultures (indicative of successful ligation and transformation) were then picked for further analysis and sequencing.

2.9 Cell Culture

2.9.1 Sterile Lymphocyte Separations

Sterile lymphocyte separations were performed in order to establish permanent cell lines containing germ line DNA from patients and controls under investigation. Cell lines were established through immortilisation of lymphocytes with Epstein-Barr virus (CRUK cell services). All of the steps for lymphocyte separation and cell line production were undertaken in sterile conditions.

25ml of peripheral venous blood was collected via venesection into a Falcon tube containing 25ml of sodium citrate medium. The 50ml of blood and sodium citrate medium were poured in to a 250ml flask, the tube was then rinsed with 4ml of RPMI medium (CRUK) at room temperature. Defibrination of the whole blood was performed by adding approximately 25 glass beads (BDH) and 600µl of **1M $CaCl_2$** (BDH) to the flask which was then placed on a gyratory shaker (source) at 250rpm for 15 minutes at room temperature. 20ml of RPMI was then added to the flask and the sample split between two falcon tubes each containing 15ml of lymphoprep (Robbins scientific). Each sample was layered carefully over the lymphoprep solution with a pipette. The tubes were then spun at 1800rpm for 20 minutes in a centrifuge with a swing out rotor (with the brake off) which allowed the defibrinated sample to be passed thorough the lymphoprep solution forming a gradient with different cellular components being present in each layer. The interface containing the lymphocytes was aspirated off using a pipette, transferred to a new 50ml falcon tube and centrifuged at 2300rom for 10 minutes. The lymphocyte cell pellets were re-suspended in 2ml of **freeze mix (90% foetal calf serum / 10% DMSO)**, divided equally between 2 cryotubes (Corning) and placed immediately at -80°C overnight. The samples were then placed in liquid nitrogen until ready for transformation.

2.9.2 Feeding Cell Lines

Once the lymphocytes had been successfully transformed and a growing culture established they would require regular feeding or spinning down for DNA or RNA extraction (as described previously). Lymphoblastoid cells lines were cultured in **RPMI/10%FCS** (CRUK) medium which is used for cells in suspension. Colon cancer cell lines (eg HCT116) were cultured in **E4/10%FCS** meduim (CRUK) which is used for adherent cells.
Cells in culture were examined daily under a microscope to determine viability and density. If cells were being deliberately left to be cultured they would be "split" when they became confluent, 50% of the cultured medium was removed under sterile conditions and replaced with fresh culture medium. Culture flasks (Falcon) were incubated at 37°C in 10% CO_2. Cells were then either left for further culture or spun down for their required protocol.

2.9.3 Freezing down and re-suspending cells to replace stocks

To ensure a permanent cell line resource an aliquot of the growing cells in culture were frozen down and stored in liquid nitrogen. 50ml of the growing culture was removed in to a falcon tube under sterile conditions and spun at 2000rpm for 5 minutes. The supernatant was removed and the tube in verted to dry. The pellet was re-suspended in 2ml **freeze mix (90% foetal calf serum / 10% DMSO)** and aliquoted in to 2 cryotubes (Corning) for long term storage. Tubes were stored at -80°C overnight and then in liquid nitrogen.

2.10 Comparative Genomic Hybridisation

Comparative genomic hybridisation (CGH) enables the screening of the whole genome for chromosomal losses and gains in a single experiment. This technique has been used widely to study tumour karyotypes . (Kallioniemi, Kallioniemi et al. 1992). Conventional CGH (resolution 5-10 Mb) has been

super-ceded by microarray CGH (aCGH) with a higher resolution of screening across the genome. I used 1Mb resolution arrays designed by Nigel Carters group at the Wellcome Trust Sanger Centre (Cambridge, UK). These arrays consist of 3125 human Bacterial Artificial Chromosome (BAC) clones, amplified by degenerate oligonucleotide primer PCR (DOP-PCR) and printed in duplicate on to glass slides. In addition 6 BAC clones from *Drosophila melanogaster* were also printed on to the array as a control for background hybridisation.

The BAC clones were selected from the Golden Path at a spacing of approximately 1Mb across the whole genome, excluding the short arms of the acrocentric chromosomes. Clones FISH-mapped to a single location or localised to known oncogenes and tumour suppressors were preferred, but the selection was arbirtrary in the majority of cases (Fiegler, Carr et al. 2003).

1. Array preparation

Array printing was performed by Cordelia Langford at the Wellcome Trust Sanger Centre (Cambridge, UK). Aminolinked PCR products were diluted into 1x printing buffer (250mM sodium phosphate pH 9.0, $1x10^{-6}$ % N-laurylsarcosine) and filtered through 0.22μm filter plates (Millipore), before re-arraying in to 384-well plates. The DNA products were printed on to Codelink™ activated slides (GE Healthcare) using a Microgrid II array spotter (Biorobotics). Printed slides were transferred to a humid chamber at room temperature for 72 hours to drive the covalent attachment of the DNA to the slides. Slides were then immersed in 1% w/v ammonium hydroxide for 5 minutes, 0.1% sodium dodecyl sulphate for 5 minutes and then rinsed in water. The bound DNA was denatured by immersing the slides in water at 95°C for 2 minutes before being rinsed in ice-cold water and finally the slides were dried by centrifugation.

2. DNA labelling and purification

450ng of normal ("reference") and tumour ("test") DNA were labelled with Cy3-dCTP and Cy5-dCTP (Amersham) respectively, using the Bioprime array CGH labelling kit (Invitrogen), according to the manufacturers instructions. Briefly, DNA was diluted to a volume of 21μl nuclease-free water and combined with 20μl random octamer primers in 2.5x buffer (125mM Tris-HCl

(pH 6.8), 12.5mM $MgCl_2$, 25mM π-mercaptoethanol, 750μg/ml random octamers). The sample was incubated at 100°C for 10 minutes and immediately cooled on ice. 5μl of dNTP mix (1.2mM dATP, dGTP and dCTP), 3μl of Cy3- or Cy5-dCTP (1μM) and 1μl of Exo-Klenow fragment (40U/μl) were mixed with the cooled sample. The samples were incubated overnight at 37°C. Reactions were then stopped by the addition of 5μl of 0.5M EDTA.

Labelled DNA was then purified using Microspin G-50 columns (Amersham) according to the manufacturer's protocol. DNA samples were run on a 2% TBE-agarose gel at 120V for 20 minutes to confirm DNA labelling. Successfully labelled samples would produce a low-molecular weight smear (~50-200bp) when viewed under UV light.

3. DNA precipitation and hybridisation

Slides were prepared for hybridisation by first forming a seal around the arrayed area of the slide by applying 2 layers of adhesive PCR film (AB-gene, AB-0558), cut to size with reference to a "dummy" printed slide.

Labelled test and reference DNA samples were combined and precipitated with 135μg Cot1 DNA (Roche) in 0.1 volumes 3M sodium acetate (pH 5.2) and 2.5 volumes of ice-cold ethanol at -80°C for 30 minutes. Concurrently, 10μg of Herring sperm DNA was precipitated with 135μg Cot1DNA. Precipitated DNA was then pelleted by centrifugation at 16,000g for 15 minutes. The resultant pellet was washed with 80% ice-cold ethanol and re-pelleted at 16,000g for 5 minutes. The supernatant was removed and the pellet dried.

The labelled pellet was then re-suspended in 80μl hybridisation buffer (50% deionised formamide, 10% dextran sulphate, 0.1% Tween-20, 2xSSC, 10mM Tris (pH 7.4)) and 8μl yeast tRNA (100μg/μl, Invitrogen). The herring sperm pellet was then re-suspended in 180μl hybridisation buffer. Both samples were heated at 80°C and frequently mixed by vortex until the pellets were re-suspended. The labelled DNA sample was then placed at 37°C for 1 hour to allow the labelled samples to compete with the Cot1 DNA, blocking repetitive sequences. The re-suspended herring sperm DNA mixture was carefully pipetted on to the prepared slide to pre-hybridise for 1 hour at 37°C in a humid

chamber formed of a slide box containing 3mm paper (Whatman) soaked in 40% formamide/2xSSC. Following competition, the labelled DNA sample was applied to the pre-hybridised array via pipette. The humidity chamber was sealed with electrical tape to form a firm seal. The array was then incubated at 37°C on a rocking platform for 48 hours.

4. Microarray CGH slide washing protocol

All steps were performed in the dark to preserve the fluorochromes (Cy3 and Cy5).

Arrays were removed from the humidity chamber and placed in wash buffer 1 (2x SSC/0.1% Tween-20) in a coplin jar at room temperature. The seal was then removed with forceps after approximately 30 seconds. The arrays were then washed in this solution on a rocking platform for 5 minutes. Arrays were then washed again in buffer 1 at 65 °C for 5 minutes. Arrays were then washed in buffer 2 (0.2 x SSC) at room temperature for 5 minutes – 3 washes in buffer 2 were performed with fresh buffer for each wash (1 wash for 2 minutes, 2 washes for 20 minutes). Arrays were then transferred to wash buffer 3 (1xPBS, 0.1% Tween-20), for 5 minutes, then wash buffer 4 (1xPBS) for 5 minutes, and a final brief wash in dH_2O. The arrays were then dried by centrifugation at 500g for 3 minutes in slide boxes lined with bleach-free tissue paper. Slides were then stored in the dark at room temperature until scanning.

5. Microarray CGH slide scanning and data analysis

A Scanarray confocal scanner and software (Perkin Elmer) was used to scan the arrays. Every array was pre-scanned and settings adjusted to ensure even signal detection from both Cy3 and Cy5 fluorochromes. Detailed scanning was then performed at 10μm resolution and TIFF image files produced for each array for further analysis.

Microarray based experiments produce very large quantities of data for analysis which requires handling in a constant and robust manner in order to be able to compare experimental results between research groups. There are two important factors which need addressing. One is appropriate normalisation of the data – whereby raw ratios are transformed to a defined baseline allowing for experimental artefacts such as uneven hybridisation. The second is accurate selection of significant regions of change for further study.

Fielger et al addressed these issues by braking down microarray data analysis into five steps (Fiegler, Carr et al. 2003).

i) Overlaying of image files and data-point quantification – individual output files for each fluorescent dye channel are overlaid and the intensity of each individual spot calculated.

ii) Data rejection – individual spots are accepted of rejected on the basis of spot quality and the level of "background" hybridisation. Data is then normalised to the number of copies of test genome per copy of reference genome. In the arrays used, this rejection was determined by the presence of 6 *Drosophila melanogaster* clones which are known not to hybridise to human DNA. These were therefore controls for non-specific hybridisation.

iii) Normalisation – Accepted data values are then normalised across the array to give a ratio of the number of test genomes per copy of the reference genome.

iv) Duplicate rejection – variability of data for duplicated BAC clones is compared and if excessively variable the data is rejected.

v) Identification of significant changes – calculated log2 ratios are used to identify regions of altered copy number in the test DNA sample with respect to the test sample.

Spot software (Jain, Tokuyasu et al. 2002) was used for overlaying Cy3 and Cy5 array images. This software calculates intensity values for each spot on the array using a local histogram method. Normalisation was performed using a Microsoft Excel spreadsheet written by Heike Fiegler in Nigel Carter's group (Fiegler, Carr et al. 2003). Duplicate clone spots were then compared to determine that both were giving an identical hybridisation ratio. This was determined by taking the median of the normalised ratios between the test and reference signals – and assessing for any deviation between these and the originals. If a duplicate had greater than 10% variance when compared to the calculated median it was rejected, if not the median was then used to calculate the final log2 ratio for this clone.

Finally, the identification of areas of significant change was undertaken using a file from UCSF Spot (Jain, Tokuyasu et al. 2002) using the statistical package R (Team 2006). In theory, the log2 output for each (duplicated) clone on the array should be representative of the number of copies of the test

genome per copy of the reference genome. Therefore a diploid tumour losing one copy of a particular chromosome would result in a ratio of 0.5 – one copy of test genome per two copies of reference genome. In practice it can be difficult to meet these theoretical thresholds due to experimental artefacts such as contaminating normal DNA in the test (tumour) samples which would dilute the observed change.

The determination of copy number changes was performed using the program DNAcopy(http://www.bioconductor.org/repository/release1.5/package/html/DNAcopy.html), supplemented by a formal paired t-test comparing tumour:normal and normal:normal hybridisations to determine regions of significant copy number change using a threshold of $p<0.001$. Only autosomes were analysed.

2.11 Expression-Microarray Analysis

RNA from lymphoblastoid cell lines was extracted using the trizol method (as described previously) and cleaned up with the Qiagen RNeasy kit following manufacturers instructions. Quality and quantity of extracted RNA was assessed using the Agilent 2100 bioanalyzer.

Purified total RNA (5μg) was labelled and hybridised on to Affymetrix®

U133 Plus 2.0 GeneChip oligonucleotide arrays (Affymetrix, Santa Clara,

CA). The following is a summary of the hybridisation protocol.

Full details can be found at -

https://www.affymetrix.com/support/downloads/manuals/expression_s2_manual.pdf.

U133 Plus 2.0 Expression Micro-array protocol.

All reagents used were supplied by Affymetrix unless otherwise specified.

In summary, first and second round cDNA was made from the extracted purified RNA. cRNA was then made from the cDNA. This was purified and

quantified then 20μg subsequently fragmented prior to hybridisation on to the oligonucleotide arrays.

1. First Strand cDNA synthesis

Poly-A control stock was diluted with poly-A control buffer 1:20, then 1:50, and finally 1:10 in preparation. 2μl of the diluted poly-A control was then added to 2μl of T7-Oligo(dT) Primer, 50 μM, and 8μl sample RNA to a total volume of 12μl. This was incubated at 70°C for 10 mins, then cooled at 4°C for a further 2 mins. A first strand master mix was prepared consisting of 4μl 5x 1st strand reaction mix, 2μl 0.1M DTT and 1μl 10mM dNTP (total 7μl volume). These were mixed together to make up a 19μl volume which was then incubated immediately at 42°C x 2 min. 1μl Superscript II was then added and the mix of 20μl incubated for 1 hour at 42°C, then cooled for at least 2 minutes at 4°C.

2. Second Strand cDNA synthesis

A master mix of 130μl was prepared with: 91μl RNase-free water, 30μl 5x 2nd strand reaction mix, 3μl dNTP 10mM, 1μl *E coli* DNA ligase, 4μl *E coli* DNA polymerase I, 1μl RNase H. This was added to the 20μl from the first strand synthesis and incubated for 2 hours at 16°C. 2μl of T4 DNA polymerase was then added and incubated at 16°C for 5 mins. The reaction was stopped by the addition of 10μl EDTA 0.5M.

3. Cleanup of cDNA

600μl of the cDNA binding buffer was added to the double-stranded cDNA preparation and mixed by vortexing. 500μl of this mixture was pipetted into a cDNA cleanup column sitting in a collection tube then centrifuged for 1 min at ≥8000g. The eluate was discarded and the spin column re-loaded with the remaining mixture, repeating the spin as above. The collection tube was changed and 750μl of cDNA wash buffer was applied and the spin repeated as above. The eluate was discarded and spun once more at maximum speed. The collection tube was changed and 14μl of cDNA elution buffer was applied via pipette, it was then spun for 1 minute at maximum speed.

4. cRNA synthesis

12μl of the eluate was mixed with 10μl RNase-free water, 4μl 10x IVT labelling buffer, 12μl IVT labelling NTP mix and 4μl IVT labelling enzyme to make a final volume of 40μl which was then incubated at 37°C for 16 hours.

5. Cleanup and quantification of cRNA

60µl RNase-free water was added to the IVT reaction and mixed by vortexing. 350µl IVT cRNA binding buffer was added to this and vortexed again. Finally 250µl ethanol (96-100%) was added and mixed with a pipette. This mix was applied to the cRNA cleanup column placed in a collection tube. The column was then centrifuged for 15 seconds at ≥ 8000g. The column membrane was washed with 500µl IVT cRNA wash buffer, then spun for 15 seconds at ≥ 8000g. 500µl 80% ethanol was then added to the column and spun for 15 seconds at ≥ 8000g. The eluate was discarded and the column spun for a further 5 min at maximum speed, then transferred to a new tube. 11µl of RNase-free water was applied to the spin column membrane and centrifuged for 1 min at maximum speed to elute the cRNA. This step was then repeated with a further 10µl RNase-free to maximise the quantity of eluted cRNA. The eluate in was diluted 1:50 with dH_2O to determine the final concentration and then analysed on the ND-3100 Nanodrop.

6. Fragmentation of cRNA

20µg of cRNA (1 to 21µl depending on concentration) was added to 8µl fragmentation buffer (Affymetrix cleanup kit) and made up to 40µl with RNase free water. This was incubated at 94°C for 35 min, then placed on ice. The fragmentation product was then run on a 2% agarose gel at 120V for 30 mins for confirmation of fragmentation.

7. Hybridisation

The following mix was made: 36µl fragmented cRNA, 5µl 3nM control oligonucleotide B2, 15µl 20x eukaryotic hybridisation controls (the 20x eukaryotic hybridisation controls were heated to 65°C for 5 min before aliquoting.), 3µl herring sperm DNA, 3µl BSA (50mg/ml), 150µl 2x hybridisation buffer, 30µl DMSO and H_2O to a total volume of 300µl. This was then heated to 99°C for 5 mins in a heat block. Meanwhile the array was wet by filling it with 1x hybridisation buffer, and incubated at 45°C in the hybridisation oven for 10 min. The hybridisation cocktail was transferred from the 99°C block to a 45°C block and then spun for 5 mins at maximum speed to remove insoluble material. The buffer solution in the array was then exchanged for the hybridisation cocktail and placed back in the hybridisation oven for 16 hours at 45°C.

8. Washing and Staining

SAPE stain solution was made by mixing 600µl 2x stain buffer, 48µl 50mg/ml BSA, 12µl 1mg/ml SAPE and 540µl ddH2O making a final volume of 1200µl. Antibody solution was made by mixing 300µl 2x stain buffer, 24µl 50mg/ml BSA, 6µl 10mg/ml Goat IgG stock (Sigma-Aldrich), 3.6µl 0.5mg/ml biotinylated antibody and 266.4µl dH_2O. The arrays are washed and stained using the automated Affymetrix wash station using the protocol EukGE_w52v5.450.

9. Scanning

This was performed using the Affymetrix GeneChip 3000 scanner. Affymetrix GCOS software (v1.4) was used to obtain DAT image files which were then converted to CEL files containing information about the expression levels of the individual probes.

Unsupervised analysis of microarray data aims to detect groups of samples or outliers without knowledge of the clinical features of each sample. Hierarchical clustering is an unsupervised method for organizing expression data into groups with similar signatures, which is represented by a cluster dendrogram. A 'volcano plot' arranges genes along dimensions of biological and statistical significance. The first axis indicates biological impact of the change; the second indicates the statistical evidence, or reliability of the change.

My data was analysed using the R statistical package (Team 2006) by the Bioinformatics department at CRUK. The standard test statistic used for comparing the two groups was the t-statistic:

$t = (xi,1 - xi,2) / si,$

where xi,1 is the mean value of gene i in group 1, xi,2 is the mean in group 2, and si is the (non-pooled) within-groups standard error (SE) for gene i. Usually the majority of genes are not consistently changed between groups. For the unchanged genes, the values of their t-statistic would follow the t-distribution indexed by n1+n2 – 2 degrees of freedom, in repeated trials, provided there are no outliers in the samples. As a matter of practice, in almost all cases, the values of the t-statistics for all of the unchanged genes in a single experiment also follow a t-distribution. If the researcher expects only a small number of genes are greatly changed, then a convenient way of assessing the

most likely true positives is to plot the t-scores obtained, against the t-distribution. Usually the t-scores of the unchanged genes follow the t-distribution; if the unchanged genes are the overwhelming majority, then this plot will be a straight line at 45°. The t-scores for the few really significant genes are more extreme, and stand out from the straight line, where they can be easily seen.

Cluster dendrograms were produced to demonstrate hierarchical clustering between the sample analysed. Dendrograms graphically present information regarding each individual sample analysed which are then grouped together at various levels of similarity. At the bottom of the dendrogram each observation is considered as having its own cluster and identity. Vertical lines extend up for each observation, and at various similarity values these lines are connected to the lines from other observations with a horizontal line. The observations continue to combine until, at the top of the dendrogram, all observations are grouped together. The height of the vertical lines and the range of the similarity axis give visual clues about the strength of the clustering. Long vertical lines indicate more distinct separation between the groups. Long vertical lines at the top of the dendrogram indicate that the groups represented by those lines are well separated from one another. Shorter lines indicate groups that are not as distinct.

The 'volcano plot' arranges genes along dimensions of biological and statistical significance. The first (horizontal) dimension is the fold change between the two groups (on a log scale, so that up and down regulation appear symmetric), and the second (vertical) axis represents the p-value for a t-test of differences between samples (most conveniently on a negative log scale – so smaller p-values appear higher up). The first axis indicates biological impact of the change; the second indicates the statistical evidence, or reliability of the change.

The data presented in this thesis will include both dendrograms and volcano plots.

2.12 Laser Capture Microdissection

Laser capture microdissection (LCM) is a technique used for isolation of highly pure cell populations from a heterogeneous tissue section, cytological preparation or a live cell culture via direct visualisation of the cells. There are two main classes of laser microdissection, infra-red capture systems and ultraviolet (UV) cutting systems. A UV cutting system on the P.A.L.M. laser capture dissection microscope (P.A.L.M Microlaser Technologies, GmbH, http://www.zeiss.com) (Micke, Ostman et al. 2005). This system allows both UV laser cutting and catapulting of the cut tissue into a collecting cap using a UV laser pulse.

The principle components of LCM are –

1. visualisation of the cells of interest via microscopy
2. transfer of laser energy with photo volatisation of cells surrounding a selected area
3. Removal of cells of interest from the heterogeneous tissue section (with UV laser pulse)

Using LCM, both frozen and fixed tissues can be dissected and recovered cells can be used for DNA, RNA and protein analysis.

Sections were cut from paraffin embedded archival tissue. Six 6μm section were taken from paraffin embedded tissue on to PALM slides (PALM Laser technologies, GmbH, 82347, Germany). The slides have a polymer membrane and were pre-treated with UV light (302 nm) for 30 minutes. Two haematoxylin and eosin (H&E) slides were taken for reference for each sample – one at the beginning and one at the end. Individual crypts from adenomas at their earliest stages were then cut in to caps (PALM Laser technologies, GmbH, 82347, Germany. Ref 1440-0250) for extraction of DNA. In order to obtain suitable amount of DNA for performing mutation detection, six sequential sections of the same crypt were cut in to each individual cap. These samples were digested overnight in proteinase K and buffer (PicoPure DNA Extraction kit (Kit:0103), Molecular Devices Corporation, CA94089-1136, USA). See method for extraction of DNA from LCM dissected crypts for further details.

2.13 Immunohistochemistry

Immunohistochemistry was performed staining for β–catenin and PMS2.

1. Slide preparation

4μm sections from paraffin embedded archival tissue were placed on to glass slides. Slides were then dewaxed in xylene (BDH) for 5 minutes then 100% ethanol (BDH) for 3 minutes, **90% ethanol** for 3 minutes and **70% ethanol** for 3 minutes.

Endogenous peroxidase was blocked by incubating the slides in **3% hydrogen peroxide** (H_2O_2, BDH)/**phosphate buffered saline** (PBS) for 30 minutes.

2. Exposing antigen and applying primary antibody

Citrate buffer was heated to boiling in a pressure cooker and slides were placed in the pressure cooker on full pressure for four minutes. Slides were then allowed to cool in the citrate buffer and rinsed in **phosphate buffered saline** (PBS) (pH 7.45).

The slides were incubated in normal rabbit serum (NGS–1:25, DAKO Ltd.) for 10 minutes to block non-specific binding. 75μl of primary antibody (β-catenin, 1:100 dilution, Transduction Labs, (20μl antibody in 1980μl PBS)) and PMS2 (purified mouse anti-PMS2 monoclonal antibody, BD Pharmingen, 1:40 concentration, (40\mu l in 1000ml PBS)) were added to the slides and incubated for 45 minutes. Positive and negative control slides were included in every run

3. Application of secondary antibody and counterstaining

Slides were rinsed in PBS for 5 minutes and then incubated with secondary antibody (biotinylated rabbit anti-mouse Ig, DAKO Ltd.) for 35 minutes. The slides were incubated for 30 minutes at room temperature, washed in PBS and then incubated with streptavidin-peroxidase conjugate (1:500, P397, DAKO Ltd.) for 35 minutes at room temperature. The peroxidase activity was demonstrated by activated 3,3'-diaminobenzidinetetrahydrochloride solution (DAB) (Sigma D5637) and **0.1% H_2O_2**. Finally slides were dehydrated through a series of ethanol washes of 70%, 90% and 100%, then xylene before being mounted using Pertex mountant (CellPath).

2.14 Mouse husbandry

Animals were bred at Cancer Research United Kingdom Laboratories (South Mimms, UK). Experiments were conducted in full accordance with the United Kingdom Animal Procedures Act 1986. All animals were sacrificed under schedule 1 regulations. Any sick animal was reviewed by the resident Vet at Clare Hall laboroatories and either treated for its condition or sacrificed and post mortem examination undertaken.

The C57BL/6J-*ApcMin*$^{+/-}$ mice were originally a gift from A. R. Moser (McArdle Laboratory, University of Wisconsin, Madison, WI). The 129/C57BL/*6JMyh*$^{+/-}$ mice were a gift from J. Miller (Molecular Biology Institute, University of California, Los Angeles, USA). AKR wild type mice used for backcrossing were obtained from CRUK stocks in the animal unit at Clare Hall laboratories (CRUK).

2.15 Ethical Approval

All samples and clinico-pathological data were obtained with informed consent and local ethical review board approval in accordance with the tenets of the Declaration of Helsinki. All patients were recruited to the CORGI (COloRectal Gene Identification) study, MREC 99/2/14.

2.16 Solutions / Media

Ammonium acetate (saturated)

148g NH_4Ac (BDH), 50ml dH_2O

Ampicillin, 100g/ml

1g ampicillin (Sigma), 10ml dH_2O, stored at -20°C

$CaCl_2$ 1M

14.7g $CaCl_2$ (BDH) in 100ml dH_2O, mixed thoroughly and filtered (0.22μm filter)

Citrate buffer stock pH6.0

210.14g citric acid (BDH) in 1000ml dH_2O, adjusted to pH6.0 using NaOH pellets (BDH)

Citrate buffer solution

20mls citrate stock (pH6.0), 1980mls dH_2O

DAB

5mg DAB (Sigma D5637), 10ml PBS, 20μl H_2O_2

Ethanol

70% - 700ml absolute ethanol (BDH) and 300ml dH_2O
75% - 750ml absolute ethanol (BDH) and 250ml dH_2O
90% - 900ml absolute ethanol (BDH) and 100ml dH_2O
95% - 950ml absolute ethanlol (BDH) and 50ml dH_2O
100% - absolute ethanol (BDH)

Ethylene-diamine-tetra-acetate (EDTA) 0.5M for 1l

Na-EDTA 184.1g, pH 8.0, autoclave

Ethidium bromide (10mg/ml)

0.1g Ethidium bromide (Pierce) dissolved in 10ml dH_2O. Store in dark

Formamide wash solution (2xSSC, 50% formamide)

50ml 20xSSC, 250ml formamide (BDH), made up to 500ml with dH_2O

Freeze Mix (90% FCS/10%DMSO)

9ml foetal calf serum (GibcoBRL) mixed with 1ml dimethyl-sulphoxide (BDH)

Growth medium E4/FCS

180ml E4 cell culture medium (CRUK), 20ml foetal calf serum (GibcoBRL)

Growth medium RPMI/FCS

180ml RPMI cell culture medium (CRUK), 20ml foetal calf serum (GibcoBRL)

Hybridisation buffer (2xSSC, 50% formamide, 10% dextran sulphate)

1ml 20xSSC, 5ml formamide (BDH), 1g dextran sulphate (BDH), made up to 10ml with dH_2O

H_2O_2 0.1%

600ml methanol, 1.8ml H2O2 (30%)

H_2O_2 3%

600ml methanol, 54ml H_2O_2 (30%)

IPTG (0.1M)

1.2g IPTG (Promega), 50ml dH2O, filter-sterilised (0.22μm filter), stored at -20°C

Luria broth (LB)

10g sodium chloride, 5g bacto yeast extract, 10g bacto-trytone, 900ml dH_2O, pH 7.0, autoclaved

LB agar plates

LB medium prepared as above, 15g bacto-agar added prior to autoclaving

NP-40 0.1%

200µl nonidet P40 (BDH), 200ml dH_2O

Nuclei lysis buffer (50ml)

10mM Tris (500µl 1M), 400mM NaCl (4ml 5M), 2mM EDTA (200µl 0.5M (BDH)), 45.3ml dH_2O

Phosphate buffered saline (1x), for 1l

NaCl 8g (137mM), KCl 0.25g (2.7mM), Na_2HPO_4 1.43g (10mM PO_4), KH_2PO_4 (0.25g), pH 7.4, autoclave

PBS/5% Tween-20

9.5ml PBS, 500µl Tween-20 (Sigma)

PBS/0.5% Tween-20

9ml PBS, 500µl Tween-20 (Sigma), 500µl BSA (NEB)

Proteinase K buffer (store 4°C)

2mg proteinase K (Merck) in 1ml dH_2O

RNAseA, 10mg/ml

100mg RNAseA (Advanced biotechnologies), 10ml dH_2O, stored at -20°C

SE buffer

75mM NaCl (7.5ml 5M), 25mM EDTA pH 8.0 (2.5ml 0.5M), 1% SDS (50ml 10%) made up to 500ml with dH_2O, filtered 0.22μm filter.

Sodium acetate (3M)

61.52g sodium acetate (BDH), 200ml dH_2O, pH 6.0 made up to 250ml with dH_2O, autoclaved

Sodium chloride (5M)

73.1g NaCl (BDH), made up to 250ml with dH_2O, autoclaved

Sodium chloride (0.9%) pH 1.5

4.5g NaCl, 400ml dH_2O adjusted to pH1.5 with HCl (BDH), made up to 500ml with dH_2O

Sodium dodecyl sulphate (SDS)

10% w/v volume SDS (BDH) in sterile dH_2O

Sodium hydroxide 0.3M

1.2g NaOH pellets (BDH), 100ml dH_2O

SSC buffer (20x) for 1l

NaCl 175.32g (3M), Na-citrate 88.23g (0.3M), pH 7.0, autoclave

Tail lysis buffer

50mM Tris/HCl pH8.0, 100mM EDTA, 100mM NaCl, 1%SDS, store at room temperature

TBE buffer (10x) for 1l

Tris base 108g (0.89M), boric acid 55g (0.89M), Na-EDTA 9.3g (0.02M), pH 8.3, autoclave

TE buffer (1x) for 1l

10 ml 1M Tris (pH 8.0), 2ml 0.5M EDTA (pH 8.0), filter (0.2μm) and UV sterilise for 15 minutes

Tris 1M for 1l

Tris base 121.14g, pH as required using HCl (BDH), autoclave

Tris-HCl 0.5M pH 6.8

78.8g TRIZMA HCl (Sigma), 400ml dH2O, adjusted to pH8.0 with HCl (BDH), made up to 500ml with dH_2O

3 Clinical *MYH* related studies - Determination of clinico-pathological features and potential genotype-phenotype correlations in *MYH*

3.1 Introduction

In this Chapter I set out to review and refine MAP in terms of its clinical and pathological features in order to improve the understanding of MAP pathogenesis, selection of individuals for genetic screening and subsequent clinical management.

The development of the understanding of genotype-phenotype correlation in FAP and AFAP has improved clinical and molecular diagnosis, appropriate surveillance and intervention. For example, in patients with severe phenotype of 1000's of adenomas are more likely to have germline mutations between codons 1250 and 1464 of *APC*. The presence of extracolonic features also guides molecular screening in FAP, with CHRPE being associated with mutations between codons 457 and 1444 and desmoids having an association with mutations between codons 1395 and 2000. In AFAP, patients harbour germline mutations in the 5', 3' regions of *APC* or the alternatively spliced region of exon 9.

See Table 3–1 for an overview of the phenotypes and extracolonic features of FAP, HNPCC and MAP.

	Upper GI polyps	Colonic polyp burden	Skin/mesodermal manifestations	Extracolonic cancers	Average age CRC	Heterozygote allele frequency
FAP	Both gastric and duodenal polyps	Typically 100's - 1000's	Sebaceous cysts, osteomas, CHRPE, desmoids, dental abnormalities	Duodenal cancer hepatoblastoma	40	1:10 000
HNPCC	none	10's	Café-au-lait macules in homozygotes	Endometrium, stomach, brain,ovary, urothelium	50	1:1000
MYH	Both gastric and duodenal polyps	10's - >1000	As yet undetermined	As yet undetermined	50	1:100

Table 3–1 Comparison of phenotype and extracolonic features of FAP, HNPCC and MAP

Historically, microadenomas (a collection of less than 20 dysplastic crypts measuring <1mm) have been associated with adenoma formation in FAP. During colonoscopy, microadenomas can be identified using dye spray with indigo-carmine staining of the colonic epithelium.

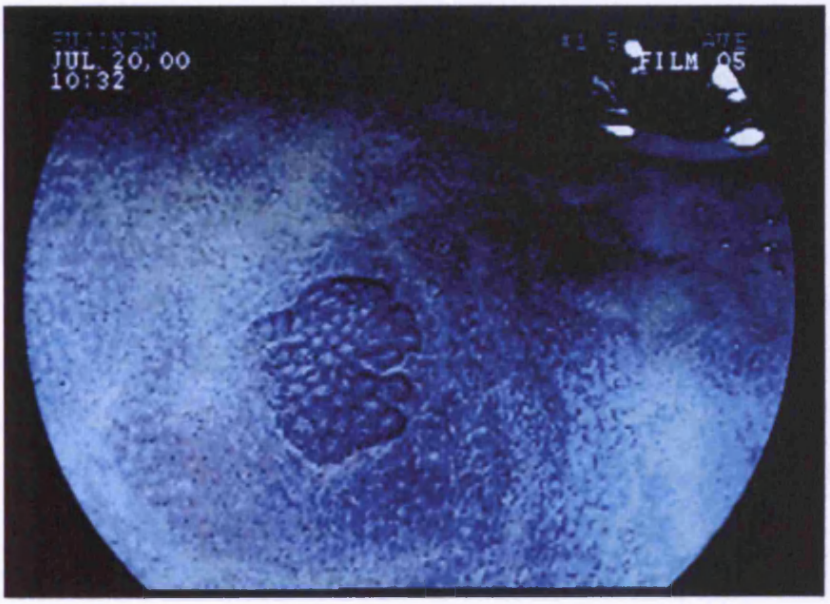

Figure 3–1 Dye spray colonoscopy demonstrating a microadenoma highlighted by the use of indigo-carmine dye spray.

To date, there has been no hard evidence to suggest that microadenomas (see Figure 3–1) are present in MAP. If present it would suggest that two "hits" at *APC* would be required for adenoma formation to be initiated in MAP. It therefore follows that the presence or absence of microadenomas in MAP

would also aid clinical diagnosis at colonoscopy and guide molecular diagnosis.

The identification of potential genotype-phenotype correlations in MAP whether it be for colonic or extra-colonic manifestations would be instructive in the further understanding of the pathogenesis of MAP and potentially lead to clues as the why the GI tract appears to be targeted in *MYH* deficiency.

Furthermore, improved knowledge of any genotype-phenotype correlation and associated ethnic correlation would further improve cost-effective genetic mutation analysis and clinical protocols for management and surveillance of MAP patients.

3.2 Methods

A restrospective study of MAP patients (both homozygous and heterozygous) from St Marks Hospital was undertaken to determine whether any genotype-phenotype correlations exist in MAP. Colonoscopy and histopathology reports were examined and clinical examination of patients was undertaken looking for specific extracolonic features. This cohort includes the largest collection reported to date of individuals with the E466X mutation found in the asian population. The colonoscopy reports of 41 asymptomatic heterozygote carriers were also examined.

All individuals included in this study were recruited through St Mark's Hospital Polyposis Registry or Family Cancer Clinic, London, UK. Every individual had confirmed pathogenic germline mutations in *MYH*. The clinical notes and pathological reports of 41 patients were reviewed and 19 patients were examined specifically for any extra-colonic features including skin lesions, tooth abnormalities, and soft tissue lesions. Thirty-four patients had bi-allelic germline mutations and four had one germline mutation, so called "affected-carriers". These individuals had all exons of *MYH* screened for a second mutation and three had MLPA performed; in all cases these results were negative. See table 1-2 for a summary of bi-allelic germline mutations in the study group.

In addition H&E slides from colectomy samples of 6 patients were examined for evidence of microadenomas.

3.3 Results

Eighty-nine patients were identified with confirmed pathogenic germline mutations in *MYH*. Fifty-one were simple heterozygotes undergoing review and surveillance. Twenty-four patients were homozygous carriers of *MYH* mutations, and 10 were compound *MYH* heterozygotes. Of the homozygous *MYH* carriers, a curiosity was that 6 were also heterozygote carriers for the *APC* missense variant E1317Q. Four patients had a mono-allelic identified germline mutation (1 Y165C, 1 G382D and 2 E466X) and also had 2-593 (median 70) colorectal adenomas and/or colorectal cancer – so-called "affected carriers". The "affected carriers" presented at 44-67 (median 50) years, 3 were female and 1 was male. These individuals presumably have a second occult *MYH* mutation as yet unidentified, despite screening of all exons of *MYH*, and use of MLPA.

Two of these patients developed CRC (1 Dukes A and 1 Dukes B) at 44 and 67 years of age. One of these, (an apparent G382D heterozygote) had a mixture of adenomatous and hyperplastic polyps, concentrated on the right side of the colon. These patients were excluded for the purposes of further analysis, as their genotype information is likely to be incomplete.

Germline mutation	No. patients
E466X/E466X	18
Y165C/G382D	7
Y165C/Y165C	4
G382D/G382D	2
Y165C/1452 del C	2
G382D/1103 del C	1

Table 3–2 Summary of bi-allelic germline *MYH* mutations of the 34 individuals studied

Of the relatives, 7 were affected by CRC, 8 had colorectal adenomas and 1 had pancreatic cancer and colorectal adenomas. All patients with E466X mutation were of Indian origin, while all Y165C and G382D homozygotes were caucasians.

3.3.1 Colonic Disease

Colonic adenoma burden at presentation in E466X homozygotes ranged from 20 to 6250 (median 120). Two were counted at colonoscopy for surveillance and 16 at colectomy the most common procedure being ileo-rectal anastomosis (see Figure 3–2).

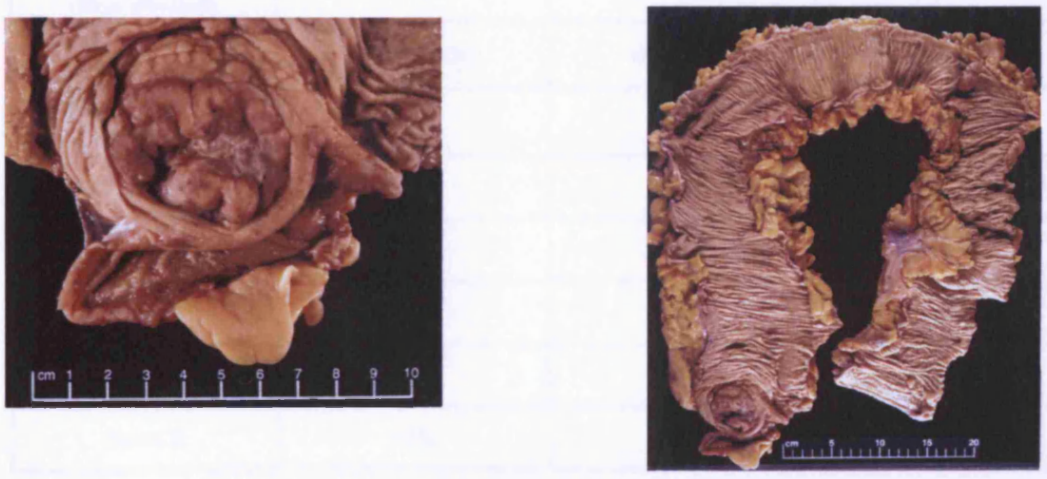

Figure 3–2 Colon of *MYH* E466X homozygous patient (48 years of age)

In caucasian Y165C and G382D homozygotes adenoma burden ranged from 25 to 265 (median 70). In compound heterozygotes adenoma burden ranged from 18 to 300 (median 70). Of the caucasian mutations, 3 were counted at colonoscopy and 13 at colectomy. There was wide variation in adenoma size ranging between 1 and 360mm. There was no statistically significant difference in adenoma size between the asian and caucasian patient groups (p=0.25 for E466X versus all Caucasian mutations, t-test). The majority of adenomas were of tubular or tubulovillous type, although 2 patients also had hyperplastic polyps (1 individual had 1 HPP 4mm and 1individual had 2 HPPs 3 and 5mm). Of the patients that underwent colonoscopic surveillance, microadenomas were present in both groups (using indigo-carmine dye spray

colonoscopy only). The microadenomas identified by indigo-carmine spray were not confirmed histologically as colectomy specimens were not available. No statistically significant difference in polyp burden or CRC incidence or age at presentation was observed on comparison by genotype (p=0.25 for adenoma burden E466X versus Caucasian and p=0.31 for age at diagnosis E466X vs Caucasian, t-test). However, the stage at which CRC presented was statistically significant with a higher number of individuals with bi-allelic E466X mutations presenting with Dukes C and D (36% vs 10% for Dukes C and 18% vs 0% for Dukes D). A summary is shown in Table 3–3.

	E466X homozygotes (n=18)	**Y165C/G382D hom and compound hets (n=16)**	**Mann Whitney *U* test**
Age diagnosis range (median)	30-74 (45)	25-71 (55)	**p=0.03**
Adenoma number range (median)	20-6250 (120)	18-300 (70)	p=0.08
Microadenomas (dye spray)	3/6	7/12	
CRC incidence	61%	62%	
Dukes A	18%	30%	p=0.10
Dukes B	28%	60%	p=0.001
Dukes C	36%	10%	**p=0.001**
Dukes D	18%	0%	**p=0.03**

Table 3–3 Comparison of bi-allelic E466X and Caucasian phenotypes

3.3.2 Upper Gastro-intestinal disease

Seventeen patients underwent upper gastrointestinal endoscopy, all were offered endoscopy but a number of individuals declined. Table 3–4 shows a summary of upper gastrointestinal disease by genotype.

	E466X/E466X hom	Y165C/G382D hom/comp hets
no. patients undergoing upper GI endoscopy	14	11
length of follow up (years)	3.72 (SD 1.48)	4.70 (SD 0.94)
Fundal polyps median (range)	3/14 4 (2-8) all cystic	2/11 4 (2-6) all cystic
Duodenal polyps median (range) size (mm)	3/14 6 (1-20) 1-30 mm	3/11 5 (2-10) 3-10 mm

Table 3–4 Upper gastro-intestinal disease by germline *MYH* mutation

Duodenal polyps were found in 5 of 19 (26%) homozygote patients (3 E466X and 2 Y165C), and 3 of 10 (30%) compound heterozygotes (all Y165C/G382D). Duodenal polyps were generally a few mm in size, but some large polyps were found in E466X homozygotes, up to 3cm. In addition, cystic fundal polyps were found in 5 homozygotes (4 E466X – 3 of which also had duodenal polyps and 1 G382D) and one compound heterozygote (Y165C/G382D – also had duodenal polyps). There were no gastric or duodenal cancers in this patient cohort.

3.3.3 Extra-intestinal Manifestations

Eleven E466X homozygotes and eleven Y165C/G382D homozygotes and compound heterozygotes were retrospectively examined by a clinical nurse specialist (J. Wright, St Marks Hospital) for specific skin, bone, dentitian and soft tissue manifestations. On clinical examination, café-au-lait spots were found in five of 11 patients with homozygous E466X mutations (46%) and one Y165C homozygous mutation carrier. These varied in diameter from 1 – 5cm and were found on the arms, abdomen, neck and trunk. Four individuals had one or two café-au-lait spots with one individual having three. There were no café-au-lait spots in compound heterozygotes. Two E466X homozygotes had sebaceous cysts and two E466X homozygotes and 2 Y165C/G382D compound heterozygotes had abnormal dentition (supernumerary teeth). Extracolonic cancers included sarcoma and melanoma in two E466X

homozygotes. No extracolonic cancer was diagnosed at an age younger or higher frequency than that expected in the general population (see Table 3–5).

	E466X/E466X	Y165C/G382D hom and compound hets
No. patients examined	11	8
Café-au-lait spots	5	1
Sebaceous cysts	1	1
Abnormal teeth	1	3
Extracolonic CRC (age diagnosis)	1 sarcoma (74 years)	1 melanoma (66 years)

Table 3–5 Comparison of extracolonic features and extracolonic cancers between E466X and Y165C/G382D germline *MYH* mutation carriers

3.3.4 Heterozygote carriers under follow up

There were 51 family members of this cohort who were asymptomatic unaffected heterozygotes under follow up. Forty one E466X heterozygotes underwent colonoscopy (as part of screening at St Marks Colorectal Unit), 1 individual had 1 hyperplastic polyp (1mm) at 20 years of age and one had 2 hyperplastic polyps (both 1mm) at 21 years of age. One individual was diagnosed with ulcerative colitis (asymptomatic) as a consequence of the investigation. Eight Y165C heterozygotes were offered colonoscopy, 1 declined, 4 are due when reaching 25 years of age and 3 underwent colonoscopy, all of which were normal. Two G382D heterozygotes underwent colonoscopy, one of which was normal and the other found evidence of ischaemic colitis. All individuals had one colonoscopy only with no further colonoscopic follow up planned.

3.3.5 Microadenoma detection

Microadenomas were present in 3 of 16 sections from colectomy samples examined (by myself and confirmed by a Gastro-intestinal Histopathologist M.Novelli, Dept. Histopathology, University College Hospital) from 6 patients included in this study (1 G382D homozygote and 2 Y165C/G382D compound hets). The number of samples available for study was limited by the low number of individuals undergoing colectomy. In cases where microadenomas were present, they occurred at 0.01 microadenomas per mm^2 of colonic mucosa examined. See Figure 3–3.

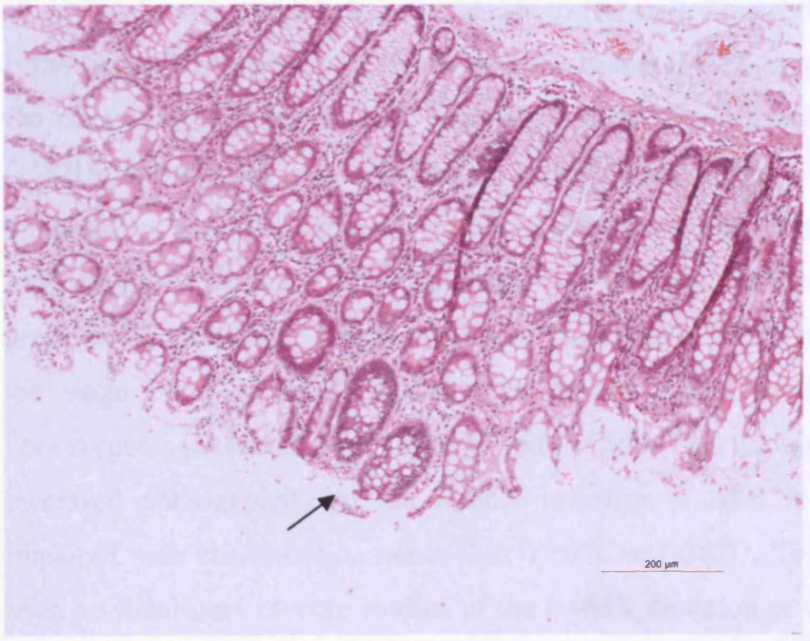

Figure 3–3 Microadenoma in *MYH* E466X homozygote, 2 dysplastic crypts (arrowed)

Microadenomas were detected at colonoscopy using dye spray in ten individuals (3 E466X homozygotes, 3 Y165C or G382D homozygotes and 4 Y165C/G382D compound heterozygotes). None of these were confirmed histologically as tissue was not taken for sampling.

3.4 Discussion

3.4.1 Is there genotype-phenotype correlation in MAP?

As MAP is a relatively recently identified syndrome accounting for approximately 1% of all CRC, it is difficult to draw firm conclusions from studies involving small numbers of individuals. Published cohorts to date include data ranging from 4 to 25 individuals including the Y165C, G382D, 1395delGAA and rarer missense variants G175E, P391L (Sieber, Lipton et al. 2003) (Sampson, Dolwani et al. 2003) (Gismondi, Meta et al. 2004) (Enholm, Hienonen et al. 2003) (Balaguer, Castellvi-Bel et al. 2007) (Croitoru, Cleary et al. 2007) (Kanter-Smoler, Bjork et al. 2006) (Russell, Zhang et al. 2006). This is the first cohort including patients with the Indian E466X mutation.

On comparison of the E466X individuals with the Caucasian Y165C and G382D individuals, no significant genotype-phenotype correlation was observed in terms of adenoma number (apart from one exceptional E466X homozygote who had 6250 adenomas), age of onset, incidence of CRC or presence of extra-colonic manifestations. There was a significant difference in the stage of CRC at presentation in that a higher number of E466X homozygotes presented with Dukes C and D CRC. This finding may be due to increased pathogenicity of the E466X mutation if BER is more severely impaired with this mutation rather than Y165C or G382D. To date there have been no functional in-vitro studies of the E466X mutation to study the ability of repair of 8-oxoG lesions with this germline mutation. Studies of this nature would shed some light as to whether individuals with this mutation may progress more quickly as a result of a higher degree of impaired BER. In-vitro studies of site directed mutageneis in *E.coli* for the Y165C and G382D equivalent mutations (Y82C and G253D) have found and 80 times reduction in the ability to repair 8-oxoG in Y165C and 6 times reduction in G382D (Chmiel, Livingston et al. 2003).

These findings may also be related to cultural differences between the Asian and Caucasian population, three of the E466X homozygous patients presented in overt bowel obstruction secondary to their underlying CRC requiring emergency laparotomy, in comparison none of the Caucasian patients did,

indicating that the Asian patients may present at a later stage than Caucasian patients.

This finding is of importance when considering screening and surgical intervention in these individuals, and certainly justifies bi-annual colonoscopy. Previously, the MAP phenotype has been described and understood as an "attenuated" polyposis described a phenotype developing between 10-100 adenomas. In this study it was found that this is not the case as eight E466X patients developed >100 and <1000 adenomas and one E466X patient had several thousand (6250) adenomas. In the Caucasian group, four patients had >100 and <1000 and none had >1000. A Portuguese case study has recently reported two siblings with homozygous 1103delC *MYH* mutations one with four synchronous adenocarcinomas (and ~30 coloreactal adenomas) and one with severe Spiegelmans III duodenal adenomas. Their heterozygote parents had 5 and 2 colorectal adenomas respectively (De Ferro, Lage et al. 2007). These findings are relevant when considering which polyposis patients to screen for *MYH* when making a molecular diagnosis.

This study supports previous findings that upper gastrointestinal disease is less severe than that found in FAP - but is still present in a significant number of patients to necessitate the need for upper GI surveillance endoscopically. Thirty percent of compound heterozygote patients and 26% of homozygote patients developed duodenal adenomas. Bougen *et al* reported gastric and duodenal adenomas in 1 of 11 *MYH* homozygotes in a recently reported study (Bouguen, Manfredi et al. 2007). No upper gastrointestinal malignancies were found in this patient cohort although they have been reported in MAP (Sampson, Dolwani et al. 2003; Croitoru, Cleary et al. 2007).

When considering extra-colonic manifestations there was an increased (but not significantly) incidence of café-au-lait spots, sebaceous cysts and dental abnormalities in E466X patients. Sebaceous adenomas have been reported in one Italian patient (1395delGAA) and one Indian (Gujarati) individual (E466X) with MAP (Gismondi, Meta et al. 2004; Ajith Kumar, Gold et al. 2007). Café-au-lait spots have also been reported in Turcot's syndrome (associated with homozygous mutations in *PMS2* and *MLH1*) (Bandipalliam 2005).

Barnetson and colleagues screened 225 endometrial cancer patients for germline *MYH* mutations. One individual was found to be a compound heterozygote with Y165C and G382D mutations, along with endometrial cancer she was found to have a sebaceous carcinoma (a feature of Muir-Torre syndrome). Five heterozygote carriers were also identified (3 G382D and 2 Y165C) which is 2.2% of the cohort. This finding is not surprising as the heterozygote carrier rate in the general population is ~ 2% (Barnetson, Devlin et al. 2007).

The extra-intestinal cancers evident in 2 patients in this cohort occurred at an age similar to that found in the general population. It therefore appears that homozygote *MYH* mutation carriers appear to develop extracolonic features associated with other hereditary colorectal cancer syndromes including FAP, HNPCC, and syndromes related to defective DNA repair, Turcot's and Muir-Torre.

It is still not understood why the GI tract is targeted by defective BER associated with germline *MYH* mutations. Theoretically, other tissues with high epithelial turnover or with high exposure to oxidative damage might also be targeted – such as the skin or the lung in smokers. To date no firm associations have been made, although there have been two reports benign lesions (sebaceous adenomas). The most common form of damage to the skin is through UV damage which is repaired by nucleotide excision repair (NER). In one study in individuals with lung cancer, no germline mutations in MYH (Al-Tassan, Eisen et al. 2004). A *Myh/Ogg1* double knockout mouse has been found to have higher levels of 8-oxoG in the liver and the lung (Xie, Yang et al. 2004). However, to date no germline mutations in *OGG1* (or *MTH1*) have been found in individuals with lung cancer or multiple adenomas.

3.4.2 *MYH* and the APC missense variant E1317Q

It was through work on the *APC* missense variant E1317Q that *MYH* was discovered. The association between *APC* E1317Q and the MAP was re-examined in this study. The original family through which *MYH* was discovered are also heterozygous carriers of the *APC* missense variant E1317Q (Al-Tassan, Chmiel et al. 2002). In this study 6 of the homozygote

patients included in the study were also heterozygous carriers for E1317Q. In this group there was no evidence to suggest any significant effect this has on phenotype in terms of either colonic adenoma burden or extra-colonic manifestations. There doesn't appear to be any reason for this association except chance. It is possible that E1317Q might act as a phenotypic modifier of MAP (perhaps by preventing nonsense G:C>T:A mutations at codon 1317), but this was not borne out in the clinico-pathological findings of these 6 patients.

When combining these findings with those of collaborators in the UK, Italy, Australia, Finland and Portugal, of 96 individuals with homozygote germline *MYH* mutations, 9 were found who also harboured the *APC* missense variant E1317Q. Again, examination of the phenotype and extracolonic features found no obvious genotype phenotype correlation or evidence of a modifer effect.

3.4.3 The significance of the heterozygous state

In the 48 asymptomatic heterozygote family members which underwent screening, 3 hyperplastic polyps were found at a relatively young age (20 and 21 years respectively). However, hyperplastic polyps have previously been found in individuals as young as 10 years of age in a study of hyperplastic polyposis (Carvajal-Carmona, Howarth et al. 2007). One asymptomatic individual was diagnosed with ulcerative colitis as a result of this screening. There has been some interest in a potential link between *MYH* deficiency and inflammatory bowel disease as it is likely there would be increased levels of oxidative damage secondary to the underlying inflammatory process. In a small study (of 6 individuals) in our laboratory no *MYH* heterozygotes were identified in screening individuals with ulcerative colitits (unpublished data).

It may be prudent to screen heterozygote carriers "once off", however there is little justification for aggressive colonoscopic screening of heterozygote family members at this time apart from in the research setting.

3.4.4 Microadenomas occur in MAP

Historically, microadenomas have been thought to be pathognomonic of FAP. They are classified as a collection of dysplastic crypts (< 20 crypts less than 1mm in diameter in total). Microadenomas were present in 3 of 16 sections examined (by a Gastointestinal Histopathologist M. Novelli) from six patients included in this study (see figure 1-3). The density of microadenomas was significantly less than those detected in FAP (0.01 per mm^2 of mucosa examined in MAP and 0.22 per mm^2 in FAP). Given that some FAP microadenomas harbour somatic mutations at *APC* (see Chapter 9) it is likely that they are the earliest detectable lesion which has been 'initiated' by 'two hits' at *APC* (germline plus somatic mutation for (A)FAP, or two somatic mutations for MAP).

3.4.5 Current management protocols for MAP – how this study may help to improve screening criteria

Since its discovery in 2002, screening for the common *MYH* mutations is possible in NHS molecular diagnostic laboratories. *MYH* screening should be considered in patients with MCRAs – not just those with an "attenuated" phenotype, and/or early-onset CRC (Wang, Baudhuin et al. 2004), although *APC* remains a much stronger candidate in families with vertical transmission of disease. Mutation testing should be tailored to the ethnic group, with mutations Y165C and G382D more common in Caucasians, Y90X in Pakistanis, E466X in Indians and nt1395delGGA in those of southern Mediterranean origin (Gismondi, Meta et al. 2004) (Enholm, Hienonen et al. 2003) (Jones, Emmerson et al. 2002) (Halford, Rowan et al. 2003). MLPA is now available for *MYH*, and it would therefore be appropriate to perform this in "affected heterozygous" patients in whom only one germline mutation has been found. Abnormal methylation in the germline of *MLH1* is responsible for one genotype causing for HNPCC (Suter, Martin et al. 2004). To date germline methylation studies have not been undertaken in *MYH*. This might account for the "affected heterozygotes" identified in this study.

When screening a new index case, the initial germline *MYH* screening should be directed towards the common mutations depending on the ethnicity of the individual. If only one mutation is found the whole gene should then be screened prior to MLPA analysis. Due to the recessive inheritance in MAP, screening of the index case's spouse for common mutations (ethnicity specific) should be undertaken to define the risk conferred and guide appropriate further testing and surveillance of their offspring.

The follow up of heterozygotes at this time varies from centre to centre. Current recommendations include a one-off colonoscopy at 50 years in some centres (Oxford) and screening starting at 35 years (St Marks Colorectal Unit) with repeat colonoscopy five yearly thereafter, in others. In certain situations, colonoscopies have been undertaken at the individual heterozygote's request, usually following a diagnosis of MAP-associated CRC in other young family members. The results of my study do not support routine regular colonoscopy in heterozygote carriers.

In the white, northern European population, the incidence of UC is 43.6/100 000 and in the Asian population it is 5.6/100 000 (Baumgart and Carding 2007). Therefore the coincidental finding of ulcerative colitis in one individual and a hyperplastic polyp in another individual was not significantly higher than would be expected in the general population.

At this time, and due to the recessive nature of the disease and hence limited family history, the majority of novel or founder bi-allelic *MYH* mutation carriers are not detected at an early enough age to prevent colectomy.

In light of the finding that the E466X patients in this study presented with a higher Dukes stage of CRC, further studies incorporating larger patient numbers are required to determine whether it is necessary to screen these individuals more regularly than individuals with the Caucasian mutations is necessary.

As the numbers of individuals diagnosed with MAP is increasing, it is vital that collaborative studies continue to develop to facilitate the understanding of the pathogenesis of MAP, in order to identify novel pathogenic and ethnic mutations and subsequently to continue to improve genetic counselling, clinical management and outcome in the future.

4 Clinical *MYH* related studies – Determination of presence and potential underlying mechanisms of genomic instability in MAP

4.1 Introduction

4.1.1 Chromosomal instability (CIN) and colorectal cancer

The mechanism(s) underlying genomic instability in the pathogenesis of MAP are yet to be fully determined. Genomic instability can be defined as an increased intrinsic mutation rate and hypermutation either through chromosomal instability (CIN) or microsatellite instability (MSI) (Lengauer, Kinzler et al. 1998). Historically, CIN has been associated with FAP through mutations in the tumour suppressor gene *APC* and MSI associated with defects in the MMR "housekeeping" genes.

The effects of defective BER in MAP are observed by the presence of G:C>T:A transversions found somatically at *APC* and *K-ras* suggesting an underlying "mutator phenotype" (Lipton, Halford et al. 2003) (van Puijenbroek, Nielsen et al. 2008). However, the genome wide implications of defective BER in MAP and whether it leads to chromosomal instability are not fully understood.

The stage at which CIN occurs during tumorigenesis and indeed how to define CIN in the first instance is a subject of ongoing debate. Some suggest that CIN initiates colorectal tumorigenesis (Nowak, Komarova et al. 2002) whilst others believe that it occurs early in adenoma growth (Alberici, de Pater et al. 2007). Further groups suggest it occurs after the adenoma-carcinoma transition (Hermsen, Postma et al. 2002; Sieber, Heinimann et al. 2002).

APC mutations occur in about 75% of human CRCs, roughly 70% of these cases also demonstrate CIN. There is, therefore a case that *APC* deficiency may be one cause of CIN. Further evidence supporting this has been demonstrated in mouse ES cells homozygous for the Apc^{1638T} mutation. The

Apc-mutant ES cells demonstrated CIN with multiple numerical and structural chromosomal abnormalities (Fodde, Kuipers et al. 2001).

4.1.2 Methods of measuring CIN

CIN can be measured using flow cytometry, fluorescent in-situ hybridisation (FISH), conventional CGH (resolution 5-10Mb), array CGH (resolution 1Mb), SNP-LOH and conventional LOH utilising microsatellite markers.

Variation in the definition of CIN may in part be due to the different experimental techniques used to detect it. Flow cytometry and FISH identify changes at gross whole or part-chromosome level whereas aCGH and LOH analysis provides information at the molecular level.

Array CGH identifies chromosomal or sub-chromosomal copy number changes (gains and deletions) in relation to total genome dosage. Therefore this method can detect aneuploidy but will not detect polyploidy (as this can be copy number neutral). However in previous studies CIN+ cancers demonstrate a higher number of aCGH changes than CIN- cancers as aneuploidy and polyploidy often co-exist.

Array CGH analysis is prone to intra and inter-experimental variation. It is sensitive at detecting small regions of chromosomal losses and gains but is less reliable at detecting polyploidy and aneuploidy. For example, regions of normal copy number in a diploid nucleus (2:2) and tetraploid nucleus (4:4) have a ratio of 1 and a $\log_2$ ratio of 0. In true aneuploidy the situation is harder to interpret, if a tetraploid tumour has a single copy loss (3:4 ratio) the log2 ratio becomes -0.41 (Table 4–1).

Diploid	Tetraploid	Ratio	log_2 ratio
0:2	0:4	0	-∞
-	1:4	0.25	-2
1:2	2:4	0.5	-1
-	3:4	0.75	-0.41
2:2	4:4	1	0
-	5:4	1.25	0.32
3:2	6:4	1.5	0.58
-	7:4	1.75	0.81
4:2	8:4	2	1
10:2	20:4	5	2.32
20:2	40:4	10	3.32

Table 4–1 aCGH fluorescence ratios with corresponding log_2 ratios for diploid and tetraploid tumours

In aCGH analysis thresholds are set in order identify true "signal" (copy number change) from "noise" (region where log_2 deviation from zero is due to experimental variation). The threshold used in this study was a log_2 ratio of ≤ -0.5 or ≥0.5 based on work by Fiegler et al (Fiegler, Carr et al. 2003). This threshold would not however detect tetraploid tumours with nuclear ratios of 3:4 or 5:4, particularly if normal tissue is included in the study sample (Table 4–1).

Each individual clone (replicated on the aCGH slide) generates its own log_2 ratio. Therefore variation in hybridisation can be observed and relative log_2 values of surrounding clones can be incorporated in to the analysis (see methods chapter for further details). In the past some groups have used "moving thresholds" whereby the value of surrounding clones are taken into account for each region of loss and gain (Clark, Edwards et al. 2003) (Clark, Edwards et al. 2002) (Pollack, Sorlie et al. 2002).

LOH analysis utilising microsatellite markers in principle measures the dosage of the maternal allele against the paternal allele at the site of the microsatellite polymorphism, relative to normal. Three situations may occur in which LOH may be detected without a change in copy number (Gaasenbeek, Howarth et al. 2006)-

i) deletion of one chromosomal homologue and regain of the other homologue through duplication, resulting in whole chromosome LOH

ii) LOH extending from a telomere involving whole or part of a chromosome arm – "mitotic recombination"

iii) LOH in an interstitial region as a result of mitotic recombination also termed "mitotic gene conversion"

When using flow cytometry, sporadic and familial colorectal adenomas (including MAP adenomas) are usually near-diploid, especially when small and of low grade (Sieber, Heinimann et al. 2002) (Lipton, Halford et al. 2003). These findings have been criticised on the grounds that this method is not sufficiently sensitive to detect more subtle manifestations of CIN, such as occasional aneusomy (Cardoso, Molenaar et al. 2006). Conventional CGH and more recently aCGH alongside digital SNP PCR (dS-PCR) and aCGH have also been used to demonstrate aneusomies in CRAs (Rowan, Halford et al. 2005; Cardoso, Molenaar et al. 2006).(Alberici, de Pater et al. 2007) (Shih, Zhou et al. 2001).

Conventionally, cancers demonstrating CIN are held to be aneuploid/polyploid with large-scale gains and deletions (Douglas, Fiegler et al. 2004; Rajagopalan and Lengauer 2004). The majority of cancers contain cells with abnormal numbers of chromosomes (commonly between 60-90) which commonly have structural abnormalities very rarely seen in normal cells. These include inversions, translocations, duplications and deletions (Rajagopalan and Lengauer 2004).

In reality the term CIN can also be used to describe small scale changes with gains and deletions of a few Mb, as well as larger scale changes with translocations and gross ploidy changes. The underlying mechanisms leading to these changes differ in that cell cycle check point abnormalities result in gross ploidy changes and translocations where-as smaller scale changes may be due to defective housekeeping genes (such as MMR genes. It is therefore likely that different types of CIN exist with differing underlying pathogenesis (Douglas, Fiegler et al. 2004; Jones, Douglas et al. 2005) (Gaasenbeek, Howarth et al. 2006). CIN could therefore be described as both an initiating element and a consequence of tumorigenesis, some believe that it is an essential event for tumorigenesis to occur (Lengauer, Kinzler et al. 1998).

One theory is that CIN is caused by a two-step process whereby an initial development of a polyploid, (yet euploid) karyotype occurs followed by smaller scale chromosomal gains and losses (Shackney, Smith et al. 1989). Wang et al suggested that specific mutations or gene silencing may cause CIN either directly or indirectly (Wang, Cummins et al. 2004). In this situation a large number of underlying defects may be responsible such as dysfunction of microtubules, centromere or centrosomes, chromosome breakage and telomere erosion.

Specific genes have been identified *in vitro* as causing CIN in CRC. The tumour suppressor gene *APC* (Fodde, Kuipers et al. 2001), G1/S checkpoint regulators *CDC4/FBXW7* (Rajagopalan, Jallepalli et al. 2004), mitotic checkpoint regulators *BUB1/BUBR1* (Cahill, Lengauer et al. 1998) and centrosome dysfunction through mutations in aurora kinases (Zhou, Kuang et al. 1998). *APC* is the only gene in which somatic mutations are consistently found in all CRC karyotypes *in vivo* (Rowan, Halford et al. 2005).

CIN is likely to confer a survival advantage in cancerous cells through acceleration of LOH of tumour suppressor genes and amplification of oncogenes through chromosomal duplication (Rajagopalan and Lengauer 2004). CRCs and adenomas can be classified on the presence of MSI or CIN (Jass, Whitehall et al. 2002). Very rarely are CRCs found to be MSI and CIN+ when using older methods for measuring CIN.

Cancer cells which demonstrate MSI have an intrinsic mutation rate at the nucleotide level 2-3 times higher than observed in normal cells (Boyer, Umar et al. 1995). Using flow cytometry and FISH analysis MSI+ CRCs have been found to be diploid or near-diploid (Lengauer, Kinzler et al. 1997). More recently CIN has been observed in MSI cell lines using SNP-LOH and array CGH (Gaasenbeek, Howarth et al. 2006), the underlying MSI mutator phenotype may in these cases be responsible for the small scale changes observed in this study.

4.1.3 Current understanding of CIN in sporadic colorectal adenomas and CRC's using aCGH

A number of studies have been undertaken using aCGH to study adenomas, CRCs and CRC cell lines (see Table 4–2 for an overview). Loss of chromosome 4q and 18q has been reported by several groups using conventional and aCGH (Douglas, Fiegler et al. 2004) (Jones, Douglas et al. 2005) (Gaasenbeek, Howarth et al. 2006).

When analysed according to the type of genomic instability exhibited - "conventional" CIN (determined by flow cytometry / FISH analysis) or MSI, a greater number of copy number changes were observed in CIN CRC's and cell lines than MSI+ tumours. A higher incidence of amplification of chromosome 20 was also observed (Douglas, Fiegler et al. 2004). The pattern of copy number changes observed was very similar between cell lines and primary cancers.

Jones *et al* studied a set of 23 MSI-/CIN- CRC's finding little evidence of genomic instability. When compared to subsets of MSI+/CIN- and MSI-/CIN+ CRCs the MSI-/CIN- cancers had significantly fewer chromosomal losses and gains than both the MSI+/CIN- and MSI-/CIN+ tumours (Jones, Douglas et al. 2005). A degree of heterogeneity was observed in the MSI-/CIN- CRC's in that two subgroups were identified, those with <6 chromosomal scale changes and those with >10 chromosomal changes resembling the changes observed in MSI-/CIN+ CRC's. No specific changes by clone were identified in the MSI-/CIN- group. However low frequencies of 5q loss, 9p and 19p gain and high frequency of 20p gain were seen (Jones, Douglas et al. 2005).

Sample type	No. samples	Chromosomal losses	Chromosomal gains	Methods	Ref.
CRC both MSI+ and CIN+	37	18q, 4q34-q35	8q, 13, 20	aCGH	Douglas *et al*
CRC cell lines both MSI+ and CIN+	48	18q, 4q34-q35, 6	8q, 13, 20 12p, 15	aCGH	Douglas *et al*
CRC MSI-/CIN-	23	5q (infrequent)	9p, 19p (low freq) 20p (high freq)	aCGH	Jones *et al*
CRC MSI-/CIN+ cell lines	34	18q, 17p (LOH or deletion) Freq LOH genome wide	Freq LOH genome wide	aCGH / SNP-LOH	Gaasenbeek *et al*
CRC MSI+/CIN- cell lines	11	none	none	aCGH / SNP-LOH	Gaasenbeek *et al*

Table 4–2 Overview of aCGH studies in CRC

One of the first studies to incorporate SNP-LOH alongside aCGH in analysis in CRC cell lines found that on examination of 11 MSI+ and 34 MSI- CRC cell lines the array based CGH changes found were not identified by SNP-LOH analysis (as they did not demonstrate reduction-to-homozygosity) (Gaasenbeek, Howarth et al. 2006). Regions of SNP-LOH were also observed without aCGH changes – the majority of cell lines demonstrating whole chromosome LOH of 2 chromosomes, 1-2 terminal regions of LOH (mitotic recombination sites) and 1 interstitial region of LOH. The MSI+ cell lines rarely demonstrated chromosomal gains and deletions or whole chromosome LOH. However, the near-diploid karyotype of this group concealed mitotic recombination frequencies similar to the MSI- group. From this study the relationships between LOH, CIN and copy number change are far from clear and that it is possible to have LOH without copy number change.

Until recently, examination of MAP adenomas and cancers has found these tumours to be near diploid (using flow cytometry) and microsatellite stable (Lipton, Halford et al. 2003). The mutational signature of defective BER is detected in the somatic mutation spectra of *APC* and *K-ras* (Lipton, Halford et al. 2003). It is thought that through hyper-mutation of *APC* that MAP tumourigenesis is driven. *K-ras* mutations are known to occur in adenomas from MAP patients – targeting the mutational hotspot at codon 12 (Lipton,

Halford et al. 2003). In keeping with defective BER all mutations reported to date are G:C>T:A tranversions.

Somatic mutations in *BRAF* have not been observed in these tumours.

Cardoso et al (Cardoso, Molenaar et al. 2006) at the same time as this study was undertaken used array-comparative genomic hybridisation (aCGH) to analyse approximately 0.6mm^2 dissected tissue from adenomas of 5 MAP and 8 FAP patients. Tumour samples were microdissected and subsequently amplified with whole genomic amplification prior to hybridisation. Small copy number changes were observed in both MAP (80%) and FAP (60%) frequently with losses at chromosomes 1p, 17, 19 and 22 with gains on chromosomes 7 and 13. It was concluded from this study that CIN is observed in both of these syndromes. However, some caution should be used when interpreting these results as the process of whole genome amplification is likely to introduce artefactual losses and gains.

4.1.4 Aims of this chapter

The primary objectives of this study were to identify underlying mechanisms of genomic instability in MAP using a variety of experimental approaches to address the following areas -

1: As CIN does not occur in MMR deficient cancers should it occur in BER deficient tumours?

2: To confirm the findings of CIN in MAP tumours described by Cardoso *et al* (undertaken at the same time as my work) without using whole-genome amplification

3: If CIN is present – what are the underlying mechanisms for this?

The results of this study are discussed alongside results obtained from aCGH analysis performed on FAP and sporadic CRAs undertaken by other laboratory members (A Jones and W Chambers).

4.2 Methods

Array CGH was performed on adenomas from 4 MAP patients with confirmed germline MYH mutations (1 Y165C homozygote and 3 E466X homozygotes). Fourteen adenomas and 1 carcinoma were analysed with aCGH, SNP LOH and microsatellite analysis from 4 MAP individuals

Adenomas were snap frozen and analysed against paired blood or morphologically normal tissue. The clinico-pathological features of these tumours are in Table 3. Histological review was undertaken to confirm at least 65% dysplastic tissue was present in each tumour.

DNA extraction, aCGH analysis, LOH analysis (including SNP-LOH) was undertaken as described in the Methods 2.1.10 and 2.1.6.4. Chromosome maps and clone positions (Mb) were taken from the Sanger Centre and UCSC websites (http://www.sanger.ac.uk, http://genome.ucsc.edu). Where copy number changes were found, confirmation of the copy number changes was then undertaken using microsatellite-based LOH analysis on the same DNA extracted from the whole tumours that had been used for the aCGH analysis.

For increased genome-wide resolution and the ability to detect copy-neutral LOH, SNP-LOH analysis was carried out on 3 MAP tumours where sufficient DNA was available for analysis.

For microsatellite LOH analysis, whole tumours were initially analysed. Subsequently, for analysis of potential spatially distributed sub-clones within the tumour, frozen sections of MAP adenomas were cut onto slides and 12 samples of epithelium (each about the size of a white needle tip) were removed with the aid of the dissecting microscope. Whole tumours, each of the twelve dissected samples and paired normal tissue were genotyped at 17 microsatellite markers (D1S201, D1S2729, D1S2749, D1S470, D9S1818, D9S1826, D9S1829, D9S1830, D17S786, D17S1832, D17S1353, D17S1844, D19S886, D19S878, D19S215, D19S565 and D19S591) with standard reaction conditions (see Appendix 1 for primer sequences and conditions).

4.3 Results

4.3.1 Overview of aCGH analysis

Of the 14 MAP adenomas analysed, eleven (78%) had changes; four adenomas had 1-3 changes, six had 6-7 changes and one had 17 changes (median 3 (range 0-17) and IQR 1-7). Sixty-seven changes were observed in total; 11 of these were of a whole chromosome. The MAP CRC analysed identified 2 whole chromosome deletions (chromosomes 1 and 10), and a whole chromosome gain of chromosome 7. Regions of loss were observed on chromosome 8p and 8q and regions of gain observed on regions 5p and 9p. (See Table 4-3 and Figures 4-1 to 4-6 for clinico-pathological features and examples of aCGH changes).

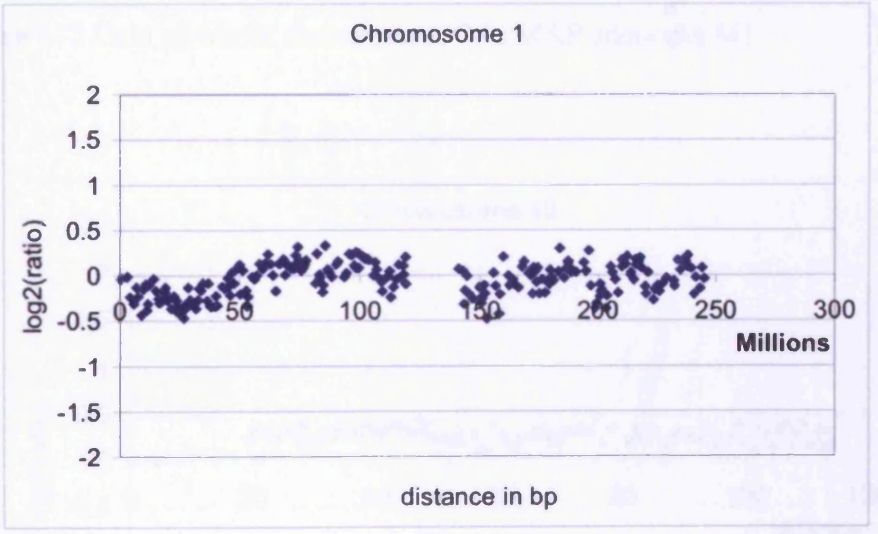

Figure 4–1 Loss of 1p (0-46 Mb) in MAP adenoma M12

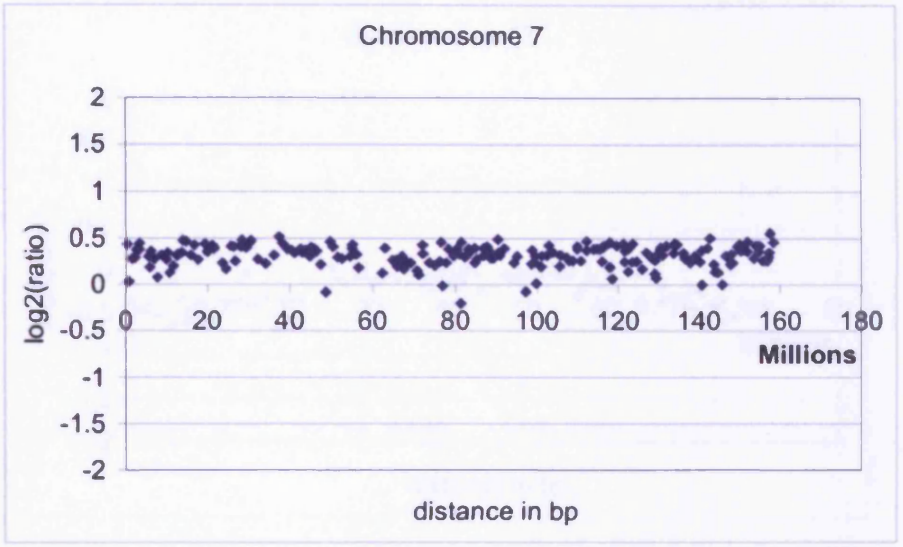

Figure 4–2 Gain of whole chromosome 7 in MAP adenoma M1

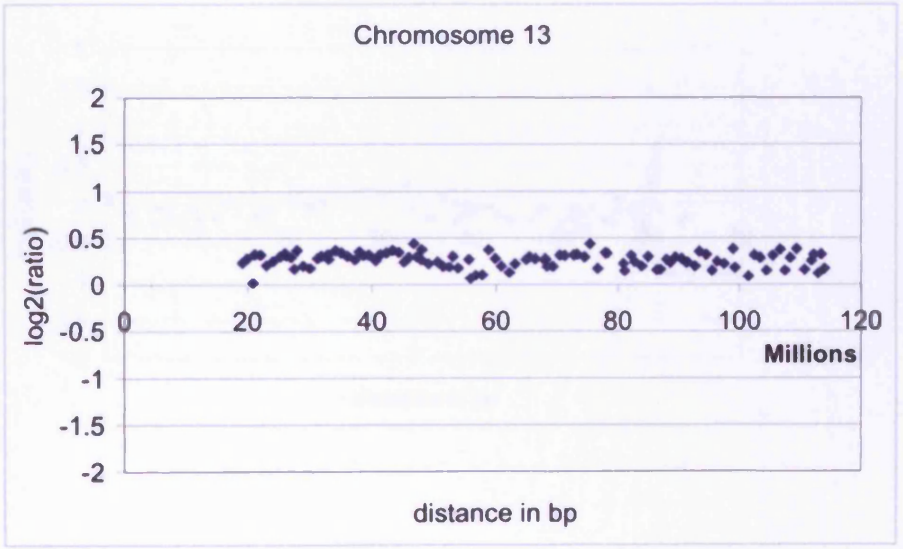

Figure 4–3 Gain of whole of chromosome 13 in MAP adenoma M5

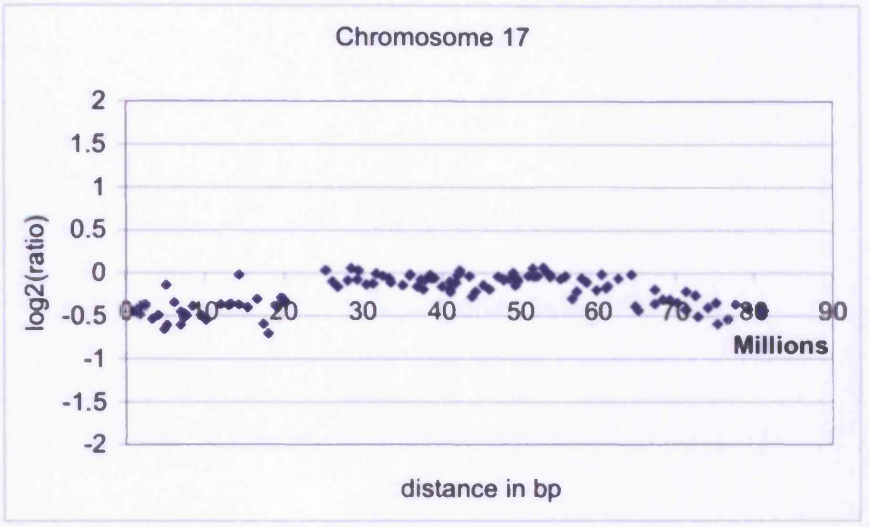

Figure 4–4 Loss of 17p (0-20 Mb) and 17q (65-ter) in MAP adenoma M3

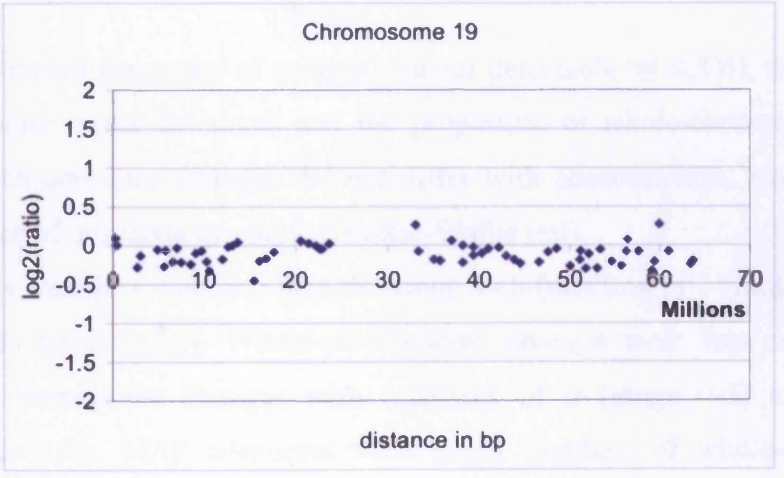

Figure 4–5 Deletion of whole of chromosome 19 in MAP adenoma M3

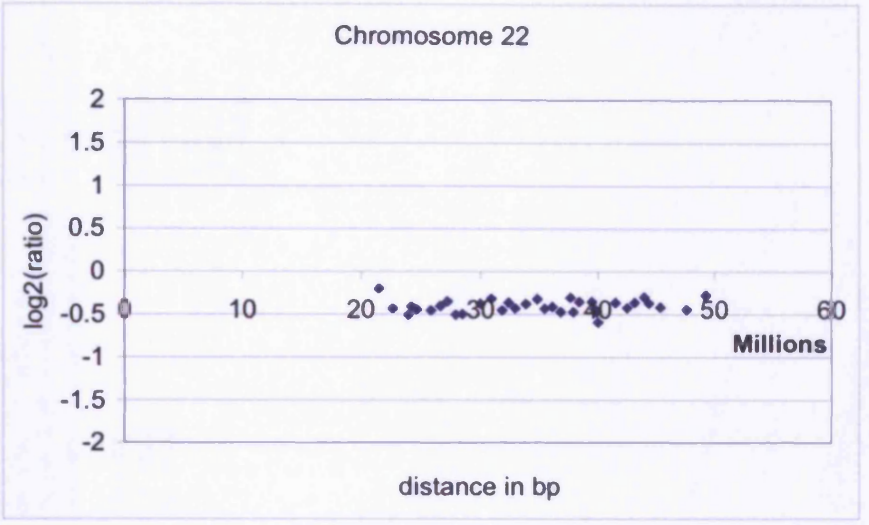

Figure 4–6 Loss of whole chromosome 22 in MAP adenoma M3

The overall frequency of genetic changes detectable by aCGH, the proportion of gains versus deletions, and the proportion of whole-chromosome versus part-chromosome changes did not differ with adenoma size, morphology, or degree of dysplasia (p= 0.25, Kruskal-Wallis test).

Gains were less common than deletions with (medians of 1 (range 0-4) and 3 (0-13) respectively). Whole-chromosome changes were less common than part-chromosome changes with (medians of 0 (range 0-3) and 3 (0-15) respectively. MAP adenomas with larger numbers of whole-chromosome changes tended to have more part-chromosome changes (linear regression analysis, t=2.23, p=0.033), and tumours with higher numbers of gains tended also to have higher numbers of deletions (linear regression analysis, t=3.17, p=0.003). See Figures 4-7 to 4-9 for overview of chromosomal losses and gains for all MAP adenomas studied.

ID	M1	M2	M3	M4	M5	M6	M7	M8	M9
Germline mutation	E466X hom	E466X hom	E466X hom	Y165C hom	Y165C hom	E466X hom	E466X hom	E466X hom	E466X hom
No. adenomas	242	242	242	265	265	242	242	>100	>100
size adenoma	35mm TA	12mm TVA	14mm TVA	8mm TA	9mm TA	29mm TA	33mm TA	6.3mm TA	4.1mm TA
histological grade	mild dysplasia	severe dysplasia	severe dysplasia	mild dysplasia	mild dysplasia	mild dysplasia	mild dysplasia	moderate dysplasia	moderate dysplasia
position in colon	desc colon	rectum	rectum	hep flexure	sigmoid colon	asc colon	desc colon	transverse colon	ascending colon
chromosomal losses and gains	**7,all, gain** 19, all, del 20,all,gain	17,0-10,del 19,all,del	1,27-46,del **8,0-31,del** **17,0-20,del** **17,65-ter,del** **18,all,del** 19,all,del **22,all,del**	1,0-41,del 1,145-162,del 3,49-58,del 4,0-8,del 4,14-ter,gain 6,33-37,del 7,78-127,gain 9,121-ter,del 12,111-ter,del 13,56-96,gain 14,88-ter,del 17,18-50,del 17,71-ter,del 19,all,del 20,29-ter,del 21,13-31,gain 22,all,del	**13,all,gain**	1,0-46,del 9,121-ter,del 13,59-96,gain 17,0-10,del 17,35-46,del 19,0-17,del 19,38-ter,del	1,0-51,del 17,0-12,del 19,0-18,del		1,28-46,del 3,19-36,gain 9,121-ter,del 12,111-ter,del 19,all,del 21,0-29,gain
No. aCGH changes	3	2	7	17	1	7	3	0	6

changes in bold = log2T:N ratio >0.5

Table 4-3 aCGH analysis of 15 MAP tumours

ID	M10	M11	M12	M13	M14	M15
Germline mutation	E466X hom	E466X hom	E466X hom	E466X hom	E466X hom	E466X hom
No. adenomas	>100	>100	242	242	242	>100
size adenoma	6.8mm TA	7.3mm TA	29mm TA	21mm TA	30mm TA	45mm adenocarcinoma
histological grade	mild dysplasia	moderate dysplasia	mild dysplasia	mild dysplasia	mild dysplasia	adenocarcinoma
position in colon	transverse colon	sigmoid colon	ascending colon	transverse colon	descending colon	descending colon
chromosomal losses and gains			1,0-46,del 9,121-ter,del 13,59-96,gain 17,0-10,del 17,35-46,del 19,0-17,del 19,38-ter,del	1,0-46,del 9,121-ter,del 13,59-96,gain 17,0-10,del 17,35-46,del 19,0-17,del 19,38-ter,del	1,0-46,del 9,121-ter,del 13,59-96,gain 17,0-10,del 17,35-46,del 19,0-17,del 19,38-ter,del	1,all,del 5,0-45,gain 7,all,gain 8,0-42,del 8,48-ter,del 9,0-30,gain 10,all,del
No. aCGH changes	0	0	7	7	7	7

changes in bold = log2T:N ratio >0.5

Table 4-3 aCGH analysis of 15 MAP tumours

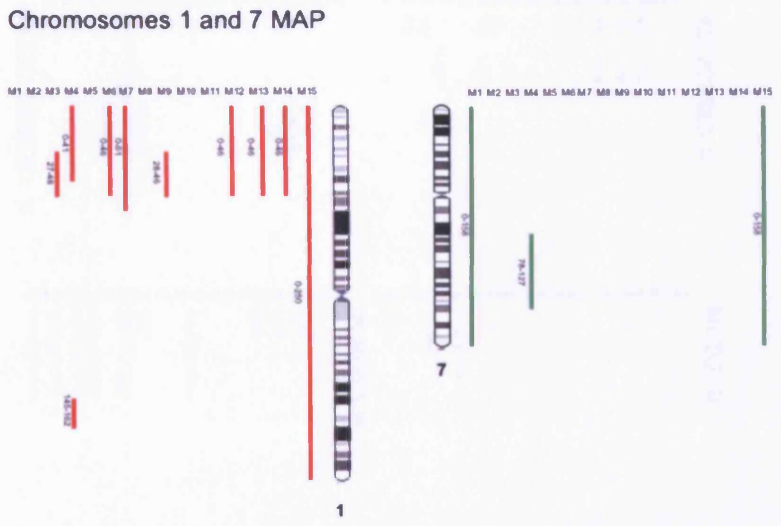

Figure 4–7 Summary of aCGH changes in all MAP adenomas for chromosomes 1 and 7

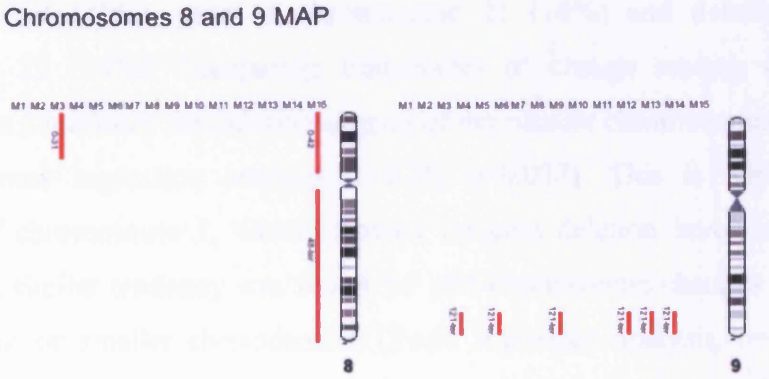

Figure 4–8 Summary of aCGH changes in all MAP adenomas for chromosomes 8 and 9

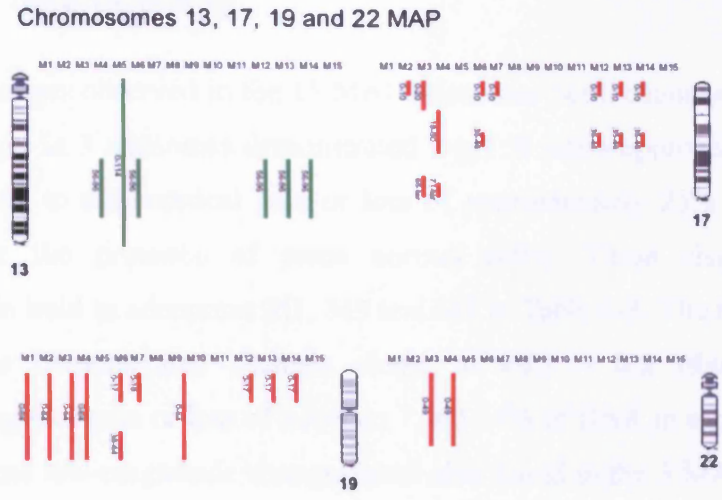

Figure 4–9 Summary of aCGH changes for chromosomes 13, 17, 19 and 22

4.3.2 Genomic locations of aCGH changes

Particularly frequent sites of change were deletion of chromosome 1p (57% of adenomas), gain of chromosome 13 (43%), deletion of 17p (64%), deletion of chromosome 19 (71%), gain of chromosome 21 (14%) and deletion of chromosome 22 (14%). Comparing frequencies of change among whole chromosomes a tendency for deletion or gain of the smaller chromosomes was observed (linear regression analysis, t=2.25, p=0.032). This is with the exception of chromosome 1, which showed frequent deletion involving its short arm. A similar tendency was found for part-chromosome changes to be more frequent on smaller chromosomes (linear regression analysis, t=-3.11, p=0.006). In order to determine if the chromosome 1p losses were artefactual or due to poor hybridisation, dye swap experiments were performed and the 1p loss was still observed. Conventional LOH analysis was also performed on whole tumours using microsatellite markers from 1p (D1S201, D1S2729, D1S2749 and D1S470) but no LOH was observed.

LOH was observed in one MAP adenoma (MAP 9) at marker D1S470 when microdissected.

4.3.3 Magnitude of copy number changes and the possibility of genetic heterogeneity

Of the 67 changes observed in the 11 MAP adenomas (with changes present), only 7 changes in 3 adenomas demonstrated $\log_2$T:N ratios approaching ±0.5 (corresponding to a theoretical gain or loss of approximately 25% of DNA, allowing for the presence of some normal cells). These changes are highlighted in bold in adenomas M1, M3 and M5 in Table 4-3. The remainder of adenomas demonstrated changes closer to ±0.1 – 0.2 (theoretically corresponding to a gain or loss of between 7 and 14% of DNA in each tumour sample). These low-magnitude changes were also found in the 3 MAP polyps which also harboured changes with $\log_2$T:N ratios close to ±0.5. A plausible explanation is that the copy number changes detected were present in tumour sub-clones.

4.3.4 Conventional LOH analysis

No LOH was found on chromosomes 1, 9, 17 and 19 when microsatellite-based LOH analysis, on the same DNA extracted from the whole tumours that had been used for the aCGH analysis. However, when LOH analysis was then undertaken on frozen sections using the same microsatellites in a single adenoma (M9) that had shown small-scale deletions by aCGH, LOH was observed in the region of 1p and 17q. Twelve different regions of tumour epithelium were micro-dissected, no chromosome 9 or 19 LOH was found, but LOH was observed in two of 12 tumour regions using chromosome 1 markers (D1S470) and in a different two regions using chromosome 17 markers (D17S786 adjacent to p53). Neither of these were the regions that showed LOH contiguous within the tumour. See Figure 4–10.

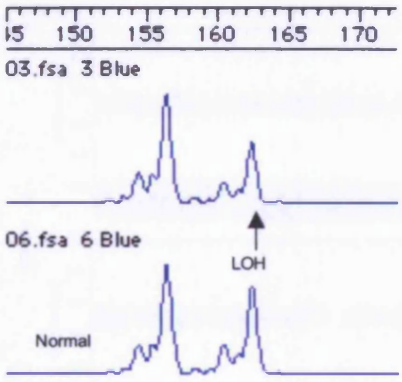

Figure 4–10 LOH at D1S470 in microdissected adenoma MAP 9 (upper tracing), normal tissue (lower tracing)

4.3.5 SNP-LOH analysis

In order to determine whether LOH was present in copy number neutral regions on aCGH analysis SNP-LOH was performed using the Infinium II assay.

Three MAP adenomas (M8, M10 and M11) were analysed for SNP-LOH analysis (this procedure was performed by A. Jones). None of these adenomas had changes on aCGH analysis. One MAP polyp (M10), a tubular adenoma with mild dysplasia measuring 6.8mm without any aCGH changes, showed copy number-neutral LOH involving the whole of chromosomes 7 and 12 (Figure 4–11). Adenomas M8 and M13 displayed no evidence of copy neutral LOH or gross CIN on aCGH.

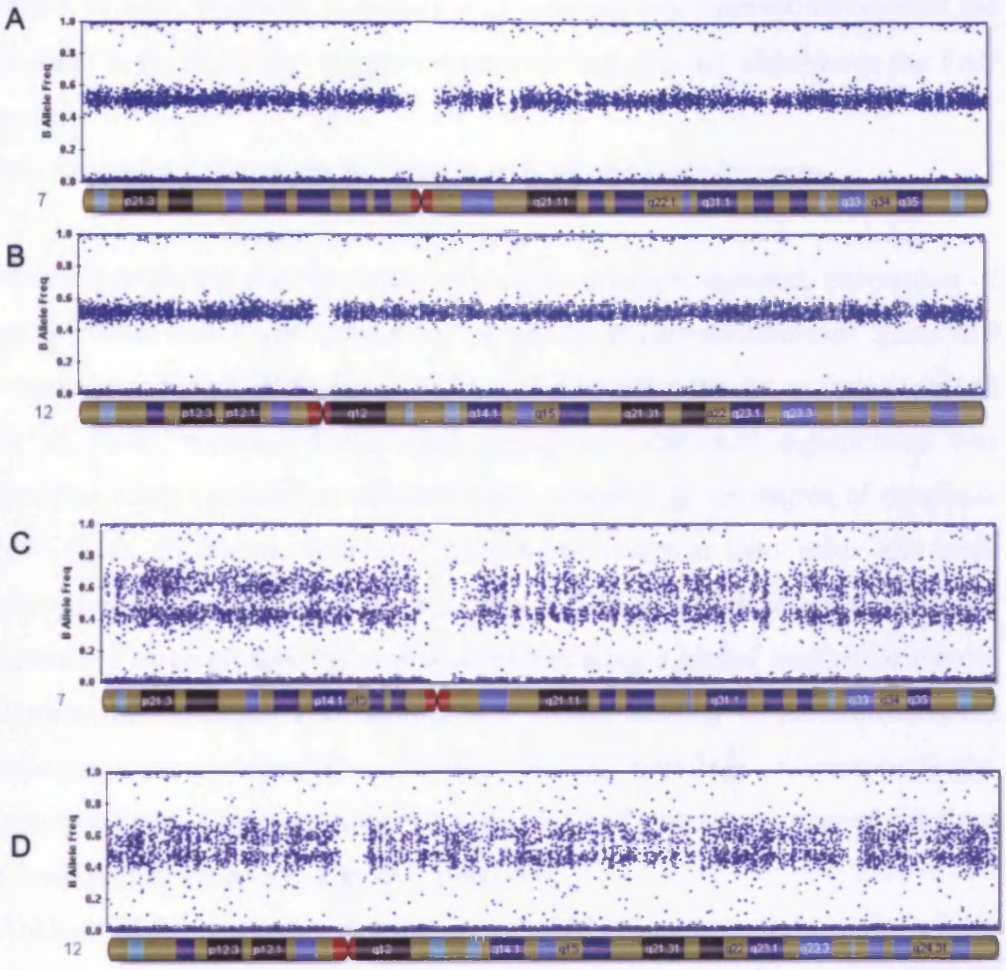

Figure 4–11 SNP-LOH data for MAP adenoma M10. Chromosomes 7 (upper panel **A** and **C**) 12 (lower panel **B** and **D**). **A** and **B** = normal controls, with no LOH. Copy number neutral LOH present in **C** and **D**

4.3.6 Comparison of MAP aCGH changes with FAP and sporadic adenomas

Small-scale aCGH changes were observed in 66% (6/9) of FAP adenomas and 71% (10/14) of sporadic adenomas studied (by A.Jones and W.Chambers). Of the FAP adenomas four had 1-3 changes, one had 7 and one had 9 changes. Of the sporadic adenomas six had 1-3 changes, two had 4 changes, one had 12 changes and one had 13 changes. Only MAP tumours had any $\log_2$T:N changes of ≥0.5 whereas all of the FAP and sporadic changes were in the

region of ≥0.1. A similar distribution of changes was observed throughout the genome in the MAP and sporadic adenomas that was not observed in the FAP group.
See Appendix 2 for details of changes in FAP and sporadic cases.

When considering the frequency of genetic changes detected, proportion of gains versus losses and proportion of whole or part-chromosome gains and losses, no statistical difference was observed between the three groups ($p>0.45$ in all cases, Kruskal-Wallis test). Again, no statistical significance was detected when considering adenoma size, morphology or degree of dysplasia ($p>0.48$ in all cases). Deletions were more common than gains and part-chromosome changes were more common than whole-chromosome changes across the three groups. Adenomas demonstrating a higher number of whole-chromosome changes also harboured a greater number of part-chromosome changes (linear regression analysis $t=2.23$, $p=0.033$). Correspondingly, adenomas with a higher number of gains also had a higher number of deletions (linear regression analysis $t=3.17$, $p=0.003$).
Analysis of the frequency distribution of aCGH changes found that the whole-chromosome changes fitted a Poisson distribution well with a mean of 0.94 ($z=0.34$, $p=0.73$). For part-chromosome changes the dataset failed to fit the Poisson distribution ($z=4.02$, $p<0.001$) even with the exclusion of the two adenomas with the greatest number of changes (Sporadic 8 and MAP 4). When excluding the six adenomas in the dataset which harboured >5 aCGH changes (removing non-random distribution bias) the remaining 28 adenomas fitted the Poisson distribution well ($z=0.76$, $p=0.45$).

4.4 Discussion

4.4.1 Evidence of CIN in MAP

When considering whether CIN is present in this sample set, subtle changes alongside large-scale chromosomal changes (observed in "true" CIN) need to be considered. These include the tendency for individual tumours to harbour specific changes relating to an underlying defect in cell division or DNA

repair, a deviation from the number of changes observed in Poisson or normal distribution and an excess of changes that might be expected in "normal" tissue.

Using these criteria, this data suggest that CIN is present in MAP.

Small amplitude copy number changes both whole and part-chromosome were observed in both whole and part chromosomes in 78% of MAP adenomas suggesting that CIN occurs in MAP. With the exception of one MAP adenoma and one sporadic adenoma the number of aCGH changes followed Poisson distributions for whole and part-chromosome changes. The two "outlying" adenomas (causing deviation from the Poisson distribution) had a large number of part-chromosome changes suggesting a high level of double DNA strand breaks. The higher frequency of part-chromosome changes observed in these adenomas may have been a consequence of them having progressed further along the adenoma-carcinoma sequence. However histologically they did not exhibit any exceptional morphology with the MAP adenoma displaying "mild dysplasia" and the sporadic adenoma "moderate dysplasia".

Only a small subset of the MAP adenomas harboured aCGH changes with $\log_2$T:N ratios of ≥0.5, the ratio was nearer 0.1 for all the FAP and sporadic samples.

A similar distribution of copy number changes throughout the genome was observed between the MAP and sporadic adenomas suggesting a similar underlying cause of genomic instability, this distribution was not seen in the FAP adenomas analysed by aCGH.

Based on their size (0.6-3.5 cm), none of the adenomas studied would be described as "early" lesions, previous studies of similar sized adenomas would almost certainly find them to be diploid using flow cytometry (Sieber, Heinimann et al. 2002) (Sieber, Tomlinson et al. 2005).

It is possible that some of the low-magnitude changes observed in this study were artefacts of the aCGH technique (some studies have reported these in gene- and GC-rich regions such as chromosome 19) (N. Carter, personal communication). It has been previously speculated that aCGH data smoothing algorithms might not be effective at removing regional differences in hybridisation efficiency resulting in systematic over- or under-reporting of Cy3:Cy5 ratios. Loss of chromosome 1p is frequently reported and it has been

suggested that this region is prone to erroneous reporting (N. Carter, personal communication). It is possible that some of the changes in this region in this study are in fact artefactual.

Previous aCGH studies of early CRC tumour samples have found frequent losses at chromosomes 4q and 18q (Hermsen, Postma et al. 2002; Douglas, Fiegler et al. 2004) (Jones, Douglas et al. 2005) (Gaasenbeek, Howarth et al. 2006). In this study loss at 4q was seen in one MAP adenoma and loss of the whole of chromosome 18 in another. In the FAP adenomas no changes were observed at 4q and 1 18q deletion and 1 whole chromosome 18 deletion were seen. The sporadic adenomas demonstrated no 4q changes and one 18q loss in a single adenoma. It is therefore likely that these changes occur later in the pathway of progression from adenoma to carcinoma.

Bartkova et al (Bartkova, Horejsi et al. 2005) have suggested that CIN occurs in CRA's through an elevated rate of chromosomal breakage at fragile sites as a consequence of elevated DNA damage response. Chromosomes 8p23.1/8p21.3, 9q32 and 11p15.1 were cited as fragile sites in their study. None of the changes observed in the three adenoma groups studied were breakages at these fragile sites and therefore do not provide any evidence to support this hypothesis.

The sites of chromosomal loss and gain throughout the genome in the MAP adenomas were similar to those observed by Cardoso *et al* (Cardoso, Molenaar et al. 2006), with the exception that this dataset found no gains of whole-chromosome 7. Cardoso *et al* studied 17 MAP tumours from 5 patients and found aCGH changes in 6 of these. Multiple small regions (approx $0.6mm^2$) were microdissected and analysed with the aim of identifying aneusomic subclones within the tumour. Array CGH changes were found on chromosomes 1p, 7, 13, 17p, 19 and 22. Array CGH changes were also seen in samples from "normal" colorectal mucosa. In this study copy number changes were scored for any smoothed data point lying outside the 15 and 85% quantile bands. This approach may lead to high sensitivity at the cost of specificity. In both this and Cardoso's study a high incidence of changes in chromosome 19 were observed. It is known that chromosome 19 is gene rich and therefore prone to aberrant behaviour in both conventional and aCGH

experiments. Therefore results for this chromosome should be interpreted with caution.

Overall, these results super-cede Cardoso *et al* (Cardoso, Molenaar et al. 2006) as DNA used for this studies did not undergo whole-genome amplification prior to aCGH analysis. The process of whole-genome amplification can introduce artefactual changes would could be interpreted as small-scale chromosomal losses and gains.

4.4.2 Conventional LOH analysis did not replicate aCGH changes

Microsatellite LOH analysis on chromosomes 1, 9, 17 and 19 of whole adenoma samples found no evidence of LOH. This may in part be due the fact the majority of aCGH changes detected were small scale with very small quantitative changes in gene dosage (approx 7% for $\log_2$T:N ratio of ≥0.1).

Therefore it could be suggested that the non-artefactual changes observed are from sub-clones within the tumour rather than the bulk of the tumour tissue. The LOH analysis undertaken on microdissected samples support this theory.

4.4.3 SNP-LOH demonstrates copy number neutral LOH in MAP

Analysis of 3 MAP adenomas with SNP-LOH found evidence of copy number neutral LOH on chromosome 7 and 12 in one MAP adenoma (MAP 10) which harboured no changes on aCGH. This suggests the presence of CIN in the absence of aCGH changes.

The remaining MAP adenomas examined found no evidence of LOH or copy number neutral LOH.

This study would have been improved should there have been sufficient DNA to analyse all of the adenomas by SNP-LOH therefore enabling comparison of SNP-LOH data from adenomas with whole or part-chromosome changes on aCGH.

4.4.4 Evidence of LOH in sub-clones within MAP adenomas

LOH was found in micro-dissected clones from one MAP adenoma (M9) in 2/12 dissected regions on chromosomes 1p and 17q. In the same sample no LOH was detected on analysis of the whole adenoma. These findings also support the finding of 6 small scale changes (5 part-chromosome and 1 whole-chromosome) observed on aCGH analysis of the same sample. The adenoma analysed was relatively small at 4.1mm exhibiting moderate dysplasia.

This data suggest the possibility that sub-clones may develop from hypothetical tumour stem cells leading to faster progression to carcinoma.

4.5 Conclusions

CIN occurs with both small-scale part and whole-chromosomal losses and gains in 78% of MAP adenomas and whole chromosomal losses and gains in a minority of MAP adenomas. Copy number neutral LOH was observed in one of three MAP adenomas analysed by SNP-LOH analysis.

No correlation was identified between the size or grade of dysplasia of the adenoma and the number of chromosomal losses and gains observed with aCGH.

The majority of losses and gains were of a magnitude far below predicted levels for single copy number loss and gain; SNP-LOH and conventional LOH found the majority of these subsequently to be either artefactual or occurring in sub-clones within the adenoma.

The finding of LOH in microdissected sub-clones may represent a faster progression towards carcinoma. It is very difficult to predict however whether these clones would have in fact progressed to carcinoma if left in situ.

5 Development of a mouse model of MAP

5.1 Introduction

In humans, MAP is a rare disorder accounting for ~ 1% of CRC. Development of a mouse model reflecting human disease is desirable in order to study the pathogenesis of MAP from its earliest stages, to study MAP cases in numbers which are statistically high enough and also to consider experimentally controlled environmental factors such as oxidative stress and diet.

Once developed, a mouse model of MAP could be used to determine the impact of therapeutic interventions such as the use of NSAIDs and anti-oxidants both in the prophylactic setting and in the treatment of adenomas. A MAP mouse model would be useful for studying the impact of the $MYH^{+/-}$ carrier state.

Knockout mice for the BER genes *Mth1*, *Ogg1* and *Myh* have previously been generated (Hirano, Tominaga et al. 2003) (Klungland, Rosewell et al. 1999) (Minowa, Arai et al. 2000) (Sakumi, Tominaga et al. 2003). When knocked out, none of these mouse lines developed intestinal adenomas. $Mth1^{-/-}$ deficient mice have a higher incidence of lung liver and stomach cancers compared to $Mth1^{+/+}$ mice (Tsuzuki, Egashira et al. 2001). $Mth1^{-/-}$ deficient mice when crossed with MMR deficient ($Msh2^{+/-}$) mice developed a higher frequency of G:C>T:A transversions on examination of the spleens of these animals(Egashira, Yamauchi et al. 2002). When *Myh* and *Ogg1* are knocked out together, mice develop a higher frequency of lymphoma, lung and ovarian cancers (Russo, De Luca et al. 2004).

Two mouse models of MAP were developed as part of this thesis. The first model was under development (by O.Sieber) as I joined the laboratory and I became involved as the animals were culled for analysis. The second mouse model was developed following initial pathological and mutational findings of the first model; this was solely my work.

The first mouse model of MAP was determined on the basis that as $Myh^{-/-}$ mice do not develop adenomas the majority of MAP adenomas in humans harbour bi-allelic *APC* mutations (Jones, Emmerson et al. 2002) (Lipton,

Halford et al. 2003), by crossing *Myh* deficient mice with $Apc^{Min+/-}$ mice, tumorigenesis would be driven at a higher rate without deviating far from the pathway of $Myh^{-/-}$ driven polyposis. $Apc^{Min+/-}$ mice harbour a germline mutation (truncating C>T) in codon 850 of *Apc*. These mice develop multiple adenomas in the small intestine, mammary tumours, desmoids and epidermoid cysts (Shoemaker, Gould et al. 1997). As homozygosity for the *Min* allele is embryonic lethal, $Apc^{Min+/-}$ mice were used in both models of MAP. Results of the first MAP mouse model have since been published (Sieber, Howarth et al. 2004).

Initial results from the first MAP mouse model (described in detail in this chapter) indicated that despite G:C>T:A transversions being present in three adenomas of *Myh* deficient mice, the majority of "second hits" at *Apc* were through LOH (associated with $Apc^{Min+/-}$ mice bred on the C57BL6 background). Shoemaker *et al* (Shoemaker, Moser et al. 1998) investigated the effect of murine genetic background on tumour multiplicity in $Apc^{Min+/-}$ mice demonstrating a reduction of tumour frequency from 100% (68/68 animals) in C57BL6 $Min^{+/-}$mice to 25% (43/170 animals) in AKR $Min^{+/-}$ mice at 85 and 138 days respectively. Fewer adenomas developed due to a lower incidence of LOH as the "second hit" at *Apc* in AKR $Min^{+/-}$ mice. Luongo *et al* have also demonstrated that the predominant somatic loss of *Apc* function in C57BL6 $Apc^{Min+/-}$ ($Myh^{+/+}$) mice is through LOH (Luongo, Moser et al. 1994).

Haigis *et al* whilst studying mechanisms of tumour regionality in the mouse demonstrated that when AKR $Min^{+/-}$ mice were crossed with *Mlh* knockout mice tumour multiplicity returned on the introduction of defective MMR. The AKR $Min^{+/-}/Mlh^{+/+}$ mice developed a mean of 3.7 +/- 1.6 tumours, AKR $Min^{+/-}/Mlh^{+/-}$ mice developed 4.0 +/- 3.5 tumours and AKR $Min^{+/-}/Mlh^{-/-}$ mice developed 34 +/- 6.4 tumours. The average lifespan was 149, 177 and 95 days respectively (Haigis, Hoff et al. 2004).

AKR mice are homozygous carriers of the resistant allele of Modifier of Min 1 ($Mom1^{R/R}$) locus found on chromosome 4, which is thought to confer resistance to tumour formation (colonic>small intestine) by acting as a modifer. The prime candidate gene for this modifer effect is the secretory phospholipase *Pla2g2a*, although a locus just distal to *D4mit64* has also been identified as a complementary resistance loci for *Mom1* resistance (Cormier,

Bilger et al. 2000). When $Mom1^{R/R}$ was introduced to C57BL6 mice (which are homozygous for the sensitive allele of $Mom1^{S/S}$), tumour multiplicity was reduced by 50% in $Mom1^{S/R}$ mice and by 75% in $Mom1^{R/R}$ mice (Gould, Dietrich et al. 1996). All mice were therefore genotyped for *Mom1* in both MAP mouse models developed in this Chapter.

Therefore on developing the second MAP mouse model it was hypothesised that if $Apc^{Min+/-}/Myh^{-/-}$ were bred on the AKR genetic background fewer of their adenomas would lose the second allele of *Apc* through LOH, consequently it would be expected that a higher proportion of adenomas would demonstrate G:C>T:A transversions somatically at *Apc*. By the introduction of defective BER to AKR $Apc^{Min+/-}$ mice it would be predicted that tumour multiplicity would return in $Apc^{Min+/-}/Myh^{-/-}$ mice bred on the AKR background.

5.1.1 Aims of this Chapter

The aim of this Chapter was to develop a faithful mouse model of MAP in order to study the development of MAP from its earliest stages and in significant numbers.

5.2 Methods

All animals were bred, housed and experiments carried out in accordance with the United Kingdom Animal Procedures Act 1986. Animals were housed at the Cancer Research United Kingdom Laboratories (South Mimms).

5.2.1 Mouse breeding

The original C57BL/6J-*Apc*$^{Min+/-}$ mice were obtained from A.R Moser (McArdle Laboratory, University of Wisconsin, USA). The SV129/C57BL/6J-*Myh*$^{+/-}$ mice were a gift from J. Miller (Molecular Biology Institute, University of California, Los Angeles, USA).

When breeding the first MAP mouse on the C57BL/6J background, male *Apc*$^{Min+/-}$ mice were bred with female *Myh*$^{+/-}$ mice, from the F_1 generation male *Apc*$^{Min+/-}$ /*Myh*$^{+/-}$ mice were inter-crossed with *Apc*$^{+/+}$ /*Myh*$^{+/-}$ females.

The *Apc*$^{Min+/-}$ mutation was carried through the male line when setting up mating pairs and trios. The F_2 generation onwards were used for analysis as these mice would share equivalent contribution from the two genetic backgrounds (C57BL/6J and SV129).

When breeding the second MAP mouse on the AKR genetic background, the C57BL/6J-*Apc*$^{Min+/-}$ and SV129/C57BL/6J-*Myh*$^{+/-}$ were backcrossed ten times on to the AKR genetic background before setting up inter-crosses as described above.

The following study groups were set up for both mouse models of MAP. *Apc*$^{Min+/-}$ /*Myh*$^{+/+}$, *Apc*$^{Min+/-}$ /*Myh*$^{+/-}$ and *Apc*$^{Min+/-}$ /*Myh*$^{-/-}$; the three comparison groups were *Apc*$^{+/+}$ /*Myh*$^{+/+}$, *Apc*$^{+/+}$ /*Myh*$^{+/-}$ and *Apc*$^{+/+}$ /*Myh*$^{-/-}$.

5.2.2 Genotyping

DNA was extracted from tail snips as described in Methods 2.1.1.6. All mice were genotyped for *Apc, Myh* and *Mom1* (AKR resistant allele).

The original *Myh* knockout mouse was developed by Jeffrey Millers group using a targeted vector pMC-neoR (neomycin cassette) in exon 6 of *Myh* as described by Xie *et al* (Xie, Yang et al. 2004). *Myh* was genotyped with a

three primer allele specific PCR assay across exon 6 where neomycin cassette insertion occurs. Primers P1 and P2 amplify wt *Myh* (262 bp product) and primers P1 and P3 amplify mutant *Myh* (376 bp product).

Apc and *Mom1(Pla2g2a)* were genotyped by sequencing directly across the Min mutation at codon 850 of *Apc* and the resistant allele of *Mom1* located on chromosome 4. AKR mice are homozygous for the resistant allele $Mom1^{R/R}$ and C57/BL6 mice are homozygous for the sensitive allele $Mom1^{S/S}$.
All primer sequences and conditions can be found in Appendix 1.

5.2.3 Adenoma, cystic crypt and aberrant crypt focus counts

Mice in the first MAP mouse study were sacrificed between 110 and 130 days by CO_2 asphyxiation for adenoma, cystic crypt and aberrant crypt focus counts.
Four of the second MAP mice bred on the AKR background were sacrificed between 110 and 130 days, but as they had no intestinal phenotype the remainder were left, initially with the intention of analysing them at 18 months. However, the majority of the mice developed lymphoma and necessarily had to be sacrificed prior to this.
The intestinal tract was removed and dissected into four segments – 3 small intestine (proximal, middle and distal) and 1 colonic. Each segment was flushed with PBS and opened longitudinally. Bowel preparations were fixed with Carnoy's medium for 3 hours and stored in 70% ethanol. Tissue was stained with 0.2% methylene blue for 3 minutes and washied in PBS for 20 minutes. Adenomas and cystic crypts were counted on a dissecting microscope at x3 magnification. Cystic crypts in the small intestine and aberrant crypt foci in the colon were counted at x3 and x5 magnification. In the first MAP mouse the preparations were counted by both O.Seiber and myself to confirm accuracy of results.

5.2.4 Histology

Following adenoma, cystic crypt and aberrant crypt foci counts, five of animals from each study group had their small intestine and colon rolled, embedded in paraffin, sectioned at 4μm intervals and stained with haematoxylin and eosin. These sections were examined by a pathologist blinded to the genotype of the mice (G.Stamp) to determine the number of aberrant crypt foci in the colon. Any abnormal tissue identified at post-mortem was also taken for histological analysis (eg mammary tumours and thymic masses).

5.2.5 Molecular analysis of adenomas

Adenomas were dissected from whole-mount preparations using a dissection microscope at x3 magnification. Each adenoma was sized as either <1mm, 1-2mm or >2mm. All samples were placed directly in to corning tubes on dry ice. A separate scalpel was used for each individual adenoma to prevent contamination and care was taken to avoid sampling of the normal surrounding epithelium. Tail tissue and normal bowel epithelium were also sampled. DNA was extracted as described in Methods 2.1.1.6.

LOH analysis at Apc and Myh

Adenomas were analysed for LOH at *Apc* was using fluorescent SSCP analysis distinguishing the wt and Min alleles. LOH at *Myh* was analysed with the same allele specific assay as used for genotyping with the common P1 primer fluorescently labelled. See Methods 2.1.6.4 for LOH analysis and Appendix 1 for primer details and conditions.

Mutation analysis

Exons 5-14 of *Apc*, *Myh* exons 2-15 and *K-ras* exon 1 were screened to determine the mutation frequency and mutational signature in the adenomas dissected. Exon 15 of *Apc* (codons 652 – 1648) was covered by 10 overlapping primer pairs. *Apc* and *Myh* were screened with fluorescent SSCP analysis followed by direct sequencing of samples with aberrant SSCP bands. *K-ras* exon 1 was sequenced directly. See Methods 2.1.6.1 for details of SSCP

analysis, Methods 2.1.7 for details of fluorescent cycling sequencing and Appendix 1 for primer details and conditions.

When somatic mutations were identified, these were confirmed by cloning the PCR product from the tumour sample. See Methods 2.1.8.

5.3 Results

5.3.1 $Apc^{Min+/-}/Myh^{-/-}$ mice bred on C57BL6/SV129 background

In total, 134 small intestine and 6 colonic adenomas were dissected from 12 $Apc^{Min+/-}/Myh^{+/+}$mice , 147 small intestine and 21 colonic adenomas from 16 $Apc^{Min+/-}/Myh^{+/-}$ mice and 167 small intestine and 16 colonic adenomas from 13 $Apc^{Min+/-}/Myh^{-/-}$ mice. Adenoma, cystic crypt and aberrant crypt foci counts were performed in 15 $Apc^{Min+/-}/Myh^{+/+}$, 25 $Apc^{Min+/-}/Myh^{+/-}$ and 15 $Apc^{Min+/-}/Myh^{-/-}$ mice and 15 animals from each of the three control groups $Apc^{+/+}/Myh^{+/+}$, $Apc^{+/+}/Myh^{+/-}$ and $Apc^{+/+}/Myh^{-/-}$. The three study groups had similar male:female ratios 8:7 for $Apc^{Min+/-}/Myh^{+/+}$, 11:14 for $Apc^{Min+/-}/Myh^{+/-}$ and 6:9 for $Apc^{Min+/-}/Myh^{-/-}$.

5.3.1.1 Enhanced adenoma and cystic crypt formation observed in the small intestine of $Apc^{Min+/-}/Myh^{-/-}$ mice

In the small intestine tumour multiplicity was increased by 53% in the $Apc^{Min+/-}/Myh^{-/-}$ mice when compared to $Apc^{Min+/-}/Myh^{+/+}$ mice (p=0.016, Mann Whitney *U* test). A higher number of adenomas developed in the proximal and middle segments of small intestine examined than the distal segment (p=0.01, ANOVA for interaction).

No significant increase in tumour multiplicity was seen in the $Apc^{Min+/-}/Myh^{+/-}$ mice when compared to $Apc^{Min+/-}/Myh^{+/+}$ mice (p=0.83 Mann Whitney *U* test). See Table 5–1.

	$Apc^{Min/+}$ Myh+/+ (n=15)	$Apc^{Min/+}$ Myh-/+ (n=25)	$Apc^{Min/+}$ Myh-/- (n=15)
Adenomas	161 ± 58	164 ± 92	228 ± 84 **(p=0.016)**
Proximal	21 ± 8	25 ± 16	44 ± 21
Middle	62 ± 23	60 ± 34	85 ± 35
Distal	78 ± 33	79 ± 47	99 ± 36
Cystic crypts	20 ± 24	24 ± 32	46 ± 50

Table 5–1 Summary of adenoma and cystic crypt formation in the small intestine mean and SD shown (p=0.016 for no. adenomas $Apc^{Min+/-}$ /$Myh^{+/+}$ versus $Apc^{Min+/-}$ /$Myh^{-/-}$ Mann Whitney *U* test)

When considering adenoma size, no significant difference was seen between the $Apc^{Min+/-}$ /$Myh^{+/-}$ and $Apc^{Min+/-}$ /$Myh^{-/-}$ mice when compared with $Apc^{Min+/-}$ /$Myh^{+/+}$ mice (p=0.10 for $Apc^{Min+/-}$ /$Myh^{+/+}$ versus $Apc^{Min+/-}$ /$Myh^{+/-}$ mice; p=1.0 for $Apc^{Min+/-}$ /$Myh^{+/+}$ versus $Apc^{Min+/-}$ /$Myh^{-/-}$ mice, χ^2 test).

An increased number of cystic crypts was observed in the $Apc^{Min+/-}$ /$Myh^{-/-}$ mice (mean = 46 in $Apc^{Min+/-}$ /$Myh^{-/-}$, 24 in $Apc^{Min+/-}$ /$Myh^{+/-}$ and 20 in $Apc^{Min+/-}$ /$Myh^{+/+}$ mice) however, this was not statistically significant (p=0.17 Mann Whitney *U* test). A sub-population of cystic crypts demonstrated dysplastic features (see Figure 5–1). Animals with a higher adenoma burden also had a higher cystic crypt count (R^2=0.57, p=<0.001, linear regression analysis).

No adenomas or cystic crypts were found in the small intestine of any of the animals in the three control groups ($Apc^{+/+}$ /$Myh^{+/+}$, $Apc^{+/+}$ /$Myh^{+/-}$ and $Apc^{+/+}$ /$Myh^{-/-}$).

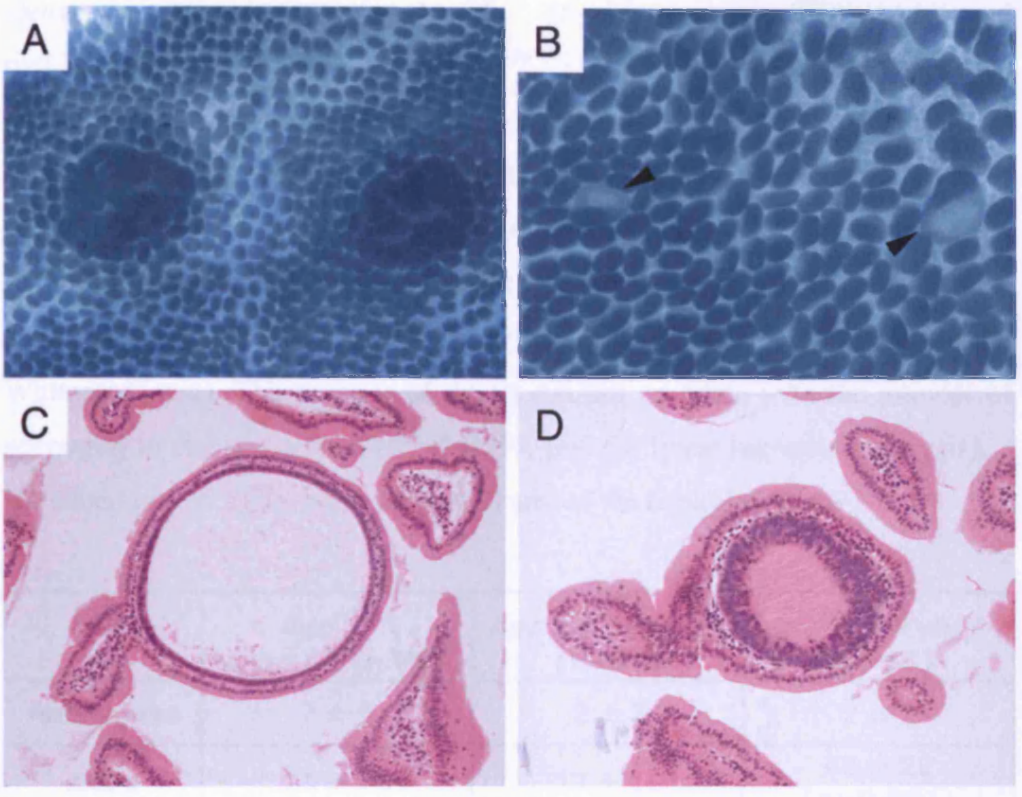

Figure 5–1 Adenomas and cystic crypts in the small intestine of *Myh* deficient mice

The above figure demonstrates adenomas and cystic crypts in the small intestine of $Apc^{Min+/-}$ $/Myh^{-/-}$ mice. Methylene blue stained adenomas and cystic crypts are shown in (**A**) and (**B**), cystic crypts are arrowed. H&E stained transverse sections of small intestine demonstrate cystic crypts with normal pathology (**C**) and dysplasia (**D**).

5.3.1.2 Increased number of aberrant crypt foci observed in the colon of $Apc^{Min+/-}/Myh^{-/-}$ mice

$Apc^{Min+/-}$ $/Myh^{+/+}$, $Apc^{Min+/-}$ $/Myh^{+/-}$ and $Apc^{Min+/-}$ $/Myh^{-/-}$ mice all developed a mean of 2 adenomas in the colon (p=0.18 for $Apc^{Min+/-}$ $/Myh^{+/+}$ versus $Apc^{Min+/-}$ $/Myh^{+/-}$ mice and p=0.16 for $Apc^{Min+/-}$ $/Myh^{+/+}$ versus $Apc^{Min+/-}$ $/Myh^{-/-}$ mice, Mann Whitney *U* test). No significant difference in size of adenoma was observed between study groups with 82% (19/23) $Apc^{Min+/-}$ $/Myh^{+/+}$, 60%

(28/47) $Apc^{Min+/-}$ /$Myh^{+/-}$ and 88% (21/24) $Apc^{Min+/-}$ /$Myh^{-/-}$ of adenomas measuring >2mm (p=0.06 for $Apc^{Min+/-}$ /$Myh^{+/+}$ versus $Apc^{Min+/-}$ /$Myh^{+/-}$ and p=0.7 for $Apc^{Min+/-}$ /$Myh^{+/+}$ versus $Apc^{Min+/-}$ /$Myh^{-/-}$, Fishers Exact test).

Myh deficient mice developed an approximately 2-fold increase in number of aberrant crypt foci (ACF) predominantly in the distal colon. $Apc^{Min+/-}$ /$Myh^{+/+}$, $Apc^{Min+/-}$ /$Myh^{+/-}$ and $Apc^{Min+/-}$ /$Myh^{-/-}$ mice developing a mean number of 23, 17 and 48 ACFs respectively (p=0.001 for $Apc^{Min+/-}$ /$Myh^{+/+}$ versus $Apc^{Min+/-}$ /$Myh^{-/-}$ and p=0.10 for $Apc^{Min+/-}$ /$Myh^{+/+}$ versus $Apc^{Min+/-}$ /$Myh^{+/-}$ Mann Whitney *U* test). The number of ACFs did not correlate with the number of adenomas in any one animal (R^2=0.0054, p=0.61, linear regression analysis). No adenomas of ACFs were present in any of the control groups.

	$Apc^{Min/+}$ *Myh+/+* (n=15)	$Apc^{Min/+}$ *Myh-/+* (n=25)	$Apc^{Min/+}$ *Myh-/-* (n=15)
Adenomas	2 ± 3	2 ± 2	2 ± 1
ACFs	23 ± 13	17 ± 12	48 ± 22 **(p=0.001)**

Table 5–2 Summary of adenoma and aberrant crypt focus counts in *Myh* deficient mice (mean +/- SD, p=0.001 for $Apc^{Min+/-}$ /$Myh^{+/+}$ versus $Apc^{Min+/-}$ Mann Whitney *U* test)

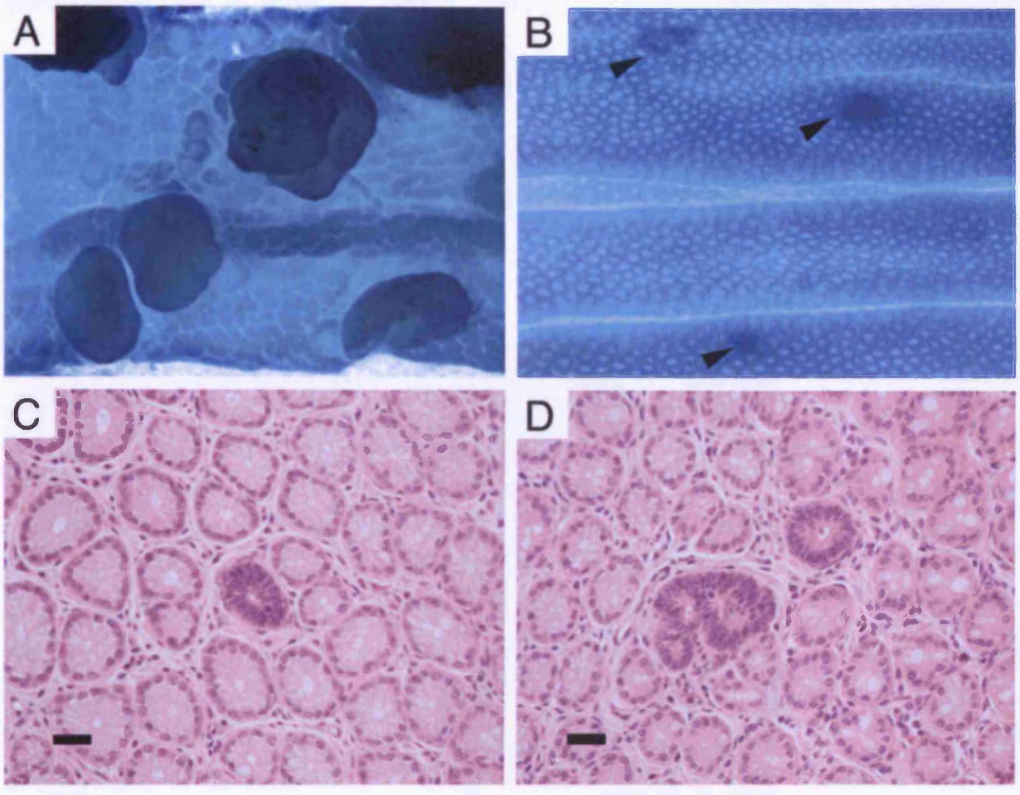

Figure 5–2 Adenomas and aberrant crypt foci in the colon of *Myh* deficient mice, bar size = 500μm

The above figure demonstrates adenomas and ACFs in the colons of $Apc^{Min+/-}$ /$Myh^{-/-}$ mice. Methylene blue-stained adenomatous polys are shown in (**A**), with ACFs demonstrated (with arrow heads) in (**B**). H&E transverse sections demonstrate a monocryptal ACF (**C**) and polycryptal ACF (**D**), scale bars = 500μm.

5.3.1.3 No evidence of progression from adenoma – carcinoma in $Apc^{Min+/-}/Myh^{-/-}$ mice

Analysis of 8 small intestine and 8 colonic adenomas from $Apc^{Min+/-}$ /$Myh^{+/+}$, 21 small intestine and 17 colonic adenomas from $Apc^{Min+/-}$ /$Myh^{+/-}$ and 30 small intestine and 17 colonic adenomas from $Apc^{Min+/-}$ /$Myh^{-/-}$ mice found no evidence of progression from adenoma to carcinoma by 120 - 130 days of age.

5.3.1.4 An increased frequency of mammary gland tumours was observed in $Apc^{Min+/-}/Myh^{-/-}$ mice

Mammary gland tumours were found in 0% (0/16) $Apc^{Min+/-}/Myh^{+/+}$, 7% (3/43) $Apc^{Min+/-}/Myh^{+/-}$ and 27% (4/15) $Apc^{Min+/-}/Myh^{-/-}$ mice (p=0.028 when comparing $Myh^{-/-}$ with both $Myh^{+/-}$ and $Myh^{+/+}$ mice, Fishers exact test). See Figure 5–3.

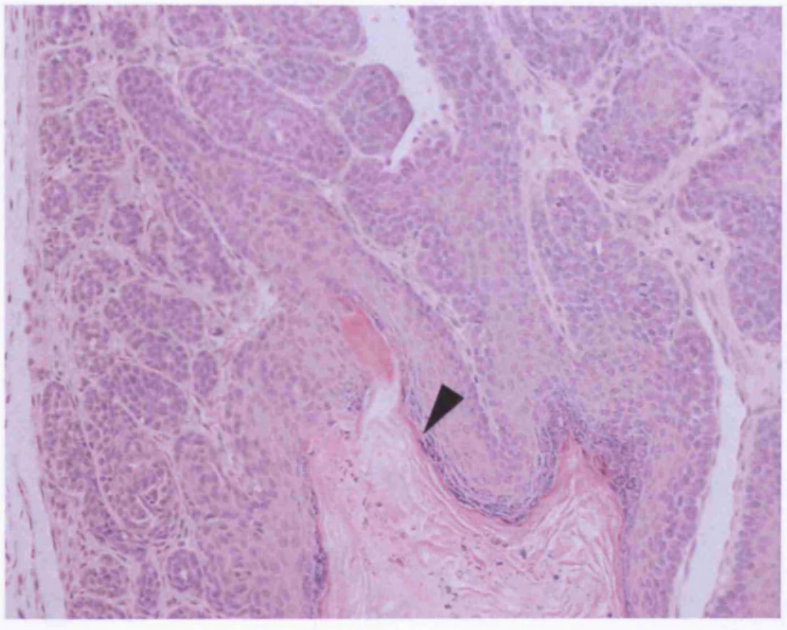

Figure 5–3 H&E stain of mammary gland tumour in $ApcMin^{+/-}/Myh^{-/-}$ mouse (x20) with squamous cell differentiation arrowed

5.3.1.5 Molecular analysis of adenomas from $Apc^{Min+/-}/Myh^{-/-}$ mice

LOH analysis at Apc

As all mice in the study groups were $Apc^{Min+/-}$, initial analysis of all adenomas for LOH at *Apc* was undertaken to determine the mechanism of loss of the second *Apc* allele, either through LOH or through G:C>T:A transversions through *Myh* deficiency.

Ninety-three percent (118/127) adenomas from $Apc^{Min+/-}/Myh^{+/+}$, 89% (87/98) adenomas from $Apc^{Min+/-}/Myh^{+/-}$ and 81% (121/150) from $Apc^{Min+/-}/Myh^{-/-}$

mice were found to have lost the wt allele of *Apc* ($p<0.001$ for *Myh* deficient mice versus *Myh* heterozygous and wt mice, Fishers Exact test).

LOH analysis of colonic adenomas found no significant difference in the frequency of allelic loss at *Apc*. One hundred percent (6/6) of adenomas from $Apc^{Min+/-}$ /$Myh^{+/+}$, 100% (18/18) $Apc^{Min+/-}$ /$Myh^{+/-}$ and 94% (15/16) adenomas from $Apc^{Min+/-}$ /$Myh^{-/-}$ mice had loss of the wt *Apc* allele ($p=0.10$ for *Myh* deficient versus *Myh* wt mice, Fishers Exact test).

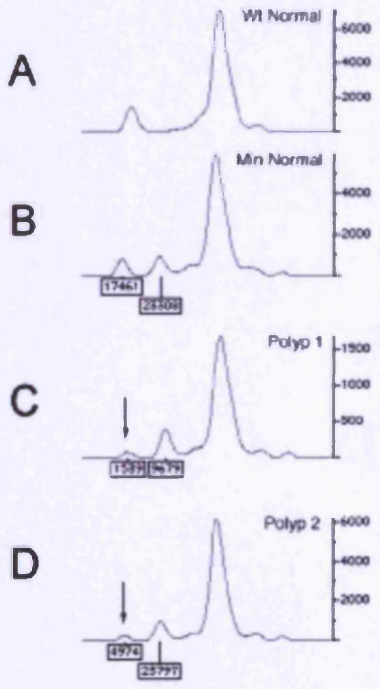

Figure 5–4 LOH analysis at *Apc* (A – wt normal, B – Min normal tissue) in adenomas from $Apc^{Min+/-}$ /$Myh^{+/+}$ (C) and $Apc^{Min+/-}$ /$Myh^{-/-}$ (D) mice. LOH at *Apc* when present, occurred at the wt allele (arrowed)

G:C>T:A transversions occur in adenomas of $Apc^{Min+/-}$ /$Myh^{-/-}$ *mice*

Twenty-nine adenomas from $Apc^{Min+/-}$ /$Myh^{-/-}$, eight adenomas from $Apc^{Min+/-}$ /$Myh^{+/-}$ and 9 adenomas from $Apc^{Min+/-}$ /$Myh^{+/+}$ mice which had not demonstrated LOH for the wt allele of *Apc* underwent somatic mutation analysis at *Apc*.

Somatic mutations were detected in 10% (3) adenomas of $Apc^{Min+/-}$ /$Myh^{-/-}$ mice. All were G:C>T:A transversions (2x G>T nt 3919 (E1307X), 1x C>A nt

4754 (S1585X). The sequence motif around the E1307X mutation (AAAGAGA) is the same as that identified in human MAP as a sequence prone to hyper-mutation as a consequence of defective BER. No somatic mutations were identified in adenomas from $Apc^{Min+/-}$ /$Myh^{+/-}$ and $Apc^{Min+/-}$ /$Myh^{+/+}$ mice.

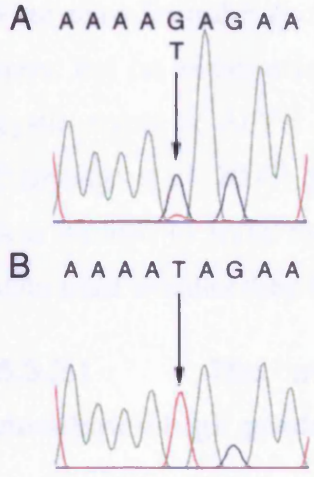

Figure 5–5 Somatic G>T transversion at nt 3919 of *Apc* resulting in E1307X termination codon, **A** – forward sequence from adenoma DNA and **B** – cloned mutant allele

Adenomas from $Apc^{Min+/-}$ /$Myh^{-/-}$ mice did not harbour K-ras mutations

No mutations in exon 1 of *K-ras* were found in 40 adenomas analysed from $Apc^{Min+/-}$ /$Myh^{-/-}$ mice and 20 adenomas from $Apc^{Min+/-}$ /$Myh^{+/+}$ mice.

No LOH at Myh was observed in $Apc^{Min+/-}$ /$Myh^{+/-}$ mice

In order to determine whether inactivation of the wt allele is selected in tumour development in *Myh* heterozygotes, 137 adenomas from $Apc^{Min+/-}$ /$Myh^{+/-}$ mice were screened for LOH at *Myh*. One percent (2/137) adenomas harboured allelic loss at *Myh*, and in one of these cases the LOH targeted the inherited mutant allele rather than the wt allele. Eighty-two adenomas were subsequently screened for somatic mutations in exons 2-15 of *Myh,* but no mutations were identified.

5.3.2 $Apc^{Min+/-}/Myh^{-/-}$ mice bred on AKR background

Following backcrossing of $Apc^{Min+/-}$ and $Myh^{+/-}$ onto AKR and inter-crossing of $Apc^{Min+/-}$ and $Myh^{+/-}$ as described earlier in this chapter, the same study groups were set up on the AKR genetic background. Twenty-two $Apc^{Min+/-}/Myh^{-/-}$, 44 $Apc^{Min+/-}/Myh^{+/-}$, 20 $Apc^{Min+/-}/Myh^{+/+}$ and 30 $Apc^{+/+}/Myh^{+/+}$ mice were studied.

Four mice from the $Apc^{Min+/-}/Myh^{-/-}$ group were culled between 110 and 130 days, but on examination, none of these animals had developed adenomas, cystic crypts or ACFs. In light of these findings and those of (Sakamoto, Tominaga et al. 2007) (published whilst this experiment was in progress), it was decided to leave these animals for up to 18 months of age in order to determine whether they would in fact develop a gastro-intestinal phenotype.

5.3.2.1 The majority of mice across all study groups developed high grade lymphoma

Whilst waiting for the mice to mature all of the animals became sick necessitating culling. Full post mortems were carried out and none of the mice in any of the study groups had developed adenomas, cyctic crypts or ACFs. The majority of the animals had developed high grade lymphoma and had died as a consequence of metastatic spread to other organs and bone marrow failure –see Table 5–3 and Table 5–4.

Animal ID	Genotype	Age at death (weeks)	*PM findings* Cause of death	weight (g)	LN size	thymus	spleen	comments
1	$MYH^{-/-}$ / $Min^{+/-}$	8	lymphoma	21.6	5-10x	10x	NAD	
2	$MYH^{-/-}$ / $Min^{+/-}$	24	no obvious cause	39.8	NAD	NAD	NAD	subcutaneous chest wall nodule
3	$MYH^{-/-}$ / $Min^{+/-}$	24	no obvious cause	28.9	NAD	NAD	NAD	stomach distended
4	$MYH^{-/-}$ / $Min^{+/-}$	28	lymphoma	29.1	5x	10x	NAD	
5	$MYH^{-/-}$ / $Min^{+/-}$	36	lymphoma	30.9	2x	10x	3x	
6	$MYH^{-/-}$ / $Min^{+/-}$	24	lymphoma	32.5	2x	5x	3x	liver infiltrated
7	$MYH^{-/-}$ / $Min^{+/-}$	28	lymphoma	33.4	10x	NAD	NAD	right inguinal LN 10x size
8	$MYH^{-/-}$ / $Min^{+/-}$	36	lymphoma	50.2	NAD	NAD	NAD	2 subcutaneous abscesses non-active
9	$MYH^{-/-}$ / $Min^{+/-}$	26	lymphoma	26.2	3-5x	10x	3x	
10	$MYH^{-/-}$ / $Min^{+/-}$	26	no obvious cause	26.7	3-5x	10x	3x	
11	$MYH^{-/-}$ / $Min^{+/-}$	21	no obvious cause	31.1	NAD	NAD	NAD	hyperplasia of the uterus
12	$MYH^{-/-}$ / $Min^{+/-}$	28	lymphoma	35.1	NAD	NAD	NAD	culled as piloerect and rapid breathing
13	$MYH^{-/-}$ / $Min^{+/-}$	16	lymphoma	34.1	2x	10x	NAD	
14	$MYH^{-/-}$ / $Min^{+/-}$	24	lymphoma	36.3	3-5x	10x	3x	
15	$MYH^{-/-}$ / $Min^{+/-}$	38	no obvious cause	30.1	2x	10x	NAD	liver infiltrated
16	$MYH^{-/-}$ / $Min^{+/-}$	38	lymphoma	33.9	3-5x	10x	5x	liver infiltrated
17	$MYH^{-/-}$ / $Min^{+/-}$	40	no obvious cause	44.8	NAD	10x	NAD	
18	$MYH^{-/-}$ / $Min^{+/-}$	22	lymphoma	25.9	2x	10x	NAD	liver infiltrated
19	$MYH^{-/-}$ / $Min^{+/-}$	30	no obvious cause	32.5	NAD	NAD	NAD	
20	$MYH^{-/-}$ / $Min^{+/-}$	30	no obvious cause	37.1	NAD	NAD	NAD	
21	$MYH^{-/-}$ / $Min^{+/-}$	32	no obvious cause	46.4	NAD	30x	NAD	
22	$MYH^{-/-}$ / $Min^{+/-}$	32	no obvious cause	51.7	NAD	30x	NAD	subcutanous cyst under chin

Table 5–3 Summary of cause of death and post mortem findings for the $Myh^{-/-}$ / $Min^{+/-}$ mice (NAD = no abnormality detected)

Genotype AKR background	no.	age at death (weeks) median (range)	weight (g) median (range)	lymphoma
$MYH^{-/-}$ / $Min^{+/-}$	22	28 (8-40)	32.5 (21.6-51.7)	12/22 (55%)
$MYH^{+/-}$ / $Min^{+/-}$	44	26 (2-32)	33.4 (25.7-41.2)	28/44 (63%)
$MYH^{+/+}$ / $Min^{+/-}$	20	28 (8-44)	31.4 (17.9-46.6)	10/20 (50%)
$MYH^{+/+}$ / $Apc^{+/+}$	30	32 (15-45)	39.6 (21.7-35.4)	21/30 (70%)

Table 5–4 Summary of age and weight at death and incidence of lymphoma at post mortem

No significant difference was observed in either the age or weight at death between any of the study groups (p=0.22 for $Apc^{Min+/-}$ /$Myh^{-/-}$ versus $Apc^{Min+/-}$ /$Myh^{+/-}$, p=0.84 for $Apc^{Min+/-}$ /$Myh^{-/-}$ versus $Apc^{Min+/-}$ /$Myh^{+/-}$, p=0.08 for $Apc^{Min+/-}$ /$Myh^{-/-}$ versus $Apc^{+/+}$ /$Myh^{+/+}$ for age at death; p=0.68 for $Apc^{Min+/-}$ /$Myh^{-/-}$ versus $Apc^{Min+/-}$ /$Myh^{+/-}$, p=0.58 for $Apc^{Min+/-}$ /$Myh^{-/-}$ versus $Apc^{Min+/-}$ /$Myh^{+/+}$ and p=0.46 for $Apc^{Min+/-}$ /$Myh^{-/-}$ versus $Apc^{+/+}$ /$Myh^{+/+}$ for weight at death, t-test).

When considering the incidence of lymphoma, no significant difference was observed across the study groups (p=0.16 for $Apc^{Min+/-}$ /$Myh^{-/-}$ versus $Apc^{Min+/-}$

$/Myh^{+/-}$, p=0.23 for $Apc^{Min+/-}$ $/Myh^{-/-}$ versus $Apc^{Min+/-}$ $/Myh^{+/+}$ and p=0.12 for $Apc^{Min+/-}$ $/Myh^{-/-}$ versus $Apc^{+/+}$ $/Myh^{+/+}$ Fishers Exact test).

5.3.2.2 Histological findings at post mortem

Full post mortems were performed and gut preparations examined for adenomas, cystic cryps and ACFs. As none were seen in any animals for all study groups, a sub-set of 5 $Apc^{Min+/-}$ $/Myh^{-/-}$ and 5 $Apc^{+/+}$ $/Myh^{+/+}$ animals had full gut rolls prepared and were examined by a Histopathologist (G.Stamp) for any evidence of cystic crypts ot ACFs. One ACF was identified in the colon of one $Apc^{Min+/-}$ $/Myh^{-/-}$ animal.

The figures below show gross pathological and H&E-stained preparations of the thymus, mesenteric lymph nodes, spleen and bowel mucosa from both $Apc^{Min+/-}$ $/Myh^{-/-}$ and wt C57BL6 animals for comparison.

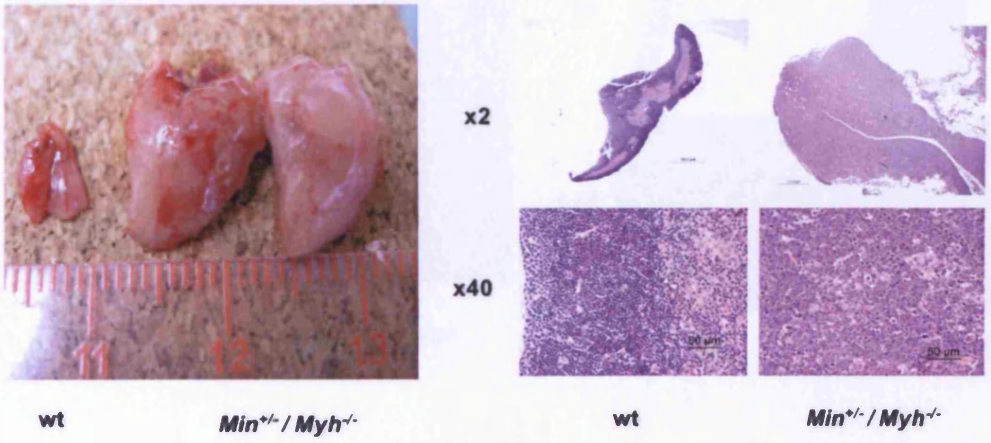

Figure 5–6 Thymus from $Apc^{Min+/-}$ / $Myh^{-/-}$ mouse, H&E sections on the right demonstrate loss of abnormal parenchymal architecture (x2) and lymphocytic infiltration with high grade lymphomatous cells (x40)

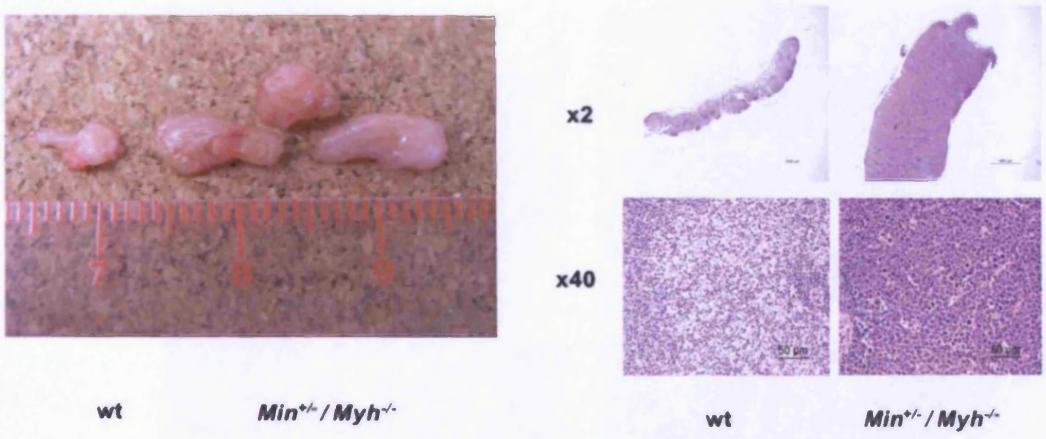

Figure 5–7 Mesenteric lymph nodes from *Apc*$^{Min+/-}$ / *Myh*$^{-/-}$ mouse, H&E sections on the right demonstrate loss of abnormal parenchymal architecture (x2) and lymphocytic infiltration with high grade lymphomatous cells (x40)

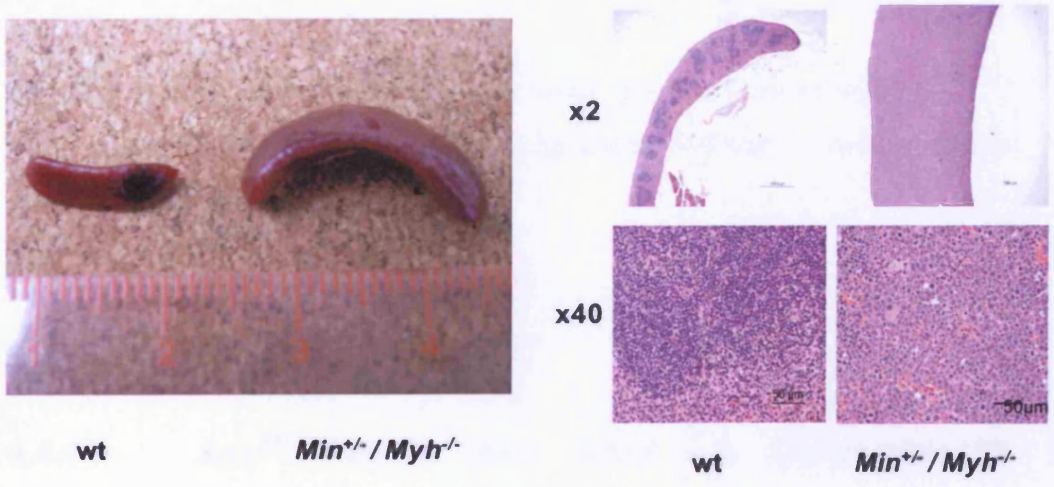

Figure 5–8 Spleen from *Apc*$^{Min+/-}$ / *Myh*$^{-/-}$ mouse, H&E sections on the right demonstrate loss of abnormal parenchymal architecture (x2) and lymphocytic infiltration with high grade lymphomatous cells (x40)

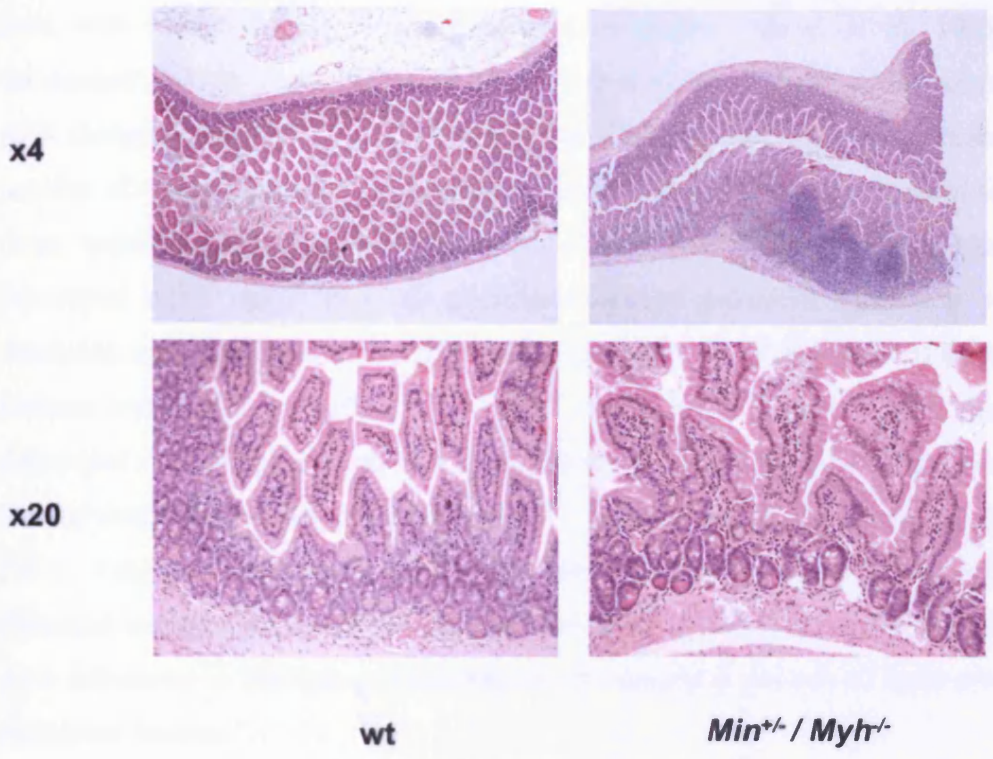

Figure 5–9 Transverse H&E sections of small intestine from wt and $Apc^{Min+/-}$ / $Myh^{-/-}$ mice. No adenomas are seen, lymphocytic infiltrate is evident in the $Apc^{Min+/-}$ / $Myh^{-/-}$section at x4 power

5.4 Discussion

5.4.1 $Apc^{Min+/-}/Myh^{-/-}$ mice bred on C57BL6/SV129 background

The first mouse model of MAP bred on a mixed C57B6/SV129 genetic background demonstrated an additive effect of defective *Myh* when crossed with $Apc^{Min+/-}$ mice both in the development of intestinal and extra-intestinal tumour development.

A significantly increased number of adenomas developed in the small intestine of $Apc^{Min+/-}$ /$Myh^{-/-}$ mice and a higher number (not statistically significant) of cystic crypts was also observed. Cystic crypts are lesions of unknown neoplastic potential which occur in the small intestine of $Apc^{Min+/-}$ mice and increase in number when mice are treated with ethylnitrosourea (ENU) or are

bred with MMR (*Mlh1*) deficient mice (Shoemaker, Moser et al. 1995; Shoemaker, Haigis et al. 2000). It is possible that the addition of defective BER alongside the $Apc^{Min+/-}$ mutation may have caused the observed increased number of cystic crypts through similar (as yet undetermined) mechanisms to those underlying the $Apc^{Min+/-}/Mlh^{-/-}$ mice. The $Apc^{Min+/-}/Mlh^{-/-}$ mice also developed other extra-intestinal manifestations of defective *Apc* such as desmoids and epidermoid cysts (Shoemaker, Haigis et al. 2000), none of these features were seen in the $Apc^{Min+/-}/Myh^{-/-}$ mice. $Apc^{Min+/-}/Mlh^{-/-}$ mice also developed ~ 2 fold greater number of ACFs which are putative pre-malignant lesions developing in the colon of $Apc^{Min+/-}$ mice (Paulsen, Steffensen et al. 2001; Yamada, Hata et al. 2002) and that are following treatment with chemical carcinogens (Wargovich, Jimenez et al. 2000). This suggests that *Myh* deficiency in the mouse promotes the development of both of these pre-malignant lesions.

The proportion of adenomas in $Apc^{Min+/-}/Myh^{-/-}$ mice without LOH of the wt allele of *Apc* was similar to that in previous studies in other BER and MMR deficient mice – *Mbd4, Mlh1, Msh2* and *Pms2* (Wong, Yang et al. 2002) (Shoemaker, Haigis et al. 2000) (Reitmair, Cai et al. 1996) (Baker, Harris et al. 1998).

The presence of G:C>T:A transversions at *Apc* in adenomas from $Apc^{Min+/-}/Myh^{-/-}$ mice was indicative that defective BER was promoting tumorigenesis in these animals. As no G:C>T:A transversions at *Apc* were seen in adenomas from the $Apc^{Min+/-}/Myh^{+/-}$ and $Apc^{Min+/-}/Myh^{+/+}$ mice, it can be concluded that the pathogenesis in those adenomas demonstrating G:C>T:A transversions similar to that occurring in humans (Al-Tassan, Chmiel et al. 2002) (Jones, Emmerson et al. 2002).

The low frequency of somatic truncating mutations at *Apc* observed in the $Apc^{Min+/-}/Myh^{-/-}$ mice may be due to increasing evidence that adenomas from $Apc^{Min+/-}$ mice and germline *APC* mutation carriers in humans (FAP) are polyclonal (Merritt, Gould et al. 1997) (Novelli, Williamson et al. 1996) (discussed further in Chapter 9). In this situation the overall contribution to the tumour DNA from the mutant allele may be too small to be detected (unless samples are micro-dissected). This is supported by the finding that the somatic

mutation (G>T transversion at nt 3919) cited in this chapter (Figure 5–5) could only be confirmed on cloning of the PCR product.

The distribution of adenomas within the small intestine of $Apc^{Min+/-}$ /$Myh^{-/-}$ mice with a greater proportion developing in the proximal and middle segments of the small intestine in part reflect the distribution of adenomas in humans MAP (where duodenal and gastric adenomas can occur). When $Apc^{Min+/-}$ mice are crossed with MMR deficient (*Mlh1*) mice a uniform distribution of adenomas is observed (Shoemaker, Haigis et al. 2000). This observation in both human and murine MAP may reflect varying levels of oxidative stress throughout the GI tract or may relate to the level of activity or functional redundancy of *MYH* in different anatomical regions of the GI tract.

The first MAP mouse model was very useful in determination of the significance of the heterozygous state in *MYH*. The finding that $Apc^{Min+/-}$ /$Myh^{+/-}$ mice did not develop a significantly higher number of adenomas than $Apc^{Min+/-}$ /$Myh^{+/+}$ mice indicated that being a heterozygous carrier of *MYH* did not confer a higher risk of developing adenomas and CRC. This study and its publication (in 2004) came before subsequent population based studies confirming this finding (Webb, Rudd et al. 2006).

The first mouse model of MAP demonstrated elements of tumorigenesis similar to that found in the human form of the disease, however adenomas were found to have a much higher incidence of LOH at *Apc* as the "second hit" and lower incidence of somatic G:C>T:A transversions at *Apc*.

It was on the basis of these findings that the second MAP model was bred in order to develop a more "faithful" model of the disease.

5.4.2 $Apc^{Min+/-}/Myh^{-/-}$ mice bred on AKR background

It is known that AKR mice are prone to developing leukaemia and lymphoma (http://jaxmice.jax.org) with a lifetime incidence of 60-90%. However previous studies back-crossing $Apc^{Min+/-}$ on to AKR and subsequent inter-crossing with *Mlh1* led to the development of a gasto-intestinal phenotype (Haigis, Hoff et al. 2004). In the study by Haigis *et al*, $Apc^{Min+/-}$ /$Mlh1^{-/-}$ mice also developed thymic lymphoma at an average age of 100 days.

As four AKR $Apc^{Min+/-}/Myh^{-/-}$ mice in my study had not developed a gastro-intestinal phenotype or lymphoma by 110 to 130 days and following the findings of Sakamoto *et al* (Sakamoto, Tominaga et al. 2007), the study and control groups in this experiment were left for longer (ideally > 1 year) prior to culling.

Sakamoto *et al* developed a $Myh^{-/-}$ mouse bred on the C57BL6 background whilst this study was in progress. This mouse develops both spontaneous adenomas at > 18 months of age and a significantly higher number of adenomas when fed $KBrO_3$ in drinking water. At 18 months of age 109 wt and 121 $Myh^{-/-}$ mice were sacrificed and examined for development of adenomas and extra-intestinal tumour development, at this time no increased mortality was observed in the $Myh^{-/-}$ mice. Four adenomas and seven carcinomas were found in the intestines (small intestine / colon not specified) of 10 $Myh^{-/-}$ mice and none were found in the wt controls. When oxidative stress was induced with $KBrO_3$ in drinking water, a higher number of adenomas was observed in 16 $Myh^{-/-}$ and 15 wt mice (mean no. adenomas = 61.88 in $Myh^{-/-}$ and 0.85 in wt) when animals were culled at 12 months. The adenomas in the $Myh^{-/-}$ mice were found predominantly in the proximal small intestine (as found in the first MAP mouse above). None of the wt or $Myh^{-/-}$ animals which were not fed $KBrO_3$ developed adenomas by 12 months of age. No mutational analysis was undertaken in these studies to determine whether the adenomas which developed in the $Myh^{-/-}$ mice had an excess of G:C>T:A transversions.

The main obstacle in development of the second MAP mouse model was the discrepancy between the length of time required for a "simple" $Myh^{-/-}$ knockout mouse (on C57BL6) to develop a phenotype (18 months of age) (Sakamoto, Tominaga et al. 2007), and even then this is found in only 8% (10/121) of animals and the incidence of lymphoma inherent in the AKR genetic background. In excess of 90% of AKR mice develop lymphoma by 18 months of age.

Interestingly, no difference was observed in either the age of death or incidence of lymphoma in any of the study groups or controls in the second MAP mouse .There was a suggestion in the data that the $Apc^{Min+/-}$ mice died at a younger age and weight, but this was not significant. The presence of

Apc$^{Min+/-}$ allele either with or without *Myh* deficiency did not significantly affect the age or cause of death when all of the study and control groups were compared. Mouse models of lymphoma (with associated microsatellite instability) include MMR deficient (*Msh2* and *Mlh1*) mice which are thought to lead to a higher number of errors in T-cell and B-cell gene rearrangements of the immunoglobulin gene superfamily, but little is known of the target genes for defective MMR in this situation. *Msh2* deficent murine lymphomas develop insertion/deletion muations in *Tgfß* type 2 gene (Lowsky, Magliocco et al. 2000). Up to 75% of *Mlh1* deficient mice develop lymphomas which harbour somatic mutations in the transcription factor *ikaros* (Kakinuma, Kodama et al. 2007).

In the AKR *Apc*$^{Min+/-}$/*Myh*$^{-/-}$ model, defective BER should not cause the same mutation spectra in either T and B cell gene rearrangement (as BER is not directly involved in T and B cell gene rearrangement) or *Tgfß* – and would not lead to the development of lymphoma at a faster rate than wt animals. This is reflected in the observed results presented in this Chapter.

It seems that some other mechanism is required alongside *Myh*$^{-/-}$ deficiency to drive tumorigenesis in mouse models of MAP – either through environmental oxidative stress or a predisposition to adenoma development through the *Apc*$^{Min+/-}$ allele.

5.5 Conclusions

The first mouse model of MAP (*Apc*$^{Min+/-}$/*Myh*$^{-/-}$ mice bred on C57BL6/SV129 genetic background) developed several features in keeping with the human MAP syndrome – those of intestinal adenoma development, with a proximal distribution in the GI tract and evidence of somatic G:C>T:A transversions at *Apc*.

Further studies have provided evidence that mouse models of MAP (on both the C57B6 and AKR genetic background) appear to require a second promoter of tumorigenesis either through external oxidative stress or inherited mutations in *Apc*.

6 Identification of potential pathogenic mechanisms underlying the multiple colorectal adenoma phenotype.

6.1 Introduction

The multiple colorectal adenoma (MCRA) phenotype is can be defined as any individual who develops between 5-100 adenomas in their lifetime.

These individuals carry an increased risk of developing CRC. Up to 35% of MCRA individuals are homozygous carriers of *MYH* germline mutations (Sieber, Lipton et al. 2003) (Sampson, Dolwani et al. 2003), and a further 15% harbour a germline mutation in *APC* ("attenuated" FAP, (AFAP)) (Spirio, Green et al. 1999). The remaining ~50% of MCRA cases are likely to have some genetic component which is as yet unidentified.

The concept of utilising molecular profiling alongside histopathological features in adenoma classification has continued to develop since the introduction of the "adenoma – carcinoma sequence" in the late 1980's. This paradigm describes the progression from normal colonic epithelium through adenoma to carcinoma initiated by bi-allelic loss of *APC* followed by activating *K-ras* mutation and culminating with inactivation of p53 resulting in transition to carcinoma (the "classical" pathway)(Vogelstein, Fearon et al. 1988).

Activating *K-ras* mutations have historically been associated with advanced adenoma and a higher degree of "aggressiveness" of an adenoma (Maltzman, Knoll et al. 2001). However, *K-ras* mutations are also found in microadenomas and small tubular adenomas indicating a limited potential for progression (Takayama, Ohi et al. 2001). Taking this alongside the finding that only 30% of CRC's harbour *K-ras* mutations (Jass, Whitehall et al. 2002)

indicates that its historical position in the adenoma – carcinoma sequence could be questioned.

The concept of an alternative "serrated" pathway of colorectal tumorigenesis was introduced on the finding that serrated adenomas, hyperplastic polyps and mixed polyps harbour mutations in *BRAF* (Chan, Zhao et al. 2003; Kambara, Simms et al. 2004) (Yang, Farraye et al. 2004). They are also commonly microsatellite unstable and demonstrate extensive DNA methylation (O'Brien, Yang et al. 2004) (Jass 2005).

In reality it is likely that there is a molecular spectrum of (epi)genetic mutations and histological findings which are observed in sporadic adenomas, serrated adenomas and hyperplastic polyps. It has been suggested that molecular "crossover" from the serrated to the classical pathway may occur conferring enhanced aggressiveness in certain adenomas (Jass, Baker et al. 2006).

The histopathological features (the majority being tubular adenomas) of MCRAs suggest that they would follow the classical pathway. However, prior to this study this area not been specifically explored or studied.

In this study I utilised several approaches in tandem to identify potential pathogenic mechanisms leading to the development of MCRAs in a group of patients in whom *MYH* and *APC* mutations had been excluded.

I set out to identify potential pathological mechanisms by looking for clues as to the development of MCRAs from their earliest stages by examination of histological slides for the presence or absence of microadenomas, searching for evidence of disruption of Wnt signalling through performing immuno-histochemistry for β-catenin and examining adenomas for evidence of a somatic mutation spectrum suggestive of an underlying disruption of DNA repair. Somatic mutation spectra in *K-ras* and *BRAF* were also determined to further molecularly classify the MCRA phenotype .

The significance of the presence of microadenomas

The primary tumour predisposition in FAP and MAP is through the formation of colorectal adenomas via *APC* mutation. FAP and MAP patients develop not only macroscopic adenomatous polyps, but also microadenomas – each comprising at most a few dysplastic crypts (Lipton, Halford et al. 2003) and

more recently described in the duodenum (Preston, Leedham et al. 2008). This is consistent with an increased rate of adenoma initiation in FAP and MAP. In HNPCC, by contrast, the primary predisposition is probably to carcinoma (or progression from adenoma to carcinoma) and microadenomas are generally absent. The presence or absence of microadenomas in the colonic mucosa of MCRA patients would therefore provide evidence as to the origins of the disease.

A similar line of reasoning can be applied to the observation that (A)FAP and MAP patients frequently develop extra-colonic adenomas, particularly in the duodenum. The similarity of the MAP and (A)FAP phenotypes suggests that all individuals predisposed to inactivation of *APC* may develop both colorectal and duodenal adenomas. Interestingly, HNPCC patients are at greatly increased relative risk - but low absolute risk - of small bowel cancer, but have very few adenomas at this site.

Wnt signalling disruption and adenoma formation

The relationship between *APC* and Wnt signalling has been previously described in Chapter 1 (1.1.3.4). A simple method with which to assess disruption of *APC* function and Wnt signalling is through cellular expression of *β-catenin* – a downstream product in the Wnt signalling pathway. FAP and AFAP adenomas have increased nuclear and cytoplasmic expression of *β-catenin* indicative of Wnt disruption (Seidensticker and Behrens 2000). HNPCC tumours in contrast, have relatively low frequency of nuclear *β-catenin.*

A previous study screening for germline mutations in the *TGF-β* (*SMAD4, BMPR1A*) and Wnt signalling (*APC2*, conductin, *GSK3-β)* pathways in 47 MCRA cases found only one individual to have a putative pathogenic mutation in *BMPR1A* (Lipton, Sieber et al. 2003).

Considering the complexity of the Wnt signalling pathway (including numerous inhibitory factors – the *Wif* family) this pathway warrants further study in the MCRA setting.

Determination of the presence of a somatic mutation signature

Following the precedent of the discovery of *MYH*, determination of a potential mutation signature at *APC* may lead to the identification of an underlying

defect in DNA repair. This is also evident in HNPCC where the effects of DNA mismatch repair (MMR) deficiency can be detected somatically through the presence of microsatellite instability (MSI) and frameshift mutations in short repeats within genes such as *BAX* and *TGFBR2* (Woodford-Richens, Rowan et al. 2001). It follows that, should some of the remaining MCRA cases be caused by a defect in DNA repair or by some other form of hypermutation, the somatic mutation spectrum will reflect the underlying cause of genomic instability.

6.1.1 Aims of this chapter

In order to determine the underlying pathogenesis of the MCRA phenotype I studied a collection of 25 MCRA cases in the following ways.

1: Examination for the presence of microadenomas - an indication that "2-hits" at *APC* have occurred initiating adenoma formation.
2: Identification of Wnt activation through immunohistochemistry for *β-catenin* expression to identify any underlying defect in Wnt signalling and somatic mutation screening for the two mutational hotspots found in exons 3 and 5 of *β-catenin.*
3: Examination of adenomas for somatic mutation at *APC, K-ras,* and *BRAF* in order to identify a potential somatic mutation signature relating to an underlying defect in DNA repair, using the precedent of the discovery of *MYH* as proof of principle.
4: Molecular classification of the MCRA phenotype through analysis for somatic mutations at *K-ras* and *BRAF* to determine whether the "classical" or "serrated" pathways are followed.

6.2 Methods

Sample collection and preparation

Patients were recruited through St Mark's Hospital Colorectal Cancer Unit and blood was routinely sampled. Informed consent was obtained prior to

sample collection. Inclusion criteria for the study were that patients should have between 10 and 100 synchronous or metachronous colorectal adenomas, irrespective of follow-up or (prophylactic) colectomy.

Individuals had all coding exons of *APC* and *MYH* screened for germline mutations with fluorescent SSCP and subsequent sequencing prior to entry in to the study. Primers and conditions for *APC* and *MYH* analysis are listed in appendix 1, SSCP analysis and sequencing were performed as outlined in Methods (2.6.1 and 2.7).

In addition, multiplex ligation-dependent probe amplification (MLPA) analysis was used to screen for germline deletions or duplications of *APC* using the Salsa MLPA kit P043 APC (MRC Holland), see Methods (2.6.5). This was undertaken in collaboration with E. Volikos at St. Marks Hospital.

A total of 241 formalin-fixed, paraffin-embedded adenomas were collected from the 25 patients who were eligible for the study.

Fifty-six formalin-fixed, paraffin-embedded sporadic adenomas (patients with 1 or 2 adenomas and no reported family history) were collected from 29 individuals.

Existing sets of adenomas from AFAP and MAP patients in our laboratory were available for comparison (Sieber, Lipton et al. 2003) (Lamlum, Al Tassan et al. 2000) (Sieber, Segditsas et al. 2006).

For all patients, germline DNA was extracted from peripheral blood using methods as described Methods (2.1.1.1).

Tumour and normal tissues were dissected from sections cut from archival, paraffin-embedded specimens. It was estimated that the resulting tumour DNAs were derived from at least 70% dysplastic cells. DNA was extracted from these by proteinase K digestion at 55°C as described in Methods (2.1.1.4).

Mutation detection

F-SSCP analysis was used to screen the formalin-fixed, paraffin-embedded tumours for somatic *APC* mutations between codons 1220 and 1620, corresponding to the mutation cluster region (MCR) and covering the region between the first 20-amino acid beta-catenin binding/degradation repeat

(20AAR) and the first SAMP repeat. The region was sub-divided into 12 amplicons (see Appendix 1 for details of primers and conditions). Any sample with a bandshift was sequenced directly in both orientations from a new PCR product. Exon 1 of *K-ras*, *β-catenin* exon 3, and the mutational hotspot at codon 600 of *BRAF* were screened by direct DNA sequencing in both orientations. Novel mutations were identified through comparison with the COSMIC database (http://www.sanger.ac.uk/genetics/CGP/cosmic) and the European *APC* database (Laurent-Puig, Beroud et al. 1998).

LOH analysis

Loss of heterozygosity (LOH) at *APC* was analysed using microsatellite markers just distal to the locus (D5S346, D5S421 and D5S656) on the ABI 3100 sequencer as described in Methods (2.1.6.1). Constitutionally homozygous markers (and occasional PCR failures) were scored as non-informative. In the event of discordance between microsatellite markers, precedence was given to the marker closest to the *APC* gene.

Microadenoma detection

H&E slides of adenomas from the MCRA, sporadic and MAP groups were examined for the presence of absence of microadenomas (collections of dysplastic crypts <1mm in diameter) under the guidance of a specialist gastroenterological histopathologist. (M.Novelli, Department of Histopathology, University College London).

Immunohistochemistry

Immunohistochemistry for *β–catenin* was performed on the multiple adenoma group, sporadic adenomas and, for comparison, a set of patients with FAP as described in Methods (2.1.13). Slides were then examined using a conventional light microscope and the level of expression of *β–catenin* (1, 2 or 3) was recorded separately for the nucleus, cytoplasm and cell membrane according to the intensity of staining in five random high-powered fields per slide. This was compared directly with staining in normal crypts from each

sample. For membranous expression, in order to normalise results across different runs of immunohistochemistry, the abnormal staining for each tumour was divided by the membrane staining in surrounding normal cells. Normal cytoplasmic and nuclear expression was so weak that such a correction was not required. Immunohistochemistry was scored by myself and a subset re-scored by another laboratory member (K.Howarth) to ensure consistence, all under the guidance of a specialist gastrointestinal histopathologist (M.Novelli); any differences were resolved by consensus.

6.3 Results

6.3.1 Germline screening of *APC* and *MYH* prior to inclusion into this study

Sixty-six individuals were screened for germline mutations in *APC* exons 1–15 and *MYH* exons 1–16 using fluorescent SSCP analysis. This was followed by direct sequencing of a fresh PCR product if aberrant SSCP bands were found (see Table 6–1 for summary).

One individual was found to have a 5 bp deletion in exon 15O (nt 6233) of *APC*. She had 33 adenomas and no extracolonic features. Silent mutations were found in seven individuals and missense mutations in three.

One individual had homozygous Y165C mutations in *MYH*, and one individual was a compound heterozygote for G382D and 1395delGAA. These are the known pathogenic mutations seen in northern European (Y165C, G382D) and southern European (1395delGAA) populations. A previously described *MYH* polymorphism, Q324H, was identified in 30% of individuals.

No individuals were found to have whole exon deletions or duplications at *APC* using MLPA analysis. All individuals with pathogenic or missense germline mutations were excluded from further study.

Gene and Exon	Mutation	Outcome	Pathogenic	No. indivudals harbouring mutation	No. TA's range (median)
APC					
5	intronic C>T		no	18	8-32 (15)
7	intronic G>C		no	1	29
11	nt1458 C>T	silent	no	7	10-33 (18)
13	nt1635 A>G	silent	no	35	7-53 (17)
15E	Q1122R nt3368G>A	Q->R	no	1	9
15I	nt 4479 G>A	silent	no	11	9-34 (19)
15J	nt 5034 A>G	silent	no	4	6-18 (10)
	nt4904 G>A	silent	no	1	21
15K	nt 5268 G>T	silent	no	3	7-26 (11)
15L	D1822V		no	1	13
15O	del 5bp nt6233	stop 2071	yes	1	33
15Q	C>T A2254V	A->V	no	1	15
15S	G>A ; G2502S	G->S	no	1	8, 13 HPP
15T	silent nt7704 A>G	silent	no	1	33
MYH					
x7	Y165C hom		yes	1	>30
x13	G382D het	het 1395delGAA	yes	1	>10
x12A	Q324H hom	Q324H	polymorphism	3	8-11 (5)
X12A	Q324H het	Q324H het	polymorphism	20	8-76 (17)

Table 6–1 Results of germline screening for *APC* and *MYH* mutations in 66 MCRA cases

From the 66 individuals screened, 25 were included in the following studies.

6.3.2 Features of the MCRA patients

The clinical features of the 25 MCRA patients included for further study are shown in Table 2. All were of white UK origin. The mean age at presentation was 60 years (median=61, range=44-75). Mean adenoma number at presentation was 24 (median=21, range=10-76), and the great majority of adenomas were mildly dysplastic tubular or tubulovillous adenomas less than 5mm in diameter. One patient had CRC at the time of presentation. No patient had upper gastrointestinal adenomas and there were no other notable or consistent extra-colonic features. Most MCRA patients were isolated cases, although a few patients had a single sibling affected with multiple adenomas. In no case was there multi-generational inheritance of CRAs (except case 19). In six patients, CRCs were present in other family members, although none of these individuals had been reported as having adenomas.

Patient no.	Age at diagnosis	Adenoma no.	CRC	FH MCRAs	FH CRC
1	75	20	No	No	Mother - 83yrs
2	66	25	No	No	
3	60	25	No	No	
4	71	14	No	No	
5	61	10	No	No	
6	51	26	No	No	
7	52	27	No	No	Mother - 60yrs
8	65	10	No	No	
9	61	19	No	No	
10	73	10	No	No	Sister - 64 years
11	68	23	Yes 68 years	No	
12	69	12	No	No	
13	67	27	No	No	
14	73	76	No	No	Father - 80yrs
15	55	10	No	No	Brother - 60yrs
16	55	17	No	No	
17	52	50	No	No	
18	55	18	No	No	
19	49	15	No	Yes - Father 19 adenomas	
20	66	10	No	1st cousin "multiple polyps"	
21	55	30	No	No	
22	44	33	No	No	
23	48	32	No	No	
24	64	50	No	No	
25	51	21	No	No	Mother - 85yrs, Mat GM - 70yrs

Table 6–2 Patient demographics for the 25 MCRA cases studied

The MAP patients used for comparison (Sieber, Lipton et al. 2003) presented at a median age of 57 (range=54-69), not significantly different from the MCRA patients (p=0.476, Wilcoxon test).

The AFAP patients used for comparison (Lamlum, Al Tassan et al. 2000) (Sieber, Segditsas et al. 2006) had a median age of 43 (range=27-68) and were significantly younger than the MCRA group (p=0.027, Wilcoxon test).

The family histories and phenotypes of the MCRA cases therefore resembled MAP. However, no evidence of a predisposition to extra-colonic disease was seen in the MCRA group.

6.3.3 Microadenoma detection

Examination of H&E-stained sections of large bowel from FAP, AFAP, MAP and multiple adenoma patients for the presence of microadenomas (dysplastic lesions <1mm diameter) was undertaken in otherwise normal large bowel mucosa. Microadenomas were present in 16 of 19 FAP sections examined, the mean density being 0.22 per mm of mucosa examined (see Table 6–3). In AFAP, microadenomas were present in 2 of 7 sections examined from four patients, with mean density 0.03 per mm of mucosa examined. In MAP, microadenomas were present in 3 of 16 sections examined from six patients at 0.01 per mm of mucosa examined. No microadenomas were found on examination of 16 sections from seven MCRA patients. There was a

significantly higher number of microadenomas on comparison of FAP with MCRA and FAP and MAP ($p<0.001$ (FAP versus MCRA); $p=0.04$ (FAP versus MAP) Fishers Exact test). No significant difference was observed between MCRA and MAP cases ($p=0.23$ Fishers Exact test). The majority of specimens examined were from colectomies subsequently sporadic adenoma cases could not be assessed, as it is very unusual for colectomy to be undertaken in these patients.

Adenoma type	FAP	AFAP	MAP	MCRA
no. microadenomas detected per number of sections examined	16/19 (84%)	2/7 (29%)	3/16 (19%)	0/16 (0%)
density of microadenomas per mm of colonic mucosa examined	0.22 per mm	0.03 per mm	0.01 per mm	0.00 per mm

Table 6–3 Summary of microadenoma detection in FAP, AFAP, MAP and MCRA cases

6.3.4 Somatic mutation and LOH frequencies

Truncating somatic mutations at *APC* were detected in 49 of 221 (22%) adenomas from the MCRA group (see Table 6-5). Of 190 informative tumours, 32 (17%) showed allelic loss (LOH) see Figure 1. Two truncating somatic APC changes were detected in 2 tumours and 11 tumours had a single *APC* mutation and LOH. The *APC* mutation and LOH frequencies were not significantly different from those found in the sporadic adenomas (Table 6-4); however, the AFAP and MAP tumours had significantly higher frequencies of truncating mutations and lower frequencies of LOH than the MCRA tumours (Table 6-4). No adenoma was found to have a somatic *β-catenin* mutation.

Patient ID	No. adenomas	No. adenomas analysed	Details of truncating mutations	No. adenomas with LOH only	No. ads with somatic truncating APC mutations	1 truncating somatic mutation	Type of somatic change	20aa rpts in somatic mutant allele	2 truncating somatic mutations	Type of somatic change	20aa rpts in somatic mutant alleles	LOH at APC	LOH and truncating somatic mutation	LOH only
1	20	11	1309 delAAAGA; Q1303X C>T; E1379X G>T	NI	3	1309FS	del5bp	0				0	0	0
						Q1303X	C>T	0						
						E1379X	G>T	1						
2	25	11	1350 delA	NI	1	1350FS	delA	1				0	0	0
3	25	14	1310 delAA + LOH	1	1	1310FS	del AA	0				2	1	1
						G1339S	G>A	0						
4	14	18	Q1303X C>T	2	1	Q1303X	C>T	0				4	1	3
5	10	4	E1379X G>T + LOH; E1379X G>T + LOH; E1379X G>T; E1379X G>T	0	4	E1379X	G>T	0				2	2	0
6	26	2	1354 delTT (+ NI)	0	1	1354FS	delTT	0				1	1	0
7	27	9	1465 delAG + 1461 delAA; 1465 delAG; 1465 delAG	3	3	1465FS	delAG	0	1465FS	del AG	2	4	0	4
									1461FS	del AA	2			
8	10	4	G1312X G>T + LOH; 1573 del 5bp	0	2	G1312X	G>T	0				1	1	0
						1573 FS	del5bp	0						
						I1559M	T>G	0						
9	19	6	1493 delA; 1493 delA	3	2	1493FS	delA	1				3	0	3
						P1441S	C>T	3						
10	10	4		0	0	none						1	0	1
11	23	4		1	0	none						2	0	2
12	12	7	1426 delG; 1446 delT; 1490 insC	0	3	1426FS	delG	0				0	0	0
						1446FS	delT	0						
						1490FS	insC	1						
13	27	18		4	0	none						5	0	5
14	76	3	1350 delA	NI	1	1350FS	delA	1				0	0	0
						A1485G	C>G							
15	10	2		0	0	none						1	0	1
16	17	2	1249 delAT + 1473 delT	0	1	1259FS	delAT	0	1259FS	del AT	0	1	0	1
									1473FS	del T	2			
17	50	6	1411 delT; 1472 delT + LOH	0	2	1411FS	delT	0				1	1	0
						1472FS	delT	1						
18	18	3	1490FS insC	0	1	1490FS	insC	1				0	0	0
19	15	3		0	0	none						1	0	1
20	10	3	Q1338X C>T +LOH; 1472FS insT + LOH	0	2	Q1338X	C>T	0				2	1	1
						1472FS	delT	1						
21	30	35	1489FS insT; 1431FS delA; 1489FS insC; 1489FS insT; 1493FS delA; 1472FS del55bp; 1488FS delTT; 1465FS del2bp; 1465FS del2bp + LOH; 1465FS del2bp; 1465FS delG + LOH; 1465FS insT	3	12	1489FS	insT	0				0	0	0
						1431FS	delA	0						
						1489FS	insC	0						
						1489FS	insT	0						
						1493FS	delA	0						
						1472FS	del55bp	0						
						1488FS	delTT	0						
22	33	16	1319FS delC; 1319FS delC; 1466FS del2bp	2	3	1319FS	delC	1				6	0	6
						1466FS	del2bp	2						
23	32	16	1465FS delG +LOH; 1491FS delT; 1491FS delT; 1491FS delT; 1491FS delT; 1491FS delT; 1491FS delT; 1491FS delT; 1491FS delT; 1501FS delT; 1481FS delT; 1500FS delA; 1500FS delA + LOH	1	13	1465FS	delG	2				4	3	1
						1491FS	delT	2						
						1491FS	delT	2						
						1491FS	delT	2						
						1491FS	delT	2						
						1491FS	delT	2						
						1491FS	delT	2						
						1491FS	delT	2						
						1491FS	delT	2						
						1501FS	delT	2						
						1481FS	delT	2						

Table 5: Mutation spectrum at APC including LOH for 25 MCRA cases

Patient ID	No. adenomas	No. adenomas analysed	Details of truncating mutations	No. adenomas with LOH only	No. ads with somatic truncating APC mutations	1 truncating somatic mutation	Type of somatic change	20aa rpts in somatic mutant allele	2 truncating somatic mutations	Type of somatic change	20aa rpts in somatic mutant alleles	LOH at APC	LOH and truncating somatic mutation	LOH only
						1500FS	delA	2						
						1500FS	delA	2						
24	50	7	1465FS delAG; 1491FS delT	1	2	1465FS	delAG	2				1	1	1
						1491FS	delT	2						
25	21	13	1465FS del2bp (LOH failed); 1465FS del2bp complete loss D5S346	0	2	1465FS	del2bp	2				1	1	0
						1465FS	del2bp	2						

Table 5: Mutation spectrum at APC including LOH for 25 MCRA cases

	MCRA	Sporadic	AFAP	MAP
Truncating mutation	49/221 (22%)	10/56 (18%) p=0.59	91/242 (38%) **p<0.001**	25/34 (74%) **p<0.001**
LOH	32/190 (17%)	5/56 (9%) p=0.20	19/230 (8%) **p=0.01**	1/34 (3%) **p=0.02**

Table 6–4 Comparison between *APC* mutation frequencies and LOH in MCRA, sporadic, AFAP and MAP cases. p values are comparisons with the MCRA group using Fishers Exact test

See Figure 6–1 for example of LOH and Figure 6-2 for examples of somatic *APC* mutations.

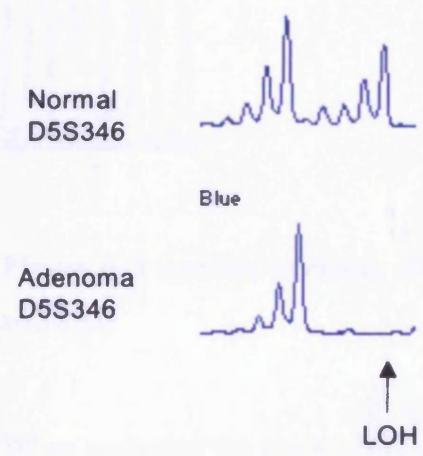

Figure 6–1 LOH at microsatellite marker D5S346 in MCRA adenoma

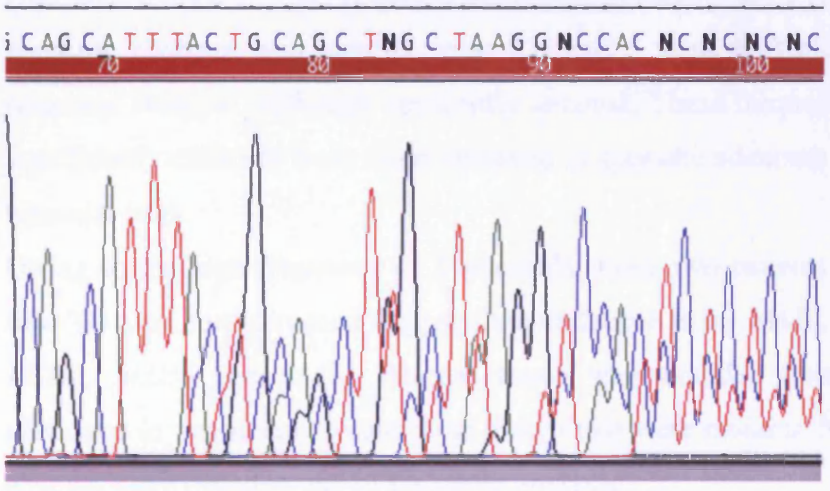

Figure 6–2 Frameshift mutation in MCRA adenoma *APC* MCR9 del A 1472 frameshift, stop @ 1506

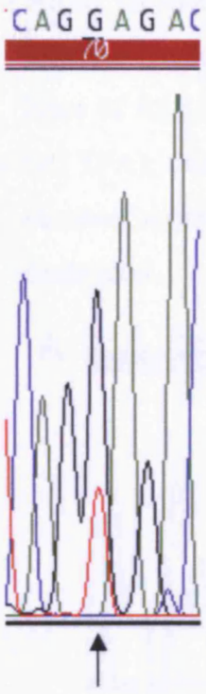

Figure 6–3 Somatic mutation in MCRA adenoma *APC* MCR5 E1379X (G>T arrowed)

When analysing the mutation spectrum on an individual patient basis none had a specific tendency to frameshift changes, specific nonsense mutations, or to LOH at *APC* (Table 6-5).

One patient (case 21) had acquired frameshift mutations in 13 tumours and no nonsense changes, and another (case 23) had 5 frameshift changes and no nonsense changes. Although apparently unusual, These frequencies were not significantly different from those observed in sporadic adenoma ($p>0.1$, exact binomial test).

Owing to the high frequency of frameshifts, these two patients (case 21 and case 23) were then screened for germline mutations in the MMR genes *MLH1, MSH2, MSH6* and *PMS2*. Normal tissue was included from around the adenomas in this screen in case these individuals were mosaics. No pathogenic changes were found in any of the genes analysed.

A total of 12 (24%) *K-ras* mutations were detected in 51 MCRA tumours analysed; 10 mutations occurred at codon 12 and two mutations, at codon 13.

All of the changes - G12A, G12D, G12V and G13D - have been previously reported to occur frequently in sporadic adenomas and CRCs.

Nine of 85 (11%) MCRA adenomas analysed had a *BRAF* mutation V600E (all T>A); this is higher that would be expected in tubular adenomas without serrated morphology. See Figure 6–4 for examples of *K-ras* and *BRAF* mutations.

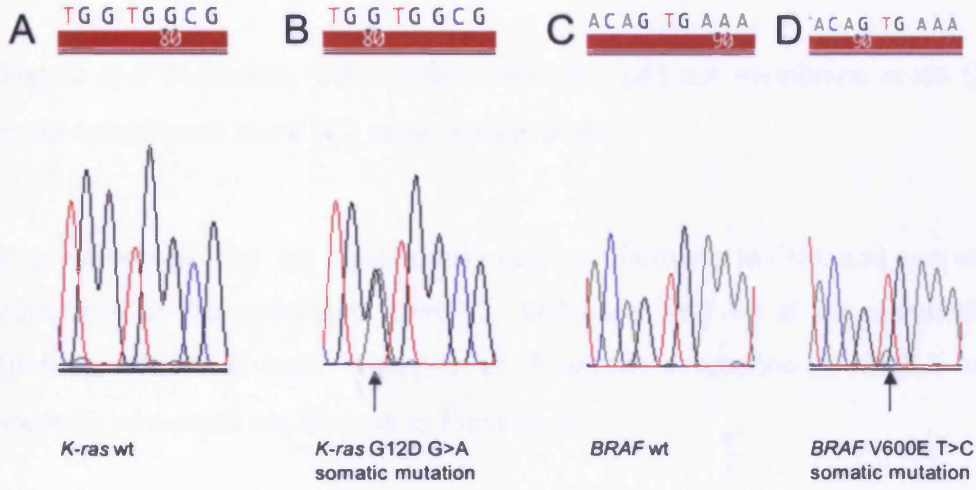

Figure 6–4 Examples of *K-ras* and *BRAF* somatic mutations in MCRA cases

No tumour harboured both *K-ras* and *BRAF* mutations. The *K-ras* and *BRAF* mutation frequencies in the MCRA tumours were not significantly different from those in the sporadic adenomas (5/34 (p=0.58) and 5/40 (p=0.73) respectively, Fisher's exact test).

6.3.5 Beta-catenin expression

The 57 MCRA tumours analysed for β–catenin expression demonstrated increased nuclear expression when compared to the 27 sporadic adenomas analysed (p=0.0087, Wilcoxon test) (see Figure 6–5). There was, however, no significant difference in nuclear β–catenin expression between the MCRA group's tumours and a set of 33 adenomas of similar size from 6 individuals with FAP (p=0.09, Wilcoxon test).

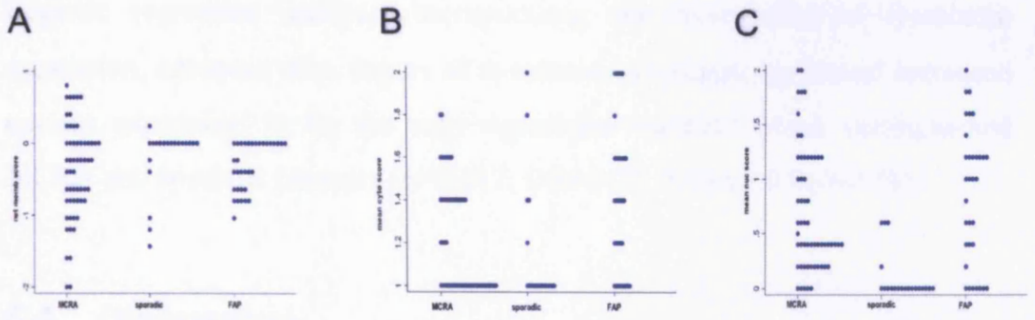

Figure 6–5 β–catenin immunohistochemistry, (**A**) net membrane score (**B**) mean cytoplasmic score (**C**) mean nuclear score

Expression was also not significantly different between MCRA and sporadic adenomas in the cytoplasm (p=0.12, Wilcoxon test) or at the membrane (p=0.63, Wilcoxon test). Examples of β–catenin expression in MCRA and sporadic adenomas can be seen in Figure 6–6.

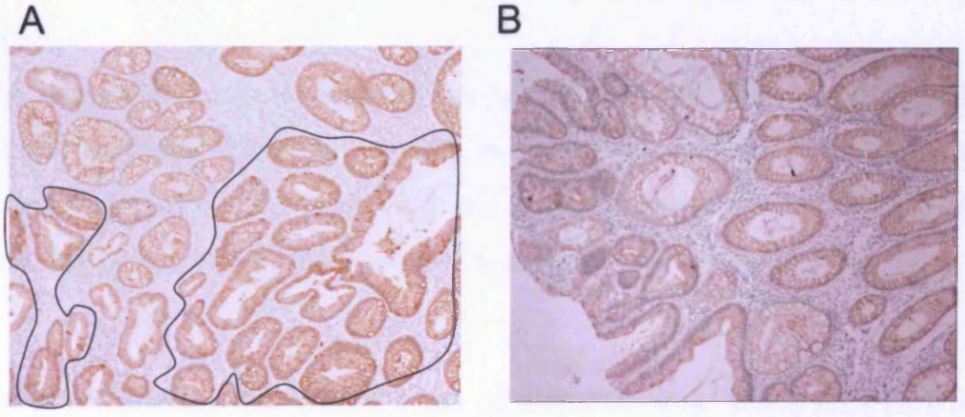

Figure 6–6 β–catenin immunohistochemistry in MCRA (**A**) and sporadic (**B**) adenoma both x100, crypts demonstrating increased nuclear staining circled

Logistic regression analysis incorporating the three sites of β–catenin expression, adenoma size, degree of dysplasia and patient age found increased nuclear expression to be the only significant variable which distinguished MCRA and sporadic tumours (p=0.017, OR=0.22, 95% CI 0.065-0.76).

6.4 Discussion

6.4.1 No microadenomas were identified in MCRA cases

Historically, microadenomas have been said to be pathognomic of FAP. This study demonstrates that they also occur in AFAP and MAP. Given that FAP microadenomas have been found to harbour somatic mutations at *APC* (see Chapter 9), it is likely that they are the earliest detectable lesion which has been "initiated" by "two hits" at *APC* (germline plus somatic mutation for AFAP, or two somatic mutations in MAP).

The finding that the number and density of microadenomas detected was highest in FAP followed by AFAP and finally MAP fits the "two hit" hypothesis of microadenoma formation with the likelihood and speed at which "two hits" would occur in the FAP group being highest and lowest in the MAP group.

The absence of microadenomas in the MCRA cases suggests that their cells are not acquiring "two hits" at *APC* at an appreciably faster rate than the general population. The mechanism of tumour predisposition in the MCRA cases may therefore involve a stage of tumorigenesis that is post-initiation.

6.4.2 No definitive mutational signature was identified in the MCRA patients' tumours

In the MCRA patients' tumours, the total of 51 truncating *APC* mutations (Table 6-5) comprised 44 frameshifts (small insertions or deletions) and 7 nonsense mutations (3 C:G>T:A transitions and 4 G:C>T:A transversions). Although the proportion of frameshift mutations was higher than in the *APC* mutation database (Laurent-Puig, Beroud et al. 1998) this may have resulted

from detection bias in small, archival tumours, which were the only samples available from the patients studied. Decreased nonsense and missense mutation detection sensitivity in such samples has previously been observed (Groves, Lamlum et al. 2002). This is in part due to the poor quality of DNA extracted from paraffin embedded samples. The DNA is often "sheared" into smaller segments through the extraction process, resulting in fragments often only ~200bp in length.

In support of this contention, the excess of frameshifts in the MCRA tumours was very similar (p=0.44, Fisher's exact test) to that in the sporadic adenomas, which had acquired 8 frameshift changes, plus one A:T>T:A transition and one G:C>T:A transversion. The *APC* mutation spectrum in the MCRA tumours contrasted with the finding that all 25 truncating mutations in the MAP tumours were G:C>T:A transversions (p<0.001, Fisher's exact test).

If the MCRA cases had, like MAP patients, a tendency to hypermutation of *APC* in the gastrointestinal tract, it might be expected that a similar spectrum of disease to MAP or (A)FAP would occur. Therefore, it is likely that MCRA results either from hypermutation of *APC* in the large bowel only, or from a distinct pathogenic mechanism that does not involve a tendency to inactivation of *APC*.

All changes in the tumours of patients case 21 and case 23 occurred in a particular region of the *APC* gene, between the 2nd and 3rd 20-amino acid *β-catenin* binding and degradation repeats. Such a spectrum of mutations might be expected in patients with a germline *APC* mutation before codon 1280 (Albuquerque, Breukel et al. 2002) (Crabtree, Sieber et al. 2003) (Lamlum, Ilyas et al. 1999) or with a deficiency in MMR that did not manifest as MSI in adenomas (Wu, Berends et al. 1999).

In the MCRA patients, the *K-ras* mutations comprised 6 G:C>A:T, 5 G:C:>T:A, and 1 G:C>C:G changes. This mutation spectrum overall was similar to that of the sporadic adenomas, which had 9 G:C>A:T, 3 G:C>T:A, and 2 T:A>A:T mutations (p=0.31, Fisher's exact test). As in the case of *APC*, these *K-ras* mutation spectra contrasted with the sole change, G12C (G:C>T:A), found in MAP tumours. As might be expected, all of the *BRAF* mutations were T:A>A:T transitions resulting in the V600E change. No

adenoma had both *K-ras* and *BRAF* mutations. There was no association between the presence of *APC* and *K-ras* or *BRAF* mutations.

Overall, these findings strongly suggested that there is no common mutational signature in the MCRA group of patients, subject to the limitations of screening large genes, such as *APC,* in DNA of relatively low quantity and poor quality. Despite these difficulties, the difference from MAP was striking, once again suggesting that there is no specific tendency to hypermutation in this set of MCRA cases.

6.4.3 Nuclear Beta-catenin expression is increased in MCRA tumours

Unlike the other molecular analyses described in this chapter, β–catenin immunohistochemistry showed clear differences between MCRA and sporadic adenomas, with expression in MCRA tumours being similar to FAP. The greater Wnt activation in MCRA patients' tumours was too consistent to be readily explained by the inclusion of one or two individuals with cryptic, as yet undetected, germline *APC* or *MYH* mutations in the MCRA group. Allowing for the fact that colorectal microadenomas probably vary in their progression to macroscopic lesions (Crabtree, Tomlinson et al. 2001), this finding raises the possibility that increased Wnt activation in MCRA may lead to microadenoma development more rapidly, or with greater probability to progress to macroadenomas. Our studies to date (Lipton, Sieber et al. 2003) have not identified causal germline mutations in Wnt pathway genes in MCRA cases. However many Wnt related genes remain to be studied in MCRA cases such as the Wnt inhibitory factors Wif, Dickkopf-1 and Snail 1 (Larriba, Valle et al. 2007).

Future work might include immunohistochemistry studies of the Wnt inhibitory factors Wif1 and Dickkopf1 in MCRA cases to determine whether their level of expression correlates with the increased nuclear expression of β–catenin in MCRA cases.

6.4.4 MCRA adenomas do not follow the "classical" pathway of tumorigenesis

All of the MCRA adenomas studied had tubular or tubulovillous morphology. It is therefore not surprising that the prevalence of *K-ras* (24%) and *BRAF* (11%) mutations detected were in keeping previous published data for these morphologies (Jass, Baker et al. 2006). In Jass's study (Jass, Baker et al. 2006) comparison of *K-ras* and *BRAF* mutation rates alongside MGMT loss in a wide variety of polyps found *K-ras* mutations in 18% and *BRAF* mutations in 5% of TAs <10mm (see Table 6-6 for summary modified from (Jass, Baker et al. 2006)). What is surprising is the higher incidence of *BRAF* mutations in the MCRA group none of which demonstrated serrated morphology.

Table 6-6 Summary of somatic *K-ras* and *BRAF* mutations and loss of expression of MGMT found in polyps of differing histology. Modified from (Jass, Baker et al. 2006)

The absence of microadenomas in the MCRA group demonstrates that the initiation step of bi-allelic *APC* mutation associated with the classical pathway of tumorigenesis does not occur.

One explanation which fits this dataset would support the "crossover" theory that sessile / serrated adenomas with predominantly *BRAF* mutations would later develop *K-ras* mutations rendering them more aggressive. A very small number of adenomas have been reported to harbour both *K-ras* and *BRAF* mutations (2% of a series of 189 polyps studied) (Jass, Baker et al. 2006). No adenomas in this study harboured both mutations.

It was not possible to screen for mutations in other known components of the classical pathway of tumorigenesis (such as *p53*) due to limited amounts of DNA extracted from paraffin embedded tissue.

6.4.5 Limitations of this study

One of the main limitations of this study was the availability and access to high quality (and quantity) of DNA for analysis in all groups undergoing analysis. This was because the majority of samples were paraffin embedded tumour blocks.

Following the finding of increased nuclear expression of β–catenin in the MCRA group, I would have wanted to proceed to screen the MCRA cases for other Wnt related factors such as the Wnt inhibitory factors should DNA have been available.

Examination for loss of MGMT expression would have helped to support / disprove the suggestion that "crossover" may occur from the serrated to the classical pathways in the MCRA group.

6.5 Conclusions

To date, Mendelian colorectal cancer syndromes can be categorised in two ways. First, the primary predisposition may be to polyps or to carcinoma. Second, the primary defect may be in either a 'gatekeeper gene' (such as *APC*, *LKB1, SMAD4/MADH4* and *ALK3/BMPR1A*) or a caretaker/DNA repair gene (such as the MMR loci and *MYH/MUTYH*). The MCRA cases studied with no germline *APC* or *MYH* mutations are likely *a priori* to have a strong genetic predisposition, given the phenotypic similarity to MAP and AFAP.

In the MCRA cases, multi-generational inheritance of multiple adenomas was not found, suggesting recessive – or, perhaps, multi-locus - inheritance.

Several possible explanations for the MCRA phenotype exist, and these patients may be a heterogeneous group.

The similar frequencies of changes at *APC*, *K-ras* and *BRAF* in MCRA and sporadic cases suggest that the genetic pathways of tumorigenesis overlap, at least with regards to these three genes.

The differences in mutation spectra observed between MAP and AFAP reinforce the likelihood that hypermutation of *APC* and/or *K-ras* does not drive tumorigenesis in this set of MCRA patients, particularly as the incidence of *K-ras* mutation is lower in MCRA group than both MAP and AFAP adenomas.

The most significant finding separating the MCRA and sporadic groups in terms of their molecular profiling was the increased nuclear expression of *β–catenin*.

Somatic mutation frequencies and spectra in MCRA adenomas were found that are very similar to comparable sporadic lesions, and distinct from AFAP and, especially, MAP. No microadenomas were found in the MCRA patients' colons. These results suggest that hypermutation of *APC* does not cause the MCRA patients' disease and indeed does not initiate the disease suggesting they do not follow the classical pathway of tumorigenesis. This strongly suggests that MAP is not a paradigm for the remaining MCRA patients. One possibility may be that those few microadenomas which do occur spontaneously in MCRA cases have an increased chance of progressing to a macroadenoma. Another possibility is that of "crossover" between the serrated and classical pathways of tumorigenesis. This model is supported by the immunohistochemical analysis of β–catenin expression in this study. If this is the case, it seems unlikely that the predisposition gene is a 'gatekeeper' type of tumour suppressor (since MCRA disease seems to be isolated or recessive), or a 'caretaker' (since no evidence of a specific DNA repair defect was found). It could be suggested that these data best fit a modified 'landscaper' model of tumorigenesis in which the intra-cellular or extra-cellular microenvironment of cells is altered to favour tumour progression from microadenoma to macroadenoma.

7 Lymphoblastoid cell line expression array analysis of MCRA cases

7.1 Introduction

To date it has proven very difficult to identify novel predisposition genes in the MRCA phenotype. This is in part due to the fact that some of these cases are inherited recessively making traditional linkage analysis harder, and also due the likelihood that these cases may be due to inheritance of mutated genes which are of moderate or low penetrance.

When considering "isolated" or possibly recessive cases in the MCRA group one approach which could identify homozygous or compound heterozygous mutations is comparison of mRNA transcripts isolated from lymphoblastoid cell line DNA in MCRA cases and normal controls. The differences in expression profiles would highlight genes and biological pathways affected by inherited germline mutations if these genes had a profound effect on transcript levels.

During cellular replication, mutant mRNA transcripts (where an error in replication may have occurred or a correct transcript from a mutated germline gene has occurred) are destroyed by a process called nonsense-mediated decay NMD, therefore maintaining the integrity cellular replication. The nonsense RNA transcripts most commonly arise from nonsense or frameshift mutations creating premature translation termination codons (PTC).NMD is activated when mulit-protein exon junction complexes (EJC) assemble around aberrant exon/exon junctions following the first round of DNA synthesis in cellular replication (Ishigaki, Li et al. 2001). The EJCs are removed from spliced mRNA during the translation step when mRNA passes through the ribosome. This mechanism works for any PTC located more than 50 nucleotides upstream if the last exon/exon junction. The unremoved EJCs found downstream of the PTC recruit the Upf protein complex subsequently initiating the degradation of the PTC containing transcript (Holbrook, Neu-Yilik et al. 2004). NMD is therefore an mRNA surveillance mechanism which

prevents the production of truncated proteins. If putative MCRA pre-disposition genes are inherited recessively, bi-allelic nonsense mutations could trigger NMD and subsequent loss of expression (if the gene of interest is expressed in lymphocytes).

Analysis of gene expression is viewed by some as the determination of a more refined phenotype as it is a measure of phenotypic variance at a molecular level (Monks, Leonardson et al. 2004). Each gene-expression phenotype can provide annotation, pathway and genome location data. In isolated or recessive diseases such as the MCRA phenotype this approach could potentially identify not only quantitative trait loci, but also identify subsequent genes, pathways and biological processes under the influence of such loci.

Jansen and Nap first described the use of expression profiling in separating populations (Jansen and Nap 2001). Soon after, differences in expression were observed between sexes in *Drosophila melanogaster* (Jin, Riley et al. 2001) which has since been observed in the study of human lymphoblastyoid cell lines (Zhang, Bleibel et al. 2007). In Zhang's study, differences in expression between the sexes were observed in pathways involving adherens junctions and cytokine-cytokine receptor interaction (based on KEGG (Kyoto Encyclopaedia of Genes and Genomes) analysis).

Differences in lymphoblastoid cell line mRNA expression between different ethnic populations has also been observed. A study of lymphoblastoid cell line expression from the full set of European and African HapMap samples found differing expression in biological processes such as ribosome biogenesis and antimicrobial humeral response were found in the 383 transcript clusters found between the two populations (Zhang, Duan et al. 2008).

Differences in expression can be also observed if culturing conditions vary – if the cell line is "stressed" (cultured for too long or cells not split / fed at the same time intervals).

In light of these findings, differences in expression between different populations, sexes and culture conditions were taken in to account on design of this study.

A previous study of lymphoblastoid cell lines from autistic cases (another heterogenous condition) and control samples demonstrated differences in expression profiling between cases and controls (Nishimura, Martin et al. 2007). Nishimura *et al* used expression microarray analysis to successfully identify differences in mRNA expression profile in lymphoblastoid cells from males with autism with known underlying germline mutations (fragile X mutation (FMR1-FM), or a 15q11-q13 duplication (dup(15q)), and non-autistic controls. I used this data as proof of principle for this study.

For this study I chose the "best" MCRA cases from my cohort, ie those individuals with the largest number of adenomas present at the youngest age.

7.1.1 Aims of this chapter

The aim of this study was to identify any differences in mRNA expression profiling in MCRA "cases" and normal "controls". These differences could help to identify underlying genetic defects or biological pathways (as a secondary aim) affected by an underlying mutated predisposition gene.

7.2 Methods

Patient samples

Venous blood was collected from eleven MCRA patients and 5 controls after obtaining informed consent.

Expression array analysis

Eleven MCRA and five control lymphoblastoid cell lines were produced from peripheral venous blood samples obtained with prior consent – see Methods (2.1.2.1).

A total of ~ 9 x 10^6 lymphoblastoid cells were seeded in a 150ml falcon culture flask (Falcon) and then incubated at 37°C in 10% CO_2 for 72 hours –

see Methods (2.1.9.1-3). mRNA was then extracted from healthy cell lines cultured in identical conditions – see Methods (2.1.2.1). RNA quality and quantity was then analysed on the Agilent 2100 Bioanalyser (Agilent, Santa Clara, CA, USA).

Complementary RNA ((cRNA) - following synthesis of cDNA) was hybridised to Affymetrix GeneChip® Human Genome U133 Plus 2.0 Expression Micro-arrays – see Methods (2.1.10). The U133 Plus 2.0 array comprises 54,000 probe sets covering 47,000 transcripts from 38,000 characterised human genes. All the probe sets are duplicated across the array. Oligonucleotide probes (25-mer) complimentary to each sequence are synthesised *in situ* on the array. Eleven pairs of probes are used to measure the level of transcription of each sequence represented on the array. Each array includes control sequences covering hybridisation quality, poly-A controls, normalization (determination of consistency of expression) and housekeeping/control genes (GAPDH, beta-Actin, ISGF-3 (STAT1). See Affymetrix website for further details - http://www.affymetrix.com/products/arrays/specific/hgu133.affx.

Statistical analysis

Statistical analysis and identification of genes with a significant >3-fold change in expression was undertaken using the statistical package R with individual programs written for data analysis by the bioinformatics department at Cancer Research UK, London Research Institute (P. East).

Probe level intensities were quantile normalised and probeset level signal intensity estimates calculated using RMA (Irizarry, Bolstad et al. 2003). A linear model was fitted to the data and differential genes between the MCRA and control groups were selected using a 0.05 FDR (false discovery rate) threshold. T-statistics were moderated prior to differential gene identification using an empirical Bayes method to converge probeset sample variances to a common value (Smyth 2004). Genes were further filtered using a 5-fold threshold. These genes are represented in a heatmap in the Results section. The analysis was carried out using the limma package from Bioconductor 2.2. (Gentleman, Carey et al. 2004). Reported annotation is from the hgu133plus2 Bioconductor annotation package.

Scatter and volcano plots were produced to confirm the quality of the experiment and robustness of the data. Heirarchical clustering using Spearman's rank correlation with average linkage clustering was then performed.

Finally, functional annotation clustering was then performed using DAVID KEGG and GO analysis. DAVID (Database for Annotation Visualisation and Integrated Discovery) is a clustering algorithm based on the hypothesis that similar annotations should have similar gene members from different biological pathways (Dennis, Sherman et al. 2003). KEGG is an integrated bioinformatics resource which combines information from three databases incorporating genomic, chemical and network information (Kaneshisa M 2004). The GO (Gene Ontology) project provides a systematic description of attributes of genes (and gene products) in three domains shared across all organisms, molecular function, biological process and cellular component (Ashburner, Ball et al. 2000).

7.3 Results

7.3.1 Expression micro-array analysis

Patient Demographics

MCRA cases were aged between 28 and 69 years (median 52 years) Adenoma burden ranged from 17 to 100 (median 23 adenomas) see Table 7–1. Two cases were diagnosed with CRC (case 6 at 67 years and case 9 at 59 years). CRC was present in 1st degree relatives of two cases (case 8 at 85 years and case 11 at 60 years). All cases were of white European origin. Germline *APC* and *MYH* mutations were excluded prior to inclusion in the study. The control set were of similar age range and ethnic background.

Pt ID	Age Diagnosis	No Ads	CRC	FH CRC	Cell line
1	28	100	N	no	JUM0287/CORGI/03/MPG
2	69	34	N	no	EIG0294/CORGI/03/MPG
3	67	27	N	no	JOH0326/CRMA/03/MPG
4	51	26	N	no	WIA0324/CRMA/03/MPG
5	52	26	N	no	FRL0237/CRMA/01/MPG
6	68	23	Y - 67 yrs	no	LEM0323/CRMA/03/MPG
7	51	21	N	M - CRC 85 yrs	ANH0207/CRMA/01/MPG
8	61	19	N	no	TER0297/CORGI/03/MPG
9	50	18	Y - 50 yrs	no	STM0315/CRMA/03/MPG
10	50	17	N	M - CRC 60 yrs	QUB0320/CRMA/03/MPG
11	55	17	N	no	WIM0313/CRMA/03/MPG

Table 7–1 Patient demographics of MCRA cases studied

Fold changes of mRNA detected in MCRA cases and controls

Overall, 1059 probes representing 881 genes were identified with a FDR threshold of 0.05. The percentage of "present" calls across all the probesets for cases and controls were similar (cases range 36.1 – 47.4, median 43.3; controls range32.5 – 46.7, median 43.7).

Transcripts representing 61 genes were expressed with a greater than 3-fold difference compared to controls and with a p value of <0.01. See Table 7–2 for list of genes with >3 fold change. See Appendix 3 for case-by-case results.

Gene Symbol	Absolute fold	Map	Gene
RGS13	7.682	1q31.2	regulator of G-protein signalling 13
APP	5.752	21q21.2;21q2	amyloid beta (A4) precursor protein
IGF2BP3	5.495	7p11	insulin-like growth factor 2 mRNA binding protein 3
FAM111B	5.336	11q12.1	family with sequence similarity 111, member B
VSIG9	5.153	3q13.31	V-set and immunoglobulin domain containing 9
SLC39A10	4.775	2q32.3	solute carrier family 39 (zinc transporter), member 10
GRK5	4.435	10q24-qter	G protein-coupled receptor kinase 5
DAPP1	4.421	4q25-q27	dual adaptor of phosphotyrosine and 3-phosphoinositides
NCOA6IP	4.296	8q11	nuclear receptor coactivator 6 interacting protein
LMO7	4.276	13q22.2	LIM domain 7
ZNF83	4.225	19q13.3	zinc finger protein 83
ZWILCH	4.148	15q22.31	Zwilch, kinetochore associated, homolog (Drosophila)
RBM25	4.137	14q24.3	RNA binding motif protein 25
TPR	4.13	1q25	translocated promoter region (to activated MET oncogene)
LYAR	4.106	4p16.2	NA
IL6ST	4.094	5q11	interleukin 6 signal transducer (gp130, oncostatin M receptor)
POLE2	3.938	14q21-q22	polymerase (DNA directed), epsilon 2 (p59 subunit)
FAM111B	3.904	11q12.1	family with sequence similarity 111, member B
CYCS	3.886	7p15.2	cytochrome c, somatic
C1orf79	3.722	1p35.3	chromosome 1 open reading frame 79
NA	3.72	NA	NA
SYNE2	3.716	14q23.2	spectrin repeat containing, nuclear envelope 2
CASC5	3.702	15q14	cancer susceptibility candidate 5
PITPNC1	3.699	17q24.2	phosphatidylinositol transfer protein, cytoplasmic 1
CD74	3.695	5q32	CD74 molecule, major histocompatibility complex
DUT	3.679	15q15-q21.1	dUTP pyrophosphatase
PON2	3.66	7q21.3	paraoxonase 2
CCNE2	3.624	8q22.1	cyclin E2
CDC42BPA	3.624	1q42.11	CDC42 binding protein kinase alpha (DMPK-like)
MLF1IP	3.621	4q35.1	MLF1 interacting protein
HNRPDL	3.599	4q13-q21	heterogeneous nuclear ribonucleoprotein D-like
CCNE2	3.596	8q22.1	cyclin E2
DDX46	3.58	5q31.1	DEAD (Asp-Glu-Ala-Asp) box polypeptide 46
POGK	3.534	1q24.1	pogo transposable element with KRAB domain
GDAP1	3.517	8q21.11	ganglioside-induced differentiation-associated protein 1
HDGFRP3	3.458	15q11.2	NA
UBD	3.432	6p21.3	ubiquitin D
HELLS	3.4	10q24.2	helicase, lymphoid-specific
WBP5	3.371	Xq22.1-q22.2	WW domain binding protein 5
CDC6	3.37	17q21.3	CDC6 cell division cycle 6 homolog (S. cerevisiae)
APP	3.366	21q21.2;21q2	amyloid beta (A4) precursor protein
RGS13	3.359	1q31.2	regulator of G-protein signalling 13
ANKRD44	3.334	2q33.1	ankyrin repeat domain 44
SCML1	3.315	Xp22.2-p22.1	sex comb on midleg-like 1 (Drosophila)
MCM4	3.289	8q11.2	MCM4 minichromosome maintenance deficient 4 (S. cerevisiae)
C21orf71	3.281	NA	chromosome 21 open reading frame 71
TFAM	3.274	10q21	transcription factor A, mitochondrial
FMNL2	3.258	2q23.3	formin-like 2
UHRF1	3.235	19p13.3	ubiquitin-like, containing PHD and RING finger domains, 1
RNF36	3.211	15q21.1	ring finger protein 36
NASP	3.2	1p34.1	nuclear autoantigenic sperm protein (histone-binding)
NA	3.151	NA	NA
TNFRSF7	3.123	12p13	tumor necrosis factor receptor superfamily, member 7
MCM10	3.118	10p13	MCM10 minichromosome maintenance deficient 10 (S. cerevisiae)
HLA-E	3.117	6p21.3	major histocompatibility complex, class I, E
UTP20	3.101	12q23	UTP20, small subunit (SSU) processome component, homolog (yeast)
PAK1IP1	3.086	6p24.2	PAK1 interacting protein 1
FUS	3.077	16p11.2	fusion (involved in t(12;16) in malignant liposarcoma)
HELLS	3.071	10q24.2	helicase, lymphoid-specific
GPATC4	3.046	1q22	G patch domain containing 4
FUT4	3.039	11q21	fucosyltransferase 4 (alpha (1,3) fucosyltransferase, myeloid-specific)
MCM4	3.025	8q11.2	MCM4 minichromosome maintenance deficient 4 (S. cerevisiae)
PCBP2	3.019	12q13.12-q13	poly(rC) binding protein 2
ZNF718	3.01	4p16.3	zinc finger protein 718

Table 7–2 Genes with > 3-fold change in expression when compared to controls with associated p value <0.01

No evidence of chromosomal loci of potential loss or gain were identified when fold changes were noted along the whole genome from chromosome 1p to 22q both with either pooled data for the MCRA cases or on a case-by-case basis. This aim of this analysis was to identify any gross chromosomal losses or gains leading to altered gene expression, however the likelihood of there being this type of change is low.

Individual cases were then reviewed noting genes of interest with markedly over or under-expressed genes. See Appendix 3 for individual case results.

The following genes of interest were over-expressed on an individual case basis *PLAGL1* (pleomorphic adenoma gene like 1, 4.77x over-expressed in case 1), *PTEN* (phosphatase and tensin homologue, 6.09x over-expressed in case 6), *PERP* (TP53 apoptosis effector, 6.81x over-expressed in case 9), *RAB31* (RAS oncogene family member 4.76x over-expressed in case 9) and *TNFRSF19* (tumour necrosis factor receptor superfamily member 19, 9.03x over-expressed in case 11). *EphrinB1* was under-expressed (5.26x) in case 9.

CXCR4, *DUT* and *POLE2* were under-expressed (> 3 fold) in several cell lines and were taken forward for further study as candidate genes in the following Chapter. See Table 7–3 for overview of fold changes across the 11 cases studied.

Pt ID	No Ads	Gene			
		CXCR4 probe 1	CXCR4 probe 2	DUT	POLE2
1	100	1.82	2.70	3.84	2.27
2	34	2.94	2.70	5.89	5.88
3	27	0.80	0.53	2.04	1.82
4	26	2.78	5.00	1.58	2.56
5	26	2.00	1.22	2.19	3.00
6	23	4.35	3.70	1.74	2.43
7	21	0.45	0.45	3.79	2.92
8	19	3.23	1.37	2.03	2.89
9	18	3.13	2.32	3.08	3.33
10	17	3.03	3.45	2.11	3.00
11	17	1.28	1.61	4.58	5.00

Table 7–3 Overview of fold changes across all cell lines in *CXCR4, DUT* and *POLE2,* dark pink - > 3fold change, light pink – ~3 fold change

Heat maps of cases and controls

The heatmap below (Figure 7–1) shows the differential genes identified between the multiple adenoma and control groups using a 0.1 FDR threshold. Genes were further filtered using a >2 fold filter. Each multiple adenoma case probeset value has seen scaled to the probeset median across all samples. The magnitude of differential expression is represented on a log2 scale (-4 to 4). The cases and controls cluster separately across the heatmap when filtered using a >2 fold filter.

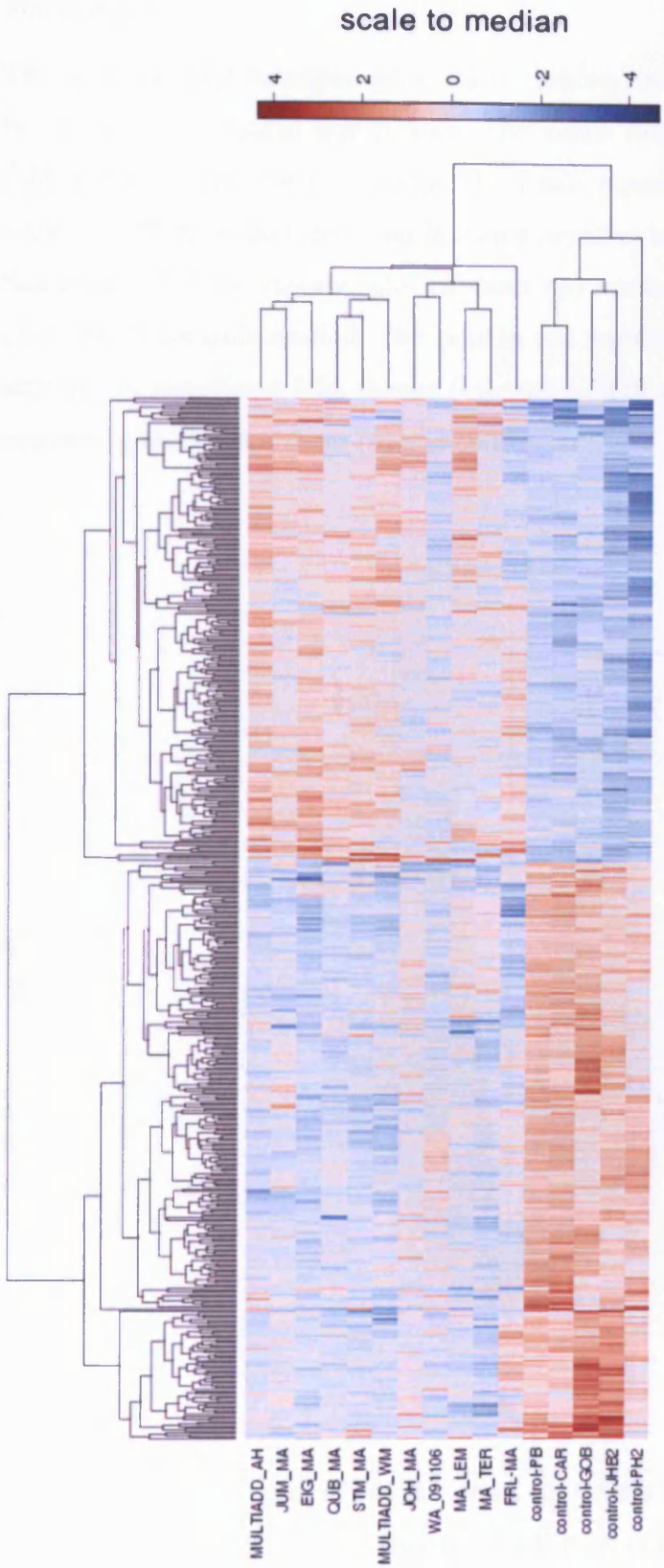

Figure 7–1 Heatmap of MCRA cases and controls demonstrating difference in expression in MCRA cases and controls when compared to the median

Volcano plot

The Volcano plot arranges gene transcriptions studied according to their biological and statistical significance. The x-axis (log scale) demonstrates the fold change between the two groups The y-axis represents the p-value for each t-test of differences between samples (on a negative log scale).

See Figure 7–2 for volcano plot of cases (p) versus controls (c) for the 11 cases and 5 controls studied. The dots in red represent the transcripts with a statistically significant fold change (>3 with a FDR of 0.05 or smaller) when comparing the MCRA cases (p) and controls (c).

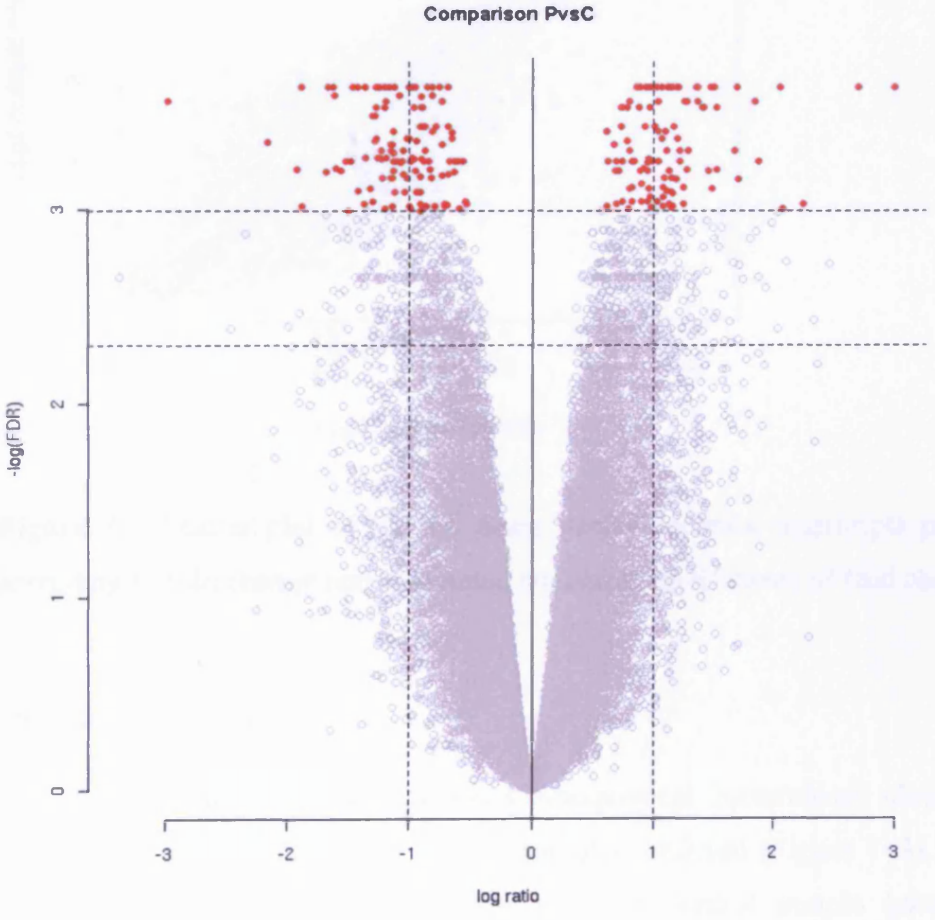

Figure 7–2 Volcano plot of MCRA cases (p) versus controls (c), the red dots represent the trancripts which are expressed in cases but not controls with > 3 fold change and FDR <0.05

Scatter plot

The scatter plot (Figure 7–3) plots gene transcripts of cases against controls according to the fold change and the associated statistical significance of the observed change. The plot of the MCRA cases against controls is symmetrical– demonstrating a "good" experiment

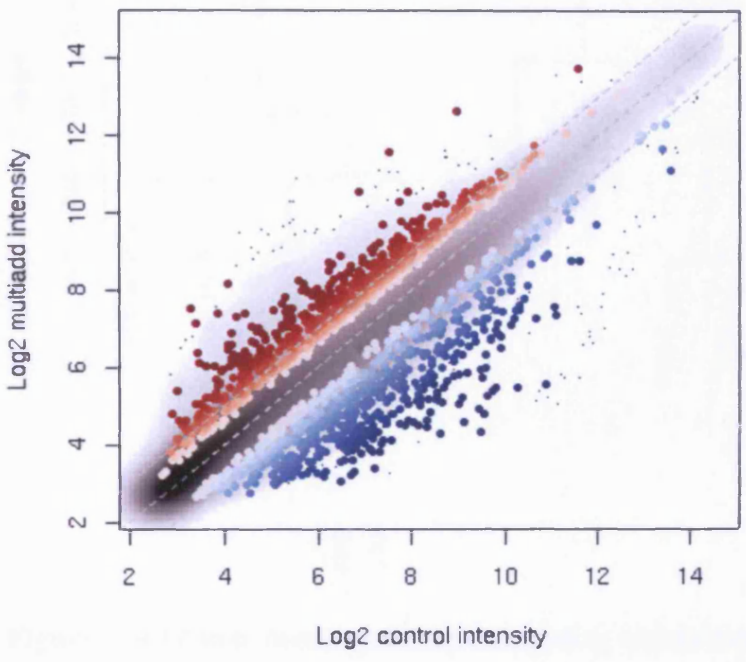

Figure 7–3 Scatter plot of MCRA cases versus controls, transcripts plotted according to fold change and associated statistical significance of fold change.

Cluster dendrogram

The cluster dendrogram demonstrates unequivocal hierarchical clustering between the MCRA cases and control samples analysed (Figure 7–4). With the exception of one MCRA sample and one control sample (clustered together on the right of the figure) all of the remaining MCRA cases and control cluster separately indicating similarities of gene expression within the groups and differing expression between the groups.

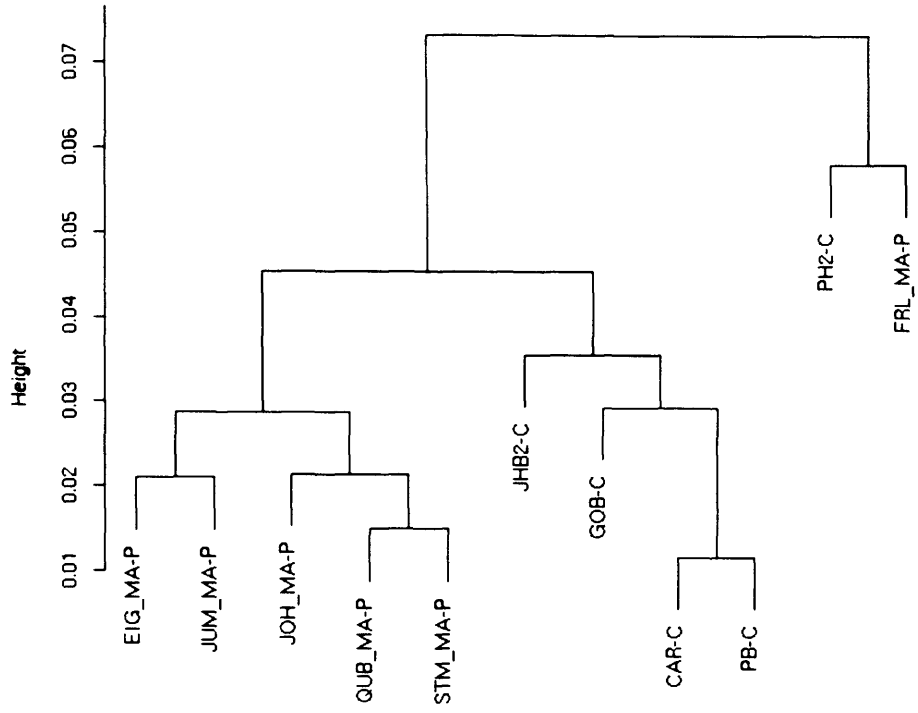

Figure 7–4 Cluster dendrogram demonstrating hierarchical clustering between MCRA cases and controls

Functional annotation and pathway analysis

No significant biological pathways were disrupted by the loss of multiple genes when using DAVID, KEGG and GO tools of analysis.

7.4 Discussion

Overall, this experimental approach enabled the identification under-expressed transcripts in MCRA cases when compared to the expression profile of controls. However, one of the most significant difficulties encountered with

this approach is the interpretation of the "missed" or "absent" probe calls. Despite the call rate across the cases and controls being equal and of a similar standard to other groups (Nishimura, Martin et al. 2007) the fact that a probe may have an "absent" call could indicate that the particular gene which it represents is not expressed by lymphocytes. In this study, results from every probe in the MCRA cases and controls (whether "absent" or not) were included in the statistical analysis.

7.4.1 Transcripts chosen for further study

The following transcripts were chosen for further study based on their fold change (across all cases) and relevance of their function in tumorigenesis. All were under expressed suggesting a loss of function.

CXCR4 is the chemokine receptor for stromal cell-derived factor-1α (SDF-1α). It is a seven-transmembrane receptor G protein coupled receptor and is known to be a co-receptor for HIV (Feng, Broder et al. 1996). In haemopoetic cells, it has been demonstrated that c-kit and *CXCR4* interact to provide homing to the bone marrow. *CXCR4* has also been shown to have a role in migration and metastasis of solid tumours such as breast, ovarian and small cell lung cancer (Muller, Homey et al. 2001) (Scotton, Wilson et al. 2001; Kijima, Maulik et al. 2002), reviewed in (Zlotnik 2008).

dUTP phosphatase (*DUT*), is a DNA repair gene which prevents mis-incorporation of uracil residues in to DNA during replication. In all known organisms uracil is not a native component of DNA. It can however become incorporated in to DNA through spontaneous deamination of cytosine residues or through dUTP utlilisation by DNA polymerases during replication (Lindahl 1993). As cytosine deamination can lead to G:C >A:T transversions, a BER repair mechanism has evolved to remove and correct mis-incorporated uracil (Lindahl 1982). To prevent dUTP utilisation during DNA replication, *DUT* hydrolyses dUTP to yield dUMP and PPi. This reaction effectively removes dUTP from the DNA biosynthetic pathway and provides a substrate (dUMP) for *de novo* synthesis of thymidylate.

POLE2 (DNA polymerase), pol ε B-subunit 2 (p59 subunit) is a replicative DNA polymerase which forms a central component in DNA replication,

repair, recombination and cell cycle control (Hubscher, Nasheuer et al. 2000). The DNA polymerase family are multi-subunit enzymes which are up-regulated by mitogenic activators. The organisation and induction of the *POLE2* promoter is similar to the promoter of *cyclin D1* (Watanabe, Albanese et al. 1998).

To date, no direct link between *POLE2* mutations and mammalian tumorigenesis have bene observed. However its role in DNA replication and repair make it a promising candidate gene to pursue.

7.4.2 Limitations of lymphoblastoid cell line work

Despite working within strict limits to prevent differences in culturing conditions, there will always be some differences of the exact conditions that each cell line studied was exposed to resulting in observed differences in expression. The analysis of the MCRA cases, both combined and on an individual basis, would have highlighted any gross differences in expression between cases.

In the cell lines used in this study NMD would theoretically have removed many of the truncated (mutated) transcripts which may have led to the identification of novel germline predisposition genes. In this scenario however a fold change (down-regulation) would have been observed. The three candidate genes chosen for further study were all down-regulated suggesting either an upstream inhibition of transcription or degradation of mutated transcripts. It is possible to inhibit mRNA translation and subsequently NMD, exploitation of this could be a useful tool to study lymphoblastoid cell line mRNA expression further – see future work.

When considering changes of expression, it is difficult in this situation to determine where in a biological pathway the initiating mutation has occurred to cause the observed effect. It would have been expected that KEGG, DAVID and GO analysis would identify any biological or biochemical pathways which were grossly affected by an underlying mutation.

7.4.3 Future work

1: Confirmation of fold changes observed

i) Real-time PCR analysis (qRT-PCR) is a useful tool which could be used to determine functional levels of proteins whose expression array levels were altered. qRT-PCR of the candidate genes chosen and of those transcripts with a more than >3 fold change of expression would help to identify functional changes in expression.

ii) Immunohistochemistry (IHC) of the protein products of down-regulated transcripts in GI mucosa (if expressed there and if probes available) would confirm any changes at a tissue level.

2: Inhibition of NMD to identify mutated transcripts

Several research groups have utilised the inhibition of NMD to identify genes carrying nonsense / frameshift mutations. This strategy is termed GINI (gene identification by NMD inhibition) and to date has been used successfully in colorectal cancer cell lines and prostate cancer cell lines (Ionov, Nowak et al. 2004) (Huusko, Ponciano-Jackson et al. 2004) (Rossi, Hawthorn et al. 2005). A limitation of earlier studies utilising inhibition of NMD was that emetine (used to inhibit translation) was a strong inducer of a stress response in the cell lines being studied, therefore causing many genes to be up and down regulated. This has been overcome in part by the addition of caffeine to culturing media (GINI2) (Ivanov, Lo et al. 2007). GINI has not yet been used successfully in lymphoblastoid cell lines to identify mutations in constitutional DNA.

One approach would be to culture lymphoblastoid cell lines from MCRA cases and controls both with and without inhibition of NMD decay. Expression array analysis of these cell lines when compared both with and without inhibition of NMD would identify transcripts which are down-regulated due to a constitutional DNA mutation rather than an error in replication.

3: Whole genome sequencing of selected MCRA cases

Whole genome sequencing has emerged as a realistic experimental approach over the last 2 years (Bentley 2006). This approach which is now available through Illumina (Solexa) allows analysis of the whole genome. It is based on parallel sequencing of millions of fragments using reversible terminator-based sequencing.

See - http://www.illumina.com/sequencing/Technology.ilmn.

Whole genome (or candidate gene region) sequencing of carefully selected MCRA cases would enable identification of constitutional mutations (with the caveat that they would be found in the 99% of the human genome re-sequenced with Solexa).

7.5 Conclusions

Expression array analysis of 11 MCRA cases and 5 controls identified 3 candidate genes *CXCR4, DUT* and *POLE2* which were all under-expressed >3 fold in the majority of MCRA cases studied. These candidate genes were then taken forward to study further in the following Chapter.

8 Candidate gene screening in MRCA cases

8.1 Introduction

Candidate gene screens are a useful tool for identification of novel predisposition genes. When considering the MCRA phenotype, genes involved in DNA repair and Wnt signalling are the most obvious point at which to start. Cell cycle checkpoint genes and regulators of apoptosis are *a priori* good candidates for any tumour type.

To date, one study has screened candidate genes from the Wnt signalling and *TGF-β* pathways in the MCRA phenotype (Lipton, Sieber et al. 2003). Lipton et al screened 47 MCRA cases (with *APC* and *MYH* mutations excluded) for germline mutations in *APC2*, conductin and *GSK3β* from the Wnt signalling pathway and *SMAD4* and *BMPR1A* from the *TGF-β* pathway. One patient was found to have a putative pathogenic mutation in *BMPR1A* (3 bp del nt 1079-81, resulting in loss of histidine residue) with no mutations found in the other genes screened.

The data presented in Chapter 6 suggests that Wnt signalling is disrupted in MCRA cases as a statistically significant increase in nuclear *β-catenin* was observed. Therefore genes (including regulatory genes) in the Wnt signalling pathway warrant further study.

A series of candidate genes was selected for further study on the basis of the results from Chapters 6 and 7 and from evidence found in current literature.

Table 8–1 provides an overview of the genes studied and the rationale for their selection.

Candidate Gene	Function	Reason for selection
OGG1	DNA repair BER	Member of BER family, following discovery of *MYH*
MTH1	DNA repair BER	Member of BER family, following discovery of *MYH*
TDG	DNA repair BER	Evidence of link with BER
MSH6	DNA repair MMR	Known interaction with *MYH*, and evidence of mutations in CRC
PMS2	DNA repair MMR	Homozygous germline mutation identified in patient with multiple CRC primaries
MGMT	DNA repair	Through literature search
MBD4	DNA repair	Through literature search
POLE2	DNA repair	Expression array work - Chapter 5
DUT	DNA repair	Expression array work - Chapter 5
CXCR4	DNA repair	Expression array work - Chapter 5
Wif1	Wnt signalling	Evidence of increased nuclear expression of B-cat - Chapter 4
DKK1	Wnt signalling	Evidence of increased nuclear expression of B-cat - Chapter 4
Ephrin B2	Wnt signalling	Evidence of increased nuclear expression of B-cat - Chapter 4
		EphB2 germline mutation idenitifed in HPP case and selected Finnish CRC cases
CDC4	Cell cycle control	Evidence of mutation in CRC
BLM	DNA helicase acivity	Ashkenazi CRC link, role in genomic instability

Table 8–1 Candidate genes chosen for study in MCRA cases

8.1.1 Selection of candidate genes

DNA repair genes

Base excision repair genes - *OGG1, MTH1, TDG*

Following the discovery of MAP (Al-Tassan, Chmiel et al. 2002) (Sieber, Lipton et al. 2003), it is possible that disruption of other BER genes may predispose to MCRA development, particularly as there is functional overlap and redundancy within the BER system.

Somatic mutations in *OGG1* have previously been reported in several human cancers including gastric, colorectal, lung, renal and leukaemia (Shinmura, Kohno et al. 1998) (Park, Choi et al. 2001) (Audebert, Chevillard et al. 2000) (Hyun, Choi et al. 2000). More recently the Korean germline *OGG1* polymorphisms R154H and S326C have been identified in sporadic CRC patients (Kim, Ku et al. 2004) and multiple adenoma cases (Kim, Ka et al. 2007) respectively.

To date, no published polymorphisms or somatic mutations in *MTH1* have been identified in human cancers, but as a pivotal member of the BER family it warrants further study in MCRA and CRC cases.

Thymidine-DNA glycosylase (*TDG*) initiates repair of G>T and G>U mismatches (which are commonly associated with CpG islands) by removing thymine and

uracil moieties. A recent study found a novel heterozygous germline missense mutation (ntA196G, R66G) in 1/94 familial CRC cases and 0/188 controls (Broderick, Bagratuni et al. 2006). The variant was identified in a 66 year old male with rectal cancer; the patient's sister died of CRC at 47. A previously identified polymorphism (V367M) was identifed in 1 case and three intronic variants were also identified (A166+12G, G167-9A and G167-19C).

Mismatch repair enzymes – *MSH6*, *PMS2*

The MMR and BER DNA repair mechanisms interact through an *MSH6* binding site present on *MYH*, therefore preventing deleterious double strand breaks. Germline *MSH6* mutations account for <5% of HNPCC cases (Plaschke, Engel et al. 2004), these cases have later onset and lower incidence of CRC when compared to *MLH1* and *MSH2* mutation carriers. The *MSH6* promoter polymorphism 159C>T has also been associated with an increased risk of CRC in a study of 929 CRC cases and 1098 controls (Mrkonjic, Raptis et al. 2007). Niessen *et al* found a higher incidence of heterozygous *MYH* carriers in individuals with missense MMR mutations (4/36 also harbouring *MSH6* mutations) (Niessen, Sijmons et al. 2006). This was further supported by the observation of both *MSH6* and *MYH* mutations in a large branch of a Dutch HNPCC family where 19 family members carried either heterozygous or compound heterozygous *MYH* mutations alongside *MSH6* mutations the phenotype of these individuals was more representative of HNPCC with evidence of MSI and an under-representation of G>T transversions (van Puijenbroek, Nielsen et al. 2007). In light of this it was hypothesised that heterozygous *MYH* mutations may act as phenotypical modifiers of HNPCC. The German HNPCC consortium investigated this hypothesis further and found no real association between *MSH6* mutation carriers and *MYH* inheritance (Steinke, Rahner et al. 2008). This study found the *MYH* carrier rate to be similar to the healthy control population when 64 *MSH6* mutation carriers were screened for *MYH* 2/64 (3.1%) harboured both *MSH6* and heterozygous *MYH* mutations.

A Danish HNPCC family presenting with CRC and adenomas at 18 years of age was found to have mutations in both *MSH6* (S612X and R1076C) and *APC* (G2502S). Immunohistochemistry for *MSH6* and *β-catenin* found lack of expression of *MSH6* alongside increased nuclear accumulation of *β-catenin* indicating a phenotypic influence of both the underlying mutations (Okkels, Sunde et al. 2006).

Therefore the role of *MSH6* in both MCRA and CRC development (outside HNPCC diagnosis) is unclear, germline mutations may play some part in the development of MCRAs.

Homozygous deletion of *PMS2,* another MMR gene, in the germline has been found to cause a severe CRC phenotype in an individual of Indian descent with parental consanguinity. This individual presented at 23 years with 10 synchronous colorectal primaries and 35 adenomas, at 25 years he was found to have duodenal adenocarcinoma, he also had dysmorphic features, mental retardation and café-au-lait spots (Will, Carvajal-Carmona et al. 2007). As this individual harboured multiple colorectal adenomas, *PMS2* warranted further investigation as a possible MCRA predisposition gene.

Other DNA repair enzymes - *MGMT, MBD4, POLE2, DUT, CXCR4*

O^6-methylguanine-DNA methyltransferase (*MGMT*) is a DNA repair gene which removes deleterious O^6-methylguanine residues from DNA. *MGMT* loss of function results in increased accumulation of O^6-methylguanine promoting tumorigenesis through G:C > A:T transversions in growth related genes such as *K-ras* and p53 (Esteller, Toyota et al. 2000) (Esteller, Risques et al. 2001). Methylation of *MGMT* can identify a subset of CRC cases with low-level microsatellite instability (Whitehall, Walsh et al. 2001). There is increasing evidence to support a role of increasing levels in *MGMT* methylation in progression from normal colonic epithelia through the adenoma-carcinoma sequence (Nagasaka, Goel et al. 2008). Somatic mutations in *MGMT* have also been identified in fresh frozen CRC tissue and CRC cell lines. Six of 113 CRCs studied by Halford *et al* harboured somatic mutations. These tumours

demonstrated defective MGMT function with G:C>A:T transversions being found at other loci such as *K-ras* and p53 (Halford, Rowan et al. 2005). Furthermore, MGMT expression was decreased or lost in over half of the CRCs studied and may therefore have a role in MCRA development.

MBD4 is known to bind to methylated CpG and TpG sites, in particular sites related to the transcriptional repressor MeCP2. It has a c-terminal domain homologous to DNA repair proteins (Hendrich and Bird 1998). *MBD4* has the ability to remove thymine or uracil from mismatched CpG sites (Hendrich, Hardeland et al. 1999). It is thought that mutations causing loss of *MBD4* function can lead to a genome wide increase in C>T transitions and therefore have a housekeeping role similar to MMR proteins (Liu, Nicolaides et al. 1995) (Herman, Umar et al. 1998). A study of *MBD4* in CRC found frameshift mutations in over 40% (9 CRC primaries and 1 cell line) of CRC cases studied (Bader, Walker et al. 1999). More recently *MBD4* has been implicated in DNA damage response and chromosomal stability (Abdel-Rahman, Knuutila et al. 2008).

The functions of *POLE2, DUT* and *CXCR4* are discussed in Chapter 5. These DNA repair genes were chosen for further study as they were down-regulated >3-fold in the majority of lymphoblastoid cell lines from MCRA cases studied using expression array analysis.

Wnt signalling

Wnt signalling related genes – *WIF1, DKK, EPHB2*

Wnt signalling inhibitory factors include *WIF1* and Dickkopf1 (*DKK*) and frizzled related proteins. These secreted molecules have been demonstrated to bind Wnt proteins and inhibit their activity. The secreted Wnt antagonists can be divided based on their function, the soluble frizzled related proteins (sFRPs) includes *WIF1*, sFRP1, 2, 4, 5 and Frisbee. These proteins bind directly to Wnts altering their ability to bind the frizzled receptors. The dickkopf class comprises *DKK 1-4*

which bind to low density lipoprotein receptor proteins (LRP5 and 6) which are contained within the Wnt receptor complex. When bound *DKK* proteins inhibit Wnt signalling by preventing normal LRP-Fz-Wnt interactions (Kawano and Kypta 2003). Byun *et al* found a difference in expression of inhibitory Wnt factors in the upper and lower GI tract. Increased zonal expression of *WIF1* was observed in colonic crypt bases on *in situ* RNA analysis suggested a role in colonic stem cell maintenance (Byun, Karimi et al. 2005). In this study *DKK1* was not expressed in normal colonic mucosa.

Epigenetic changes (promoter hypermethylation) of *WIF1* have been reported in gastric and Barretts related oesophageal cancers suggesting a role as a putative tumour suppressor gene (Taniguchi, Yamamoto et al. 2005) (Clement, Guilleret et al. 2008). Similar epigenetic changes have been observed in *DKK1* in CRC cases where hypermethylation of *DKK1* was observed in 9/54 CRCs studied (Aguilera, Fraga et al. 2006).

Ephrin receptor B2 (*EPHB2*) is a direct transcriptional target of *β-catenin.* Its protein product mediates the bi-directional migration and correct positioning of cells along the crypt axis in intestinal epithelium (Batlle, Henderson et al. 2002). In murine studies, *EPHB2* has been demonstrated to have tumour suppressor activity. When the gene is disrupted in $Apc^{min/+}$ mice acceleration of tumour growth is observed in both colon and rectum (Batlle, Bacani et al. 2005). Germline missense mutations in *EPHB2* have been identified in Finnish CRC cases (who also had a personal or family history of prostate cancer) and individuals from the UK with hyperplastic polyposis (Kokko, Laiho et al. 2006). Four missense mutations were identified, two in the CRC cases (I361V, R568W) and one (D861N) in a HPP case. The fourth missense mutation (R80H) found in a CRC case was also present in 9/281 healthy controls and is likely to be a polymorphism. As *EPHB2* has an association with serrated adenomas (Laiho, Kokko et al. 2007) it is possible that it may also play a role in MCRA development based on the findings of *BRAF* mutations in the MCRA adenomas studied in Chapter 6.

Cell cycle regulation

Cell cycle regulation *CDC4*

CDC4 is a highly conserved E3 ubiquitin ligase which is indirectly involved in regulating the G1-S cell cycle checkpoint by targeting proteins for destruction by the SCF complex (Winston, Koepp et al. 1999). Mutations in *CDC4* have previously been identified in breast and ovarian cancer cell lines (Moberg, Bell et al. 2001) (Strohmaier, Spruck et al. 2001) and more recently in a subset of CRCs (Rajagopalan, Jallepalli et al. 2004) (Kemp, Rowan et al. 2005). There has been some discussion of a putative role of *CDC4* in chromosomal instability initially suggested by Rajopalan *et al* following the observation that when *CDC4* is knocked out in CRC lines, changes occur suggestive of CIN (Rajagopalan, Jallepalli et al. 2004). Further work by Kemp *et al* found no association between *CDC4* mutation and CIN in a study of 244 colorectal tumours and 40 CRC cell lines. Six percent of tumours (including near-diplod CIN- lesions) harboured *CDC4* mutations. The mutation spectra included nonsense an missense mutations with a bias towards C:G>T:A transversions (Kemp, Rowan et al. 2005).

CDC4 was chosen for further study due to its role in cell cycle regulation and the recently identified association between somatic *CDC4* mutations and CRC.

Genomic instability / other CRC Hereditary syndromes

Other CRC Hereditary Syndromes - *BLM*

The Ashkenazi Jewish population have a 10-15% lifetime risk of developing CRC. There are known founder mutations in both *APC* (I1307K) and *MSH2* (1906G>C) in this population which although prevalent do not account for the disease burden observed (Zauber, Sabbath-Solitare et al. 2005).

Bloom syndrome is a rare autosomal recessive condition leading to immunodeficiency, growth retardation, male sterility, breast cancer and CRC. A founder mutation in the Bloom gene BLM^{ash} (frameshift mutation in exon 10) has been identified in one third of individuals with Bloom syndrome. Two groups report an increased risk (2.3 – 2.8 fold) of CRC in heterozygous carriers of the

BLM^{ash} mutation (Gruber, Ellis et al. 2002) (Cleary, Zhang et al. 2003). Although Baris *et al* reported no increased risk in heterozygous carriers over three generations (Baris, Kedar et al. 2007).

The functions of the *BLM* gene include roles in genomic stability and meiotic recombination. It has helicase activity although its natural substrates have yet to be identified (Neff, Ellis et al. 1999). Seven pathogenic missense mutations have been identified which have been mapped to seven highly conserved sequence motifs (Bernstein, Zittel et al. 2003). The *BLM* gene warrants further study due to its role in genomic stability and association with CRC.

8.1.2 Aims

The aim of this chapter was to screen a selection of MCRA candidate genes selected either through my own experimental work in Chapters 6 and 7 or based on evidence from current literature.

8.2 Methods

8.2.1 Mutation detection

Following selection, the genomic sequence of each gene was downloaded from the UCSC Genome Browser - http://www.genome.ucsc.edu/

Primers were selected using Primer 3 software - http://frodo.wi.mit.edu/cgi-bin/primer3/primer3_www.cgi and annealing conditions determined (as described in Methods 2.1.4).

All genes except *MSH6, DUT, POLE2* and *CXCR4* were screened using fluorescent SSCP (Methods 2.1.6.1).

MSH6 was screened using dHPLC WAVE analysis (Methods 2.1.6.2).

DUT, POLE2 and *CXCR4* were screened using the Lightscanner melting curve analysis (Methods 2.1.6.3).

Following identification of aberrant bands on SSCP, demonstration of abnormalities on the dHPLC chromatogram or abnormal melting profile on Lightscanner analysis, samples were sequenced in forward and reverse orientations using fluorescence cycling sequencing, see Methods 2.1.7

All non-synonymous SNPs identified were analysed using the Fred Hutchinson SIFT analysis software to determine any potential pathogenic downstream alterations in protein structure and function - http://blocks.fhcrc.org/sift/SIFT.html.

The following genes were screened with G. Guerra an Italian collaborator - *MSH6, Wif1, DKK, MGMT, MBD4, BLM.*

POLE2 and *DUT* were screened with K. Monahan a fellow PhD student.

8.2.2 Immunohistochemistry

Immunohistochemostry for PMS2 was undertaken as described in Methods 2.1.13

Paraffin embedded tissue from 20 MCRA cases were studied for altered expression of PMS2.

8.3 Results

In total, 15 candidate genes were screened, 14 (133 exons in total) through germline mutation detection using SSCP, dHPLC and Lightscanner mutation detection and 1 through immunohistochemistry to determine whether any alteration in PMS2 expression occurs in MCRA cases.

8.3.1 Mutation detection

Overall, no obvious pathogenic germline mutations were identified in the MCRA cases studied. See Table 8-2 for a summary of the mutations detected.

The majority of mutations detected were in the DNA repair group of candidate genes. Of the Wnt signalling genes a single synonymous mutation in *EPHB2* (Q875Q A>G nt 2625) was detected.

Five silent mutations were detected, two in *MSH6*, one in *MBD4* and one in *EPHB2*. Eight heterozygous missense mutations were detected, S326C (previously reported in Korean population) in *OGG1*, V83M in *MTH1*, L84F, I143V and K178R in *MGMT*, T515S in *MBD4,* V154G in *DUT* and V181I in *CXCR4*. Three homozygous missense mutations were found, S326C in *OGG1*, L84F and L88F in *MGMT*. Intronic SNPs were identified in *OGG1* and *MSH6*.

Three 3'UTR SNPs were identified two in exon 19 of *POLE2* and one in exon 7 of DUT, all of which may have some effect on gene expression. Of 47 controls examined for these 3'UTR SNPs the two SNPs identified in exon 19 of *POLE2* were found in 15% of controls suggesting that they are not pathogenic. The 3'UTR SNP associated with exon 7 of *DUT* was not found in any controls suggesting that this SNP may alter gene expression. The non-synonymous SNP V154G present in exon 7 of *DUT* is thought to be potentially pathogenic as it occurs in a highly conserved region of the gene coding for the UTPase region (as predicted by the Fred Hutchinson SIFT analysis http://www.fhcrc.org).

8.3.2 PMS2 immunohistochemistry

A total of 21 paraffin embedded tissue blocks from 20 MCRA cases were studied for altered PMS2 expression. Adenoma burden ranged from 5 – 34 (median 10) and age of individuals studied ranged from 38 – 78 (median 60 years).

No altered expression was observed in any of the cases observed when immunhistochemistry staining was compared with normal control slides included in the experiment. See Figure 8–1 for example of PMS2 immunohistochemistry.

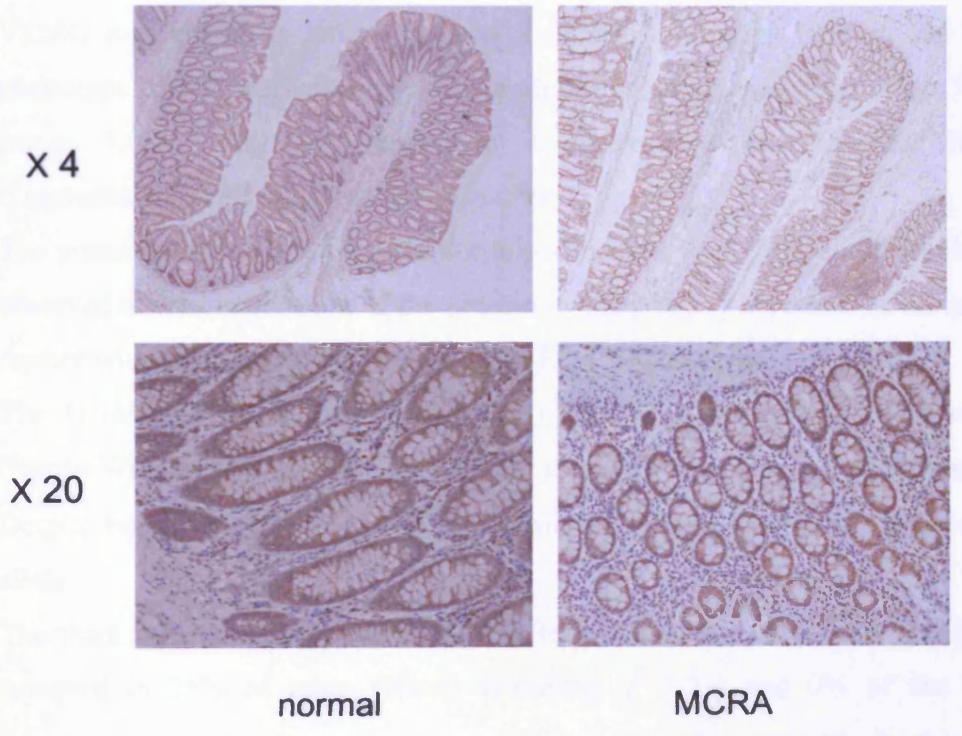

Figure 8–1 PMS2 immunohistochemistry of normal and MCRA colonic epithelium both demonstrating normal expression of the PMS2 protein

8.4 Discussion

Despite careful selection of candidate genes, no obvious pathological germline mutations in selected DNA repair, Wnt signalling or cell cycle control genes were identified in this study.

8.4.1 DNA repair gene non-synonymous SNPs – potential candidates as low risk alleles

Three non-synonymous SNPs were identified in three DNA repair genes which warrant further study.

Most interesting is the V154G heterozygous SNP (rs1802838) found in exon 7 of *DUT* which was identified in 11% of MCRA cases (Hardy-Weinberg χ^2 0.34) and 0% (0/47) of controls screened. This SNP is predicted to alter the UTPase region of the gene and could potentially be deleterious (SIFT analysis prediction). *DUT* V154G may therefore have a role as a disease modifying SNP in the MCRA phenotype. *DUT* was chosen as a candidate as decreased expression >3 fold (range 3.08 – 5.89 fold reduction in expression) was observed in 5/11 lymphoblastoid cell lines studied (Chapter 7)

The presence of the 3'UTR polymorphism in exon 7 of *DUT* could result in the observed altered expression of the protein in Chapter 5. This could be investigated further with quantitative real time PCR (qRT-PCR) analysis.

The *MGMT* K178R heterozygous SNP (rs2308327) was found in 29% of cases (Hardy-Weinberg χ^2 2.88) and 17% of the control population (HapMap Eur). Despite being "tolerated" on SIFT analysis it may still have a role as a low risk allele.

The third non-synonymous SNP T515S found in exon 6 of *MBD4* (rs3138359) occurred in 26% of cases (Hardy-Weinberg χ^2 2.23) and 0% of the control population (HapMap Eur). There is no SIFT analysis data available for this SNP.

For all of these SNPs there is a higher frequency in the MCRA cases when compared to controls. Unfortunately no germline DNA samples were available from other family members of these cases to use in co-segregation analysis of these SNPs.

In order to confirm these findings, these SNPs should be screened in another independent cohort of MCRA cases and control populations.

At this time they could be considered as potential low risk alleles contributing to the MCRA phenotype – in particular the *DUT* V154G SNP.

8.4.2 Potential role of synonymous SNPs and non-synonymous SNPs with similar frequencies in MCRA cases and control populations

Of the BER genes studied, the *OGG1* missense mutation S362C was identified in 27% of individuals screened; 13% were heterozygous and 14% homozygous for the mutation. Although not thought to be pathogenic, Goode et al (Goode, Ulrich et al. 2002) when reviewing DNA repair gene polymorphisms and cancer risk found an increased prevalence of S326C homozygous mutations in lung, oesophageal and prostate cancers. In the control groups, the genotype frequencies were 32% for the common allele, 54% for heterozygous carriers and 14% homozygous carriers of the rare allele (326C). There is discrepancy as to the allele frequencies as the European HapMap figures for these alleles (rs1052133) differ, citing 31% for S326C heterozygotes and 6.9% for S326C homozygotes. The frequency of the 326C homozygote carriers of the rare allele in my study would therefore be double (14%) that of the HapMap frequency (6.9%) suggesting that it may confer increased risk for developing MCRAs.

The *MGMT* L84F and I143V SNPs (rs12917 and rs2308321) were found to have very similar frequency as the control population (HapMap Eur) and are unlikely to have a role as either a low risk allele or disease modifying allele.

However, the presence of missense mutations in DNA repair genes may have a subtle effect as modifier genes or make an individual more susceptible to environmental exposure – such as free radicals caused by smoking or oxidative stress in the intestinal epithelium through poor diet. A candidate gene screen of other BER genes in CRC cases by Broderick et al (Broderick, Bagratuni et al. 2006) detected three missense mutations in *NEIL2* (C367A), *TDG* (A196G) and *UNG2* (C262T) which were screened alongside *NTHL1, NEIL2, MPG* and *SMUG1* in 94 CRC cases and 188 controls. The *TDG* A196G mutation was not detected in the MCRA cases in this study suggesting that if it is associated with CRC it may play a role in tumour progression rather than development.

There is increasing interest in the potentially pathogenic influence of "silent" mutations on altered protein translation kinetics on transit through the ribosome (Komar 2007). Kimchi-Sarfaty *et al* (Kimchi-Sarfaty, Oh et al. 2007) have suggested that silent SNPs can in fact alter in vivo protein folding and ultimately function. This finding could have an enormous impact in the interpretation of mutation detection studies particularly if these SNPs are occurring at a higher frequency in the disease population.

As no pathogenic mutations were found in *POLE2* and *CXCR4*, the observed reduced expressionin both of these genes in Chapter 7 may be due to downstream effects or altered expression of these genes in lymphoblastoid cells. Both of which are limitations of the experimental approach as discussed in Chapter 7. The two 3'UTR polymorphisms identified in exon 19 of *POLE2* which were present in 15% of controls screened suggest that they would not have an effect on expression. Again, qRT-PCR would be a useful tool with which this study this observation which is not within the scope of this thesis.

8.4.3 No potential pathogenic mutations identified in Wnt signalling genes

No pathogenic mutations were identified in either the Wnt signalling related genes or the *BLM* gene. Futher Wnt inhibitory factors *WIF2, DKK2, DKK3* and frizzled related proteins would be appropriate candidate genes to screen in the future.

8.5 Conclusions

Following the identification of several "good quality" candidate genes either based on my own experimental work or from published data from others no pathogenic germline mutations were identified which might lead to the development of the MCRA phenotype.

Areas of interest warranting further study include –

1: Study of the three non-synonymous SNPs *DUT* V154G, *MGMT* K178R and *MBD4* T515S identified with higher frequency in the MCRA cases, including confirmation studies in an independent cohort of MCRA cases.

2: Further investigation of the Wnt signalling pathway following the finding of increased nuclear expression of *β-catenin* in the MCRA cases.

3: Real-time PCR to investigate the expression of *DUT* and *POLE2* following identification of 3'UTR SNPs in a larger series of MCRA cases.

9 Investigation of clonal origins in FAP, AFAP and sporadic colonic adenomas

9.1 Introduction

9.1.1 The clonal origins of CRC are not fully understood

Clonality studies in colorectal adenomas and CRC have been the source of some debate since the early 1960s. The determination of the adenoma-carcinoma sequence with its associated genetic changes (Vogelstein, Fearon et al. 1988), alongside the ability to study CRC from its earliest stages through colonoscopic sampling of tissue, makes CRC an ideal tumour type in which to study clonality theories of carcinogenesis.

9.1.2 Existing markers of clonality in CRC have limitations

Early studies utilised X-chromosome inactivation in females harbouring mosaicism of G6PD isoenzymes. Beutler described a polyclonal CRC (Beutler, Collins et al. 1967) and Hsu reported polyclonal adenomas based on the findings of gel electrophoresis of X-inactivation of G6PD isoenzymes (Hsu, Luk et al. 1983). Vogelstein and Fearon *et al* studied X-inactivation patterns of the phosphoglycerate kinase (PGK) gene in DNA (rather than the expressed protein) using restriction fragment length polymorphisms. In female patients with FAP they demonstrated a monoclonal pattern of X-chromosome inactivation (Fearon, Hamilton et al. 1987) (Vogelstein, Fearon et al. 1985). The most significant limitation of these studies is the existence of X-linked patches in both normal and dysplastic tissue. It is possible that some covert polyclonal tumours appeared monoclonal as they arose within an X-linked patch of tissue. Since then, Novelli *et al* have demonstrated through further

analysis of X-linked patch size that X-inactivation studies have a significant bias towards demonstrating colorectal tumour monoclonality (Novelli, Cossu et al. 2003).

Investigation of adenomas from an individual with FAP and XO/XY mixoploid chromosome (as a consequence of a dicentric Y chromosome) led to further evidence supporting a polyclonal origin of adenoma development in FAP (Novelli, Williamson et al. 1996). In this study, clonality was assessed through probing for the Y chromosome in adenomas, This approach demonstrated that 76% of FAP adenomas were polyclonal.

Mouse studies have supported this finding, Merritt *et al* (Merritt, Gould et al. 1997) developed an $Apc^{Min+/-}$ and ROSA 26 (*lacZ* expressing) chimaeric mouse. Analysis of adenomas from these animals found 79% of adenomas to be polyclonal (heterotypic for ROSA and non-ROSA lineages), a figure very similar to Novelli *et al.*

Thliveris (Thliveris, Halberg et al. 2005) has suggested three theories of colorectal tumour polyclonality (discussed in Introduction). Adenoma mosaicism; random or regional collision between independently arising neoplasms; and active interaction between adjacent crypts. To date, none of these theories fully fits observed experimental findings in either humans or animal models.

Since the majority of adenomas harbour mutations at *APC* and as *APC* mutations are the "gatekeeper" mutations in the genesis of colorectal tumorigenesis (Kinzler and Vogelstein 1996), identification and utilisation of somatic *APC* mutations in dysplastic crypts would be a suitable clonal marker with which to study adenoma development from its earliest stages.

I set out to analyse the mutation spectrum at *APC* on a crypt-by-crypt basis by laser micro-dissecting single crypts from adenomas. The identified mutations were then utilised as clonal markers in the following adenoma types – FAP, AFAP and sporadic adenomas. I also re-examined tissue from Novelli's study of an XO/XY individual with FAP to compare two different methods of assessing tumour clonality.

9.1.3 Aims of this chapter

The aim of this chapter was to identify and utilise a simple and robust marker of clonality in CRC which could be used to study adenoma development from its earliest stages and to investigate theories of clonal development of adenomas further.

9.2 Methods

Sample collection and preparation

Patients were recruited through St Mark's Hospital Colorectal Cancer Unit, blood was routinely sampled and paraffin embedded archival tissue was collected. Informed consent was obtained prior to sample collection through the CORGI study.

A total of 5 FAP, 5 AFAP and 4 sporadic adenomas plus 3 adenomas from the individual with XO/XY chimera and FAP were studied.

The FAP individuals chosen for the study had germline *APC* mutations between codons 1040 and 1061 as it would be expected that their second hits at *APC* would occur within the MCR region. In comparison, individuals with the del 5bp deletion at codon 1309 of *APC* most commonly lose the second allele of *APC* through LOH rather than harbouring truncating somatic mutations. All of the AFAP patients had germline mutations in the alternatively spliced region of exon 9 (R332X) of *APC*.

Laser Capture Micro-dissection

For each adenoma studied, serial dysplastic crypts were laser micro-dissected from around the circumference of the adenoma see Figure 9–1. In order to obtain sufficient DNA from each crypt for sequencing analysis, the same crypt was micro-dissected from 6 serial slides. Each crypt sample was laser captured into a separate collecting tube. To determine whether any contamination may have occurred, a "blank" collecting tube was included in every batch analysed. DNA was extracted using standard proteinase K digestion overnight at 60°C.

For each crypt, a total of 10µl starting material was available for subsequent analysis.

For SSCP analysis several crypts were dissected into one collecting tube for digestion in order to obtain 30µl of starting material.

See Methods 2.1.12 for overview of technique and extraction of DNA from dissected crypts

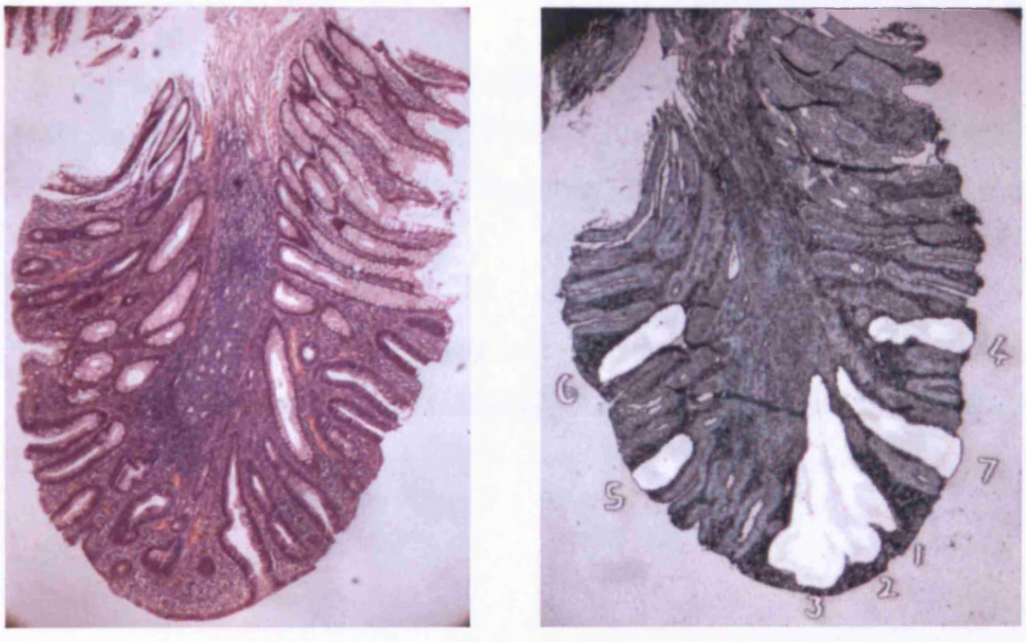

Figure 9–1 Laser micro-dissection of FAP adenoma, H&E section (x20) on left and serially micro-dissected crypts demonstrated on right

Mutation detection in single micro-dissected crypts

For each adenoma, fluorescent SSCP analysis was performed covering the mutation cluster region of *APC* (MCR 1-12) to identify somatic *APC* mutations which could be used as clonal markers (see Methods 2.1.6.1.).

Following identification of aberrant bands on fluorescent SSCP analysis the corresponding MCR region was then sequenced using nested PCR. First and second round primers were used for each MCR region (see Methods 2.1.7.).

LOH analysis at codon 1309 of *APC* was performed in single crypts dissected from adenomas from XO/XY chimeric FAP patient. The germline *APC* mutation for the individual was del 5bp at codon 1309. Subsequently loss of

the wild type allele could be determined by performing LOH analysis across the MCR3 region containing codon 1309.
All primer sequences and conditions can be found in Appendix 1.

Immunohistochemistry
Immunohistochemistry for ß-catenin, and Ki-67 was undertaken as described in Methods 2.1.13.

Fluorescent in-situ hybridisation (FISH) analysis for X and Y chromosomes
FISH for the Y chromosome in the XO/XY patient studied was performed by R. Jeffrey in the Histopathology Laboratory, Cancer Research UK, London Research Institute.

The work undertaken in this Chapter was in collaboration with SJ. Leedham a fellow PhD student in the Histopathology Laboratory, Cancer Research UK, London Research Institute.

9.3 Results

With the limited amount of DNA available for analysis from each crypt it was not always possible to identify the "second hit" at *APC*. If a neighbouring crypt to one harbouring a somatic *APC* mutation was found to be wild type, it was taken that this crypt had arisen from a different clone. All crypts dissected in the study were histologically dysplastic.

9.3.1 FAP adenomas are polyclonal

In total, 36 crypts were dissected from 5 FAP adenomas. Adenomas 1-3 were from an individual with a germline mutation at codon 1040 of *APC* and adenomas 4 and 5 were from an individual with a germline mutation at codon 1061 of *APC*. The mean adenoma size was 9.5 mm^2 (median 2.25 mm^2, range 1.0 – 40 mm^2). All of FAP adenomas were found to be polyclonal, see Table 9–1.

FAP Polyp ID	Size (mm)	Total no. crypts (analysed)	Somatic *APC* Mutations	Clonality
1	1.5 x 2.0	15 (11)	8 crypts - del 2bp nt 4219 and 2 crypts ins A nt 3925 Entrapped wild type crypt	Polyclonal
2	1.5 x 1.5	13 (5)	3 crypts - del A nt 4364 1crypt - ins C nt 4373 1 crypt - wild type for above	Polyclonal
3	1.0 x 1.0	9 (6)	4 crypts - del A nt 4243 2 crypts - wild type for above	Polyclonal
4	1.0 x 1.0	5(4)	2 crypts - del A nt 4195 2 crypts - wild type for above	Polyclonal
5	5.0 x 8.0	100 (10)	9 crypts - del C nt 4476 1 crypt - wild type for above	Polyclonal

Table 9–1 Summary of somatic *APC* mutations identified in single crypts from five FAP adenomas

Figure 9–2 shows SSCP tracings demonstrating aberrant bands in both MCR6 and MCR9 of FAP adenoma 1. Subsequent crypt-by-crypt sequencing analysis identified mutations in both of these regions, see Figure 9–3. Figure 9–4 demonstrates polyclonality in FAP adenoma 2.

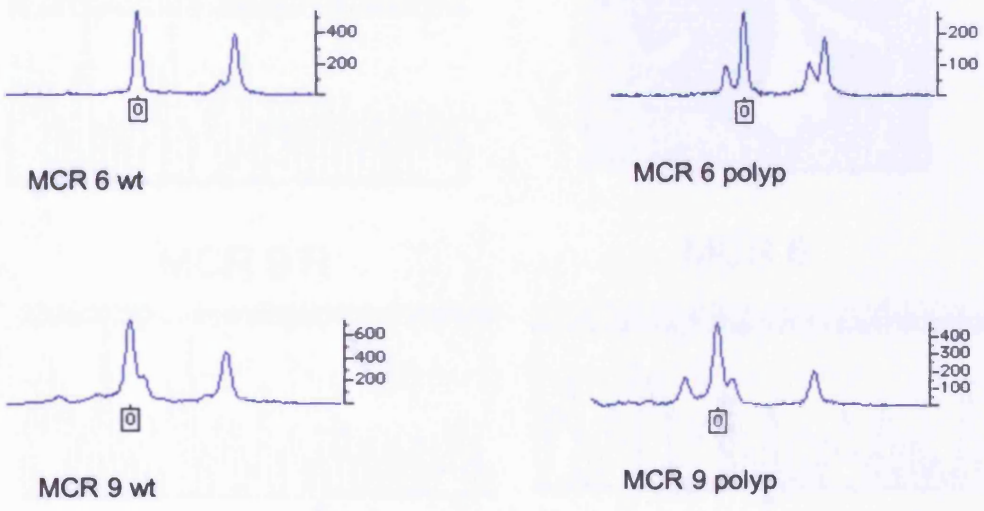

Figure 9–2 Fluorescent SSCP analysis of FAP adenoma demonstrating aberrant bands in MCR6 and MCR9, these were sequenced and are presented in Figure 9–3

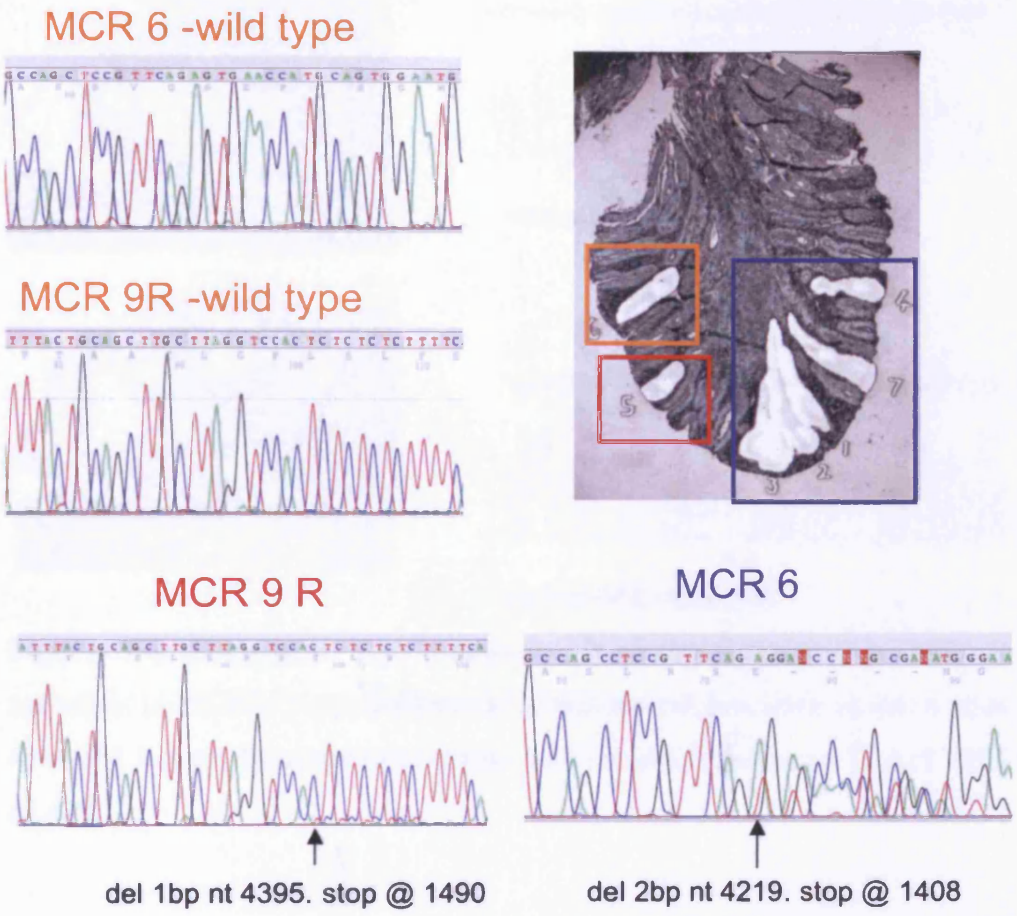

Figure 9–3 Polyclonal FAP adenoma (1), crypt in orange box wt for MCR6 and MCR9, crypt in red box truncating mutation in MCR9 and crypt in blue box truncating mutation in MCR6

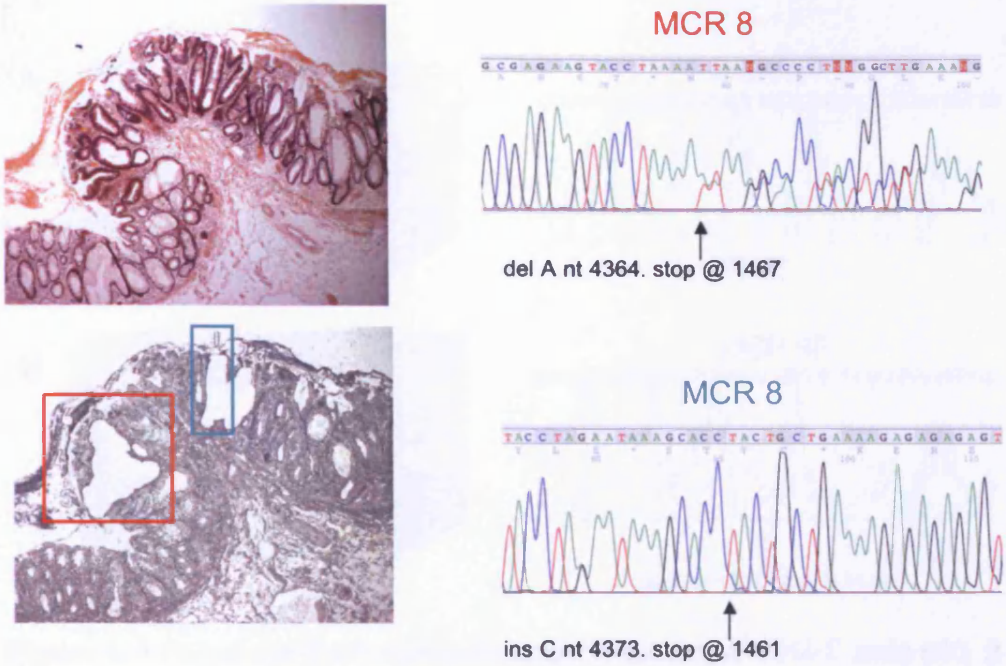

Figure 9–4 Polyclonal FAP adenoma (2) demonstrating two different mutations in MCR8, 3 crypts dissected within the red box harbour del A at nt 4364 and 1 crypt dissected from within the blue box harbours ins C at nt 4373 of *APC*

Two microadenomas (both 1mm^2) in FAP colonic epithelia were examined and both found to be polyclonal from their earliest stages, see Figure 9–5.

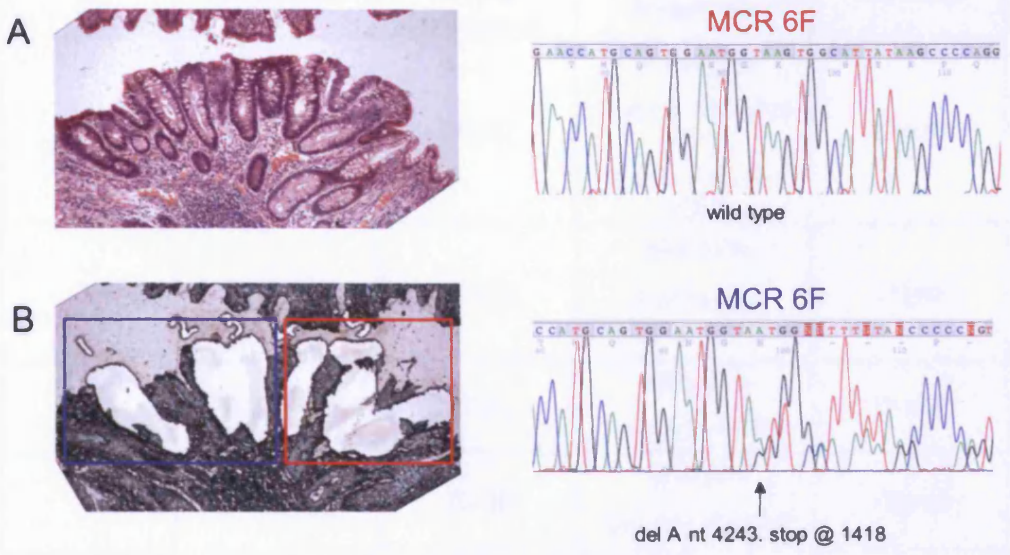

Figure 9–5 Polyclonal FAP microadenoma (3) patient, **A** – H&E stain x40, **B** – micro-dissected crypts . 3 crypts in blue box have truncating mutation in MCR6 and 3 crypts in red box are wt for MCR6

9.3.2 AFAP adenomas are clonal

In total, 36 crypts were analysed from 5 AFAP adenomas collected from 3 AFAP patients. All patients had germline mutations in the alternatively spliced region of exon 9 *APC* (R332X). The mean adenoma size was 11.6 mm^2 (median 9 mm^2, range 4 – 25 mm^2). All AFAP adenomas were found to be clonal see Table 9–2.

AFAP Polyp ID	Size (mm)	Total no. crypts (analysed)	Somatic *APC* Mutations	Clonality
1	3.0 x 3.0	35 (8)	All crypts 2nd hit - del C nt 4117 3rd hit - ins A nt 4662	Clonal
2	4.0 x 4.0	33 (8)	All crypts Nonsense mutation G1552X	Clonal
3	5.0 x 5.0	60 (6)	All crypts Ins A nt 4662	Clonal
4	2.0 x 2.0	25 (8)	All crypts Del 4bp nt 4386	Clonal
5	2.0 x 2.0	27 (6)	All crypts SNP G to A nt 4478	Clonal

Table 9–2 Summary of somatic *APC* mutations identified in single crypts from five AFAP adenomas

See Figure 9–6 and Figure 9–7 for results of adenomas 1 – 3. AFAP adenoma 1 is of particular interest in that it demonstrated both second and third hits at *APC* in every crypt dissected.

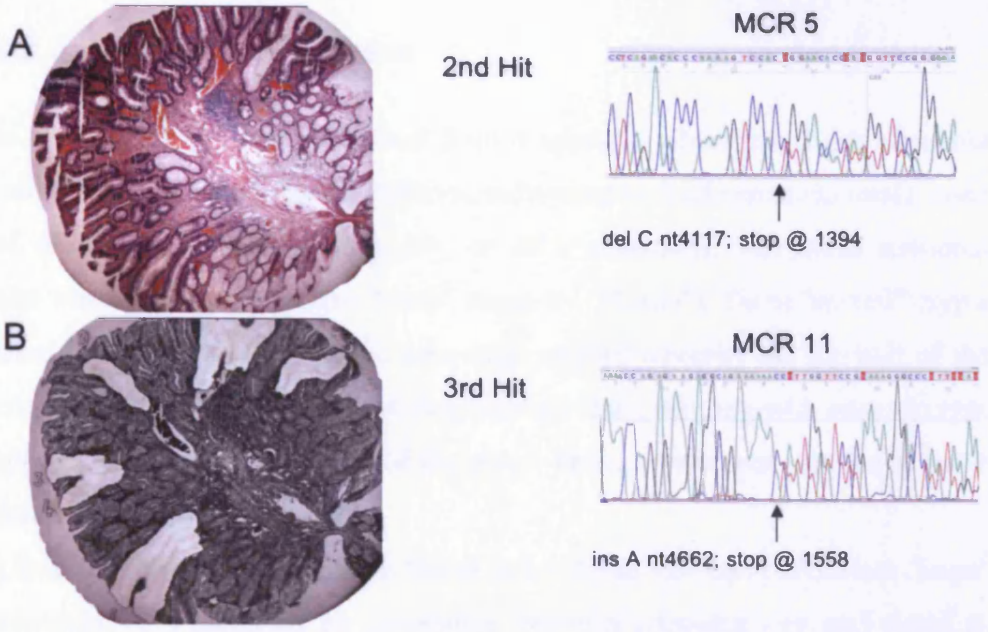

Figure 9–6 Adenoma from AFAP patient (1), **A** – H&E x40, **B** – PALM laser capture slide. Each crypt dissected was found to have second and third hits at *APC* in MCR5 and MCR11

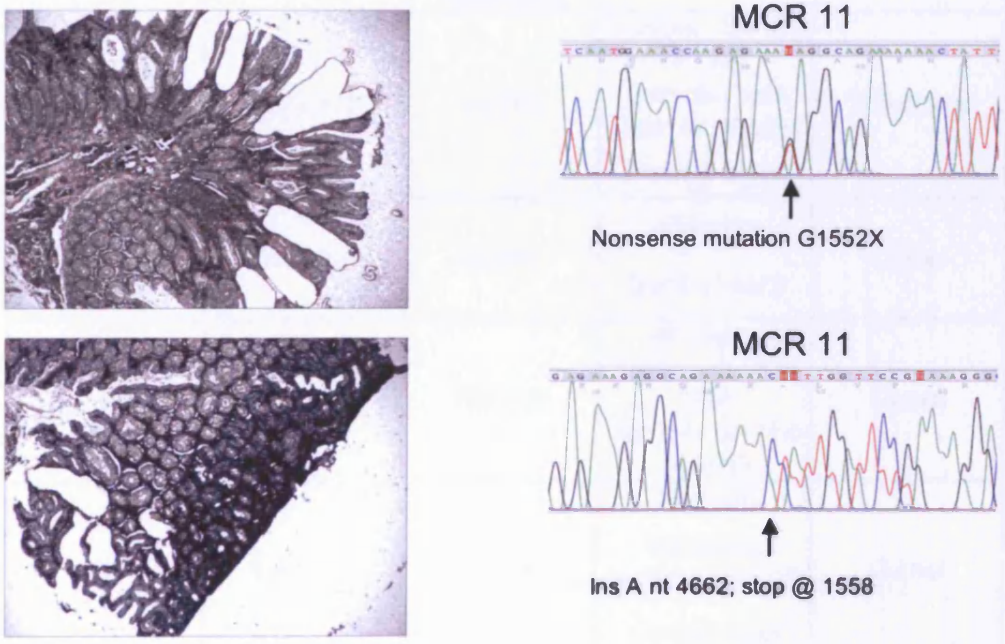

Figure 9–7 AFAP adenomas 2 (upper panel) and 3 (lower panel). Adenoma 2 harboured G1552X nonsense mutation in all crypts studied and adenoma 3 harboured ins A at nt 4662 of *APC* in each crypt

9.3.3 Sporadic adenomas

In total, 44 crypts were analysed from 4 sporadic adenomas. Each adenoma studied was collected from a different individual (< 3 adenomas in total), none of whom harboured germline *APC* or *MYH* mutations. The mean adenoma size was 18.75 mm^2 (median 9 mm^2, range 8 – 25 mm^2). Three "mixed" crypts were identified in the sporadic adenomas studied whereby the top half of the crypt demonstrated evidence of dysplasia on H&E staining with normal crypt appearances in the lower half of the crypt. These crypts were studied in more detail in the following section.

Three sporadic adenomas were found to be clonal and one polyclonal (8mm^2 adenoma 1). There was no correlation between adenoma size and clonality observed as adenoma 2 (smaller than adenoma 1) and adenoms 3, 4 (larger than adenoma 1) are all found to be clonal. See Table 9–3 for overview.

Sporadic Polyp ID	Size (mm)	Total no. crypts (analysed)	Somatic *APC* Mutations	Clonality
1	8.0 x 1.0	70 (11)	9 crypts - del 4bp nt 4388 2 crypts - wild type for above 2 mixed crypts	Polyclonal
2	3.0 x 3.0	30 (10)	All crypts Del T nt 4473	Clonal
3	5.0 x 5.0	100 (12)	All crypts 1st hit - del A nt 3700 2nd hit - del 4bp nt 4463	Clonal
4	5.0 x 5.0	50 (11)	All crypts Nonsense mutation G1312X 1 mixed crypt	Clonal

Table 9–3 Summary of somatic *APC* mutations identified in single crypts from four sporadic adenomas

9.3.4 Evidence for "top down" growth in sporadic adenoma development

Three crypts (from 2 adenomas) were identified in the sporadic adenomas which demonstrated mixed morphology. These were studied further by micro-dissecting the dysplastic region of the crypt separately to the region demonstrating normal morphology. In order to confirm progression from normal crypt architecture to histological dysplasia ß-catenin and Ki-67 immunohistochemistry was performed prior to micro-dissection see Figure 9–8.

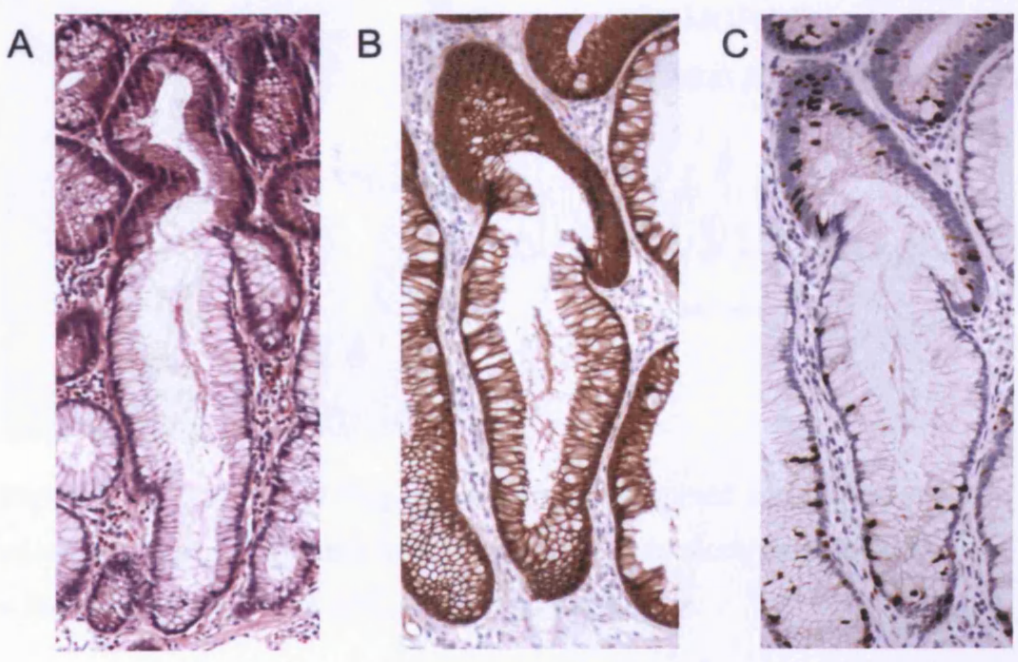

Figure 9–8 Mixed crypt identified in sporadic adenoma 1, **A** – H&E stain x40, **B** –ß-catenin immunohistochemostry demonstrating increased nuclear staining in upper half of crypt, **C** – Ki-67 immunohistochemistry demonstrating higher rate of cellular proliferation in upper half of crypt

On clonal analysis of this crypt the dyplastic top half harboured a mutation in MCR9 and the bottom half with normal histological appearances was found to be wt, see Figure 9–9.

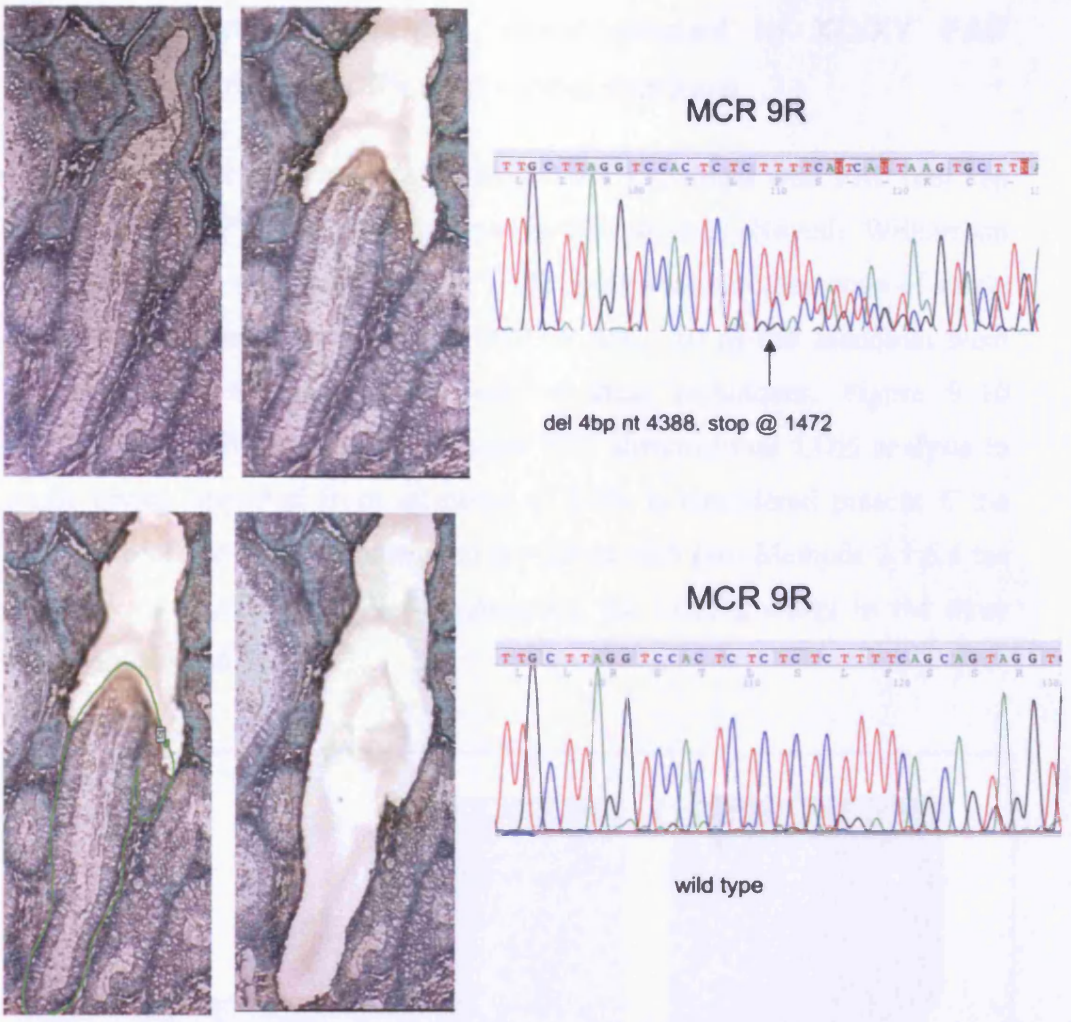

Figure 9–9 Evidence of "top down" growth in mixed crypt from sporadic adenoma, the top (dyplastic) half of the crypt when micro-dissected harboured a 4bp deletion at nt 4388 *APC*, the bottom half was wt

9.3.5 Stroma did not harbour *APC* mutations in FAP, AFAP or sporadic adenomas

When histologically normal stroma was micro-dissected from 3 FAP, 3 AFAP and 2 sporadic adenomas, none of the tissue was found to harbour the same *APC* mutations as identified through SSCP analysis and direct sequencing of the dysplastic crypts within the adenoma.

9.3.6 Polyclonal adenomas demonstrated in XO/XY FAP individual using two different clonal markers

Three informative adenomas from the XO/XY individual with FAP (del 5bp 1309 germline *APC* mutation) decribed by Novelli *et al* (Novelli, Williamson et al. 1996) were re-examined using FISH and laser-microdissection of single crypts for LOH analysis at codon 1309 of *APC*. All of the adenomas were found to be polyclonal using both of these techniques. Figure 9–10 demonstrates FISH analysis and Figure 9–11 demonstrates LOH analysis in single crypts dissected from adenoma 1. LOH is considered present if the LOH ratio of the two alleles studied is >2.0 or <0.5 (see Methods 2.1.6.4 for summary of LOH). Table 9–4 summarises the LOH findings in the three adenomas studied.

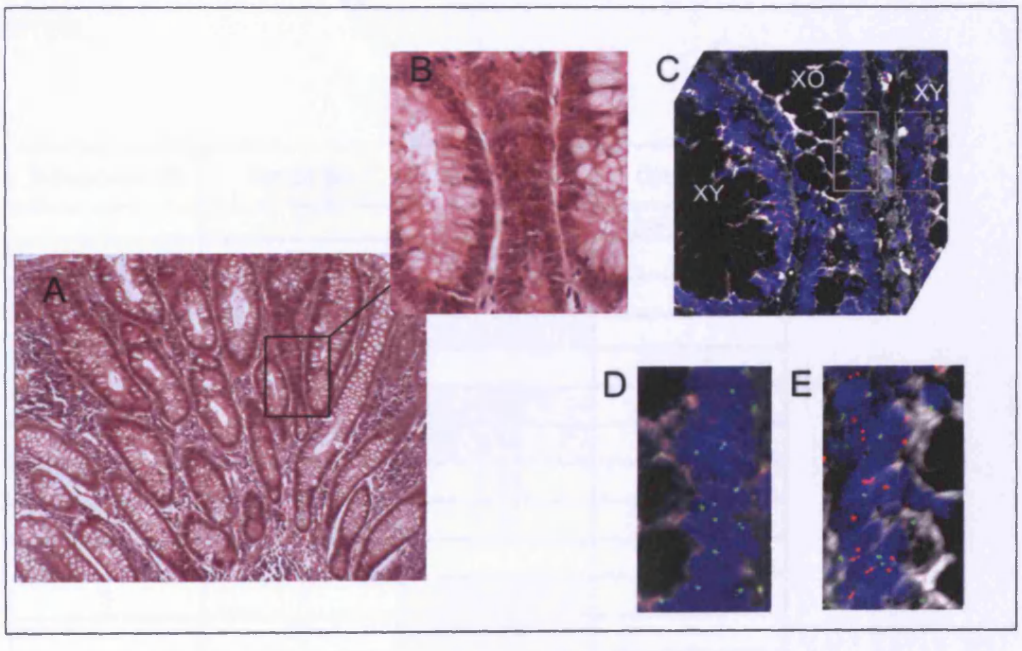

Figure 9–10 Fluorescent in-situ hybridisation for X and Y chromosomes on adenoma of XO/XY patient with FAP, **A** – H&E stain x20, **B** – crypts demonstrated with FISH, **C** – FISH demonstrating XY and XO crypts adjacent to each other, X chromosome = green and Y chromosome = red, DAPI = blue. **D** – XO crypt, **E** = XY crypt

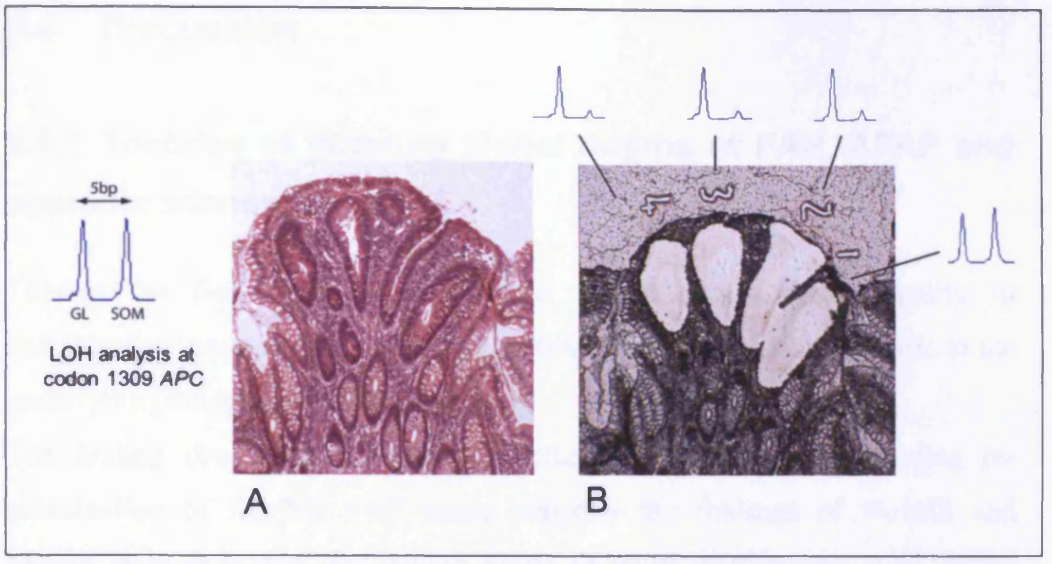

Figure 9–11 LOH analysis at codon 1309 *APC* in adenoma (1) from XO/XY patient with FAP. A – H&E stain x20, B – crypt 1 has no LOH and crypts 2-4 have LOH of the somatic (wt) allele of *APC* demonstrating different clonal origin

Adenoma ID	Crypt no	LOH ratio	Clonality
1	1	0.55	polyclonal
	2	4.26	
	3	4.23	
	4	5.27	
2	1	4.49	polyclonal
	2	2.19	
	3	1.38	
	4	1.33	
3	1	5.32	polyclonal
	2	9.19	
	3	5.42	
	4	3.65	
	5	1.24	

Table 9–4 Summary of LOH analysis at codon 1309 *APC* from single crypts dissected from XO/XY individual with FAP. Blue shading = LOH present (ratio >2.0)

9.4 Discussion

9.4.1 Theories of differing clonal origins of FAP, AFAP and sporadic adenomas

This is the first study to investigate colorectal adenoma clonality in individually dissected dysplastic crypts utilising a clonal marker specific to the underlying pathogenesis of the disease.

The finding that 100% of FAP adenomas were polyclonal including re-examination of XO/XY FAP tissue supports the findings of Novelli and Merritt in both human and mouse tissue (Novelli, Williamson et al. 1996) (Merritt, Gould et al. 1997). There are no published studies of clonality to date in AFAP, the finding that 100% of adenomas studied were of single clonal origin is intriguing and lends weight to the theories of random collision and field cancerisation (as a result of the first germline *APC* "hit"). The finding that 75% of sporadic adenomas are clonal and 25% polyclonal is of great interest. Evidence of "top down" growth as demonstrated in sporadic adenoma "mixed" crypts suggests active interaction between crypts and raises the possibility that an adjacent dysplastic crypt may induce proliferation in its neighbouring crypts.

Therefore, when considering existing theories of clonal origins in adenoma development the data presented in this chapter supports some elements of the random / regional collision, active interaction and field cancerisation theories.

Random or regional collision between independently arising neoplasms

Previously Novelli and Merritt have suggested random / regional collision as a mechanism underlying polyclonality in FAP as a consequence of high tumour burden in FAP patients (Novelli, Williamson et al. 1996) and chimeric *ApcMin*$^{+/-}$ mice (Merritt, Gould et al. 1997).

To test this hypothesis Thliveris *et al* reduced tumour multiplicity in the chimeric *ApcMin*$^{+/-}$ mouse model used by Merritt *et al* by introducing homozygosity for the tumour resistance allele of *Mom1*. Overall tumour multiplicity was reduced 8-fold but the percentage of mixed tumours ranged

from 8-63%, with a mean of 22% (Thliveris, Halberg et al. 2005). This figure is higher than would be expected if heterotypic tumours are formed by random collision when consideration of tumour burden is taken into account. Therefore it was suggested that random collision is an unlikely mechanism leading to polyclonality in the chimaeric mouse model.

The finding of a polyclonal sporadic adenoma in this study suggests a separate pathological process to that of FAP adenoma development and lends more weight to the concept of active interaction between dysplastic crypts and environmental impact on gastro-intestinal epithelia in different regions of the colon.

Active interaction between adjacent crypts

Thliveris and Novelli both believe active interaction between crypts to be the most likely cause of polyclonality observed in human and mouse models of FAP. The possible mechanisms underlying this include microheterogeneity of tumour susceptibility where local stroma promotes somatic mutation in adjacent crypts - the so-called landscaper effect, or stem cell interaction between neighbouring initiated crypts.

These concepts are supported by the observation of polyclonality in FAP microadenomas of 4 crypts diameter in this study. This may be a consequence of paracrine secretion of mitogens or stimulatory proliferogens from neighbouring dysplastic crypts. A different explanation could be the direct effects of epithelial-epithelial interactions between crypts initiating loss of control of cellular proliferation (for example through epidermal growth factor receptor signalling).

Support of epithelial-epithelial interaction causing increased cellular proliferation can be found in mouse studies where hyperplastic ("colossal") crypts found adjacent to adenomas are found to have a higher rate of proliferation (Bjerknes and Cheng 1999). The finding of increased Ki-67 expression in the upper half of the "mixed" crypts studied in sporadic adenomas supports this observation.

Field cancerisation

The theory of "field cancerisation" was first suggested in the 1950s when it was demonstrated that multiple oral tumours could arise from a field of

mutated cells following exposure to a known carcinogen (Slaughter, Southwick et al. 1953). This (albeit old) theory is easily applicable to colorectal epithelia when considering both FAP and AFAP germline first hits and the impact of environmental dietary / oxidative stress in the gastro-intestinal tract.

Histologically normal crypts in individuals with FAP (harbouring the germline *APC* mutation only) have a significantly different proliferation pattern to that of wild-type crypts – with an upwards shift (towards the top of the crypt) of DNA synthesising (S-phase) cells (Potten, Kellett et al. 1992). Mathematical modelling of stem cell kinetics in FAP crypts led to similar results where tumor initiation in the colon was thought to be due to crypt stem cell overproduction and increased proliferation (Boman, Fields et al. 2001). Methylation patterns in histologically normal FAP crypts differ to wild-type crypts, these findings were consistent with slower clonal evolution and subsequent stem cell survival advantage (Kim and Shibata 2004).

Studies of mitochondrial DNA have identified patches of clonally related crypts occuring in normal human colon (Greaves, Preston et al. 2006). Therefore if the first "hit" at *APC* alters cellular proliferation and stem cell survival as discussed above it could theoretically give rise to a morphologically normal "patch" of colonic epithelia harbouring an identical first hit mutation at *APC*. This could result in a field of stem cells harbouring a first hit at *APC* which would be more susceptible to a second hit and subsequent initiation of the adenoma – carcinoma sequence. This could explain the development of clonal adenomas observed in AFAP. Therefore in FAP and AFAP the entire colon could represent a fertile "field" for development of somatic mutations. If this theory is applied to my data it could be suggested that in FAP active interaction occurs alongside the field effect of the germline first hit resulting in polyclonal adenomas. In AFAP the germline first hit at *APC* may result in a less mutation prone "field" therefore second – and as demonstrated in this study and Sieber *et al* (Sieber, Segditsas et al. 2006) - third hits are required for initiation of the adenoma-carcinoma sequence. As this would take a longer period of time chronologically it is more likely that the resulting adenomas would be clonal.

9.4.2 Further work

These results although intriguing require further confirmation through analysis of a greater number of FAP, AFAP and sporadic adenomas. In particular AFAP adenomas from individuals with 5' and 3' germline *APC* mutations should be studied to determine whether they too are clonal in origin or whether my observations relate to AFAP cases with alternatively spliced exon 9 germline mutations only.

In order to further understand pathogenic mechanisms in *MYH* tumorigenesis and explore the effects of environmental stresses on adenoma clonality a collection of MAP adenomas should also be studied.

9.5 Conclusions

Somatic *APC* mutations can be successfully utilised as clonal markers in crypt-by-crypt analysis of adenomas from their earliest stages (including microadenomas from just 4 crypts in diameter).

The finding that FAP adenomas are polyclonal and AFAP adenomas are clonal is intriguing – this lends support to the theories of active interaction and random collision. Evidence of "top down" growth again supports active interaction and suggests that the "second hit" at *APC* would not always have to occur in the bottom of the intestinal crypt where stem cells reside.

A landscaper effect was excluded by the analysis of histologically normal tissue within adenomas which did not harbour *APC* mutations.

This is the first study to investigate colorectal adenoma clonality in individual dysplastic crypts utilising a clonal marker specific to the underlying pathogenesis.

10 Discussion and Conclusions

MYH related studies

MYH associated polyposis (MAP) is a recessively inherited colorectal cancer syndrome accounting for ~1% of all CRC. MAP is caused by inheritance of bi-allelic mutations at *MYH*, a base excision repair (BER) glycosylase. MAP leads to the development of multiple colorectal adenomas and CRC. To date, there have been reports of extra-colonic features associated with MAP, all in small case series. There are known common pathogenic variants which occur in *MYH* amongst different ethnic groups. Northern European populations have a predominance of Y165C and G382D mutations (Jones, Emmerson et al. 2002). Other variants include Y90X in patients of Pakistani origin and E466X which has been found solely in patients of Indian origin. An in frame deletion nt1395delGGA has been identified in patients of Mediterranean origin (Gismondi, Meta et al. 2004).

I studied a cohort of 34 bi-allelic carriers of *MYH* mutations, 18 E466X homozygotes, with the remainder, either Y165C, G382D homozygotes or compound heterozygotes (Y165C/G382D) in search of any genotype-phenotype correlation (Chapter 3). Although a similar incidence of CRC was observed between the Y165C, G382D and E466X homozygotes (62% and 61% respectively), a significantly higher number of the E466X homozygotes developed Dukes stage (B-D) CRC (Table 3-3) than the Northern European mutation carriers suggesting that E466X mutation carriers develop more aggressive disease. This finding is borne out when comparing adenoma burden, a total of 8 E466X homozygote carriers developed >100 and <1000 adenomas with one exceptional individual developing 6250 adenomas. This dataset includes the largest cohort of E466X homozygotes to be studied to date. Future studies to investigate the effectiveness of E466X mutation carriers to repair oxidative DNA damage should include site directed mutagenesis studies in *E.coli* (previously undertaken in Y165C and G382D mutations). If it were found that the E466X mutation were less able to repair oxidative DNA damage this would support the finding that harbouring this mutation would lead to the development of a more aggressive phenotype. Further clinical

research should include collaborative studies to investigate this finding in larger patient cohorts.

On commencing my thesis, screening and clinical surveillance guidelines for MAP were under development, and the significance of being a heterozygous *MYH* mutation carrier was the source of some debate. Through my study of bi-allelic *MYH* mutation carriers it was determined that duodenal polyps occurred in 28% and fundal polyps in 17% of homozygote patients necessitating upper GI endoscopy as screening in all bi-allelic mutation carriers. This is now accepted as best practice.

The development of a mouse model of MAP (Chapter 5) was particularly useful in determination of the significance of being a heterozygous *MYH* mutation carrier. In my study heterozygous $Myh^{+/-}$ mice had no increased risk of tumour development than $Myh^{+/+}$ mice. This data was published in 2004 before large population based studies in humans were available (Farrington, Tenesa et al. 2005) (Webb, Rudd et al. 2006).

Further study of MAP adenomas and colectomy specimens from MAP patients found the presence of microadenomas in colonic epithelium demonstrating that "2 hits" at *APC* are necessary to initiate tumourigenesis (Chapter 3). However, it is still not understood as to why *APC* (and the gastro-intestinal tract) appear to be targeted in *MYH* deficient individuals It could be postulated that the GI tract is more vulnerable to defective BER through environmental exposure to oxidative damage.

Array CGH analysis of MAP tumours (Chapter 4) demonstrated evidence of CIN in 78% (11/14) adenomas studied, with small-scale and large-scale chromosomal changes observed. This included copy number neutral LOH (in one of 3 MAP adenomas examined by SNP-LOH). The observed small-scale changes may be as a consequence of defective BER, whereas the large-scale changes may represent abnormal function of *APC* as *APC* is targeted in MAP. No correlation was identified between the size or grade of dysplasia in adenomas studied and the number of losses and gains observed on aCGH. Previous data had suggested that MAP tumours are diploid on flow-cytometry (Lipton, Halford et al. 2003). At the same time as my study, Cardoso *et al* (Cardoso, Molenaar et al. 2006) were also undertaking aCGH analysis on MAP tumours. The results of Cardoso's and mine are similar (in terms of site

and nature of chromosomal changes cross the genome). However, Cardoso *et al* used whole-genome amplification of extracted DNA prior to aCGH hybridisation. This step is likely to introduce atrefactual errors making interpretation of their data more difficult. Both aCGH and flow-cytometry are limited by their lack of sensitivity in identifying copy number neutral LOH, the finding of copy-number neutral LOH through SNP-LOH analysis is particularly interesting as it may represent small-scale genome wide changes associated with the underlying defect in BER. This data suggests that the previous analysis of MAP adenomas by flow cytometry should not be dismissed as those tumours studied may have harboured copy number neutral LOH.

The development of the first mouse model of MAP ($Apc^{Min+/-}/Myh^{-/-}$ mice bred on C57BL6/SV129 genetic background) (Chapter 5) was successful in that this mouse developed several features in keeping with the human MAP syndrome, those of intestinal adenoma development and evidence of somatic G:C>T:A transversions at *Apc*. However, due to the influence of the *Min* allele on adenoma development the majority of adenomas developed in this model lost the second allele of *Apc* through LOH rather than through truncating mutations (as observed in human MAP). Furthermore, somatic *Apc* mutation screening in these animals suggested a polyclonal origin from the $ApcMin^{+/-}$ / $Myh^{-/-}$ mice studied. This finding was explored further in the clonal analysis of adenoma development in Chapter 9.

It is still not understood why when *Myh* is knocked out alone in mice no gastrointestinal phenotype develops. The influence of the genetic background on which the mouse is bred appears to have a profound effect. This was borne out in the development of the second mouse model of MAP whereby none of the animals developed a gastro-intestinal phenotype when bred on the AKR genetic background. The basis of the second mouse model of MAP was to produce a mouse model was to reduce the incidence of LOH at *Apc* as the second hit in adenoma development by breeding $ApcMin^{+/-}$ / $Myh^{-/-}$ mice on the AKR genetic background. My study, alongside the findings of Sakamoto *et al* (Sakamoto, Tominaga et al. 2007), who developed a mouse model of MAP during the course of my thesis, have provided evidence that mouse models of MAP (on both the C57B6 and AKR genetic background) appear to

require a second promoter of tumorigenesis either through external oxidative stress (Sakamoto, Tominaga et al. 2007), or inherited mutations through the *ApcMin*$^{+/-}$ allele.

Pathogenesis and identification of potential candidate genes in the MCRA phenotype

To date, the understanding of the underlying pathogenesis of the multiple colorectal adenoma phenotype (individuals who develop between 5-100 adenomas) includes the identification of a subset cases with underlying germline *APC* mutations (AFAP) and bi-alleleic *MYH* mutation carriers, together these account for up to 50% of cases. Previously, candidate gene screens have included those involved in Wnt signalling (*APC2*, conductin and *GSK3β)* the *TGF-β* pathway (*SMAD4* and *BMPR1A)* and DNA repair (*NEIL2*, *TDG, UNG2, NTHL1, NEIL2, MPG* and *SMUG1)* (Lipton, Sieber et al. 2003) (Broderick, Bagratuni et al. 2006). No pathogenic germline predisposition genes were identified.

I set out to determine potential pathogenic mechanisms and candidate genes in the MCRA phenotype utilising several approaches in tandem.

In my study of 25 MCRA cases (with no underlying *APC* or *MYH* mutations), I demonstrated disruption of Wnt signalling in MCRA cases through increased nuclear ß-catenin expression on immunohistochemistry when compared to sporadic adenomas (Chapter 6). Somatic mutation screening at *APC* was undertaken in MCRA cases in order to identify any mutational signature indicative of an underlying defect in DNA repair. No such mutational signature was identified. However, on lymphoblastoid cell line expression array analysis on 11 MCRA cases and controls (Chapter 7), 3 candidate genes (all related to DNA repair) were identified. Expression of *DUT, CXCR4* and *POLE2* were all reduced >3 fold in MCRA cases when compared to controls. These were taken forward for screening as potential candidate genes with 12 other candidates in Chapter 8. Further work of interest in utilising expression analysis in lymphoblastoid cell lines would include the inhibition of nonsense mediated decay (NMD) in order to identify transcripts harbouring mutations, this would be within the remit that lymphocytes express the genes of interest.

On guidance of the results from Chapters 6 and 7, and from evidence in current literature, 15 candidate genes were screened in 95 MCRA cases in Chapter 8. These included Wnt related genes following the discovery of significantly increased nuclear ß-catenin expression in MCRA cases in Chapter 6 and the DNA repair genes *DUT, CXCR4* and *POLE2* as identified in Chapter 7.

The most interesting and significant finding was the V154G heterozygous SNP (rs1802838) found in exon 7 of *DUT* which was identified in 11% of MCRA cases (Hardy-Weinberg χ^2 0.34) and 0% (0/47) of controls screened. This SNP is predicted to alter the UTPase region of the gene and could potentially be deleterious. Further studies of this SNP are warranted in an independent MCRA cohort and a larger control population. At this time population based data is not available for this SNP through the HapMap consortium.

My data suggest that the remaining MCRA genes as yet to be identified would include further candidates from the Wnt signalling pathway (including Wnt inhibitory factors) and DNA repair genes. It is likely that the remaining genes are of low to moderate penetrance and multiple loci may be involved. Therefore future strategies should incorporate a genome wide association studies in selected cases and controls, and whole genome sequencing in carefully selected MCRA cases.

Investigation of clonality in adenoma development

In Chapter 9, I demonstrated that somatic *APC* mutations can be successfully utilised as clonal markers in adenoma development. This is the first clonal marker in CRC which utilises a marker relevant to the pathogenesis of the underlying disease.

Clonality in FAP, AFAP and sporadic adenomas were studied through laser-capture micro-dissection of individual crypts and subsequent analysis of DNA for somatic mutations at *APC* which were used as clonal markers.

The findings were intriguing, 100% of FAP adenomas were found to be polyclonal which support previous studies in both human and mouse models of FAP (Novelli, Williamson et al. 1996) (Merritt, Gould et al. 1997). One hundred percent of AFAP adenomas were clonal (with one adenoma

demonstrating 2nd and 3rd hits at APC in every crypt dissected). This is the first study of clonality in AFAP and supports Sieber *et al's* findings that up to three hits at *APC* are required to initiate tumorigenesis (Sieber, Segditsas et al. 2006). All AFAP adenomas studied were from individuals with a germline mutation in the alternitvely spliced region of exon 9 (R332X) therefore further studies should include individuals with both 5' and 3' germline mutations at *APC*.

Interestingly, examination of sporadic adenomas found evidence to support "top down" growth in crypts leading weight to the theory of "active interaction" between crypts in the colorectal epithelium suggested by (Thliveris, Halberg et al. 2005). This finding also questions the role of stem cells the transition from normal to dyplastic crypt architecture as stem cells reside in the bottom of the intestinal crypt. Therefore, my data (albeit in limited numbers of sporadic adenomas) supports "top down" growth as suggested by Shih *et al* (Shih, Wang et al. 2001).

Future work should include the study of a greater number of adenomas from each group including AFAP tumours from individuals with 5' and 3' germline mutations.

In terms of furthering the understanding MAP tumours particularly in light of findings of evidence of polyclonality in the MAP mouse model (although it is likely that this was driven by the *Min* allele), it is planned that this experimental technique be applied to MAP adenomas. This work is planned for the future.

In conclusion, the work in this thesis has helped to further define the clinico-pathological features of MAP, and through the development of a mouse model, demonstrate that there is no increased risk of tumour development in heterozygous carriers. I have furthered the understanding of the pathogenesis of MAP adenomas by demonstrating chromosomal instability (both small and large-scale) in 78% of adenomas from MAP patients through aCGH analysis.

On studying MCRA cases, I identified and screened potential candidate genes from the Wnt signalling signalling pathway and DNA repair. I subsequently identified a non-synonymous SNP in exon 7 of *DUT* in 11% of MCRA cases which has pathogeneic potential. Future approaches in MCRA gene

identification would include genome-wide association studies and whole genome sequencing in selected MCRA cases.

Investigation of clonality in FAP, AFAP and sporadic adenomas has furthered the understanding of pathogenesis of adenoma development, in particular AFAP, and questioned some long-held beliefs in CRC pathogenesis.

Publications and conference proceedings

1: Colorectal cancer and inherited mutations in base excision repair.
Elizabeth Chow, **Christina Thirlwell**, Lara Lipton. *Lancet Oncology* 2004; vol 5: iss 10, 600-606

2: An update on the genetics of colorectal cancer.
Z Kemp, **C Thirlwell**, O Sieber, A Silver, I Tomlinson. *Human and Molecular Genetics* 2004; 13: R177-R185

3: *Myh* Deficiency Enhances Intestinal Tumourigenesis in Multiple Intestinal Neoplasia (*ApcMin*$^{+/-}$) Mice.
Oliver M. Sieber, Kimberley M. Howarth, **Christina Thirlwell,** Nikki Mandir, Robert A. Goodlad, Ashfaq Gilkar, Bradley Spencer-Dene, Gordon Stamp, Victoria Johnson, Andrew Silver, Jeffrey H. Miller, Mohammad Ilyas, and Ian P. M. Tomlinson. *Cancer Research* 2004 15; 64 (24): 8876-81

4: Investigation of pathogenic mechanisms in multiple colorectal adenoma patients. **C Thirlwell**, KM Howarth, S Segitsas, G Guerra, HJW Thomas, RKS Phillips, IC Talbot, M Gorman, MR Novelli, OM Sieber, IPM Tomlinson. *BJC* 2007 Jun 4; 96(11): 1729-34.

5: Disease severity and genetic pathways in attenuated familial polyposis vary greatly but depend on the site of germline mutation. O. Sieber, S.Segditsas, A.. Knudsen, J.Zhang, J.Luz, A.Rowan, S.Spain, **C.Thirlwell**, K. Howarth, E.Jaeger, J.Robinson, E.Volikos, A.Silver, G.Kelly, S.Aretz, I.Frayling, P.Hutter, M.Dunlop, K.Neale, R.Phillips, L.Aaltonen, K.Heinimann and I. Tomlinson. *Gut* 2006; 55(10); 1440-48.

6: Analysis of copy number changes suggests chromosomal instability in a minority of large colorectal adenomas. Angela Jones, **Christina Thirlwell**, Kimberley Howarth, Trevor Graham, William Chambers, Stefania Segditsas, Karen Page, Robin Phillips, Huw Thomas, Oliver Sieber, Elinor Sawyer, Ian Tomlinson. *J Path* 2007 Nov; 213(3): 249-56.

Oral Proceedings

1: The clonal origin of Human tumours – is FAP different?
British Pathological Society Centenary Meeting, July 2006.

2: Utilising somatic Adenomatous Polyposis Coli (*APC*) mutations as clonal markers in colonic adenomas. International Society for Gastrointestinal Hereditary Tumours, Yokohama, Japan. March 2007.

12 References

Abdel-Rahman, W. M., S. Knuutila, et al. (2008). "Truncation of MBD4 predisposes to reciprocal chromosomal translocations and alters the response to therapeutic agents in colon cancer cells." DNA Repair (Amst) **7**(2): 321-8.

Aguilera, O., M. F. Fraga, et al. (2006). "Epigenetic inactivation of the Wnt antagonist DICKKOPF-1 (DKK-1) gene in human colorectal cancer." Oncogene **25**(29): 4116-21.

Ajith Kumar, V. K., J. A. Gold, et al. (2007). "Sebaceous adenomas in an MYH associated polyposis patient of Indian (Gujarati) origin." Fam Cancer.

Al-Tassan, N., N. H. Chmiel, et al. (2002). "Inherited variants of MYH associated with somatic G:C-->T:A mutations in colorectal tumors." Nat Genet **30**(2): 227-32.

Al-Tassan, N., T. Eisen, et al. (2004). "Inherited variants in MYH are unlikely to contribute to the risk of lung carcinoma." Hum Genet **114**(2): 207-10.

Alberici, P., E. de Pater, et al. (2007). "Aneuploidy arises at early stages of Apc-driven intestinal tumorigenesis and pinpoints conserved chromosomal loci of allelic imbalance between mouse and human." Am J Pathol **170**(1): 377-87.

Albuquerque, C., C. Breukel, et al. (2002). "The 'just-right' signaling model: APC somatic mutations are selected based on a specific level of activation of the beta-catenin signaling cascade." Hum Mol Genet **11**(13): 1549-60.

Alexander, P. (1985). "Do cancers arise from a single transformed cell or is monoclonality of tumours a late event in carcinogenesis?" Br J Cancer **51**(4): 453-7.

Anderson, G. L., M. Limacher, et al. (2004). "Effects of conjugated equine estrogen in postmenopausal women with hysterectomy: the Women's Health Initiative randomized controlled trial." Jama **291**(14): 1701-12.

Ashburner, M., C. A. Ball, et al. (2000). "Gene ontology: tool for the unification of biology. The Gene Ontology Consortium." Nat Genet **25**(1): 25-9.

Audebert, M., S. Chevillard, et al. (2000). "Alterations of the DNA repair gene OGG1 in human clear cell carcinomas of the kidney." Cancer Res **60**(17): 4740-4.

Bach, S. P., A. G. Renehan, et al. (2000). "Stem cells: the intestinal stem cell as a paradigm." Carcinogenesis **21**(3): 469-76.

Bader, S., M. Walker, et al. (1999). "Somatic frameshift mutations in the MBD4 gene of sporadic colon cancers with mismatch repair deficiency." Oncogene **18**(56): 8044-7.

Baker, S. M., A. C. Harris, et al. (1998). "Enhanced intestinal adenomatous polyp formation in Pms2-/-;Min mice." Cancer Res **58**(6): 1087-9.

Balaguer, F., S. Castellvi-Bel, et al. (2007). "Identification of MYH mutation carriers in colorectal cancer: a multicenter, case-control, population-based study." Clin Gastroenterol Hepatol **5**(3): 379-87.

Bandipalliam, P. (2005). "Syndrome of early onset colon cancers, hematologic malignancies & features of neurofibromatosis in HNPCC families with homozygous mismatch repair gene mutations." Fam Cancer **4**(4): 323-33.

Baris, H. N., I. Kedar, et al. (2007). "Prevalence of breast and colorectal cancer in Ashkenazi Jewish carriers of Fanconi anemia and Bloom syndrome." Isr Med Assoc J **9**(12): 847-50.

Barnetson, R. A., L. Devlin, et al. (2007). "Germline mutation prevalence in the base excision repair gene, MYH, in patients with endometrial cancer." Clin Genet.

Baron, J. A., B. F. Cole, et al. (2003). "A randomized trial of aspirin to prevent colorectal adenomas." N Engl J Med **348**(10): 891-9.

Bartkova, J., Z. Horejsi, et al. (2005). "DNA damage response as a candidate anti-cancer barrier in early human tumorigenesis." Nature **434**(7035): 864-70.

Batlle, E., J. Bacani, et al. (2005). "EphB receptor activity suppresses colorectal cancer progression." Nature **435**(7045): 1126-30.

Batlle, E., J. T. Henderson, et al. (2002). "Beta-catenin and TCF mediate cell positioning in the intestinal epithelium by controlling the expression of EphB/ephrinB." Cell **111**(2): 251-63.

Baumgart, D. C. and S. R. Carding (2007). "Inflammatory bowel disease: cause and immunobiology." Lancet **369**(9573): 1627-40.

Bentley, D. R. (2006). "Whole-genome re-sequencing." Curr Opin Genet Dev **16**(6): 545-52.

Bergstrom, A., P. Pisani, et al. (2001). "Overweight as an avoidable cause of cancer in Europe." Int J Cancer **91**(3): 421-30.

Bernstein, D. A., M. C. Zittel, et al. (2003). "High-resolution structure of the E.coli RecQ helicase catalytic core." Embo J **22**(19): 4910-21.

Beutler, E., Z. Collins, et al. (1967). "Value of genetic variants of glucose-6-phosphate dehydrogenase in tracing the origin of malignant tumors." N Engl J Med **276**(7): 389-91.

Bisgaard, M. L., K. Fenger, et al. (1994). "Familial adenomatous polyposis (FAP): frequency, penetrance, and mutation rate." Hum Mutat **3**(2): 121-5.

Bjerknes, M. (1986). "A test of the stochastic theory of stem cell differentiation." Biophys J **49**(6): 1223-7.

Bjerknes, M. and H. Cheng (1999). "Colossal crypts bordering colon adenomas in Apc(Min) mice express full-length Apc." Am J Pathol **154**(6): 1831-4.

Bjerknes, M., H. Cheng, et al. (1997). "APC mutation and the crypt cycle in murine and human intestine." Am J Pathol **150**(3): 833-9.

Blair, N. P. and C. L. Trempe (1980). "Hypertrophy of the retinal pigment epithelium associated with Gardner's syndrome." Am J Ophthalmol **90**(5): 661-7.

Boardman, L. A., S. N. Thibodeau, et al. (1998). "Increased risk for cancer in patients with the Peutz-Jeghers syndrome." Ann Intern Med **128**(11): 896-9.

Boman, B. M., J. Z. Fields, et al. (2001). "Computer modeling implicates stem cell overproduction in colon cancer initiation." Cancer Res **61**(23): 8408-11.

Bouguen, G., S. Manfredi, et al. (2007). "Colorectal Adenomatous Polyposis Associated with MYH Mutations: Genotype and Phenotype Characteristics." Dis Colon Rectum **50**(10): 1612-1617.

Boyer, J. C., A. Umar, et al. (1995). "Microsatellite instability, mismatch repair deficiency, and genetic defects in human cancer cell lines." Cancer Res **55**(24): 6063-70.

Broderick, P., T. Bagratuni, et al. (2006). "Evaluation of NTHL1, NEIL1, NEIL2, MPG, TDG, UNG and SMUG1 genes in familial colorectal cancer predisposition." BMC Cancer **6**: 243.

Broderick, P., L. Carvajal-Carmona, et al. (2007). "A genome-wide association study shows that common alleles of SMAD7 influence colorectal cancer risk." Nat Genet **39**(11): 1315-7.

Brownstein, M. H., A. H. Mehregan, et al. (1979). "The dermatopathology of Cowden's syndrome." Br J Dermatol **100**(6): 667-73.

Bulow, S. (1986). "Clinical features in familial polyposis coli. Results of the Danish Polyposis Register." Dis Colon Rectum **29**(2): 102-7.

Burkitt, D. P. (1969). "Related disease--related cause?" Lancet **2**(7632): 1229-31.

Burn, J., P. D. Chapman, et al. (1998). "Diet and cancer prevention: the concerted action polyp prevention (CAPP) studies." Proc Nutr Soc **57**(2): 183-6.

Burt, R. W., Jass, J.R. (2000). Hyperplastic Polyposis. Berlin, Springer-Verlag.

Byun, T., M. Karimi, et al. (2005). "Expression of secreted Wnt antagonists in gastrointestinal tissues: potential role in stem cell homeostasis." J Clin Pathol **58**(5): 515-9.

Cahill, D. P., C. Lengauer, et al. (1998). "Mutations of mitotic checkpoint genes in human cancers." Nature **392**(6673): 300-3.

Cairnie, A. B. and B. H. Millen (1975). "Fission of crypts in the small intestine of the irradiated mouse." Cell Tissue Kinet **8**(2): 189-96.

Cannon-Albright, L. A., M. H. Skolnick, et al. (1988). "Common inheritance of susceptibility to colonic adenomatous polyps and associated colorectal cancers." N Engl J Med **319**(9): 533-7.

Cardoso, J., L. Molenaar, et al. (2006). "Chromosomal instability in MYH- and APC-mutant adenomatous polyps." Cancer Res **66**(5): 2514-9.

Carvajal-Carmona, L., K. Howarth, et al. (2007). "Molecular classification and genetic pathways in hyperplastic polyposis syndrome." J Pathol.

Caspari, R., S. Olschwang, et al. (1995). "Familial adenomatous polyposis: desmoid tumours and lack of ophthalmic lesions (CHRPE) associated with APC mutations beyond codon 1444." Hum Mol Genet **4**(3): 337-40.

Castellone, M. D., H. Teramoto, et al. (2005). "Prostaglandin E2 promotes colon cancer cell growth through a Gs-axin-beta-catenin signaling axis." Science **310**(5753): 1504-10.

Chan, A. T., E. L. Giovannucci, et al. (2005). "Long-term use of aspirin and nonsteroidal anti-inflammatory drugs and risk of colorectal cancer." Jama **294**(8): 914-23.

Chan, T. L., W. Zhao, et al. (2003). "BRAF and KRAS mutations in colorectal hyperplastic polyps and serrated adenomas." Cancer Res **63**(16): 4878-81.

Cheng, H., M. Bjerknes, et al. (1986). "Crypt production in normal and diseased human colonic epithelium." Anat Rec **216**(1): 44-8.

Cheng, H. and C. P. Leblond (1974). "Origin, differentiation and renewal of the four main epithelial cell types in the mouse small intestine. V. Unitarian Theory of the origin of the four epithelial cell types." Am J Anat **141**(4): 537-61.

Chlebowski, R. T., J. Wactawski-Wende, et al. (2004). "Estrogen plus progestin and colorectal cancer in postmenopausal women." N Engl J Med **350**(10): 991-1004.

Chmiel, N. H., A. L. Livingston, et al. (2003). "Insight into the functional consequences of inherited variants of the hMYH adenine glycosylase associated with colorectal cancer: complementation assays with hMYH variants and pre-steady-state kinetics of the corresponding mutated E.coli enzymes." J Mol Biol **327**(2): 431-43.

Cho, E., S. A. Smith-Warner, et al. (2004). "Alcohol intake and colorectal cancer: a pooled analysis of 8 cohort studies." Ann Intern Med **140**(8): 603-13.

Church, J. M., V. W. Fazio, et al. (1988). "Small colorectal polyps. Are they worth treating?" Dis Colon Rectum **31**(1): 50-3.

Clark, J., S. Edwards, et al. (2003). "Genome-wide screening for complete genetic loss in prostate cancer by comparative hybridization onto cDNA microarrays." Oncogene **22**(8): 1247-52.

Clark, J., S. Edwards, et al. (2002). "Identification of amplified and expressed genes in breast cancer by comparative hybridization onto microarrays of randomly selected cDNA clones." Genes Chromosomes Cancer **34**(1): 104-14.

Cleary, S. P., W. Zhang, et al. (2003). "Heterozygosity for the BLM(Ash) mutation and cancer risk." Cancer Res **63**(8): 1769-71.

Clement, G., I. Guilleret, et al. (2008). "Epigenetic alteration of the Wnt inhibitory factor-1 promoter occurs early in the carcinogenesis of Barrett's esophagus." Cancer Sci **99**(1): 46-53.

Colliver, D. W., N. P. Crawford, et al. (2006). "Molecular profiling of ulcerative colitis-associated neoplastic progression." Exp Mol Pathol **80**(1): 1-10.

Coogan, P. F., J. Smith, et al. (2007). "Statin use and risk of colorectal cancer." J Natl Cancer Inst **99**(1): 32-40.

Cormier, R. T., A. Bilger, et al. (2000). "The Mom1AKR intestinal tumor resistance region consists of Pla2g2a and a locus distal to D4Mit64." Oncogene **19**(28): 3182-92.

Crabtree, M., O. M. Sieber, et al. (2003). "Refining the relation between 'first hits' and 'second hits' at the APC locus: the 'loose fit' model and evidence for differences in somatic mutation spectra among patients." Oncogene **22**(27): 4257-65.

Crabtree, M. D., I. P. Tomlinson, et al. (2001). "Variability in the severity of colonic disease in familial adenomatous polyposis results from differences in tumour initiation rather than progression and depends relatively little on patient age." Gut **49**(4): 540-3.

Crawford, N. P., D. W. Colliver, et al. (2005). "Characterization of genotype-phenotype relationships and stratification by the CARD15 variant genotype for inflammatory bowel disease susceptibility loci using

multiple short tandem repeat genetic markers." Hum Mutat **25**(2): 156-66.

Croitoru, M. E., S. P. Cleary, et al. (2007). "Germline MYH mutations in a clinic-based series of Canadian multiple colorectal adenoma patients." J Surg Oncol **95**(6): 499-506.

Csizmadi, I., J. P. Collet, et al. (2004). "The effects of transdermal and oral oestrogen replacement therapy on colorectal cancer risk in postmenopausal women." Br J Cancer **90**(1): 76-81.

Cummings, J. H. and H. N. Englyst (1987). "Fermentation in the human large intestine and the available substrates." Am J Clin Nutr **45**(5 Suppl): 1243-55.

Cybulski, C., B. Gorski, et al. (2004). "CHEK2 is a multiorgan cancer susceptibility gene." Am J Hum Genet **75**(6): 1131-5.

De Ferro, S. M., P. Lage, et al. (2007). "[MYH associated poliposis: severe phenotype in the homozigoty for the 1103delC mutation]." Acta Med Port **20**(3): 243-7.

de Jong, M. M., I. M. Nolte, et al. (2002). "Low-penetrance genes and their involvement in colorectal cancer susceptibility." Cancer Epidemiol Biomarkers Prev **11**(11): 1332-52.

Debinski, H. S., J. Trojan, et al. (1995). "Effect of sulindac on small polyps in familial adenomatous polyposis." Lancet **345**(8953): 855-6.

Deka, J., J. Kuhlmann, et al. (1998). "A domain within the tumor suppressor protein APC shows very similar biochemical properties as the microtubule-associated protein tau." Eur J Biochem **253**(3): 591-7.

Demple, B. and L. Harrison (1994). "Repair of oxidative damage to DNA: enzymology and biology." Annu Rev Biochem **63**: 915-48.

Dennis, G., Jr., B. T. Sherman, et al. (2003). "DAVID: Database for Annotation, Visualization, and Integrated Discovery." Genome Biol **4**(5): P3.

Dietrich, W. F., E. S. Lander, et al. (1993). "Genetic identification of Mom-1, a major modifier locus affecting Min-induced intestinal neoplasia in the mouse." Cell **75**(4): 631-9.

Doll (2003). Epidemiology of Cancer. C. T. Warrell D, Oxford University Press.

Doll, R. and R. Peto (1981). "The causes of cancer: quantitative estimates of avoidable risks of cancer in the United States today." J Natl Cancer Inst **66**(6): 1191-308.

Dormond, O., A. Foletti, et al. (2001). "NSAIDs inhibit alpha V beta 3 integrin-mediated and Cdc42/Rac-dependent endothelial-cell spreading, migration and angiogenesis." Nat Med **7**(9): 1041-7.

Douglas, E. J., H. Fiegler, et al. (2004). "Array comparative genomic hybridization analysis of colorectal cancer cell lines and primary carcinomas." Cancer Res **64**(14): 4817-25.

Dubois, R. N., S. B. Abramson, et al. (1998). "Cyclooxygenase in biology and disease." Faseb J **12**(12): 1063-73.

DuBois, R. N., F. M. Giardiello, et al. (1996). "Nonsteroidal anti-inflammatory drugs, eicosanoids, and colorectal cancer prevention." Gastroenterol Clin North Am **25**(4): 773-91.

Eberhart, C. E., R. J. Coffey, et al. (1994). "Up-regulation of cyclooxygenase 2 gene expression in human colorectal adenomas and adenocarcinomas." Gastroenterology **107**(4): 1183-8.

Egashira, A., K. Yamauchi, et al. (2002). "Mutational specificity of mice defective in the MTH1 and/or the MSH2 genes." DNA Repair (Amst) **1**(11): 881-93.

Englyst, H. N., H. Trowell, et al. (1987). "Dietary fiber and resistant starch." Am J Clin Nutr **46**(6): 873-4.

Enholm, S., T. Hienonen, et al. (2003). "Proportion and phenotype of MYH-associated colorectal neoplasia in a population-based series of Finnish colorectal cancer patients." Am J Pathol **163**(3): 827-32.

Esteller, M., R. A. Risques, et al. (2001). "Promoter hypermethylation of the DNA repair gene O(6)-methylguanine-DNA methyltransferase is associated with the presence of G:C to A:T transition mutations in p53 in human colorectal tumorigenesis." Cancer Res **61**(12): 4689-92.

Esteller, M., A. Sparks, et al. (2000). "Analysis of adenomatous polyposis coli promoter hypermethylation in human cancer." Cancer Res **60**(16): 4366-71.

Esteller, M., M. Toyota, et al. (2000). "Inactivation of the DNA repair gene O6-methylguanine-DNA methyltransferase by promoter

hypermethylation is associated with G to A mutations in K-ras in colorectal tumorigenesis." Cancer Res **60**(9): 2368-71.

Evertsson, S., A. Lindblom, et al. (2001). "APC I1307K and E1317Q variants are rare or do not occur in Swedish colorectal cancer patients." Eur J Cancer **37**(4): 499-502.

Farrington, S. M., A. Tenesa, et al. (2005). "Germline susceptibility to colorectal cancer due to base-excision repair gene defects." Am J Hum Genet **77**(1): 112-9.

Fearnhead, N. S., J. L. Wilding, et al. (2004). "Multiple rare variants in different genes account for multifactorial inherited susceptibility to colorectal adenomas." Proc Natl Acad Sci U S A **101**(45): 15992-7.

Fearon, E. R., S. R. Hamilton, et al. (1987). "Clonal analysis of human colorectal tumors." Science **238**(4824): 193-7.

Feng, Y., C. C. Broder, et al. (1996). "HIV-1 entry cofactor: functional cDNA cloning of a seven-transmembrane, G protein-coupled receptor." Science **272**(5263): 872-7.

Fernandez, E., C. La Vecchia, et al. (2001). "Oral contraceptives and colorectal cancer risk: a meta-analysis." Br J Cancer **84**(5): 722-7.

Fiegler, H., P. Carr, et al. (2003). "DNA microarrays for comparative genomic hybridization based on DOP-PCR amplification of BAC and PAC clones." Genes Chromosomes Cancer **36**(4): 361-74.

Figer, A., R. Shtoyerman-Chen, et al. (2001). "Phenotypic characteristics of colo-rectal cancer in I1307K APC germline mutation carriers compared with sporadic cases." Br J Cancer **85**(9): 1368-71.

Fodde, R., J. Kuipers, et al. (2001). "Mutations in the APC tumour suppressor gene cause chromosomal instability." Nat Cell Biol **3**(4): 433-8.

Frayling, I. M., N. E. Beck, et al. (1998). "The APC variants I1307K and E1317Q are associated with colorectal tumors, but not always with a family history." Proc Natl Acad Sci U S A **95**(18): 10722-7.

Fromme, J. C., A. Banerjee, et al. (2004). "Structural basis for removal of adenine mispaired with 8-oxoguanine by MutY adenine DNA glycosylase." Nature **427**(6975): 652-6.

Gaasenbeek, M., K. Howarth, et al. (2006). "Combined array-comparative genomic hybridization and single-nucleotide polymorphism-loss of

heterozygosity analysis reveals complex changes and multiple forms of chromosomal instability in colorectal cancers." Cancer Res **66**(7): 3471-9.

Gentleman, R. C., V. J. Carey, et al. (2004). "Bioconductor: open software development for computational biology and bioinformatics." Genome Biol **5**(10): R80.

Giardiello, F. M. (1994). "Sulindac and polyp regression." Cancer Metastasis Rev **13**(3-4): 279-83.

Giardiello, F. M., J. D. Brensinger, et al. (2000). "Very high risk of cancer in familial Peutz-Jeghers syndrome." Gastroenterology **119**(6): 1447-53.

Giardiello, F. M., S. B. Welsh, et al. (1987). "Increased risk of cancer in the Peutz-Jeghers syndrome." N Engl J Med **316**(24): 1511-4.

Gillen, C. D., R. S. Walmsley, et al. (1994). "Ulcerative colitis and Crohn's disease: a comparison of the colorectal cancer risk in extensive colitis." Gut **35**(11): 1590-2.

Gismondi, V., L. Bonelli, et al. (2002). "Prevalence of the E1317Q variant of the APC gene in Italian patients with colorectal adenomas." Genet Test **6**(4): 313-7.

Gismondi, V., M. Meta, et al. (2004). "Prevalence of the Y165C, G382D and 1395delGGA germline mutations of the MYH gene in Italian patients with adenomatous polyposis coli and colorectal adenomas." Int J Cancer **109**(5): 680-4.

Gogos, A., J. Cillo, et al. (1996). "Specific recognition of A/G and A/7,8-dihydro-8-oxoguanine (8-oxoG) mismatches by Escherichia coli MutY: removal of the C-terminal domain preferentially affects A/8-oxoG recognition." Biochemistry **35**(51): 16665-71.

Goldstein, N. S., P. Bhanot, et al. (2003). "Hyperplastic-like colon polyps that preceded microsatellite-unstable adenocarcinomas." Am J Clin Pathol **119**(6): 778-96.

Goode, E. L., C. M. Ulrich, et al. (2002). "Polymorphisms in DNA repair genes and associations with cancer risk." Cancer Epidemiol Biomarkers Prev **11**(12): 1513-30.

Gorlin, R. J., M. M. Cohen, Jr., et al. (1992). "Bannayan-Riley-Ruvalcaba syndrome." Am J Med Genet **44**(3): 307-14.

Gould, K. A., W. F. Dietrich, et al. (1996). "Mom1 is a semi-dominant modifier of intestinal adenoma size and multiplicity in Min/+ mice." Genetics **144**(4): 1769-76.

Greaves, L. C., S. L. Preston, et al. (2006). "Mitochondrial DNA mutations are established in human colonic stem cells, and mutated clones expand by crypt fission." Proc Natl Acad Sci U S A **103**(3): 714-9.

Groden, J., L. Gelbert, et al. (1993). "Mutational analysis of patients with adenomatous polyposis: identical inactivating mutations in unrelated individuals." Am J Hum Genet **52**(2): 263-72.

Groden, J., A. Thliveris, et al. (1991). "Identification and characterization of the familial adenomatous polyposis coli gene." Cell **66**(3): 589-600.

Grodstein, F., P. A. Newcomb, et al. (1999). "Postmenopausal hormone therapy and the risk of colorectal cancer: a review and meta-analysis." Am J Med **106**(5): 574-82.

Groves, C., H. Lamlum, et al. (2002). "Mutation cluster region, association between germline and somatic mutations and genotype-phenotype correlation in upper gastrointestinal familial adenomatous polyposis." Am J Pathol **160**(6): 2055-61.

Gruber, S. B., N. A. Ellis, et al. (2002). "BLM heterozygosity and the risk of colorectal cancer." Science **297**(5589): 2013.

Gryfe, R., N. Di Nicola, et al. (1998). "Somatic instability of the APC I1307K allele in colorectal neoplasia." Cancer Res **58**(18): 4040-3.

Gryfe, R., N. Di Nicola, et al. (1999). "Inherited colorectal polyposis and cancer risk of the APC I1307K polymorphism." Am J Hum Genet **64**(2): 378-84.

Guan, Y., R. C. Manuel, et al. (1998). "MutY catalytic core, mutant and bound adenine structures define specificity for DNA repair enzyme superfamily." Nat Struct Biol **5**(12): 1058-64.

Hahnloser, D., G. M. Petersen, et al. (2003). "The APC E1317Q variant in adenomatous polyps and colorectal cancers." Cancer Epidemiol Biomarkers Prev **12**(10): 1023-8.

Haigis, K. M., P. D. Hoff, et al. (2004). "Tumor regionality in the mouse intestine reflects the mechanism of loss of Apc function." Proc Natl Acad Sci U S A **101**(26): 9769-73.

Haiman, C. A., L. Le Marchand, et al. (2007). "A common genetic risk factor for colorectal and prostate cancer." Nat Genet.

Halford, S., A. Rowan, et al. (2005). "O(6)-methylguanine methyltransferase in colorectal cancers: detection of mutations, loss of expression, and weak association with G:C>A:T transitions." Gut **54**(6): 797-802.

Halford, S. E., A. J. Rowan, et al. (2003). "Germline mutations but not somatic changes at the MYH locus contribute to the pathogenesis of unselected colorectal cancers." Am J Pathol **162**(5): 1545-8.

Hamilton, S. R., B. Liu, et al. (1995). "The molecular basis of Turcot's syndrome." N Engl J Med **332**(13): 839-47.

Hayashi, H., Y. Tominaga, et al. (2002). "Replication-associated repair of adenine:8-oxoguanine mispairs by MYH." Curr Biol **12**(4): 335-9.

Heiskanen, I. and H. J. Jarvinen (1996). "Occurrence of desmoid tumours in familial adenomatous polyposis and results of treatment." Int J Colorectal Dis **11**(4): 157-62.

Heiss, K. F., D. Schaffner, et al. (1993). "Malignant risk in juvenile polyposis coli: increasing documentation in the pediatric age group." J Pediatr Surg **28**(9): 1188-93.

Hemminki, A., D. Markie, et al. (1998). "A serine/threonine kinase gene defective in Peutz-Jeghers syndrome." Nature **391**(6663): 184-7.

Hendrich, B. and A. Bird (1998). "Identification and characterization of a family of mammalian methyl-CpG binding proteins." Mol Cell Biol **18**(11): 6538-47.

Hendrich, B., U. Hardeland, et al. (1999). "The thymine glycosylase MBD4 can bind to the product of deamination at methylated CpG sites." Nature **401**(6750): 301-4.

Herman, J. G., A. Umar, et al. (1998). "Incidence and functional consequences of hMLH1 promoter hypermethylation in colorectal carcinoma." Proc Natl Acad Sci U S A **95**(12): 6870-5.

Hermsen, M., C. Postma, et al. (2002). "Colorectal adenoma to carcinoma progression follows multiple pathways of chromosomal instability." Gastroenterology **123**(4): 1109-19.

Herrmann, M. G., J. D. Durtschi, et al. (2006). "Amplicon DNA melting analysis for mutation scanning and genotyping: cross-platform comparison of instruments and dyes." Clin Chem **52**(3): 494-503.

Hes, F. J., M. Nielsen, et al. (2007). "Somatic APC Mosaicism: An Underestimated Cause Of Polyposis Coli." Gut.

Hirano, S., Y. Tominaga, et al. (2003). "Mutator phenotype of MUTYH-null mouse embryonic stem cells." J Biol Chem **278**(40): 38121-4.

Hizawa, K., M. Iida, et al. (1994). "Gastrointestinal manifestations of Cowden's disease. Report of four cases." J Clin Gastroenterol **18**(1): 13-8.

Hofting, I., G. Pott, et al. (1993). "[Familial juvenile polyposis with predominant stomach involvement]." Z Gastroenterol **31**(9): 480-3.

Holbrook, J. A., G. Neu-Yilik, et al. (2004). "Nonsense-mediated decay approaches the clinic." Nat Genet **36**(8): 801-8.

Houlston, R. S., A. Collins, et al. (1992). "Dominant genes for colorectal cancer are not rare." Ann Hum Genet **56 (Pt 2)**: 99-103.

Houlston, R. S. and I. P. Tomlinson (2000). "Detecting low penetrance genes in cancer: the way ahead." J Med Genet **37**(3): 161-7.

Houlston, R. S. and I. P. Tomlinson (2001). "Polymorphisms and colorectal tumor risk." Gastroenterology **121**(2): 282-301.

Howe, J. R., J. L. Bair, et al. (2001). "Germline mutations of the gene encoding bone morphogenetic protein receptor 1A in juvenile polyposis." Nat Genet **28**(2): 184-7.

Howe, J. R., F. A. Mitros, et al. (1998). "The risk of gastrointestinal carcinoma in familial juvenile polyposis." Ann Surg Oncol **5**(8): 751-6.

Howe, J. R., S. Roth, et al. (1998). "Mutations in the SMAD4/DPC4 gene in juvenile polyposis." Science **280**(5366): 1086-8.

Hsu, S. H., G. D. Luk, et al. (1983). "Multiclonal origin of polyps in Gardner syndrome." Science **221**(4614): 951-3.

Hubscher, U., H. P. Nasheuer, et al. (2000). "Eukaryotic DNA polymerases, a growing family." Trends Biochem Sci **25**(3): 143-7.

Huusko, P., D. Ponciano-Jackson, et al. (2004). "Nonsense-mediated decay microarray analysis identifies mutations of EPHB2 in human prostate cancer." Nat Genet **36**(9): 979-83.

Hyun, J. W., J. Y. Choi, et al. (2000). "Leukemic cell line, KG-1 has a functional loss of hOGG1 enzyme due to a point mutation and 8-hydroxydeoxyguanosine can kill KG-1." Oncogene **19**(39): 4476-9.

Ilyas, M., I. P. Tomlinson, et al. (1997). "Beta-catenin mutations in cell lines established from human colorectal cancers." Proc Natl Acad Sci U S A **94**(19): 10330-4.

Ionov, Y., N. Nowak, et al. (2004). "Manipulation of nonsense mediated decay identifies gene mutations in colon cancer Cells with microsatellite instability." Oncogene **23**(3): 639-45.

Irizarry, R. A., B. M. Bolstad, et al. (2003). "Summaries of Affymetrix GeneChip probe level data." Nucleic Acids Res **31**(4): e15.

Ishigaki, Y., X. Li, et al. (2001). "Evidence for a pioneer round of mRNA translation: mRNAs subject to nonsense-mediated decay in mammalian cells are bound by CBP80 and CBP20." Cell **106**(5): 607-17.

Ivanov, I., K. C. Lo, et al. (2007). "Identifying candidate colon cancer tumor suppressor genes using inhibition of nonsense-mediated mRNA decay in colon cancer cells." Oncogene **26**(20): 2873-84.

Izumi, T., L. R. Wiederhold, et al. (2003). "Mammalian DNA base excision repair proteins: their interactions and role in repair of oxidative DNA damage." Toxicology **193**(1-2): 43-65.

Jacoby, R. F., K. Seibert, et al. (2000). "The cyclooxygenase-2 inhibitor celecoxib is a potent preventive and therapeutic agent in the min mouse model of adenomatous polyposis." Cancer Res **60**(18): 5040-4.

Jaeger, E., E. Webb, et al. (2008). "Common genetic variants at the CRAC1 (HMPS) locus on chromosome 15q13.3 influence colorectal cancer risk." Nat Genet **40**(1): 26-8.

Jaeger, E. E., K. L. Woodford-Richens, et al. (2003). "An ancestral Ashkenazi haplotype at the HMPS/CRAC1 locus on 15q13-q14 is associated with hereditary mixed polyposis syndrome." Am J Hum Genet **72**(5): 1261-7.

Jain, A. N., T. A. Tokuyasu, et al. (2002). "Fully automatic quantification of microarray image data." Genome Res **12**(2): 325-32.

Jansen, R. C. and J. P. Nap (2001). "Genetical genomics: the added value from segregation." Trends Genet **17**(7): 388-91.

Jaruga, P., T. H. Zastawny, et al. (1994). "Oxidative DNA base damage and antioxidant enzyme activities in human lung cancer." FEBS Lett **341**(1): 59-64.

Jass, J. R. (2005). "Serrated adenoma of the colorectum and the DNA-methylator phenotype." Nat Clin Pract Oncol **2**(8): 398-405.

Jass, J. R., K. Baker, et al. (2006). "Advanced colorectal polyps with the molecular and morphological features of serrated polyps and adenomas: concept of a 'fusion' pathway to colorectal cancer." Histopathology **49**(2): 121-31.

Jass, J. R., V. L. Whitehall, et al. (2002). "Emerging concepts in colorectal neoplasia." Gastroenterology **123**(3): 862-76.

Jeevaratnam, P., D. S. Cottier, et al. (1996). "Familial giant hyperplastic polyposis predisposing to colorectal cancer: a new hereditary bowel cancer syndrome." J Pathol **179**(1): 20-5.

Jenne, D. E., H. Reimann, et al. (1998). "Peutz-Jeghers syndrome is caused by mutations in a novel serine threonine kinase." Nat Genet **18**(1): 38-43.

Jin, W., R. M. Riley, et al. (2001). "The contributions of sex, genotype and age to transcriptional variance in Drosophila melanogaster." Nat Genet **29**(4): 389-95.

Jones, A. M., E. J. Douglas, et al. (2005). "Array-CGH analysis of microsatellite-stable, near-diploid bowel cancers and comparison with other types of colorectal carcinoma." Oncogene **24**(1): 118-29.

Jones, S., P. Emmerson, et al. (2002). "Biallelic germline mutations in MYH predispose to multiple colorectal adenoma and somatic G:C-->T:A mutations." Hum Mol Genet **11**(23): 2961-7.

Joslyn, G., D. S. Richardson, et al. (1993). "Dimer formation by an N-terminal coiled coil in the APC protein." Proc Natl Acad Sci U S A **90**(23): 11109-13.

Kakinuma, S., Y. Kodama, et al. (2007). "Ikaros is a mutational target for lymphomagenesis in Mlh1-deficient mice." Oncogene **26**(20): 2945-9.

Kallioniemi, A., O. P. Kallioniemi, et al. (1992). "Comparative genomic hybridization for molecular cytogenetic analysis of solid tumors." Science **258**(5083): 818-21.

Kambara, T., L. A. Simms, et al. (2004). "BRAF mutation is associated with DNA methylation in serrated polyps and cancers of the colorectum." Gut **53**(8): 1137-44.

Kaneshisa M, S. G. (2004). "The KEGG resource for deciphering the genome." Nucleic Acid Research Database Issue **32**(D): 277-280.

Kanter-Smoler, G., J. Bjork, et al. (2006). "Novel findings in Swedish patients with MYH-associated polyposis: mutation detection and clinical characterization." Clin Gastroenterol Hepatol **4**(4): 499-506.

Kaplan, K. B., A. A. Burds, et al. (2001). "A role for the Adenomatous Polyposis Coli protein in chromosome segregation." Nat Cell Biol **3**(4): 429-32.

Karuman, P., O. Gozani, et al. (2001). "The Peutz-Jegher gene product LKB1 is a mediator of p53-dependent cell death." Mol Cell **7**(6): 1307-19.

Kawamori, T., C. V. Rao, et al. (1998). "Chemopreventive activity of celecoxib, a specific cyclooxygenase-2 inhibitor, against colon carcinogenesis." Cancer Res **58**(3): 409-12.

Kawano, Y. and R. Kypta (2003). "Secreted antagonists of the Wnt signalling pathway." J Cell Sci **116**(Pt 13): 2627-34.

Kawasaki, Y., T. Senda, et al. (2000). "Asef, a link between the tumor suppressor APC and G-protein signaling." Science **289**(5482): 1194-7.

Kemp, Z., L. Carvajal-Carmona, et al. (2006). "Evidence for a colorectal cancer susceptibility locus on chromosome 3q21-q24 from a high-density SNP genome-wide linkage scan." Hum Mol Genet **15**(19): 2903-10.

Kemp, Z., A. Rowan, et al. (2005). "CDC4 mutations occur in a subset of colorectal cancers but are not predicted to cause loss of function and are not associated with chromosomal instability." Cancer Res **65**(24): 11361-6.

Kemp, Z., C. Thirlwell, et al. (2004). "An update on the genetics of colorectal cancer." Hum Mol Genet **13 Spec No 2**: R177-85.

Kijima, T., G. Maulik, et al. (2002). "Regulation of cellular proliferation, cytoskeletal function, and signal transduction through CXCR4 and c-Kit in small cell lung cancer cells." Cancer Res **62**(21): 6304-11.

Kilpivaara, O., P. Laiho, et al. (2003). "CHEK2 1100delC and colorectal cancer." J Med Genet **40**(10): e110.

Kim, H. C., J. M. Wheeler, et al. (2000). "The E-cadherin gene (CDH1) variants T340A and L599V in gastric and colorectal cancer patients in Korea." Gut **47**(2): 262-7.

Kim, I. J., J. L. Ku, et al. (2004). "Mutational analysis of OGG1, MYH, MTH1 in FAP, HNPCC and sporadic colorectal cancer patients: R154H OGG1 polymorphism is associated with sporadic colorectal cancer patients." Hum Genet **115**(6): 498-503.

Kim, J. C., I. H. Ka, et al. (2007). "MYH, OGG1, MTH1, and APC alterations involved in the colorectal tumorigenesis of Korean patients with multiple adenomas." Virchows Arch **450**(3): 311-9.

Kim, K. M. and D. Shibata (2004). "Tracing ancestry with methylation patterns: most crypts appear distantly related in normal adult human colon." BMC Gastroenterol **4**: 8.

Kimchi-Sarfaty, C., J. M. Oh, et al. (2007). "A "silent" polymorphism in the MDR1 gene changes substrate specificity." Science **315**(5811): 525-8.

Kinzler, K. W. and B. Vogelstein (1996). "Lessons from hereditary colorectal cancer." Cell **87**(2): 159-70.

Kishida, S., H. Yamamoto, et al. (1998). "Axin, a negative regulator of the wnt signaling pathway, directly interacts with adenomatous polyposis coli and regulates the stabilization of beta-catenin." J Biol Chem **273**(18): 10823-6.

Klungland, A., I. Rosewell, et al. (1999). "Accumulation of premutagenic DNA lesions in mice defective in removal of oxidative base damage." Proc Natl Acad Sci U S A **96**(23): 13300-5.

Kokko, A., P. Laiho, et al. (2006). "EPHB2 germline variants in patients with colorectal cancer or hyperplastic polyposis." BMC Cancer **6**: 145.

Komar, A. A. (2007). "Genetics. SNPs, silent but not invisible." Science **315**(5811): 466-7.

Kuo, C. F., D. E. McRee, et al. (1992). "Crystallization and crystallographic characterization of the iron-sulfur-containing DNA-repair enzyme endonuclease III from Escherichia coli." J Mol Biol **227**(1): 347-51.

Lage, P., M. Cravo, et al. (2004). "Management of Portuguese patients with hyperplastic polyposis and screening of at-risk first-degree relatives: a contribution for future guidelines based on a clinical study." Am J Gastroenterol **99**(9): 1779-84.

Laiho, P., A. Kokko, et al. (2007). "Serrated carcinomas form a subclass of colorectal cancer with distinct molecular basis." Oncogene **26**(2): 312-20.

Laken, S. J., G. M. Petersen, et al. (1997). "Familial colorectal cancer in Ashkenazim due to a hypermutable tract in APC." Nat Genet **17**(1): 79-83.

Lambertz, S. and W. G. Ballhausen (1993). "Identification of an alternative 5' untranslated region of the adenomatous polyposis coli gene." Hum Genet **90**(6): 650-2.

Lamlum, H., N. Al Tassan, et al. (2000). "Germline APC variants in patients with multiple colorectal adenomas, with evidence for the particular importance of E1317Q." Hum Mol Genet **9**(15): 2215-21.

Lamlum, H., M. Ilyas, et al. (1999). "The type of somatic mutation at APC in familial adenomatous polyposis is determined by the site of the germline mutation: a new facet to Knudson's 'two-hit' hypothesis." Nat Med **5**(9): 1071-5.

Larriba, M. J., N. Valle, et al. (2007). "The inhibition of Wnt/beta-catenin signalling by 1alpha,25-dihydroxyvitamin D3 is abrogated by Snail1 in human colon cancer cells." Endocr Relat Cancer **14**(1): 141-51.

Laurent-Puig, P., C. Beroud, et al. (1998). "APC gene: database of germline and somatic mutations in human tumors and cell lines." Nucleic Acids Res **26**(1): 269-70.

Lengauer, C., K. W. Kinzler, et al. (1997). "Genetic instability in colorectal cancers." Nature **386**(6625): 623-7.

Lengauer, C., K. W. Kinzler, et al. (1998). "Genetic instabilities in human cancers." Nature **396**(6712): 643-9.

Levin, B. (1992). "Ulcerative colitis and colon cancer: biology and surveillance." J Cell Biochem Suppl **16G**: 47-50.

Liaw, D., D. J. Marsh, et al. (1997). "Germline mutations of the PTEN gene in Cowden disease, an inherited breast and thyroid cancer syndrome." Nat Genet **16**(1): 64-7.

Lichtenstein, P., N. V. Holm, et al. (2000). "Environmental and heritable factors in the causation of cancer--analyses of cohorts of twins from Sweden, Denmark, and Finland." N Engl J Med **343**(2): 78-85.

Liew, M., M. Seipp, et al. (2007). "Closed-tube SNP genotyping without labeled probes/a comparison between unlabeled probe and amplicon melting." Am J Clin Pathol **127**(3): 341-8.

Liljegren, A., G. Barker, et al. (2008). "Prevalence of adenomas and hyperplastic polyps in mismatch repair mutation carriers among CAPP2 participants: report by the colorectal adenoma/carcinoma prevention programme 2." J Clin Oncol **26**(20): 3434-9.

Lindahl, T. (1982). "DNA repair enzymes." Annu Rev Biochem **51**: 61-87.

Lindahl, T. (1993). "Instability and decay of the primary structure of DNA." Nature **362**(6422): 709-15.

Lindahl, T. and R. D. Wood (1999). "Quality control by DNA repair." Science **286**(5446): 1897-905.

Lipton, L., C. Fleischmann, et al. (2003). "Contribution of the CHEK2 1100delC variant to risk of multiple colorectal adenoma and carcinoma." Cancer Lett **200**(2): 149-52.

Lipton, L., S. E. Halford, et al. (2003). "Carcinogenesis in MYH-associated polyposis follows a distinct genetic pathway." Cancer Res **63**(22): 7595-9.

Lipton, L., O. M. Sieber, et al. (2003). "Germline mutations in the TGF-beta and Wnt signalling pathways are a rare cause of the "multiple" adenoma phenotype." J Med Genet **40**(4): e35.

Liu, B., N. C. Nicolaides, et al. (1995). "Mismatch repair gene defects in sporadic colorectal cancers with microsatellite instability." Nat Genet **9**(1): 48-55.

Loeb, L. A. (2001). "A mutator phenotype in cancer." Cancer Res **61**(8): 3230-9.

Lowsky, R., A. Magliocco, et al. (2000). "MSH2-deficient murine lymphomas harbor insertion/deletion mutations in the transforming growth factor beta receptor type 2 gene and display low not high frequency microsatellite instability." Blood **95**(5): 1767-72.

Lu, A. L., X. Li, et al. (2001). "Repair of oxidative DNA damage: mechanisms and functions." Cell Biochem Biophys **35**(2): 141-70.

Luongo, C., A. R. Moser, et al. (1994). "Loss of Apc+ in intestinal adenomas from Min mice." Cancer Res **54**(22): 5947-52.

Lynch, H. T. and A. de la Chapelle (2003). "Hereditary colorectal cancer." N Engl J Med **348**(10): 919-32.

Maley, C. C., P. C. Galipeau, et al. (2004). "Selectively advantageous mutations and hitchhikers in neoplasms: p16 lesions are selected in Barrett's esophagus." Cancer Res **64**(10): 3414-27.

Malins, D. C. and R. Haimanot (1991). "Major alterations in the nucleotide structure of DNA in cancer of the female breast." Cancer Res **51**(19): 5430-2.

Maltzman, T., K. Knoll, et al. (2001). "Ki-ras proto-oncogene mutations in sporadic colorectal adenomas: relationship to histologic and clinical characteristics." Gastroenterology **121**(2): 302-9.

Marnett, L. J. (2000). "Oxyradicals and DNA damage." Carcinogenesis **21**(3): 361-70.

Marsh, D. J., P. L. Dahia, et al. (1997). "Germline mutations in PTEN are present in Bannayan-Zonana syndrome." Nat Genet **16**(4): 333-4.

Maskens, A. P. and R. M. Dujardin-Loits (1981). "Kinetics of tissue proliferation in colorectal mucosa during post-natal growth." Cell Tissue Kinet **14**(5): 467-77.

Mathers, J. C., I. Mickleburgh, et al. (2003). "Can resistant starch and/or aspirin prevent the development of colonic neoplasia? The Concerted Action Polyp Prevention (CAPP) 1 Study." Proc Nutr Soc **62**(1): 51-7.

Meijers-Heijboer, H., A. van den Ouweland, et al. (2002). "Low-penetrance susceptibility to breast cancer due to CHEK2(*)1100delC in noncarriers of BRCA1 or BRCA2 mutations." Nat Genet **31**(1): 55-9.

Merritt, A. J., K. A. Gould, et al. (1997). "Polyclonal structure of intestinal adenomas in ApcMin/+ mice with concomitant loss of Apc+ from all tumor lineages." Proc Natl Acad Sci U S A **94**(25): 13927-31.

Micke, P., A. Ostman, et al. (2005). "Laser-assisted cell microdissection using the PALM system." Methods Mol Biol **293**: 151-66.

Midgley, C. A., S. White, et al. (1997). "APC expression in normal human tissues." J Pathol **181**(4): 426-33.

Minowa, O., T. Arai, et al. (2000). "Mmh/Ogg1 gene inactivation results in accumulation of 8-hydroxyguanine in mice." Proc Natl Acad Sci U S A **97**(8): 4156-61.

Miyaki, M., M. Konishi, et al. (1997). "Germline mutation of MSH6 as the cause of hereditary nonpolyposis colorectal cancer." Nat Genet **17**(3): 271-2.

Miyoshi, Y., H. Nagase, et al. (1992). "Somatic mutations of the APC gene in colorectal tumors: mutation cluster region in the APC gene." Hum Mol Genet **1**(4): 229-33.

Moberg, K. H., D. W. Bell, et al. (2001). "Archipelago regulates Cyclin E levels in Drosophila and is mutated in human cancer cell lines." Nature **413**(6853): 311-6.

Monks, S. A., A. Leonardson, et al. (2004). "Genetic inheritance of gene expression in human cell lines." Am J Hum Genet **75**(6): 1094-105.

Mrkonjic, M., S. Raptis, et al. (2007). "MSH2 118T>C and MSH6 159C>T promoter polymorphisms and the risk of colorectal cancer." Carcinogenesis **28**(12): 2575-80.

Muller, A., B. Homey, et al. (2001). "Involvement of chemokine receptors in breast cancer metastasis." Nature **410**(6824): 50-6.

Munemitsu, S., I. Albert, et al. (1995). "Regulation of intracellular beta-catenin levels by the adenomatous polyposis coli (APC) tumor-suppressor protein." Proc Natl Acad Sci U S A **92**(7): 3046-50.

Murphy, T. K., E. E. Calle, et al. (2000). "Body mass index and colon cancer mortality in a large prospective study." Am J Epidemiol **152**(9): 847-54.

Nagasaka, T., A. Goel, et al. (2008). "Methylation pattern of the O6-methylguanine-DNA methyltransferase gene in colon during progressive colorectal tumorigenesis." Int J Cancer **122**(11): 2429-36.

Nakabeppu, Y. (2001). "Regulation of intracellular localization of human MTH1, OGG1, and MYH proteins for repair of oxidative DNA damage." Prog Nucleic Acid Res Mol Biol **68**: 75-94.

Neff, N. F., N. A. Ellis, et al. (1999). "The DNA helicase activity of BLM is necessary for the correction of the genomic instability of bloom syndrome cells." Mol Biol Cell **10**(3): 665-76.

Nichols, H. B., A. Trentham-Dietz, et al. (2005). "Oral contraceptive use, reproductive factors, and colorectal cancer risk: findings from Wisconsin." Cancer Epidemiol Biomarkers Prev **14**(5): 1212-8.

Niessen, R. C., R. H. Sijmons, et al. (2006). "MUTYH and the mismatch repair system: partners in crime?" Hum Genet **119**(1-2): 206-11.

Nishimura, Y., C. L. Martin, et al. (2007). "Genome-wide expression profiling of lymphoblastoid cell lines distinguishes different forms of autism and reveals shared pathways." Hum Mol Genet **16**(14): 1682-98.

Niv, Y., G. Delpre, et al. (2003). "Hyperplastic gastric polyposis, hypergastrinaemia and colorectal neoplasia: a description of four cases." Eur J Gastroenterol Hepatol **15**(12): 1361-6.

Noll, D. M., A. Gogos, et al. (1999). "The C-terminal domain of the adenine-DNA glycosylase MutY confers specificity for 8-oxoguanine.adenine mispairs and may have evolved from MutT, an 8-oxo-dGTPase." Biochemistry **38**(20): 6374-9.

Norat, T., S. Bingham, et al. (2005). "Meat, fish, and colorectal cancer risk: the European Prospective Investigation into cancer and nutrition." J Natl Cancer Inst **97**(12): 906-16.

Novelli, M., A. Cossu, et al. (2003). "X-inactivation patch size in human female tissue confounds the assessment of tumor clonality." Proc Natl Acad Sci U S A **100**(6): 3311-4.

Novelli, M. R., J. A. Williamson, et al. (1996). "Polyclonal origin of colonic adenomas in an XO/XY patient with FAP." Science **272**(5265): 1187-90.

Nowak, M. A., N. L. Komarova, et al. (2002). "The role of chromosomal instability in tumor initiation." Proc Natl Acad Sci U S A **99**(25): 16226-31.

Nowell, P. C. (1976). "The clonal evolution of tumor cell populations." Science **194**(4260): 23-8.

Nugent, K. P., A. D. Spigelman, et al. (1993). "Life expectancy after colectomy and ileorectal anastomosis for familial adenomatous polyposis." Dis Colon Rectum **36**(11): 1059-62.

O'Brien, M. J., S. J. Winawer, et al. (1990). "The National Polyp Study. Patient and polyp characteristics associated with high-grade dysplasia in colorectal adenomas." Gastroenterology **98**(2): 371-9.

O'Brien, M. J., S. Yang, et al. (2004). "Hyperplastic (serrated) polyps of the colorectum: relationship of CpG island methylator phenotype and K-ras mutation to location and histologic subtype." Am J Surg Pathol **28**(4): 423-34.

Oberhuber, G. and M. Stolte (2000). "Gastric polyps: an update of their pathology and biological significance." Virchows Arch **437**(6): 581-90.

Okamoto, K., S. Toyokuni, et al. (1994). "Formation of 8-hydroxy-2'-deoxyguanosine and 4-hydroxy-2-nonenal-modified proteins in human renal-cell carcinoma." Int J Cancer **58**(6): 825-9.

Okkels, H., L. Sunde, et al. (2006). "Polyposis and early cancer in a patient with low penetrant mutations in MSH6 and APC: hereditary colorectal cancer as a polygenic trait." Int J Colorectal Dis **21**(8): 847-50.

Olinski, R., T. Zastawny, et al. (1992). "DNA base modifications in chromatin of human cancerous tissues." FEBS Lett **309**(2): 193-8.

Oshima, M., N. Murai, et al. (2001). "Chemoprevention of intestinal polyposis in the Apcdelta716 mouse by rofecoxib, a specific cyclooxygenase-2 inhibitor." Cancer Res **61**(4): 1733-40.

Oshima, M. and M. M. Taketo (2002). "COX selectivity and animal models for colon cancer." Curr Pharm Des **8**(12): 1021-34.

Park, H. S., R. A. Goodlad, et al. (1995). "Crypt fission in the small intestine and colon. A mechanism for the emergence of G6PD locus-mutated crypts after treatment with mutagens." Am J Pathol **147**(5): 1416-27.

Park, Y. J., E. Y. Choi, et al. (2001). "Genetic changes of hOGG1 and the activity of oh8Gua glycosylase in colon cancer." Eur J Cancer **37**(3): 340-6.

Parkes, M., J. Satsangi, et al. (2001). "Ulcerative colitis is more strongly linked to chromosome 12 than Crohn's disease." Gut **49**(2): 311.

Paul, P., T. Letteboer, et al. (1993). "Identical APC exon 15 mutations result in a variable phenotype in familial adenomatous polyposis." Hum Mol Genet **2**(7): 925-31.

Paulsen, J. E., I. L. Steffensen, et al. (2001). "Qualitative and quantitative relationship between dysplastic aberrant crypt foci and tumorigenesis in the Min/+ mouse colon." Cancer Res **61**(13): 5010-5.

Phillips, R. K., M. H. Wallace, et al. (2002). "A randomised, double blind, placebo controlled study of celecoxib, a selective cyclooxygenase 2 inhibitor, on duodenal polyposis in familial adenomatous polyposis." Gut **50**(6): 857-60.

Plaschke, J., C. Engel, et al. (2004). "Lower incidence of colorectal cancer and later age of disease onset in 27 families with pathogenic MSH6 germline mutations compared with families with MLH1 or MSH2 mutations: the German Hereditary Nonpolyposis Colorectal Cancer Consortium." J Clin Oncol **22**(22): 4486-94.

Pollack, J. R., T. Sorlie, et al. (2002). "Microarray analysis reveals a major direct role of DNA copy number alteration in the transcriptional program of human breast tumors." Proc Natl Acad Sci U S A **99**(20): 12963-8.

Popat, S., J. Stone, et al. (2000). "Prevalence of the APC E1317Q variant in colorectal cancer patients." Cancer Lett **149**(1-2): 203-6.

Porter, T. R., F. M. Richards, et al. (2002). "Contribution of cyclin d1 (CCND1) and E-cadherin (CDH1) polymorphisms to familial and sporadic colorectal cancer." Oncogene **21**(12): 1928-33.

Potten, C. S., M. Kellett, et al. (1992). "Proliferation in human gastrointestinal epithelium using bromodeoxyuridine in vivo: data for different sites, proximity to a tumour, and polyposis coli." Gut **33**(4): 524-9.

Poynter, J. N., S. B. Gruber, et al. (2005). "Statins and the risk of colorectal cancer." N Engl J Med **352**(21): 2184-92.

Preston, S. L., S. J. Leedham, et al. (2008). "The development of duodenal microadenomas in FAP patients: the human correlate of the Min mouse." J Pathol **214**(3): 294-301.

Preston, S. L., W. M. Wong, et al. (2003). "Bottom-up histogenesis of colorectal adenomas: origin in the monocryptal adenoma and initial expansion by crypt fission." Cancer Res **63**(13): 3819-25.

Rajagopalan, H., P. V. Jallepalli, et al. (2004). "Inactivation of hCDC4 can cause chromosomal instability." Nature **428**(6978): 77-81.

Rajagopalan, H. and C. Lengauer (2004). "Aneuploidy and cancer." Nature **432**(7015): 338-41.

Rajagopalan, H. and C. Lengauer (2004). "CIN-ful cancers." Cancer Chemother Pharmacol **54 Suppl 1**: S65-8.

Rashid, A., P. S. Houlihan, et al. (2000). "Phenotypic and molecular characteristics of hyperplastic polyposis." Gastroenterology **119**(2): 323-32.

Reddy, B. S., Y. Hirose, et al. (2000). "Chemoprevention of colon cancer by specific cyclooxygenase-2 inhibitor, celecoxib, administered during different stages of carcinogenesis." Cancer Res **60**(2): 293-7.

Redston, M., K. L. Nathanson, et al. (1998). "The APCI1307K allele and breast cancer risk." Nat Genet **20**(1): 13-4.

Reitmair, A. H., J. C. Cai, et al. (1996). "MSH2 deficiency contributes to accelerated APC-mediated intestinal tumorigenesis." Cancer Res **56**(13): 2922-6.

Ricchi, P., R. Zarrilli, et al. (2003). "Nonsteroidal anti-inflammatory drugs in colorectal cancer: from prevention to therapy." Br J Cancer **88**(6): 803-7.

Risch, N. (2001). "Implications of multilocus inheritance for gene-disease association studies." Theor Popul Biol **60**(3): 215-20.

Rosin-Arbesfeld, R., F. Townsley, et al. (2000). "The APC tumour suppressor has a nuclear export function." Nature **406**(6799): 1009-12.

Rossi, M. R., L. Hawthorn, et al. (2005). "Identification of inactivating mutations in the JAK1, SYNJ2, and CLPTM1 genes in prostate cancer cells using inhibition of nonsense-mediated decay and microarray analysis." Cancer Genet Cytogenet **161**(2): 97-103.

Rowan, A., S. Halford, et al. (2005). "Refining molecular analysis in the pathways of colorectal carcinogenesis." Clin Gastroenterol Hepatol **3**(11): 1115-23.

Rubin, H. (1985). "Cancer as a dynamic developmental disorder." Cancer Res **45**(7): 2935-42.

Rubinfeld, B., I. Albert, et al. (1996). "Binding of GSK3beta to the APC-beta-catenin complex and regulation of complex assembly." Science **272**(5264): 1023-6.

Rubinfeld, B., B. Souza, et al. (1993). "Association of the APC gene product with beta-catenin." Science **262**(5140): 1731-4.

Russell, A. M., J. Zhang, et al. (2006). "Prevalence of MYH germline mutations in Swiss APC mutation-negative polyposis patients." Int J Cancer **118**(8): 1937-40.

Russo, M. T., G. De Luca, et al. (2004). "Accumulation of the oxidative base lesion 8-hydroxyguanine in DNA of tumor-prone mice defective in both the Myh and Ogg1 DNA glycosylases." Cancer Res **64**(13): 4411-4.

Rutter, M., B. Saunders, et al. (2004). "Severity of inflammation is a risk factor for colorectal neoplasia in ulcerative colitis." Gastroenterology **126**(2): 451-9.

Sakamoto, K., Y. Tominaga, et al. (2007). "MUTYH-null mice are susceptible to spontaneous and oxidative stress induced intestinal tumorigenesis." Cancer Res **67**(14): 6599-604.

Sakumi, K., Y. Tominaga, et al. (2003). "Ogg1 knockout-associated lung tumorigenesis and its suppression by Mth1 gene disruption." Cancer Res **63**(5): 902-5.

Salem, O. S. and W. D. Steck (1983). "Cowden's disease (multiple hamartoma and neoplasia syndrome). A case report and review of the English literature." J Am Acad Dermatol **8**(5): 686-96.

Sampson, J. R., S. Dolwani, et al. (2003). "Autosomal recessive colorectal adenomatous polyposis due to inherited mutations of MYH." Lancet **362**(9377): 39-41.

Sandler, R. S., S. Halabi, et al. (2003). "A randomized trial of aspirin to prevent colorectal adenomas in patients with previous colorectal cancer." N Engl J Med **348**(10): 883-90.

Sanger, F., S. Nicklen, et al. (1977). "DNA sequencing with chain-terminating inhibitors." Proc Natl Acad Sci U S A **74**(12): 5463-7.

Satsangi, J., M. Parkes, et al. (1998). "Genetics of inflammatory bowel disease." Clin Sci (Lond) **94**(5): 473-8.

Sayed, M. G., A. F. Ahmed, et al. (2002). "Germline SMAD4 or BMPR1A mutations and phenotype of juvenile polyposis." Ann Surg Oncol **9**(9): 901-6.

Scott-Conner, C. E., M. Hausmann, et al. (1995). "Familial juvenile polyposis: patterns of recurrence and implications for surgical management." J Am Coll Surg **181**(5): 407-13.

Scotton, C. J., J. L. Wilson, et al. (2001). "Epithelial cancer cell migration: a role for chemokine receptors?" Cancer Res **61**(13): 4961-5.

Seidensticker, M. J. and J. Behrens (2000). "Biochemical interactions in the wnt pathway." Biochim Biophys Acta **1495**(2): 168-82.

Shackney, S. E., C. A. Smith, et al. (1989). "Model for the genetic evolution of human solid tumors." Cancer Res **49**(12): 3344-54.

Shibutani, S., M. Takeshita, et al. (1991). "Insertion of specific bases during DNA synthesis past the oxidation-damaged base 8-oxodG." Nature **349**(6308): 431-4.

Shih, I. M., T. L. Wang, et al. (2001). "Top-down morphogenesis of colorectal tumors." Proc Natl Acad Sci U S A **98**(5): 2640-5.

Shih, I. M., W. Zhou, et al. (2001). "Evidence that genetic instability occurs at an early stage of colorectal tumorigenesis." Cancer Res **61**(3): 818-22.

Shinmura, K., T. Kohno, et al. (1998). "Infrequent mutations of the hOGG1 gene, that is involved in the excision of 8-hydroxyguanine in damaged DNA, in human gastric cancer." Jpn J Cancer Res **89**(8): 825-8.

Shoemaker, A. R., K. A. Gould, et al. (1997). "Studies of neoplasia in the Min mouse." Biochim Biophys Acta **1332**(2): F25-48.

Shoemaker, A. R., K. M. Haigis, et al. (2000). "Mlh1 deficiency enhances several phenotypes of Apc(Min)/+ mice." Oncogene **19**(23): 2774-9.

Shoemaker, A. R., A. R. Moser, et al. (1995). "N-ethyl-N-nitrosourea treatment of multiple intestinal neoplasia (Min) mice: age-related effects on the formation of intestinal adenomas, cystic crypts, and epidermoid cysts." Cancer Res **55**(19): 4479-85.

Shoemaker, A. R., A. R. Moser, et al. (1998). "A resistant genetic background leading to incomplete penetrance of intestinal neoplasia and reduced loss of heterozygosity in ApcMin/+ mice." Proc Natl Acad Sci U S A **95**(18): 10826-31.

Sieber, O., S. Segditsas, et al. (2006). "Disease severity and genetic pathways in attenuated familial adenomatous polyposis vary greatly, but depend on the site of the germline mutation." Gut.

Sieber, O. M., K. Heinimann, et al. (2002). "Analysis of chromosomal instability in human colorectal adenomas with two mutational hits at APC." Proc Natl Acad Sci U S A **99**(26): 16910-5.

Sieber, O. M., K. M. Howarth, et al. (2004). "Myh deficiency enhances intestinal tumorigenesis in multiple intestinal neoplasia (ApcMin/+) mice." Cancer Res **64**(24): 8876-81.

Sieber, O. M., L. Lipton, et al. (2003). "Multiple colorectal adenomas, classic adenomatous polyposis, and germ-line mutations in MYH." N Engl J Med **348**(9): 791-9.

Sieber, O. M., I. P. Tomlinson, et al. (2000). "The adenomatous polyposis coli (APC) tumour suppressor--genetics, function and disease." Mol Med Today **6**(12): 462-9.

Sieber, O. M., S. R. Tomlinson, et al. (2005). "Tissue, cell and stage specificity of (epi)mutations in cancers." Nat Rev Cancer **5**(8): 649-55.

Slattery, M. L., S. Edwards, et al. (2003). "Physical activity and colorectal cancer." Am J Epidemiol **158**(3): 214-24.

Slaughter, D. P., H. W. Southwick, et al. (1953). "Field cancerization in oral stratified squamous epithelium; clinical implications of multicentric origin." Cancer **6**(5): 963-8.

Slupska, M. M., C. Baikalov, et al. (1996). "Cloning and sequencing a human homolog (hMYH) of the Escherichia coli mutY gene whose function is required for the repair of oxidative DNA damage." J Bacteriol **178**(13): 3885-92.

Slupska, M. M., W. M. Luther, et al. (1999). "Functional expression of hMYH, a human homolog of the Escherichia coli MutY protein." J Bacteriol **181**(19): 6210-3.

Smyth, G. K. (2004). "Linear models and empirical bayes methods for assessing differential expression in microarray experiments." Stat Appl Genet Mol Biol **3**: Article3.

Sparks, A. B., P. J. Morin, et al. (1998). "Mutational analysis of the APC/beta-catenin/Tcf pathway in colorectal cancer." Cancer Res **58**(6): 1130-4.

Spirio, L., J. Green, et al. (1999). "The identical 5' splice-site acceptor mutation in five attenuated APC families from Newfoundland demonstrates a founder effect." Hum Genet **105**(5): 388-98.

Spirio, L., S. Olschwang, et al. (1993). "Alleles of the APC gene: an attenuated form of familial polyposis." Cell **75**(5): 951-7.

Starink, T. M., J. P. van der Veen, et al. (1986). "The Cowden syndrome: a clinical and genetic study in 21 patients." Clin Genet **29**(3): 222-33.

Steinke, V., N. Rahner, et al. (2008). "No association between MUTYH and MSH6 germline mutations in 64 HNPCC patients." Eur J Hum Genet **16**(5): 587-92.

Strohmaier, H., C. H. Spruck, et al. (2001). "Human F-box protein hCdc4 targets cyclin E for proteolysis and is mutated in a breast cancer cell line." Nature **413**(6853): 316-22.

Su, L. K., M. Burrell, et al. (1995). "APC binds to the novel protein EB1." Cancer Res **55**(14): 2972-7.

Su, L. K., B. Vogelstein, et al. (1993). "Association of the APC tumor suppressor protein with catenins." Science **262**(5140): 1734-7.

Sugita, A., D. B. Sachar, et al. (1991). "Colorectal cancer in ulcerative colitis. Influence of anatomical extent and age at onset on colitis-cancer interval." Gut **32**(2): 167-9.

Sulekova, Z. and W. G. Ballhausen (1995). "A novel coding exon of the human adenomatous polyposis coli gene." Hum Genet **96**(4): 469-71.

Survey, N. S. H. (2005). National Statistics Health Survey for England 2004 - 2005.

Suter, C. M., D. I. Martin, et al. (2004). "Germline epimutation of MLH1 in individuals with multiple cancers." Nat Genet **36**(5): 497-501.

Takayama, T., M. Ohi, et al. (2001). "Analysis of K-ras, APC, and beta-catenin in aberrant crypt foci in sporadic adenoma, cancer, and familial adenomatous polyposis." Gastroenterology **121**(3): 599-611.

Taniguchi, H., H. Yamamoto, et al. (2005). "Frequent epigenetic inactivation of Wnt inhibitory factor-1 in human gastrointestinal cancers." Oncogene **24**(53): 7946-52.

Taylor, R. W., M. J. Barron, et al. (2003). "Mitochondrial DNA mutations in human colonic crypt stem cells." J Clin Invest **112**(9): 1351-60.

Tenesa, A., S. M. Farrington, et al. (2008). "Genome-wide association scan identifies a colorectal cancer susceptibility locus on 11q23 and replicates risk loci at 8q24 and 18q21." Nat Genet **40**(5): 631-7.

Thibodeau, S. N., A. J. French, et al. (1998). "Microsatellite instability in colorectal cancer: different mutator phenotypes and the principal involvement of hMLH1." Cancer Res **58**(8): 1713-8.

Thliveris, A. T., R. B. Halberg, et al. (2005). "Polyclonality of familial murine adenomas: analyses of mouse chimeras with low tumor multiplicity suggest short-range interactions." Proc Natl Acad Sci U S A **102**(19): 6960-5.

Tomlinson, I. and W. Bodmer (1999). "Selection, the mutation rate and cancer: ensuring that the tail does not wag the dog." Nat Med **5**(1): 11-2.

Tomlinson, I., P. Sasieni, et al. (2002). "How many mutations in a cancer?" Am J Pathol **160**(3): 755-8.

Tomlinson, I., E. Webb, et al. (2007). "A genome-wide association scan of tag SNPs identifies a susceptibility variant for colorectal cancer at 8q24.21." Nat Genet.

Tomlinson, I. P., E. Webb, et al. (2008). "A genome-wide association study identifies colorectal cancer susceptibility loci on chromosomes 10p14 and 8q23.3." Nat Genet **40**(5): 623-30.

Totafurno, J., M. Bjerknes, et al. (1987). "The crypt cycle. Crypt and villus production in the adult intestinal epithelium." Biophys J **52**(2): 279-94.

Tsuzuki, T., A. Egashira, et al. (2001). "Spontaneous tumorigenesis in mice defective in the MTH1 gene encoding 8-oxo-dGTPase." Proc Natl Acad Sci U S A **98**(20): 11456-61.

Van Meir, E. G. (1998). ""Turcot's syndrome": phenotype of brain tumors, survival and mode of inheritance." Int J Cancer **75**(1): 162-4.

van Puijenbroek, M., M. Nielsen, et al. (2007). "The natural history of a combined defect in MSH6 and MUTYH in a HNPCC family." Fam Cancer **6**(1): 43-51.

van Puijenbroek, M., M. Nielsen, et al. (2008). "Identification of patients with (atypical) MUTYH-associated polyposis by KRAS2 c.34G > T prescreening followed by MUTYH hotspot analysis in formalin-fixed paraffin-embedded tissue." Clin Cancer Res **14**(1): 139-42.

Vasen, H. F., G. Griffioen, et al. (1993). "Familial adenomatous polyposis and its clinical surveillance." Neth J Med **42**(3-4): 105-8.

Vasen, H. F., P. Watson, et al. (1999). "New clinical criteria for hereditary nonpolyposis colorectal cancer (HNPCC, Lynch syndrome) proposed by the International Collaborative group on HNPCC." Gastroenterology **116**(6): 1453-6.

Veale, A. M., I. McColl, et al. (1966). "Juvenile polyposis coli." J Med Genet **3**(1): 5-16.

Viano H, B. F. (2002). IARC handbooks of cancer prevention: Weight control and physical activity., IARC Press.

Vogelstein, B., E. R. Fearon, et al. (1985). "Use of restriction fragment length polymorphisms to determine the clonal origin of human tumors." Science **227**(4687): 642-5.

Vogelstein, B., E. R. Fearon, et al. (1988). "Genetic alterations during colorectal-tumor development." N Engl J Med **319**(9): 525-32.

Volk, D. E., P. G. House, et al. (2000). "Structural similarities between MutT and the C-terminal domain of MutY." Biochemistry **39**(25): 7331-6.

Waite, K. A. and C. Eng (2002). "Protean PTEN: form and function." Am J Hum Genet **70**(4): 829-44.

Wallis, Y. L., D. G. Morton, et al. (1999). "Molecular analysis of the APC gene in 205 families: extended genotype-phenotype correlations in FAP and evidence for the role of APC amino acid changes in colorectal cancer predisposition." J Med Genet **36**(1): 14-20.

Wang, L., L. M. Baudhuin, et al. (2004). "MYH mutations in patients with attenuated and classic polyposis and with young-onset colorectal cancer without polyps." Gastroenterology **127**(1): 9-16.

Wang, Z., J. M. Cummins, et al. (2004). "Three classes of genes mutated in colorectal cancers with chromosomal instability." Cancer Res **64**(9): 2998-3001.

Wargovich, M. J., A. Jimenez, et al. (2000). "Efficacy of potential chemopreventive agents on rat colon aberrant crypt formation and progression." Carcinogenesis **21**(6): 1149-55.

Wasan, H. S., H. S. Park, et al. (1998). "APC in the regulation of intestinal crypt fission." J Pathol **185**(3): 246-55.

Watanabe, G., C. Albanese, et al. (1998). "Inhibition of cyclin D1 kinase activity is associated with E2F-mediated inhibition of cyclin D1 promoter activity through E2F and Sp1." Mol Cell Biol **18**(6): 3212-22.

Webb, E. L., M. F. Rudd, et al. (2006). "Colorectal cancer risk in monoallelic carriers of MYH variants." Am J Hum Genet **79**(4): 768-71; author reply 771-2.

Wei, E. K., E. Giovannucci, et al. (2004). "Comparison of risk factors for colon and rectal cancer." Int J Cancer **108**(3): 433-42.

White, S., V. J. Bubb, et al. (1996). "Germline APC mutation (Gln1317) in a cancer-prone family that does not result in familial adenomatous polyposis." Genes Chromosomes Cancer **15**(2): 122-8.

Whitehall, V. L., M. D. Walsh, et al. (2001). "Methylation of O-6-methylguanine DNA methyltransferase characterizes a subset of colorectal cancer with low-level DNA microsatellite instability." Cancer Res **61**(3): 827-30.

Whitelaw, S. C., V. A. Murday, et al. (1997). "Clinical and molecular features of the hereditary mixed polyposis syndrome." Gastroenterology **112**(2): 327-34.

Will, O., L. G. Carvajal-Carmona, et al. (2007). "Homozygous PMS2 deletion causes a severe colorectal cancer and multiple adenoma phenotype without extraintestinal cancer." Gastroenterology **132**(2): 527-30.

Williams, C. S., A. J. Watson, et al. (2000). "Celecoxib prevents tumor growth in vivo without toxicity to normal gut: lack of correlation between in vitro and in vivo models." Cancer Res **60**(21): 6045-51.

Winston, J. T., D. M. Koepp, et al. (1999). "A family of mammalian F-box proteins." Curr Biol **9**(20): 1180-2.

Wong, E., K. Yang, et al. (2002). "Mbd4 inactivation increases Cright-arrowT transition mutations and promotes gastrointestinal tumor formation." Proc Natl Acad Sci U S A **99**(23): 14937-42.

Wong, W. M., N. Mandir, et al. (2002). "Histogenesis of human colorectal adenomas and hyperplastic polyps: the role of cell proliferation and crypt fission." Gut **50**(2): 212-7.

Wong, W. M. and N. A. Wright (1999). "Cell proliferation in gastrointestinal mucosa." J Clin Pathol **52**(5): 321-33.

Wood, R. D. (1996). "DNA repair in eukaryotes." Annu Rev Biochem **65**: 135-67.

Woodford-Richens, K. L., A. J. Rowan, et al. (2001). "SMAD4 mutations in colorectal cancer probably occur before chromosomal instability, but after divergence of the microsatellite instability pathway." Proc Natl Acad Sci U S A **98**(17): 9719-23.

Wu, Y., M. J. Berends, et al. (1999). "Association of hereditary nonpolyposis colorectal cancer-related tumors displaying low microsatellite instability with MSH6 germline mutations." Am J Hum Genet **65**(5): 1291-8.

Xie, Y., H. Yang, et al. (2004). "Deficiencies in mouse Myh and Ogg1 result in tumor predisposition and G to T mutations in codon 12 of the K-ras oncogene in lung tumors." Cancer Res **64**(9): 3096-102.

Xie, Y., H. Yang, et al. (2008). "Cells deficient in oxidative DNA damage repair genes Myh and Ogg1 are sensitive to oxidants with increased G2/M arrest and multinucleation." Carcinogenesis **29**(4): 722-8.

Yamada, Y., K. Hata, et al. (2002). "Microadenomatous lesions involving loss of Apc heterozygosity in the colon of adult Apc(Min/+) mice." Cancer Res **62**(22): 6367-70.

Yang, S., F. A. Farraye, et al. (2004). "BRAF and KRAS Mutations in hyperplastic polyps and serrated adenomas of the colorectum:

relationship to histology and CpG island methylation status." Am J Surg Pathol **28**(11): 1452-9.

Yoo, L. I., D. C. Chung, et al. (2002). "LKB1--a master tumour suppressor of the small intestine and beyond." Nat Rev Cancer **2**(7): 529-35.

Zanke, B. W., C. M. Greenwood, et al. (2007). "Genome-wide association scan identifies a colorectal cancer susceptibility locus on chromosome 8q24." Nat Genet.

Zauber, N. P., M. Sabbath-Solitare, et al. (2005). "Clinical and genetic findings in an Ashkenazi Jewish population with colorectal neoplasms." Cancer **104**(4): 719-29.

Zauber, N. P., M. Sabbath-Solitare, et al. (2003). "The characterization of somatic APC mutations in colonic adenomas and carcinomas in Ashkenazi Jews with the APC I1307K variant using linkage disequilibrium." J Pathol **199**(2): 146-51.

Zhang, W., W. K. Bleibel, et al. (2007). "Gender-specific differences in expression in human lymphoblastoid cell lines." Pharmacogenet Genomics **17**(6): 447-50.

Zhang, W., S. Duan, et al. (2008). "Evaluation of genetic variation contributing to differences in gene expression between populations." Am J Hum Genet **82**(3): 631-40.

Zhou, H., J. Kuang, et al. (1998). "Tumour amplified kinase STK15/BTAK induces centrosome amplification, aneuploidy and transformation." Nat Genet **20**(2): 189-93.

Zlotnik, A. (2008). "New insights on the role of CXCR4 in cancer metastasis." J Pathol **215**(3): 211-3.

"Nothing great is easy"

Capt. Matthew Webb

England ~ France 21 hours 45 minutes, Aug 24th 1875

Chrissie Thirlwell

England ~ France 19 hours 18 minutes, Sept 6th 2007

Gene name	Primer name	Primer sequence 5' to 3'	Label	Amplicon Size, bp	Mg mM	Q soln. (Qiagen)	Annealing Temp °C	No. Cycles
APC								
Exon 1	1F	ATTAACACAATTCTTCTTAAACGTC	FAM	300	1.5		57	35
	1R	TGGATAAACTACAATTAAAAGTCACAG	FAM					
Exon 2	2F	AAATACAGAATCATGTCTTGAAGT	TET	200	1.5		57	35
	2R	ACACCTAAAGATGACAATTTGAG	TET					
Exon 3	3F	TAACTTAGATAGCAGTAATTTCCC	HEX	212	2		57	35
	3R	ACCTCTCTTTCTCAAGTTCTTCTAAA	HEX					
Exon 4	4F	ATAGGTCATTGCTTCTTGCTGAT	FAM	185	1		57	35
	4R	TGAATTTTAATGGATTACCTAGGT	FAM					
Exon 5	5F	CTTTTTTTGCTTTTACTGATTAACG	TET	248	2		57	35
	5R	TGTAATTCATTTTATTCCTAATAGCTC	TET					
Exon 6	6F	GGTAGCCATAGTATGATTATTTCT	HEX	200	1.5		55	35
	6R	CTACCTATTTTTATACCCACAAAC	HEX					
Exon 7	7F	AAGAAAGCCTACACCATTTTTGC	FAM	250	2		57	35
	7R	GATCATTCTTAGAACCATCTTGC	FAM					
Exon 8	8F	ACCTATAGTCTAAATTATACCATC	TET	190	2		57	35
	8R	GTCATGGCATTAGTGACCAG	TET					
Exon 9A	9(I)F	AGTCGTAATTTTGTTTCTAAACTC	HEX	495	1.5		55	35
	9(I)R	ATGTAAAAGCTGGATGAGGA	HEX					
Exon 9B	9(II)F	GCTATGTCTAGCTCCCAAGA	FAM	225	1.5		55	35
	9(II)R	CTCTCTTGTCATCAGGCTGT	FAM					
Exon 9C	9(III)F	CAACATCATTCACTCACAGC	TET	185	1.5		55	35
	9(III)R	CTTTGAAACATGCACTACGA	TET					
Exon 10	10F	AAACATCATTGCTCTTCAAATAAC	HEX	220	2		57	35
	10R	TACCATGATTTAAAAATCCACCAG	HEX					
Exon 10A	10AF	AATCATAACAGGAAGGGGAT	FAM	290	2		55	35
	10AR	CAGTCACACCCCCAGAGG	FAM					
Exon 11	11F	GATGATTGTCTTTTTCCTCTTGC	TET	220	1.5		55	35
	11R	CTGAGCTATCTTAAGAAATACATG	TET					
Exon 12	12F	TTTTAAATGATCCTCTATTCTGTAT	HEX	180	2		60	35
	12R	ACAGAGTCAGACCCTGCCTCAAAG	HEX					
Exon 13	13F	TTTCTATTCTTACTGCTAGCATT	FAM	300	1.5		55	35
	13R	ATACACAGGTAAGAAATTAGGA	FAM					
Exon 14	14F	TAGATGACCCATATTCTGTTTC	HEX	325	1.5		55	35
	14R	CAATTAGGTCTTTTTGAGAGTA	HEX					
Exon 15A	15AF	GTTACTGCATACACATTGTGAC	FAM	417	1.5		55	35
	15AR	GCTTTTTGTTTCCTAACATGAAG	FAM					
Exon 15B	15BF	AGTACAAGGATGCCAATATTATG	TET	346	1.5		55	35
	15BR	ACTTCTATCTTTTTCAGAACGAG	TET					

Appendix 1: Primers and conditions

Exon 15C	15CF	ATTTGAATACTACAGTGTTACCC	HEX	399	2		59	35
	15CR	CTTGTATTCTAATTTGGCATAAGG	HEX					
Exon 15D	15DF	CTGCCCATACACATTCAAACAC	FAM	382	1.5		55	35
	15DR	TGTTTGGGTCTTGCCCATCTT	FAM					
Exon 15E	15EF	AGTCTTAAATATTCAGATGAGCAG	TET	420	1.5		55	35
	15ER	GTTTCTCTTCATTATATTTTATGCTA	TET					
Exon 15F	15FF	AAGCCTACCAATTATAGTGAACG	HEX	428	1.5		55	35
	15FR	AGCTGATGACAAAGATGATAATG	HEX					
Exon 15G	15GF	AAGAAACAATACAGACTTATTGTG	FAM	382	1.5		55	35
	15GR	ATGAGTGGGGTCTCCTGAAC	FAM					
Exon 15H	15HF	ATCTCCCTCCAAAAGTGGTGC	TET	420	1.5		55	35
	15HR	TCCATCTGGAGTACTTTCTGTG	TET					
Exon 15I	15IF	AGTAAATGCTGCAGTTCAGAGG	HEX	508	1	yes	60	35
	15IR	CCGTGGCATATCATCCCCC	HEX					
Exon 15J	15JF	CCCAGACTGCTTCAAAATTACC	FAM	317	1.5		55	35
	15JR	GAGCCTCATCTGTACTTCTGC	FAM					
Exon 15K	15KF	CCCTCCAAATGAGTTAGCTGC	FAM	352	1.5		55	35
	15KR	TTGTGGTATAGGTTTTACTGGTG	FAM					
Exon 15L	15LF	ACCCAACAAAAATCAGTTAGATG	TET	417	1.5		55	35
	15LR	GTGGCTGGTAACTTTAGCCTC	TET					
Exon 15M	15MF	ATGATGTTGACCTTTCCAGGG	FAM	250	1.5		55	35
	15MR	ATTGTGTAACTTTTCATCAGTTGC	FAM					
Exon 15N	15NF	AAAGACATACCAGACAGAGGG	TET	338	1.5		55	35
	15NR	CTTTTTTGGCATTGCGGAGCT	TET					
Exon 15O	15OF	AAGATGACCTGTTGCAGGAATG	FAM	291	1.5		55	35
	15OR	GAATCAGACGAAGCTTGTCTAGAT	FAM					
Exon 15P	15PF	CCATAGTAAGTAGTTTACATCAAG	TET	400	1.5		55	35
	15PR	AAACAGGACTTGTACTGTAGGA	TET					
Exon 15Q	15QF	CAGCCCCTTCAAGCAAACATG	FAM	373	1.5		55	35
	15QR	GAGGACTTATTCCATTTCTACC	FAM					
Exon 15R	15RF	CAGTCTCCTGGCCGAAACTC	TET	361	1.5		55	35
	15RR	GTTGACTGGCGTACTAATACAG	TET					
Exon 15S	15SF	TGGTAATGGAGCCAATAAAAAGG	FAM	306	1.5		55	35
	15SR	TGGGAGTTTTCGCCATCCAC	FAM					
Exon 15T	15TF	TGTCTCTATCCACACATTCGTC	TET	301	2		58	35
	15TR	ATGTTTTTCATCCTCACTTTTTGC	TET					
Exon 15U	15UF	GGAGAAGAACTGGAAGTTCATC	FAM	401	1.5		57	35
	15UR	TTGAATCTTTAATGTTTGGATTTGC	FAM					
Exon 15V	15VF	TCTCCCACAGGTAATACTCCC	TET	275	1.5		55	35
	15VR	GCTAGAACTGAATGGGGTACG	TET					

Appendix 1: Primers and conditions

Exon 15W	15WF	CAGGACAAAATAATCCTGTCCC	FAM	341	1.5		58	35
	15WR	ATTTTCTTAGTTTCATTCTTCCTC	FAM					
***APC* MCR region**	**Paraffin samples**							
exon 15 F	MCR 1F	CAAGCAGTGAGAATACGTCCA	FAM	134	1		55	35
	MCR 1R	TTTCTTGGTTAATAGAAGAAACTTTGC	FAM					
exon 15 F-G	MCR 2F	GCCACTTGCAAAGTTTCTTCT	FAM	144	2	yes	55	35
	MCR 2R	TGCTTCCTGTGTCGTCTGA	FAM					
exon 15 G	MCR 3-2F	CAGACGACACAGGAAGCAGA	FAM	182	1		60	35
	MCR 3-2F	TGGAACTTCGCTCACAGGAT	FAM					
exon 15 G	MCR 4F	GATCCTGTGAGCGAAGTTCC	HEX	149	1		58	35
	MCR 4R	CTGAGCACCACTTTTGGAGG	HEX					
exon 15 G-H	MCR 5F	AGAATCAGCCAGGCACAAAG	FAM	173	1		55	35
	MCR 5R	GCAATCGAACGACTCTCAAA	FAM					
exon 15 H	MCR 6F	CACTATGTTCAGGAGACCCCA	FAM	149	1		58	35
	MCR 6R	TGGAAGATCACTGGGGCTTA	FAM					
exon 15 H	MCR 7F	GTGAACCATGCAGTGGAATG	HEX	135	1		60	35
	MCR 7R	ACTTCTCGCTTGGTTTGAGC	HEX					
exon 15 H	MCR 8F	AAACACCTCCACCACCTCCT	HEX	145	1		58	35
	MCR 8R	AGCATCTGGAAGAACCTGGA	HEX					
exon 15 I-H	MCR 9F	CCTAAAAATAAAGCACCTACTGCTG	FAM	165	3		60	35
	MCR 9R	CACTCAGGCTGGATGAACAA	FAM					
exon 15 I	MCR 10F	ACATTTTGCCACGGAAAGTA	HEX	158	2		55	35
	MCR 10R	GGCTGCTCTGATTCTGTTTC	HEX					
exon 15 I	MCR 11F	CAGGAAAATGACAATGGGAAT	FAM	168	2		55	35
	MCR 11R	TGGCATGGCAGAAATAATACA	FAM					
exon 15 I	MCR 12F	GGACCTATTAGATGATTCAGATGATG	HEX	148	2		55	35
	MCR 12R	ACTTGGTTTCCTTGCCACAG	HEX					
***APC* MCR region**	**1st round PCR**							
exon 15 F	MCR 1F	GGACAAAGCAGTAAAACCGAAC		220	1		60	35
	MCR 1R	AACTACATCTTGAAAAACATATTGGA						
exon 15 F-G	MCR 2F	AAGTGGTCAGCCTCAAAAGG		198	3	yes	60	35
	MCR 2R	GCTATTTGCAGGGTATTAGCA						
exon 15 G	MCR 3F	GATACTCCAATATGTTTTTCAAGATG		250	1		55	35
	MCR 3R	GCCTGGCTGATTCTGAAGAT						
exon 15 G-H	MCR 5F	CAGACTGCAGGGTTCTAGTTTATC		235	2		60	35
	MCR 5R	CATTCCACTGCATGGTTCAC						
exon 15 H	MCR 6F	CCAAAAGTGGTGCTCAGACA		209	2		60	35
	MCR 6R	CATGGTTTGTCCAGGGCTAT						
exon 15 H	MCR 7F	TTTGAGAGTCGTTCGATTGC		204	1		60	35
	MCR 7R	TCTCTTTTCAGCAGTAGGTGCTT						

Appendix 1: Primers and conditions

Exon 15W	15WF	CAGGACAAAATAATCCTGTCCC	FAM	341	1.5		58	35
	15WR	ATTTTCTTAGTTTCATTCTTCCTC	FAM					
***APC* MCR region**	**Paraffin samples**							
exon 15 F	MCR 1F	CAAGCAGTGAGAATACGTCCA	FAM	134	1		55	35
	MCR 1R	TTTCTTGGTTAATAGAAGAAACTTTGC	FAM					
exon 15 F-G	MCR 2F	GCCACTTGCAAAGTTTCTTCT	FAM	144	2	yes	55	35
	MCR 2R	TGCTTCCTGTGTCGTCTGA	FAM					
exon 15 G	MCR 3-2F	CAGACGACACAGGAAGCAGA	FAM	182	1		60	35
	MCR 3-2F	TGGAACTTCGCTCACAGGAT	FAM					
exon 15 G	MCR 4F	GATCCTGTGAGCGAAGTTCC	HEX	149	1		58	35
	MCR 4R	CTGAGCACCACTTTTGGAGG	HEX					
exon 15 G-H	MCR 5F	AGAATCAGCCAGGCACAAAG	FAM	173	1		55	35
	MCR 5R	GCAATCGAACGACTCTCAAA	FAM					
exon 15 H	MCR 6F	CACTATGTTCAGGAGACCCCA	FAM	149	1		58	35
	MCR 6R	TGGAAGATCACTGGGGCTTA	FAM					
exon 15 H	MCR 7F	GTGAACCATGCAGTGGAATG	HEX	135	1		60	35
	MCR 7R	ACTTCTCGCTTGGTTTGAGC	HEX					
exon 15 H	MCR 8F	AAACACCTCCACCACCTCCT	HEX	145	1		58	35
	MCR 8R	AGCATCTGGAAGAACCTGGA	HEX					
exon 15 I-H	MCR 9F	CCTAAAAATAAAGCACCTACTGCTG	FAM	165	3		60	35
	MCR 9R	CACTCAGGCTGGATGAACAA	FAM					
exon 15 I	MCR 10F	ACATTTTGCCACGGAAAGTA	HEX	158	2		55	35
	MCR 10R	GGCTGCTCTGATTCTGTTTC	HEX					
exon 15 I	MCR 11F	CAGGAAAATGACAATGGGAAT	FAM	168	2		55	35
	MCR 11R	TGGCATGGCAGAAATAATACA	FAM					
exon 15 I	MCR 12F	GGACCTATTAGATGATTCAGATGATG	HEX	148	2		55	35
	MCR 12R	ACTTGGTTTCCTTGCCACAG	HEX					
***APC* MCR region**	**1st round PCR**							
exon 15 F	MCR 1F	GGACAAAGCAGTAAAACCGAAC		220	1		60	35
	MCR 1R	AACTACATCTTGAAAAACATATTGGA						
exon 15 F-G	MCR 2F	AAGTGGTCAGCCTCAAAAGG		198	3	yes	60	35
	MCR 2R	GCTATTTGCAGGGTATTAGCA						
exon 15 G	MCR 3F	GATACTCCAATATGTTTTTCAAGATG		250	1		55	35
	MCR 3R	GCCTGGCTGATTCTGAAGAT						
exon 15 G-H	MCR 5F	CAGACTGCAGGGTTCTAGTTTATC		235	2		60	35
	MCR 5R	CATTCCACTGCATGGTTCAC						
exon 15 H	MCR 6F	CCAAAAGTGGTGCTCAGACA		209	2		60	35
	MCR 6R	CATGGTTTGTCCAGGGCTAT						
exon 15 H	MCR 7F	TTTGAGAGTCGTTCGATTGC		204	1		60	35
	MCR 7R	TCTCTTTTCAGCAGTAGGTGCTT						

Appendix 1: Primers and conditions

exon 15 H	MCR 8F	CATGCAGTGGAATGGTAAGT		199	2		55	35
	MCR 8R	GCAGCATTTACTGCAGCTT						
exon 15 I-H	MCR 9F	CAAGCGAGAAGTACCTAAAAA		210	2		55	35
	MCR 9R	TTCTGTATAAATGGCTCATCG						
exon 15 I	MCR 10F	GGTTCTTCCAGATGCTGATA		209	2		55	35
	MCR 10R	CTTGGTTTTCATTTGATTCTTT						
exon 15 I	MCR 11F	AATTAAGAATAATGCCTCCAGT		209	2		55	35
	MCR 11R	TTTACGTGATGACTTTGTTGG						
exon 15 I	MCR 12F	CCAAGAGAAAGAGGCAGAAAAA		217	1	yes	55	35
	MCR 12R	TGATGGTAGAAGTTTGTACACAGG						
***APC* microsatellite markers**								
D5S346	346F	ACTCACTCTAGTGATAAATCGGG	FAM	125	1		55	35
	346R	AGCAGATAAGACAGTATTACTAGTT						
D5S421	421F	TGGAAATAGAATCCAGGCTT	FAM	170	1		55	35
	421R	TCTATCGTTAACTTTATTGATTCAG						
D5S656	656F	GCTAAGAAAATACGACAACTAAATG	FAM	187	1		55	35
	656R	CATAATAAACTGATGTTGACACAC						
***hMYH* region**								
exon 1	1F	TGAAGGCTACCTCTGGGAAG	FAM	141	1		55	35
	1R	AGGAGACGGACCGCAAGT	FAM					
exon 2	2F	GGCTGGGTCTTTTTGTTTCA	HEX	164	1		60	35
	2R	GGGCCACAACCTAGTTCCTT	HEX					
exon 3	3AF	CTGTGTCCCAAGACCCTGAT	HEX	187	3	yes	55	35
	3AR	TTGGTCGTACCAGCTTAGCA	HEX					
exon 3	3BF	AGCTGAAGTCACAGCCTTCC	FAM	110	1		60	35
	3BR	CACCCACTGTCCCTGCTC	FAM					
exon 4	4F	CCTCCACCCTAACTCCTCATC	FAM	110	1		55	35
	4R	AAAGTGGCCCTGCTCTCAG	FAM					
exon 5	5F	CAGGTCAGCAGTGTCCTCAT	FAM	152	2		60	35
	5R	GTCTGACCCATGACCCTTCC	FAM					
exon 6	6F	GTCTCTTTCTGCCTGCCTGT	FAM	125	2		60	35
	6R	TCACCCGTCAGTCCCTCTAT	FAM					
exon 7	7F	CGGGTGATCTCTTTGACCTC	FAM	134	2		60	35
	7R	GTTCCTACCCTCCTGCCATC	FAM					
exon 8	8F	TCTTGAGTCTTGCACTCCAATC	HEX	164	1		55	35
	8R	AAAGTGGGGGTGGGCTGT	HEX					
exon 9	9F	GCTAACTCTTTGGCCCCTCT	FAM	150	3	yes	60	35
	9R	CACCCTTGTTACCCCAACAT	FAM					
exon 10	10F	CTGCTTCACAGCAGTGTTCC	HEX	208	2	yes	60	35
	10R	GACTTCTCACTGCCCCTTCC	HEX					

Appendix 1: Primers and conditions

exon 11	11F	ACACTCAACCCTGTGCCTCT	FAM	147	1		60	35
	11R	GGAATGGGGCTTCTGACTG	FAM					
exon 12A	12AF	CTTGGCTTGAGTAGGGTTCG	HEX	179	1	yes	60	35
	12AR	GGCTGTTCCAGAACACAGGT	HEX					
exon 12B	12BF	GAGTGGTCAACTTCCCCAGA	FAM	146	1		60	35
	12BR	CACGCCCAGTATCCAGGTA	FAM					
exon 13	13F	AGGGAATCGGCAGCTGAG	HEX	209	1		60	35
	13R	GCTATTCCGCTGCTCACTTA	HEX					
exon 14	14F	AGGCCTATTTGAACCCCTTG	HEX	210	1		60	35
	14R	CAACAAAGACAACAAAGGTAGTGC	HEX					
exon 15	15F	CCCTCACCTCCCTGTCTTCT	HEX	159	3	yes	55	35
	15R	TGTTCACCCAGACATTCGTT	HEX					
exon 16A	16AF	CTACAAGGCCTCCCTCCTTC	HEX	158	1	yes	55	35
	16AR	GCTGCACTGTTGAGGCTGT	HEX					
exon 16B	16BF	GCCAGCAAGTCCTGGATAAT	HEX	181	2		60	35
	16BR	ACATAGCGAGACCCCCATCT	HEX					
***hMTH1* region**								
exon 2	2F	GCCTTATCGCAAGGACAGAG	HEX	241	3	yes	60	35
	2R	TGATGGAACCATGAGTTTGG	HEX					
exon 3	3F	TGACTCTGCCCTCTCACCTT	FAM	224	1		60	35
	3R	CGGTTCTATGGCCAGACCT	FAM					
exon 4	4F	TCCCTGGGCTGTGTGTAGAT	HEX	270	1		60	35
	4R	GAGCAGGCCCTGTGAGACT	HEX					
exon 5	5F	CTCTTCCCCCATTGGTACAG	FAM	240	1		60	35
	5R	CTGTTCAGCAGCCACGTCT	FAM					
***hOGG1* region**								
exon 1	1F	GGGTAGGCGGGGCTACTAC	HEX	266	1		55	35
	1R	CCCCAAATTCCTTTGTACCC	HEX					
exon 2	2F	AATTGAGTGCCAGGGTTGTC	FAM	313	1		55	35
	2R	CTAACCCCAGCCCAGGTC	FAM					
exon 3	3F	CAGCAGGTACCTCTCCTACCC	FAM	269	2	yes	55	35
	3R	TCTTGAAAGCTGATGGAAGG	FAM					
exon 4	4F	TTGAAGATGCCTGATGCTTG	HEX	258	1		55	35
	4R	TAGAGAGGGCAGCTCCTACC	HEX					
exon 5	5F	TCTTCCACAAGGGCTCATTC	HEX	232	1		55	35
	5R	TCTACCATCCCAGCCCACT	HEX					
exon 6	6F	TCACAGAAGGGGTCAGATAACTT	HEX	197	3		60	35
	6R	GGCTGGAGAGTCCTTTAGGG	HEX					
exon 7	7F	GACCCCAGTGTACCCTCCTC	FAM	311	1		55	35
	7R	ATATCCCCCACCCCATCTT	FAM					

Appendix 1: Primers and conditions

exon 8	8F	ATTCTCCATGCTGCCTTCCT	FAM	346	1		55	35
	8R	GTAAGCTGGCTTGCATCACA	FAM					
***hMSH6* region**								
exon 1	1F	AGATGCGGTGCTTTTAGGAG		473	1.5	yes	60	35
	1R	TGCACTCATTCAAGCCAACT						
exon 2	2F	TGCCAGAAGACTTGGAATTG		448	1.5	yes	60	35
	2R	CATGCCAGAAGCTTTCACAA						
exon 3	3F	CTCCCAAAATGCTGGGATTA		486	2.5	yes	60	35
	3R	GGGAACTACAGAAGTATGCATGT						
exon 4	4AF	TGAACTGTCTTACATTATGGTTTTCC		468	2.5	yes	60	35
	4AR	GGGCAGAGAAAGCTCTCAAA						
exon 4	4BF	AAAGGAAAAGCTCTAGGAAGGAA		494	1.5	yes	55	35
	4BR	TGCACCAGGGAATCTGAAT						
exon 4	4CF	CAGTGAACTGGGGCTGGTAT		488	1.5	yes	55	35
	4CR	TTTTAGTTTCCTTTGAGAGATTTCC						
exon 4	4DF	GGACTCTAGTGGCACACTATCC		500	2.5	yes	55	35
	4DR	TCCATTCAGAAAAATCTCCAAG						
exon 4	4EF	CAAAGCCTATCAACGAATGG		497	1.5	yes	60	35
	4ER	GAGAGATGACCTGCTTAAGGATT						
exon 4	4FF	AAAATCCTTAAGCAGGTCATCTC		578	2.5	yes	60	35
	4FR	CAGCTGGCAAACAGCACTAC						
exon 5	5F	AAAGAAGACCTATAAAACACTTAGGC		428	2.5	yes	60	35
	5R	CTGTGTTTGGAAAATGATCACC						
exon 6	6F	TGGATTTCAGAACAGAACCAA		391	1.5	yes	55	35
	6R	TGATGTTTTTAAAGTAACACCAGAAAA						
exon 7	7F	CTCCCAAAGTGCTGGGATTA		356	1.5	yes	55	35
	7R	TTTTTAGAGCACGCACTCA						
exon 8	8F	CCGATGTTGCTTTTCTGTCC		454	1.5	yes	55	35
	8R	CCTTGCTGCATTAAAGCCATA						
exon 9	9F	TGAGAGGGCACTTCTCTTGC		396	2.5	yes	60	35
	9R	CCAGGCAAACTTCCCTTAAA						
exon 10	10F	ACCCCAGCCAGGAGACTATT		425	2.5	yes	60	35
	10R	CCACCTTTGTCAGAAGTCAAC						
***Kras* region**								
exon 1	1F	TTAACCTTATGTGTGACATGTTCTAA		220	1		55	35
	1R	GGTCCTGCACCAGTAATATGC						
***Braf* region**								
exon 15	15F	TCATAATGCTTGCTCTGATAGGA		224	1.5		55	35
	15R	GGCCAAAAATTTAATCAGTGGA						
***B-catenin* region**								

Appendix 1: Primers and conditions

exon 3	3F	ATTGATGGAGTTGGACATGGC		236	1.5		55	35
	3R	CCAGCTACTTGTTCTTGACTGAAGG						
exon 5	5F	GGTGGTTAATAAGGCTGCAGTT		231	1.5		55	35
	5R	ATTTTCACCAGGGCAGGAAT						
BLM								
exon 1	1F	TTCAAGTGTCACTAGTTGTAAATGTCA		500	1.5	yes	60	35
	1R	CAGGAACCATGCAAAGATGA						
exon 2A	2AF	CTTTGCTCAGTTGGGATACAA		500	2.5	yes	60	35
	2AR	TCATCCATATCATCCCAATCAT						
exon 2B	2BF	GCAGACTCCGAAGGAAGTTG		542	1.5	yes	60	35
	2BR	TCATGACTATTCCCAATGGCTA						
exon 3	3F	AAAGGGAGAGGATCCATACAAA		486	2.5	yes	60	35
	3R	TGGGACTTCATCTTTAGAATGC						
exon 4	4F	TGAAAAGGGCTCTTTCTGGA		494	2.5	yes	60	35
	4R	TCAGGCAAATGCTGGCTAAC						
exon 5	5F	TGACAGGGTCTCACTGTGTTG		478	1.5	yes	55	35
	5R	CGAATGTTAAAGGAGTGGTTTG						
exon 6A	6AF	TTTTGCTACAATTTCTATTTGGTATGA		472	2.5	yes	60	35
	6AR	CAGCAGTGCTTGTGAGAACA						
exon 6B	6BF	AGTAGCAACTGGGCTGAAACA		499	2.5	yes	60	35
	6BR	AGAAATTTGCATAGCAACAATG						
exon 7	7F	GCAAGTTTTTGGTGGCTTTG		493	1.5	yes	60	35
	7R	TGGTACAGGAGGTTTAAGAGGTC						
exon 8	8F	CCTGGGCAACAGAATGAGAC		497	1.5	yes	55	35
	8R	TGCAAATTTAACTGCTGTGCTT						
exon 9	9F	GCCCTGCCTGAGTTATGCT		476	2.5	yes	60	35
	9R	TGCAGAGAGAGAATACAAAGCAA						
exon 10	10F	TGTTGGTTAGGCTGGTCACA		485	2.5	yes	60	35
	10R	TCAGACTACTTGGAGCTTCCTTC						
exon 11	11F	TCCGGAAATACCGATAAATACA		478	2.5	yes	55	35
	11R	CTGCCATCGGGTTACAACTT						
exon 12	12F	ATATGCGGGTGGGGAGAG		488	2.5	yes	60	35
	12R	TTTCCAGAATTGAGAGAGTTGC						
exon 13	13F	GCACACATGAATTCCTTGCTT		491	2.5	yes	60	35
	13R	GCAACTTTAGAAGTCTCAAAGAAAA						
exon 14	14F	AATGGCATTGCAAGTTATCAG		530	2.5	yes	60	35
	14R	TTGCCAATCTGTATAAACTCCTC						
exon 15	15F	ATGCCATGTTGACAATGCTG		452	1.5	yes	60	35
	15R	GGAAGCTGTCTTTCCCCTGT						
exon 16	16F	TGAAATTTCCGTAGGTTTTGG		497	2.5	yes	55	35

Appendix 1: Primers and conditions

	16R	TTCTTTGTATGTGAAACCATCTCAA						
exon 17	17F	CGGGGTTTGTGATCTATTCC		491	2.5	yes	55	35
	17R	GGTTGAATTTTAAGATCTCTTTCCA						
exon 18	18F	AGAATGCACAGCCCCTGTT		491	1.5	yes	55	35
	18R	GGGTGACACAGCGAGACC						
exon 19	19F	GTCTGCTGCCTCTGAGGTG		476	1.5	yes	60	35
	19R	CACAGGGGGCATAAGCACTA						
exon 20	20F	GAATCCATATGGCAGGGAAG		472	1.5	yes	60	35
	20R	CTCCATTAACAACTGTCATTCCA						
exon 21	21F	GGGTTGGTCACAAGTCAGAAA		498	1.5	yes	60	35
	21R	TGGTCAGATGCTGACAAACA						
CDC4								
exon 1	1F	CAGGAGCAGGAGCTTTCACT		144	2.5	yes	55	35
	1R	TTTTCACTAAAAGAGGCCAAGG						
exon 2	2F	CCATGCTGACTCAAGATTTGATA		164	2.5	yes	55	35
	2R	TTCCGGTAATCTCAAAATGTGTT						
exon 3	3F	TGCCAGATCATCATTCTTTG		142	2.5	yes	55	35
	3R	GCAGCAATTAAGTGAGGCATT						
exon 4	4F	GCCTGTAATTTGGGACATCTG		135	2.5	yes	55	35
	4R	CACCCAATGAAGAATGTAATTGA						
exon 5	5F	TCAAGTATCTCATCCTGTGGAGAA		124	2.5	yes	55	35
	5R	TTTCAGAATCACTCTGCTTTTCA						
exon 6	6F	TGGTGAAGGCAATTTACTCTTG		137	2.5	yes	55	35
	6R	AACGGTTTCTGTTACATTGTGC						
exon 7	7F	ATCTGCACATCTTTCTTATAGGTGCT		114	2.5	yes	55	35
	7R	GAAGAGTAAACTTACTTTGCCTGTGA						
exon 8	8F	TCACTTTTCCTTTCTACCCAAAA		182	2.5	yes	55	35
	8R	GGAAGAAGTCCCAACCATGA						
exon 9	9F	TTTTTCTGTTTCTCCCTCTGC		226	2.5	yes	55	35
	9R	TTCATCAGGAGAGCATTTAAGG						
exon 10	10F	TCCTCTTCCCCCTTTCCTAC		211	2.5	yes	55	35
	10R	TTTGTGATGCTAAGGCTCCA						
MBD4								
exon 1	1F	ATCTTACTCCGCCCCACAC		206	1.5		60	35
	1R	GTGAAACTGAGGCCCAAAAG						
exon 2	2F	AATCACTTAGACTTTGTTTTTCCAG		295	2.5	yes	55	35
	2R	TCATTTGGCTGTACTATCTTTACCA						
exon 3A	3AF	ACCTATGGCAACATTTGGAA		680	2.5	yes	55	35
	3AR	TCACACTGAGGGTCTCACCA						
exon 3B	3BF	TGATAGCAAAAGAGAATCTGTGTG		496	2.5	yes	55	35

Appendix 1: Primers and conditions

	3BR	GGCACGAATACAAGATGCAG						
exon 4 - 5	4-5F	GCCTGGCATGCTTTGTAATA		496	2.5	yes	55	35
	4-5R	TCCCAGGTGACACACTCAAA						
exon 6	6F	GCCCACCTGGAGTCTTGTAA		225	2.5	yes	55	35
	6R	TGTTTTTCCTTTGGGTGTATAGG						
exon 7	7F	CACATTTTGGGAGGGTGTCT		212	1.5	yes	55	35
	7R	GCCTCAGAGACCAAATGTGC						
exon 8	8F	ATGTACTGTCCCCCAGCAAA		202	1		55	35
	8R	TGAGCTTGAAAGCTGCAGAG						
MGMT								
exon 2	2F	CGACCAGCCTCTTACCTATACA		211	2		60	35
	2R	AGGATCACGTGGGCTCATAC						
exon 3	3F	GGTGTTTGCTTTTCCGATGT		195	2	yes	55	35
	3R	ACACCGCAGATGGCTTAGTT						
exon 4	4F	TCCTGCATTCTTCCTTTCAG		243	1		55	35
	4R	GAGGAAACACGTGGGATCAG						
exon 5	5F	CGTTGTCCAGATCCCTGACT		299	2		60	35
	5R	TACACGTGTGTGTCGCTCAA						
TDG								
exon1	1F	TCTCTGGGGTTGTCTTACC		225	1.5	yes	55	35
	1R	GGCCGGGATTTAAAAGAC						
exon 2	2F	AGATTTTTGTACAGCTGATCATT		299	1.5	yes	55	35
	2R	AATTCACCATGAAACCCTTT						
exon 3	3F	TTCTGCATTTCTGGAAATTAT		299	2.5	yes	55	35
	3R	AATCCAACGAGGACAAAGAT						
exon 4	4F	TCCTCCATAGAAACGCTAAG		222	1.5	yes	55	35
	4R	AACACAATTGGTTTTTCTGA						
exon 5	5F	TACACTCTAGCCTGGGTGAC		246	1.5	yes	55	35
	5R	AAGGTTCCAACCCATAAAAG						
exon 6	6F	AAGCTGTCTGAATTTAGCATATTA		208	2.5	yes	55	35
	6R	ACATTGCCCATAATGTTAGC						
exon 7	7F	AAATATCAGCCACGAATAGC		250	1.5	yes	55	35
	7R	TTCACATTTAGCTGATTTACAA						
exon 8	8F	CCCAAATAAAGACAAATATTCTAA		289	1.5	yes	55	35
	8R	TGAATAAAAGGAATGAGGACA						
exon 9	9F	TTCATGATTTCTGAATAAAGCTA		249	1.5	yes	55	35
	9R	GACCAAACCGTCTTTGAA						
exon 10	10F	TGGGCGATAGAGTAAGACC		288	2.5	yes	55	35
	10R	TTGTTGACAACTGCATTAAAA						

Appendix 1: Primers and conditions

CXCR4								
exon 1	1F	GTAGCAAAGTGACGCCGAG		149	1		60	35
	1R	AGAGGGGCTGCGCTCTAAG						
exon 2-1	2-1F	TGCTTGCTGAATTGGAAGTG		170	1		60	35
	2-1R	GAGTAGATGGTGGGCAGGAA						
exon 2-2	2-2F	GGATTGGTCATCCTGGTCAT		174	2		60	35
	2-2R	GACATGGACTGCCTTGCATA						
exon 2-3	2-3F	TATGCAAGGCAGTCCATGTC		215	1		60	35
	2-3R	CTCACTGACGTTGGCAAAGA						
exon 2-4	2-4F	TGACTTGTGGGTGGTTGTGT		165	1		60	35
	2-4R	GCCAGGATGAGGATGACTGT						
exon 2-5	2-5F	ATTGGGATCAGCATCGACTC		154	2		60	35
	2-5R	TGGCTCCAAGGAAAGCATAG						
exon 2-6	2-6F	AAGCGAGGTGGACATTCATC		176	1		55	35
	2-6R	AAATCCAACAAGCAATAAAAACTG						
exon 2-7	2-7F	TGCTTGTTGGATTTTTGTCTTG		180	1		55	35
	2-7R	CACGCTCTGGAATGTTCAGT						
exon 2-8	2-8F	CATTCCAGAGCGTGTAGTGAA		295	1		60	35
	2-8R	GCCAAAAGAATGTCAACAGAAA						
DUT								
exon 1a	1aF	GCAAGACTCAAGACGCCAAC		270	1		60	35
	1aR	TGAGCGAAGCAGAGACGTAA						
exon 1b	1bF	GGGGAAATGACTCCCCTCT		362	1		60	35
	1bR	CACCCTACTTCCCCCACAG						
exon 2	2F	CTCATCGTGCGCTCTC		278	2		55	35
	2R	GTTTCTAGCTGTGGCAGCG						
exon 3	3F	CACTGAAAGTAATTTTGTATGCTTGG		272	2		60	35
	3R	GCCTGCTTATTACCCCAAATG						
exon 4	4F	TGACATGCTTAAATTGCATCAG		279	1		60	35
	4R	AAAATAACCACAAAGCTTTTCCTC						
exon 5	5F	CAATTGTAAGAATACAAATCTCAGAGC		244	1		55	35
	5R	CACATACATGACTCTGAAAATTCACTA						
exon 6	6F	AATTTTAGTGAATTTTCAGAGTCATGT		290	2		55	35
	6R	TTACAAACAGCATATTAAATTCTCAAG						
exon 7	7F	AATTTTAGTGAATTTTCAGAGTCATGT		254	1		60	35
	7R	TGCAAAACACCAAAACACTTG						
POLE2								
exon 1	1F	TAACAGGGTTTAGCGCC		289	2		55	35
	1R	AATTTAAGGTCAAGCCCC						

Appendix 1: Primers and conditions

exon 2	2F	CCTTTCAGTGCCAGATTG		308	1		55	35
	2R	GGGACATCTTAATAGTGAAGC						
exon 3	3F	TGGGAAAAGAGCTGTCTG		242	1		55	35
	3R	TTGATCACTAATAATTTTCCAAG						
exon 4	4F	CTTATAATGCAAGTTATCATGTTC		247	1		55	35
	4R	GTGAGCCAAAAGTGAAGC						
exon 5	5F	TCTCTTGCTTCACTTTTGG		246	2		55	35
	5R	CCCTGAGATTTCCCTAAAC						
exon 6	6F	ACAGTGTTTCATCAGGGC		291	2		55	35
	6R	GCAGCCCATCCAGTTAG						
exon 7	7F	TTGTAGGACAAAATTAAACATCC		358	1		55	35
	7R	CATTCCTGTGCCCACTAC						
exon 8	8F	TTTTAAAATCCACTTTCTCCC		302	1		55	35
	8R	ACATTCCTACACCAGCAAC						
exon 9	9F	TTAGAAGCCTTGTTGGACTC		206	1		55	35
	9R	AACATATTTTACCCAAAGCAG						
exon 10	10F	GTTCACAGGGCATGAGAC		290	2		55	35
	10R	GACACAAAGCCTGACACC						
exon 11	11F	CTCAAAAAGATAAATAGAATACTCAAA		381	1		55	35
	11R	CAAAGAGTACCTTTTTACACTGG						
exon 12	12F	AATTTGCATATAATGCCATAAA		385	2		55	35
	12R	AATGAATGGCTACTGTTATTAGTATT						
exon 13	13F	AAGCTTTGAAAGGTATTAACG		331	1		55	35
	13R	TCCTTAGTTTTGTAATAATTGCTG						
exon 14-15	14-15F	AACTTGCTTTTAAGCTATTGG		417	1		55	35
	14-15R	AACTCCAAGCAACCTGC						
exon 16	16F	GGAATGGGGTTGTATTGTAAG		285	2		55	35
	16R	CCCAAGGACAAATTATTAAGTG						
exon 17	17F	GCATATTTTTACTTCGACAATAATC		407	1		55	35
	17R	TTCCTAGTTTCTCAAATTTTCTG						
exon 18	18F	AGCCTGGGTGATGAGAG		358	2		55	35
	18R	CCGTGATAAGCTCAGCC						
exon 19	19F	TTTGGGAGCAGAAAAGG		327	1		55	35
	19R	ACAAATTTAAGCAGAACATCC						
DKK1								
exon1A	1AF	GCAAGACTCAAGACGCCAAC		277	2		60	35
	1AR	TGAGCGAAGCAGAGACGTAA						
exon 1B	1BF	GGGGAAATGACTCCCCTCT		362	1		60	35
	1BR	CACCCTACTTCCCCCACAG						
exon 2	2F	CTCATCGTGCGCTCTCC		278	1		60	35

Appendix 1: Primers and conditions

	2R	GTTTCTAGCTGTGGCAGCG						
exon 3	3F	CACTGAAAGTAATTTTGTATGCTTGG		272	2		60	35
	3R	GCCTGCTTATTACCCCAAATG						
exon 4	4F	TGACATGCTTAAATTGCATCAG		279	1		60	35
	4R	AAAATAACCACAAAGCTTTTCCTC						
exon 5	5F	CAATTGTAAGAATACAAATCTCAGAGC		244	2		55	35
	5R	CACATACATGACTCTGAAAATTCACTA						
exon 6	6F	AATTTTAGTGAATTTTCAGAGTCATGT		290	1		55	35
	6R	TTACAAACAGCATATTAAATTCTCAAG						
exon 7	7F	GGAGCTGGAGAGGAAAACTG		218	1		60	35
	7R	TGCAAAACACCAAAACACTTG						
EPHB2								
exon 1	1F	CTGGATGGCTCATTCTGCTG	FAM	433	1		55	35
	1R	CTCCTCCTGGCACAGTCAAT						
exon 2	2F	AGATTGACAGCGCCTGGTAG	HEX	220	1		55	35
	2R	AGGGGGAAAGGGGTTAGAAT						
exon 3A	3AF	CCTTACCTCCCCACCTGAC	HEX	195	1		55	35
	3AR	CGCACCGAAAACTTCATCT						
exon 3B	3BF	CCACGTGGAGATGAAGTTTTC	HEX	250	2		55	35
	3BR	CGGTGTTGATTTTCATGACG						
exon 3C	3CF	CCGCGTCATGAAAATCAAC	FAM	412	2		55	35
	3CR	AGTCTGCAGCCAAGACCAGT						
exon 4	4F	TCCAGTTTCCTGGTGACTCT	HEX	250	1		60	35
	4R	GCAGGTAGACCTGGGACTC						
exon 5	5F	GGGAATAGTACCCCCTGAGC	FAM	464	1		55	35
	5R	CTTTTGTGAGGACTGCAGGA						
exon 6	6F	CTCCCTGATCCCTGACCTCT	HEX	237	1		55	35
	6R	CAGAACTCCCAGGCCTCA						
exon 7	7F	CCCACTATGAGCCACAACCT	HEX	250	2		55	35
	7R	AGTCTGTGCCCTCCTCTTGC						
exon 8	8F	CTGAGAATGCCCTACCATGC	HEX	194	2		60	35
	8R	GAGAGAAGCCATCTGGGACA						
exon 9	9F	GCTCCAGCCCTTTGCTCT	FAM	161	2		55	35
	9R	TAAGAGGTCACTGGGGAACC						
exon 10	10F	CTCCCGCTTTTCCTTTTTGT	HEX	236	1		55	35
	10R	GCCATGGCTAAGGTCATAGTACA						
exon 11	11F	GGCAAGTGACATCCTGTCTG	FAM	336	1		60	35
	11R	CTTTTCCTGCCCCATTCAT						
exon 12	12F	TTTACTCTGTGTTTTCCCCACTT	FAM	296	2		55	35
	12R	CCCTCTTCTCTGGCTCTGTG						

Appendix 1: Primers and conditions

exon 13	13F	ACCCACAAACCCTCCTCTTT	HEX	206	2		55	35
	13R	CTTGCCTATCCCCTTGGAG						
exon 14	14F	AACCCCACTGCACTCCTG	FAM	281	2		60	35
	14R	ATGGGAGACGGGAAGAGG						
exon 15	15F	GTGCCCTGACCATCTCTGTC	HEX	238	2		60	35
	15R	AGAGGGGGTGCTAAGGTGAC						
exon 16	16F	CCCGCATATTTCCCTAACAC	FAM	500	1		60	35
	16R	AACTGCTTTTGTCTCCGATTG						
Wif1								
exon 1	1F	CTCTCGCAGGCTCCTTGG	FAM	356	1		55	35
	1R	GAGGACATAGGCAGGGGAAG						
exon 2	2F	TCAAGTCTACCTGGTTTGATCG	HEX	231	1		55	35
	2R	TGCCATAAGGCAGTGGAAAT						
exon 3	3F	GCCTTCTCCCTCTCTGGTTT	FAM	189	1		60	35
	3R	CCTTTCTTCAGGCAAAGACC						
exon 4	4F	CTTGGTTCCCAAGATTTCTG	FAM	248	2		55	35
	4R	TCTTCTCTTGAATCACCATCG						
exon 5	5F	GGCTGTGATTCACCCAACAT	FAM	236	1		55	35
	5R	ACAATACACATGGGGCTCCT						
exon 6	6F	TGGCCTTAATCAGGGTTCTC	HEX	243	2		60	35
	6R	CCCTAAGCCATACATTCTCAGAGC						
exon 7	7F	GAAATGGGCAAGTAGCAAGC	HEX	247	2		55	35
	7R	CTCCCCAAGTCAAAAGAACG						
exon 8	8F	TGAATGAAGCACCAGGTTCC	FAM	242	1		55	35
	8R	CAGGCAACATGCACTAAGCA						
exon 9	9F	CCAACTTATGACTGGAGACTGAC	HEX	350	1		55	35
	9R	AGCCAAGAAACCGAAGTGAA						
exon 10A	10AF	GAATCTGAAGAGCCTGGTTTTG	HEX	195	1		55	35
	10AR	TCAGATGTCGGAGTTCACCA						
exon 10B	10BF	GCCTTTGTTAACCTTTCATGTG	FAM	276	2		55	35
	10BR	GCCCCCAGACACCATAAAT						
exon 10C	10CF	CAATGCATTTATGGTGTCTGG	FAM	224	2		60	35
	10CR	CTGAATCTCTGGAATAATGGTAAGG						
exon 10D	10DF	ACACTGTGGTAGTGGCATTT	HEX	218	1		55	35
	10DR	GCATGTGCAAAGATCACCTC						
Microsatellite markers								
chromosome 1	D1S201F	GGTATGGAAGTCACCCAACA	FAM	186	1.5	yes	55	35
	D1S201R	CTCAAAATGACTGATGGGGT						
	D1S2729F	TACTTGCCTAATGCTGTGTG	FAM	208	1.5	yes	55	35
	D1S2729R	TATCAATCCTTGGGAGACC						

Appendix 1: Primers and conditions

	D1S2749F	GATCCTGCCTTTACTGCTTG	FAM	195	1.5	yes	55	35
	D1S2749R	GGCCATGTGTAGCCTTTC						
	D1S470F	AAATGGGGCTAATAAATCTCCTGG	FAM	155	1.5	yes	55	35
	D1S470R	CTACACCATAGGCATAGGTGCAA						
chromosome 9	D9S1818F	GGATCTATGCTGGCTACTTCATAAC	FAM	133	1.5	yes	55	35
	D9S1818R	TATTTGGACTCTGTAGTGCTGAAC						
	D9S1826F	ATGTTGATTGCCGCAGTG	FAM	133	1.5	yes	55	35
	D9S1826R	TGCAGAACCAGGTCTTATTCG						
	D9S1829F	AGCTACTCAGGAGGCTAAGG	FAM	198	1.5	yes	55	35
	D9S1829R	GCGAACTTCAGAAAAACATC						
	D9S1830F	CAGAGTGGTGGGACTCAA	FAM	107	1.5	yes	55	35
	D9S1830R	AGCTGCAGACTGCCTTC						
chromosome 17	D17S786F	TACAGGGATAGGTAGCCGAG	FAM	135	1.5	yes	55	35
	D17S786R	GGATTTGGGCTCTTTTGTAA						
	D17S1832F	ACGCCTTGACATAGTTGC	FAM	151	1.5	yes	55	35
	D17S1832R	TGTGTGACTGTTCAGCCTC						
	D17S1353F	CTGAGGCACGAGAATTGCAC	FAM	184	1.5	yes	55	35
	D17S1353R	TACTATTCAGCCCGAGGTGC						
	D17S1844F	CATTCCAGCCTGGGTGA	FAM	227	1.5	yes	55	35
	D17S1844R	GGAACCATAGGAGGCGTTTT						
chromosome 19	D19S886F	TGGATCTACACTCCGGC	FAM	134	1.5	yes	55	35
	D19S886R	ATTTTACTGGCTGGCACTTG						
	D19S878F	GCCTGGGCGACAGAGAAT	FAM	208	1.5	yes	55	35
	D19S878R	GGTTGCCCGCAGAGTG						
	D19S215F	CATGCATTAAAAATGACAACTGT	FAM	252	1.5	yes	55	35
	D19S215R	GCTCTGCANTCCATTACTCA						
	D19S656F	GTGATTGCACCACGGG	FAM	168	1.5	yes	55	35
	D19S656R	TCAAGTCATTGGGTTGGC						
	D19S591F	TTCCAGCCTAGGTAGCAGTG	FAM	96	1.5	yes	55	35
	D19S591R	GCAACTGAGGAAATGCATCT						

Mouse Primer sequences

Gene name	Primer name	Primer sequence 5' to 3'	Label	Amplicon Size, bp	Mg mM	Q soln. (Qiagen)	Annealing Temp °C	No. Cycles
APC								
	mAPC x15AF	CTTGTTGTCACTAATCACATTTTC		550	2		55	35
	mAPC x15AR	TCCAGTATTGAAATTGTCTGACC						
	mApc x15BF	GACGCCAATCGACATGAT		547	2		55	35
	mApc x15BF	CAACTGAGGGTTTCATTTGG						
	mApc x15CF	TGATGGATATGGTAAAAGAGG		544	2		55	35
	mApc x15CR	TTCTTCCTCAGAATAACGTTCAC						

Appendix 1: Primers and conditions

	mApc x15DF	TGAAGATGATAAACCTACCAAC		545	2		55	35
	mApc x15DF	CAGCTGACCGAGTTACATCA						
	mApc x15EF	TGCAGACAGCAGAAGTAAAAGA		504	2		60	35
	mApc x15EF	GCTTAGGCCCACTCTCTCTC						
	mApc x15FF	AGTAAAGTCCCTGCTGCTGA		453	2		55	35
	mApc x15FR	TGCCACAGGTGGAGGTAAT						
	mApc LOH 1F	TACGGTATTGCCCAGCTCTT	FAM	153	2		55	35
	mApc LOH 1R	TGCAGACCTCGTTTTGATGA						
	mAPC x15 (-1)F	TGCCCCTTTACTTGTTGTCA	FAM	308	1		55	35
	mAPC x15 (-1)R	TCTGTTTGCCATGAGATTCCT	FAM					
	mAPC x15 (0)F	CCTCATTCATTCCAAGCACA	FAM	376	1		55	35
	mAPC x15 (0)F	AGAGCTGGGCAATACCGTAG	FAM					
	mAPC x15 (LOH5&6)F	TTTTGACGCCAATCGACAT	FAM	310	2		60	35
	mAPC x15 (LOH5&6)R	GTCGTCCTGGGAGGTATGAA	FAM					
	mAPC x15 (1)F	GCCAAAGTTATGGAAGAAGTATCA	FAM	411	1		60	35
	mAPC x15 (1)R	TGGTGTATCCAGTTCTCCATCA	FAM					
	mAPC x15 (2)F	CAGTGCAAATCATATGGATGATAA	HEX	372	2		55	35
	mAPC x15 (2)R	TCTTCCTGACACAGAGACTGG	HEX					
	mAPC x15 (3)F	TCGAATGGGTTCTAGTCATGC	FAM	418	1		60	35
	mAPC x15 (3)R	GGGGACTTTGCAAGTAGTGC	FAM					
	mAPC x15 (4)F	GCACAAAGAAATGGCCAGAC	HEX	391	2		55	35
	mAPC x15 (4)R	CACCACTTTTGGAGGGAGAC	HEX					
	mApc x6F	CCCATGTCAAGACACTCCAG	FAM	204	1		55	35
	mApc x6R	TGTACCAGAAGGGGGCTTTA	FAM					
	mApc x7F	TTCATCGAGAGTTTTGAAGCAA	HEX	228	2		55	35
	mApc x7R	CAGACAGGACTTGTCAGTTTGAA	HEX					
	mApc x8F	AATTGGGAGCTTCAGAGTGG	FAM	196	2	yes	55	35
	mApc x8R	GCAAGAGGGTTTGTAATCTGC	FAM					
	mAPC x9F	TAAACTCATTTGGCCCACAG	FAM	555	1		60	35
	mAPC x9R	CAGGGAAATGCAGATTTAAGC	FAM					
	mApc x10F	TGAGGGATGTGTCAATAACGTC	FAM	223	3		60	35
	mApc x10R	ATTTGTGGCGTTAGGAAAGC	FAM					
	mApc x11F	TGTTTCCTTTTGCCCTTGTT	HEX	272	2	yes	55	35
	mApc x11R	GTTCAACTGGGCTGCTGTG	HEX					
	mAPC x12F	TCAGGCAGATTCCTTGATGA	FAM	208	1		55	35
	mAPC x12R	GCCATACTTTAACACAAGCCACT	FAM					
	mAPC x13F	CCTCTAGCATTAGAAACAAAAAGACA	HEX	226	1		55	35
	mAPC x13R	CCTATTCCAGCACCCAACAT	HEX					
	mAPC x14F	CAGCACTGACCCAAATTTCA	HEX	475	1		55	35
	mAPC x14F	GGCCTCTTTGCTTAGAGCTT	HEX					

Appendix 1: Primers and conditions

Mom 1								
	Mom1F	GTCCAAGGGAACATTGCG		465	1		55	35
	Mom1R	AGAACAGGTGATTTGGCCC						
Kras								
	mKras x1F	TTTTTATTGTAAGGCCTGCTGA		161	2		55	35
	mKras x1R	GCACGCAGACTGTAGAGCAG						
BRAF								
	mBRAFx15F	AGGCCTGGGACAGCTTAAAA		529	3	yes	65	35
	mBRAFx15R	CAGCTTTCTAAGTGCTGGGATT						
MYH								
	mMYH x1F	CTTTGCCCTTTTGTTTCGAG	FAM	199	2		60	35
	mMYH x1R	GAAACTGGTGAGGGACAAGC	FAM					
	mMYH x2F	CTGAGTTCCCCTGGCTGTC	FAM	199	2		55	35
	mMYH x2R	CACTGTCTCTGTCCCATCCA	FAM					
	mMYH x3&4F	TTCACCCTTGGTTTTATTGACA	FAM	278	2		60	35
	mMYH x3&4R	CTCCCTCCCCAACATCAC	FAM					
	mMYH x5&6F	TTTTTGCCTGTCTTGGGTTT	FAM	254	1		60	35
	mMYH x5&6R	CACCGGGCTATTTTTCAGTG	FAM					
	mMYH x7&8F	CTGTGAGCTTCCTGCTCCAT	FAM	337	2		60	35
	mMYH x7&8R	CCCGTCACCTCATTACCCTA	FAM					
	mMYH x9&10F	AAGGGCCTTTGCTTACAGAA	FAM	357	2		60	35
	mMYH x9&10R	CTCTGAAAGGGACAGGGATG	FAM					
	mMYH x11&12F	GCTGGGAATCTTTGTTTCCA	FAM	466	2	yes	60	35
	mMYH x11&12R	CCCTGTCACCTTTGCTAACC	FAM					
	mMYH x13&14F	CAGACCTGGTTCGGTCTCTT	FAM	460	2		60	35
	mMYH x13&14R	GAAGAGGGCGGAATGCAC	FAM					
	mMYH x15F	GGGTAGAAGAGTCCCTGGTG	FAM	201	2		60	35
	mMYH x15R	TTTGGGTAGGGAATCCCAGT	FAM					
***MYH* genotyping**								
	P1 (21-mer)	CAAGTGCTGGGATCAAAGGTG			1		55	35
	P2 (20-mer)	GCTCCTTCTTGTAGCCGACG	P1/P2	262				
	P3 (neo, 21-mer)	TCCTCGTGCTTTACGGTATCG	P1/P3	376				

Appendix 1: Primers and conditions

Mom 1								
	Mom1F	GTCCAAGGGAACATTGCG		465	1		55	35
	Mom1R	AGAACAGGTGATTTGGCCC						
Kras								
	mKras x1F	TTTTTATTGTAAGGCCTGCTGA		161	2		55	35
	mKras x1R	GCACGCAGACTGTAGAGCAG						
BRAF								
	mBRAFx15F	AGGCCTGGGACAGCTTAAAA		529	3	yes	65	35
	mBRAFx15R	CAGCTTTCTAAGTGCTGGGATT						
MYH								
	mMYH x1F	CTTTGCCCTTTTGTTTCGAG	FAM	199	2		60	35
	mMYH x1R	GAAACTGGTGAGGGACAAGC	FAM					
	mMYH x2F	CTGAGTTCCCCTGGCTGTC	FAM	199	2		55	35
	mMYH x2R	CACTGTCTCTGTCCCATCCA	FAM					
	mMYH x3&4F	TTCACCCTTGGTTTTATTGACA	FAM	278	2		60	35
	mMYH x3&4R	CTCCCTCCCCAACATCAC	FAM					
	mMYH x5&6F	TTTTTGCCTGTCTTGGGTTT	FAM	254	1		60	35
	mMYH x5&6R	CACCGGGCTATTTTTCAGTG	FAM					
	mMYH x7&8F	CTGTGAGCTTCCTGCTCCAT	FAM	337	2		60	35
	mMYH x7&8R	CCCGTCACCTCATTACCCTA	FAM					
	mMYH x9&10F	AAGGGCCTTTGCTTACAGAA	FAM	357	2		60	35
	mMYH x9&10R	CTCTGAAAGGGACAGGGATG	FAM					
	mMYH x11&12F	GCTGGGAATCTTTGTTTCCA	FAM	466	2	yes	60	35
	mMYH x11&12R	CCCTGTCACCTTTGCTAACC	FAM					
	mMYH x13&14F	CAGACCTGGTTCGGTCTCTT	FAM	460	2		60	35
	mMYH x13&14R	GAAGAGGGCGGAATGCAC	FAM					
	mMYH x15F	GGGTAGAAGAGTCCCTGGTG	FAM	201	2		60	35
	mMYH x15R	TTTGGGTAGGGAATCCCAGT	FAM					
***MYH* genotyping**								
	P1 (21-mer)	CAAGTGCTGGGATCAAAGGTG			1		55	35
	P2 (20-mer)	GCTCCTTCTTGTAGCCGACG	P1/P2	262				
	P3 (neo, 21-mer)	TCCTCGTGCTTTACGGTATCG	P1/P3	376				

Appendix 1: Primers and conditions

ID	FAP 1	FAP 2	FAP 3	FAP 4	FAP 5	FAP 6	FAP 7	FAP 8	FAP 9
hitological morphology	TA	TA	TA	TA	TA	TA	TA	TA	TA
size adenoma (cm)	2.1	3	2.6	1.5	1	2.6	1.8	3.5	2.3
histological grade	mild dysplasia	mild dysplasia	mod dysplasia	mild dysplasia	mild dysplasia	mild dysplasia	mod dysplasia	mod dysplasia	mild dysplasia
chromosomal losses and gains	none	17,0-8,del 19,0-18,del 19,51-ter,del	none	1,76-112,del 1,188-218,del 13,53-96,del 16,all gain 17,all gain 18,24-39,del 19,all gain 21,33-ter,gain 22,all gain	1,183-196,del 13,54-104,del 21,all gain	21,41-ter,gain	1,0-118,del 1,143-244,gain 5,55-165,del 6,all gain 13,all gain 18,all del 20,all gain	19,0-18,del	none
No. aCGH changes	0	3	0	9	3	1	7	1	0

ID	Sporadic 1	Sporadic 2	Sporadic 3	Sporadic 4	Sporadic 5	Sporadic 6	Sporadic 7	Sporadic 8	Sporadic 9	Sporadic 10	Sporadic 11
hitological morphology	TA	TVA	TA	TA	TA	TA	TVA	VA	TVA	TVA	TVA
size adenoma	1	1.3	1.6	3	1	1.5	1	6	7	3.8	2.4
histological grade	mild dysplasia	mod dysplasia	mild dysplasia	mild dysplasia	mild dysplasia	mild dysplasia	mild dysplasia	mod dysplasia	mod dysplasia	mod dysplasia	mod dysplasia
chromosomal losses and gains	1,0-54,del 6,33-47,del 8,all gain 9,122-ter,del 13,all gain 16,0-31,del 16,67-ter,del 17,0-50,del 19,all del 20,all gain 21,all gain 22,all del	1,0-51,del 2,123-152,del 17,all del 19,all del	1,0-57,del 9,104-111,del 17,0-50,del	1,0-47,del 17,0-50,del 22,all del	none	1,0-46,del 17,44-50,del	1,0-46,del 10,91-103,del 18,51-64,del 19,?all del	1,0-46,del 7,62-74,del 9,123-ter,del 12,111-ter,del 13,53-96,gain 16,0-31,del 16,66-ter,del 17,0-50,del 17,72-ter,del 19,0-18,del 19,38-ter,del 20,31-36,del 22,all del	none	1,0-51 del	13,all gain
No. aCGH changes	12	4	3	3	0	2	4	13	0	1	1

Appendix 2: FAP and Sporadic aCGH changes

ID
hitological morphology
size adenoma (cm)
histological grade
chromosomal losses and gains
No. aCGH changes

ID	Sporadic 12	Sporadic 13	Sporadic 14
hitological morphology	TVA	TVA	TA
size adenoma	1.5	3.5	1
histological grade	mild dysplasia	mod dysplasia	mild dysplasia
chromosomal losses and gains	none	17,0-14,del	none
No. aCGH changes	0	1	0

Appendix 2: FAP and Sporadic aCGH changes

Ind 1 JUM-MA				
Probe ID	fold change	gene.symbol	map	description
204517_at	6.97	PPIC	5q23.2	peptidylprolyl isomerase C (cyclophilin C)
206366_x_at	6.95	XCL1	1q23	chemokine (C motif) ligand 1
204983_s_at	6.07	GPC4	Xq26.1	glypican 4
203325_s_at	6.01	COL5A1	9q34.2-q34.3	collagen, type V, alpha 1
1559401_a_at	5.80	ZNF609	15q22.31	zinc finger protein 609
1569237_at	5.26	RAPGEF2	4q32.1	Rap guanine nucleotide exchange factor (GEF) 2
226665_at	5.21	AHSA2	2p15	AHA1, activator of heat shock 90kDa protein ATPase homolog 2 (yeast)
207836_s_at	5.18	RBPMS	8p12-p11	RNA binding protein with multiple splicing
236404_at	5.10	ATXN1	6p23	ataxin 1
239808_at	4.91	PITPNC1	17q24.2	phosphatidylinositol transfer protein, cytoplasmic 1
229026_at	4.89	CDC42SE2	5q31.1	CDC42 small effector 2
207002_s_at	4.77	PLAGL1	6q24-q25	pleiomorphic adenoma gene-like 1
221042_s_at	4.73	CLMN	14q32.13	calmin (calponin-like, transmembrane)
209546_s_at	4.63	APOL1	22q13.1	apolipoprotein L, 1
200988_s_at	5.03	PSME3	17q21	proteasome (prosome, macropain) activator subunit 3 (PA28 gamma; Ki)
215001_s_at	4.84	GLUL	1q31	glutamate-ammonia ligase (glutamine synthetase)
200762_at	4.51	DPYSL2	8p22-p21	dihydropyrimidinase-like 2
215073_s_at	4.45	NR2F2	15q26	nuclear receptor subfamily 2, group F, member 2
44783_s_at	4.27	HEY1	8q21	hairy/enhancer-of-split related with YRPW motif 1
202613_at	4.14	CTPS	1p34.1	CTP synthase
201360_at	4.09	CST3	20p11.21	cystatin C (amyloid angiopathy and cerebral hemorrhage)
203038_at	4	PTPRK	6q22.2-23.1	protein tyrosine phosphatase, receptor type, K
Ind 2 EIG - MA				
Probe ID	fold change	gene.symbol	map	description
213524_s_at	20.91	G0S2	1q32.2-q41	G0/G1switch 2
205220_at	13.24	GPR109B	12q24.31	G protein-coupled receptor 109B
219622_at	10.31	RAB20	13q34	RAB20, member RAS oncogene family
202581_at	8.99	HSPA1B	6p21.3	heat shock 70kDa protein 1B
225803_at	8.57	FBXO32	8q24.13	F-box protein 32
210448_s_at	8.34	P2RX5	17p13.3	purinergic receptor P2X, ligand-gated ion channel, 5
227850_x_at	7.81	CDC42EP5	19q13.42	CDC42 effector protein (Rho GTPase binding) 5
211214_s_at	6.38	DAPK1	9q34.1	death-associated protein kinase 1
202770_s_at	5.52	CCNG2	4q21.1	cyclin G2
203819_s_at	17.29	IGF2BP3	7p11	insulin-like growth factor 2 mRNA binding protein 3
203820_s_at	14.21	IGF2BP3	7p11	insulin-like growth factor 2 mRNA binding protein 3
210138_at	10.92	RGS20	8q12.1	regulator of G-protein signalling 20

Appendix 3: Expression array results for individual patients

Probe ID	fold change	gene.symbol	map	description
206618_at	10.34	IL18R1	2q12	interleukin 18 receptor 1
201387_s_at	10.36	UCHL1	4p14	ubiquitin carboxyl-terminal esterase L1 (ubiquitin thiolesterase)
204410_at	9.27	EIF1AY	Yq11.222	eukaryotic translation initiation factor 1A, Y-linked
218589_at	8.21	P2RY5	13q14	purinergic receptor P2Y, G-protein coupled, 5
205034_at	7.43	CCNE2	8q22.1	cyclin E2
210279_at	6.29	GPR18	13q32	G protein-coupled receptor 18
1552680_a_at	6.13	CASC5	15q14	cancer susceptibility candidate 5
Ind 3 JOH-MA				
Probe ID	**fold change**	**gene.symbol**	**map**	**description**
207095_at	13.91	SLC10A2	13q33	solute carrier family 10 (sodium/bile acid cotransporter family), member 2
205518_s_at	10.22	CMAH	6p21.32	cytidine monophosphate-N-acetylneuraminic acid hydroxylase (CMP-N-acetylneuraminate monooxygenase)
201125_s_at	7.53	ITGB5	3q21.2	integrin, beta 5
205991_s_at	6.58	PRRX1	1q24	paired related homeobox 1
235349_at	6.43	FAM82A	2p22.2	family with sequence similarity 82, member A
211535_s_at	6.42	FGFR1	8p11.2-p11.1	fibroblast growth factor receptor 1 (fms-related tyrosine kinase 2, Pfeiffer syndrome)
1556096_s_at	6.23	UNC13C	15q21.3	unc-13 homolog C (C. elegans)
225168_at	5.66	FRMD4A	10p13	FERM domain containing 4A
210571_s_at	5.64	CMAH	6p21.32	cytidine monophosphate-N-acetylneuraminic acid hydroxylase (CMP-N-acetylneuraminate monooxygenase)
227620_at	5.55	SLC44A1	9q31.2	solute carrier family 44, member 1
204633_s_at	5.40	RPS6KA5	14q31-q32.1	ribosomal protein S6 kinase, 90kDa, polypeptide 5
208475_at	5.29	FRMD4A	10p13	FERM domain containing 4A
222314_x_at	4.95	ITPR1	3p26-p25	inositol 1,4,5-triphosphate receptor, type 1
225167_at	4.69	FRMD4A	10p13	FERM domain containing 4A
204348_s_at	8.45	AK3L1	1p31.3	adenylate kinase 3-like 1
210643_at	8.44	TNFSF11	13q14	tumor necrosis factor (ligand) superfamily, member 11
242517_at	8.42	KISS1R	19p13.3	KISS1 receptor
218094_s_at	6.87	DBNDD2	20q13.12	dysbindin (dystrobrevin binding protein 1) domain containing 2
225342_at	6.67	AK3L1	1p31.3	adenylate kinase 3-like 1
209822_s_at	5.42	VLDLR	9p24	very low density lipoprotein receptor
221491_x_at	4.36	HLA-DRB1	6p21.3	major histocompatibility complex, class II, DR beta 1
230102_at	4.23	ETV5	3q28	ets variant gene 5 (ets-related molecule)
202435_s_at	4.21	CYP1B1	2p21	cytochrome P450, family 1, subfamily B, polypeptide 1
230967_s_at	4.12	USP7	16p13.3	ubiquitin specific peptidase 7 (herpes virus-associated)
Ind 4 WA-MA				
Probe ID	**fold change**	**gene.symbol**	**map**	**description**
1554474_a_at	8.30	MOXD1	6q23.1-23.3	monooxygenase, DBH-like 1
220684_at	8.05	TBX21	17q21.32	T-box 21

Appendix 3: Expression array results for individual patients

Probe ID	fold change	gene.symbol	map	description
225728_at	5.80	SORBS2	4q35.1	sorbin and SH3 domain containing 2
203828_s_at	5.02	IL32	16p13.3	interleukin 32
229764_at	4.86	FAM79B	3q28	family with sequence similarity 79, member B
209708_at	4.37	MOXD1	6q23.1-23.3	monooxygenase, DBH-like 1
59644_at	5.4	BMP2K	4q21.21	BMP2 inducible kinase
242903_at	4.98	IFNGR1	6q23-q24	interferon gamma receptor 1
217028_at	4.9	CXCR4	2q21	chemokine (C-X-C motif) receptor 4
230413_s_at	4.77	AP1S2	Xp22.2	adaptor-related protein complex 1, sigma 2 subunit
209604_s_at	4.77	GATA3	10p15	GATA binding protein 3
209948_at	4.69	KCNMB1	5q34	potassium large conductance calcium-activated channel, subfamily M, beta member 1
230921_s_at	4.49	PCBP2	12q13.12-q13.13	poly(rC) binding protein 2
231484_at	4.47	ATP8A1	4p14-p12	ATPase, aminophospholipid transporter (APLT), Class I, type 8A, member 1
209725_at	4.37	UTP20	12q23	UTP20, small subunit (SSU) processome component, homolog (yeast)
243916_x_at	4.18	UBLCP1	5q33.3	ubiquitin-like domain containing CTD phosphatase 1
229500_at	4.09	SLC30A9	4p13-p12	solute carrier family 30 (zinc transporter), member 9
223210_at	4.08	CHURC1	14q23.3	churchill domain containing 1
204863_s_at	4.08	IL6ST	5q11	interleukin 6 signal transducer (gp130, oncostatin M receptor)
227740_at	4.05	UHMK1	1q23.3	U2AF homology motif (UHM) kinase 1
225420_at	4.04	GPAM	10q25.2	glycerol-3-phosphate acyltransferase, mitochondrial
Ind 5 FRL-MA				
Probe ID	**fold change**	**gene.symbol**	**map**	**description**
1566403_at	12.84	SNORA68	19p13	small nucleolar RNA, H/ACA box 68
211993_at	10.49	WNK1	12p13.3	WNK lysine deficient protein kinase 1
208151_x_at	8.38	DDX17	22q13.1	DEAD (Asp-Glu-Ala-Asp) box polypeptide 17
208719_s_at	7.60	DDX17	22q13.1	DEAD (Asp-Glu-Ala-Asp) box polypeptide 17
222450_at	6.76	TMEPAI	20q13.31-q13.33	transmembrane, prostate androgen induced RNA
211082_x_at	5.37	MARK2	11q12-q13	MAP/microtubule affinity-regulating kinase 2
201008_s_at	5.26	TXNIP	1q21.1	thioredoxin interacting protein
224828_at	5.12	CPEB4	5q21	cytoplasmic polyadenylation element binding protein 4
202205_at	4.97	VASP	19q13.2-q13.3	vasodilator-stimulated phosphoprotein
208583_x_at	4.97	HIST1H2AJ	6p22-p21.3	histone 1, H2aj
208547_at	4.96	HIST1H2BB	6p21.3	histone 1, H2bb
221092_at	4.92	ZNFN1A3	17q21	zinc finger protein, subfamily 1A, 3 (Aiolos)
208496_x_at	4.89	HIST1H3G	6p21.3	histone 1, H3g
1552263_at	4.76	MAPK1	22q11.2;22q11.21	mitogen-activated protein kinase 1
228181_at	4.73	SLC30A1	1q32-q41	solute carrier family 30 (zinc transporter), member 1
222439_s_at	4.73	THRAP3	1p34.3	thyroid hormone receptor associated protein 3
202082_s_at	4.70	SEC14L1	17q25.1-17q25.2	SEC14-like 1 (S. cerevisiae)

Appendix 3: Expression array results for individual patients

Probe ID	fold change	gene.symbol	map	description
229971_at	4.69	GPR114	16q13	G protein-coupled receptor 114
205124_at	4.69	MEF2B	19p12	MADS box transcription enhancer factor 2, polypeptide B (myocyte enhancer factor 2B)
221881_s_at	4.68	CLIC4	1p36.11	chloride intracellular channel 4
223062_s_at	4.65	PSAT1	9q21.2	phosphoserine aminotransferase 1
200835_s_at	4.63	MAP4	3p21	microtubule-associated protein 4
228841_at	15.41	HINT1	5q31.2	histidine triad nucleotide binding protein 1
241163_at	14.93	NAALADL2	3q26.31	N-acetylated alpha-linked acidic dipeptidase-like 2
225092_at	11.38	NUP88	17p13.2	nucleoporin 88kDa
212195_at	11.15	IL6ST	5q11	interleukin 6 signal transducer (gp130, oncostatin M receptor)
242586_at	11.05	FSD1L	9q31	fibronectin type III and SPRY domain containing 1-like
230387_at	10.51	ATP2C1	3q22.1	ATPase, Ca++ transporting, type 2C, member 1
222805_at	9.98	MANEA	6q16.1	mannosidase, endo-alpha
1556121_at	9.2	NAP1L1	12q21.2	nucleosome assembly protein 1-like 1
212980_at	8.79	USP34	2p15	ubiquitin specific peptidase 34
212037_at	8.3	PNN	14q21.1	pinin, desmosome associated protein
213070_at	7.96	PIK3C2A	11p15.5-p14	phosphoinositide-3-kinase, class 2, alpha polypeptide
222685_at	7.66	FAM29A	9p22.1	family with sequence similarity 29, member A
229692_at	7.62	API5	11p12-q12	apoptosis inhibitor 5
230174_at	7.27	LYPLAL1	1q41	lysophospholipase-like 1
209902_at	7.17	ATR	3q22-q24	ataxia telangiectasia and Rad3 related
226998_at	7.16	NARG1	4q31.1	NMDA receptor regulated 1
212542_s_at	6.95	PHIP	6q14	pleckstrin homology domain interacting protein
212653_s_at	6.94	EHBP1	2p15	EH domain binding protein 1
212036_s_at	6.92	PNN	14q21.1	pinin, desmosome associated protein
241734_at	6.75	SRFBP1	5q23.1	serum response factor binding protein 1
1558956_s_at	6.62	IFT80	3q26.1	intraflagellar transport 80 homolog (Chlamydomonas)
235390_at	6.44	P18SRP	5q12.3	NA
206059_at	6.39	ZNF91	19p13.1-p12	zinc finger protein 91
Ind 6 LEM-MA				
Probe ID	**fold change**	**gene.symbol**	**map**	**description**
213913_s_at	25.39	KIAA0984	12q14.3	NA
228335_at	16.69	CLDN11	3q26.2-q26.3	claudin 11 (oligodendrocyte transmembrane protein)
213912_at	16.25	KIAA0984	12q14.3	NA
209839_at	6.79	DNM3	1q24.3	dynamin 3
201427_s_at	6.70	SEPP1	5q31	selenoprotein P, plasma, 1
215392_at	6.27	USP3	15q22.3	ubiquitin specific peptidase 3
214056_at	6.22	MCL1	1q21	myeloid cell leukemia sequence 1 (BCL2-related)
233314_at	6.09	PTEN	10q23.3	phosphatase and tensin homolog (mutated in multiple advanced cancers 1)

Appendix 3: Expression array results for individual patients

Probe ID	fold change	gene.symbol	map	description
223823_at	5.92	KCNMB2	3q26.2-q27.1	potassium large conductance calcium-activated channel, subfamily M, beta member 2
210473_s_at	5.76	GPR125	4p15.31	G protein-coupled receptor 125
232528_at	5.75	UBE2E3	2q32.1	ubiquitin-conjugating enzyme E2E 3 (UBC4/5 homolog, yeast)
209459_s_at	5.55	ABAT	16p13.2	4-aminobutyrate aminotransferase
205498_at	5.45	GHR	5p13-p12	growth hormone receptor
1556361_s_at	5.31	ANKRD13C	1p32.3-p31.3	ankyrin repeat domain 13C
240594_at	5.30	CDYL	6p25.1	chromodomain protein, Y-like
206032_at	5.21	DSC3	18q12.1	desmocollin 3
223434_at	5.51	GBP3	1p22.2	guanylate binding protein 3
1558217_at	5.45	SLFN13	17q12	schlafen family member 13
201692_at	5.42	OPRS1	9p13.3	opioid receptor, sigma 1
1553423_a_at	5.35	SLFN13	17q12	schlafen family member 13
237215_s_at	5.22	TFRC	3q29	transferrin receptor (p90, CD71)
201850_at	5.07	CAPG	2p11.2	capping protein (actin filament), gelsolin-like
230543_at	4.99	USP9X	Xp11.4	ubiquitin specific peptidase 9, X-linked
217728_at	4.87	S100A6	1q21	S100 calcium binding protein A6 (calcyclin)
227354_at	4.57	PAG1	8q21.13	phosphoprotein associated with glycosphingolipid microdomains 1
212999_x_at	4.44	HLA-DQB1	6p21.3	major histocompatibility complex, class II, DQ beta 1
211919_s_at	4.41	CXCR4	2q21	chemokine (C-X-C motif) receptor 4
211016_x_at	4.02	HSPA4	5q31.1-q31.2	heat shock 70kDa protein 4
Ind 7 AH-MA				
Probe ID	**fold change**	**gene.symbol**	**map**	**description**
226811_at	9.64	FAM46C	1p12	family with sequence similarity 46, member C
232112_at	8.75	RALGPS2	1q25.2	Ral GEF with PH domain and SH3 binding motif 2
202620_s_at	8.54	PLOD2	3q23-q24	procollagen-lysine, 2-oxoglutarate 5-dioxygenase 2
234792_x_at	8.53	IGHA1	14q32.33	immunoglobulin heavy constant alpha 1
207734_at	7.16	LAX1	1q32.1	lymphocyte transmembrane adaptor 1
202843_at	7.00	DNAJB9	7q31;14q24.2-q24.3	DnaJ (Hsp40) homolog, subfamily B, member 9
203574_at	6.91	NFIL3	9q22	nuclear factor, interleukin 3 regulated
239258_at	6.54	RHOQ	2p21	ras homolog gene family, member Q
204992_s_at	6.50	PFN2	3q25.1-q25.2	profilin 2
203543_s_at	6.41	KLF9	9q13	Kruppel-like factor 9
210426_x_at	6.38	RORA	15q21-q22	RAR-related orphan receptor A
217732_s_at	6.16	ITM2B	13q14.3	integral membrane protein 2B
213856_at	6.09	CD47	3q13.1-q13.2	CD47 molecule
209845_at	6.06	MKRN1	7q34	makorin, ring finger protein, 1
225464_at	6.06	FRMD6	14q22.1	FERM domain containing 6
244841_at	6.04	SEC24A	5q31.1	SEC24 related gene family, member A (S. cerevisiae)

Appendix 3: Expression array results for individual patients

Probe ID	fold change	gene.symbol	map	description
231202_at	6.01	ALDH1L2	12q23.3	aldehyde dehydrogenase 1 family, member L2
239246_at	5.96	FARP1	13q32.2	FERM, RhoGEF (ARHGEF) and pleckstrin domain protein 1 (chondrocyte-derived)
1561195_at	5.61	GPR137B	1q42-q43	G protein-coupled receptor 137B
220377_at	5.59	FAM30A	14q32.33	family with sequence similarity 30, member A
233463_at	5.56	RASSF6	4q13.3	Ras association (RalGDS/AF-6) domain family 6
225998_at	5.55	GAB1	4q31.21	GRB2-associated binding protein 1
241844_x_at	5.46	TMEM156	4p14	transmembrane protein 156
210875_s_at	5.42	TCF8	10p11.2	transcription factor 8 (represses interleukin 2 expression)
207901_at	5.39	IL12B	5q31.1-q33.1	interleukin 12B (natural killer cell stimulatory factor 2, cytotoxic lymphocyte maturation factor 2, p40)
1554462_a_at	5.37	DNAJB9	7q31;14q24.2-q24.3	DnaJ (Hsp40) homolog, subfamily B, member 9
210479_s_at	5.37	RORA	15q21-q22	RAR-related orphan receptor A
1557257_at	5.32	BCL10	1p22	B-cell CLL/lymphoma 10
215641_at	5.31	SEC24D	4q26	SEC24 related gene family, member D (S. cerevisiae)
205890_s_at	7.83	UBD	6p21.3	ubiquitin D
208814_at	4.66	HSPA4	5q31.1-q31.2	heat shock 70kDa protein 4
208712_at	4.65	CCND1	11q13	cyclin D1
241403_at	4.50	CLK4	5q35	CDC-like kinase 4
1569025_s_at	4.43	FAM13A1	4q22.1	family with sequence similarity 13, member A1
241937_s_at	4.26	WDR4	21q22.3	WD repeat domain 4
209278_s_at	4.20	TFPI2	7q22	tissue factor pathway inhibitor 2
208711_s_at	4.14	CCND1	11q13	cyclin D1
231577_s_at	4.10	GBP1	1p22.2	guanylate binding protein 1, interferon-inducible, 67kDa
222912_at	4.06	ARRB1	11q13	arrestin, beta 1
208920_at	4.03	SRI	7q21.1	sorcin
234000_s_at	4.02	PTPLAD1	15q22.2	protein tyrosine phosphatase-like A domain containing 1
Ind 8 TER-MA				
Probe ID	**fold change**	**gene.symbol**	**map**	**description**
205659_at	6.80	HDAC9	7p21.1	histone deacetylase 9
213793_s_at	5.54	HOMER1	5q14.2	homer homolog 1 (Drosophila)
213572_s_at	4.98	SERPINB1	6p25	serpin peptidase inhibitor, clade B (ovalbumin), member 1
224800_at	4.39	WDFY1	2q36.1	WD repeat and FYVE domain containing 1
229695_at	4.39	FAM107B	10p13	family with sequence similarity 107, member B
213075_at	4.18	OLFML2A	9q33.3	olfactomedin-like 2A
223503_at	4.16	TMEM163	2q21.3	transmembrane protein 163
227803_at	4.16	ENPP5	6p21.1-p11.2	ectonucleotide pyrophosphatase/phosphodiesterase 5 (putative function)
240413_at	4.15	PYHIN1	1q23.1	pyrin and HIN domain family, member 1
236235_at	4.09	ITCH	20q11.22-q11.23	itchy homolog E3 ubiquitin protein ligase (mouse)
238002_at	4.08	GOLPH4	3q26.2	golgi phosphoprotein 4

Appendix 3: Expression array results for individual patients

Probe ID	fold change	gene.symbol	map	description
213446_s_at	11.2	IQGAP1	15q26.1	IQ motif containing GTPase activating protein 1
213122_at	10.94	TSPYL5	8q22.1	TSPY-like 5
212257_s_at	9.34	SMARCA2	9p22.3	SWI/SNF related, matrix associated, actin dependent regulator of chromatin, subfamily a, member 2
242774_at	8.73	SYNE2	14q23.2	spectrin repeat containing, nuclear envelope 2
230058_at	8.62	SDCCAG3	9q34.3	serologically defined colon cancer antigen 3
209088_s_at	7.5	UBN1	16p13.3	ubinuclein 1
223161_at	7.02	MULK	7q34	multiple substrate lipid kinase
211672_s_at	6.53	ARPC4	3p25.3	actin related protein 2/3 complex, subunit 4, 20kDa
227884_at	6.49	TAF15	17q11.1-q11.2	TAF15 RNA polymerase II, TATA box binding protein (TBP)-associated factor, 68kDa
213286_at	6.48	ZFR	5p13.3	zinc finger RNA binding protein
206983_at	6.47	CCR6	6q27	chemokine (C-C motif) receptor 6
242352_at	6.43	NIPBL	5p13.2	Nipped-B homolog (Drosophila)
1557100_s_at	6.31	HECTD1	14q12	HECT domain containing 1
1563321_s_at	5.86	MLL	11q23	myeloid/lymphoid or mixed-lineage leukemia (trithorax homolog, Drosophila)
236462_at	5.77	YEATS2	3q27.1	YEATS domain containing 2
202855_s_at	5.68	SLC16A3	17q25	solute carrier family 16, member 3 (monocarboxylic acid transporter 4)
201101_s_at	5.67	BCLAF1	6q22-q23	BCL2-associated transcription factor 1
Ind 9 STM-MA				
Probe ID	**fold change**	**gene.symbol**	**map**	**description**
209189_at	14.61	FOS	14q24.3	v-fos FBJ murine osteosarcoma viral oncogene homolog
205931_s_at	12.30	CREB5	7p15.1	cAMP responsive element binding protein 5
210942_s_at	9.22	ST3GAL6	3q12.1	ST3 beta-galactoside alpha-2,3-sialyltransferase 6
205476_at	7.76	CCL20	2q33-q37	chemokine (C-C motif) ligand 20
237485_at	7.66	SFRS3	6p21	splicing factor, arginine/serine-rich 3
203397_s_at	7.19	GALNT3	2q24-q31	UDP-N-acetyl-alpha-D-galactosamine:polypeptide N-acetylgalactosaminyltransferase 3 (GalNAc-T3)
220051_at	6.82	PRSS21	16p13.3	protease, serine, 21 (testisin)
222392_x_at	6.81	PERP	6q24	PERP, TP53 apoptosis effector
218764_at	6.73	PRKCH	14q22-q23	protein kinase C, eta
213355_at	5.71	ST3GAL6	3q12.1	ST3 beta-galactoside alpha-2,3-sialyltransferase 6
204995_at	5.56	CDK5R1	17q11.2	cyclin-dependent kinase 5, regulatory subunit 1 (p35)
212715_s_at	5.46	MICAL3	22q11.21	microtubule associated monoxygenase, calponin and LIM domain containing 3
235142_at	5.38	ZBTB8	1p35.1	zinc finger and BTB domain containing 8
241843_at	5.32	EIF5	14q32.32	eukaryotic translation initiation factor 5
1553105_s_at	5.19	DSG2	18q12.1	desmoglein 2
235458_at	5.17	HAVCR2	5q33.3	hepatitis A virus cellular receptor 2
205270_s_at	4.96	LCP2	5q33.1-qter	lymphocyte cytosolic protein 2 (SH2 domain containing leukocyte protein of 76kDa)
241745_at	4.88	FBXO30	6q24	F-box protein 30
217764_s_at	4.76	RAB31	18p11.3	RAB31, member RAS oncogene family

Appendix 3: Expression array results for individual patients

Probe ID	fold change	gene.symbol	map	description
205798_at	4.72	IL7R	5p13	interleukin 7 receptor
209682_at	4.45	CBLB	3q13.11	Cas-Br-M (murine) ecotropic retroviral transforming sequence b
204614_at	4.45	SERPINB2	18q21.3	serpin peptidase inhibitor, clade B (ovalbumin), member 2
225147_at	4.33	PSCD3	7p22.1	pleckstrin homology, Sec7 and coiled-coil domains 3
204472_at	4.30	GEM	8q13-q21	GTP binding protein overexpressed in skeletal muscle
218805_at	4.28	GIMAP5	7q36.1	GTPase, IMAP family member 5
217763_s_at	4.14	RAB31	18p11.3	RAB31, member RAS oncogene family
204174_at	5.04	ALOX5AP	13q12	arachidonate 5-lipoxygenase-activating protein
230425_at	5.02	EPHB1	3q21-q23	EPH receptor B1
230292_at	4.95	RCBTB2	13q14.3	regulator of chromosome condensation (RCC1) and BTB (POZ) domain containing protein 2
230896_at	4.82	CCDC4	4p13	coiled-coil domain containing 4
238332_at	4.71	ANKRD29	18q11.2	ankyrin repeat domain 29
203132_at	4.21	RB1	13q14.2	retinoblastoma 1 (including osteosarcoma)
242890_at	4.19	HELLS	10q24.2	helicase, lymphoid-specific
227176_at	4.02	SLC2A13	12q12	solute carrier family 2 (facilitated glucose transporter), member 13
204103_at	4.01	CCL4	17q12	chemokine (C-C motif) ligand 4
Ind 10 QUB-MA				
Probe ID	**fold change**	**gene.symbol**	**map**	**description**
205749_at	8.88	CYP1A1	15q22-q24	cytochrome P450, family 1, subfamily A, polypeptide 1
217867_x_at	8.81	BACE2	21q22.3	beta-site APP-cleaving enzyme 2
202967_at	7.97	GSTA4	6p12.1	glutathione S-transferase A4
209793_at	6.40	GRIA1	5q33;5q31.1	glutamate receptor, ionotropic, AMPA 1
58916_at	6.21	KCTD14	11q14.1	potassium channel tetramerisation domain containing 14
229893_at	5.99	FRMD3	9q21.32	FERM domain containing 3
209496_at	5.61	RARRES2	7q36.1	retinoic acid receptor responder (tazarotene induced) 2
204395_s_at	5.58	GRK5	10q24-qter	G protein-coupled receptor kinase 5
219545_at	5.51	KCTD14	11q14.1	potassium channel tetramerisation domain containing 14
221690_s_at	5.48	NALP2	19q13.42	NACHT, leucine rich repeat and PYD containing 2
206951_at	4.51	HIST1H4E	6p21.3	histone 1, H4e
205660_at	4.50	OASL	12q24.2	2'-5'-oligoadenylate synthetase-like
219637_at	4.24	ARMC9	2q37.1	armadillo repeat containing 9
219667_s_at	4.24	BANK1	4q24	B-cell scaffold protein with ankyrin repeats 1
242600_at	4.22	FRMD3	9q21.32	FERM domain containing 3
208523_x_at	4.13	HIST1H2BI	6p21.3	histone 1, H2bi
1569110_x_at	11.01	PDCD6	5pter-p15.2	programmed cell death 6
236244_at	5.20	HNRPU	1q44	heterogeneous nuclear ribonucleoprotein U (scaffold attachment factor A)
204999_s_at	4.67	ATF5	19q13.3	activating transcription factor 5

Appendix 3: Expression array results for individual patients

Probe ID	fold change	gene.symbol	map	description
230892_at	4.28	DERA	12p12.3	2-deoxyribose-5-phosphate aldolase homolog (C. elegans)
1556054_at	4.28	RPL31	2q11.2	ribosomal protein L31
213907_at	4.22	EEF1E1	6p24.3-p25.1	eukaryotic translation elongation factor 1 epsilon 1
1558102_at	4.13	TM6SF1	15q24-q26	transmembrane 6 superfamily member 1
37170_at	4.09	BMP2K	4q21.21	BMP2 inducible kinase
Ind 11 WM-MA				
Probe ID	**fold change**	**gene.symbol**	**map**	**description**
217179_x_at	33.28	IGLV1-44	22q11.2	immunoglobulin lambda variable 1-44
213245_at	11.42	ADCY1	7p13-p12	adenylate cyclase 1 (brain)
228434_at	10.58	BTNL9	5q35.3	butyrophilin-like 9
219947_at	9.53	CLEC4A	12p13	C-type lectin domain family 4, member A
223827_at	9.03	TNFRSF19	13q12.11-q12.3	tumor necrosis factor receptor superfamily, member 19
228974_at	9.01	ZNF677	19q13.41	zinc finger protein 677
206110_at	8.82	HIST1H3H	6p22-p21.3	histone 1, H3h
229985_at	8.48	BTNL9	5q35.3	butyrophilin-like 9
210299_s_at	8.45	FHL1	Xq26	four and a half LIM domains 1
207156_at	8.24	HIST1H2AG	6p22.1	histone 1, H2ag
230992_at	8.12	BTNL9	5q35.3	butyrophilin-like 9
215071_s_at	8.08	HIST1H2AC	6p21.3	histone 1, H2ac
235953_at	7.39	ZNF610	19q13.33	zinc finger protein 610
207120_at	6.67	ZNF667	19q13.43	zinc finger protein 667
1560562_a_at	6.67	ZNF677	19q13.41	zinc finger protein 677
1554679_a_at	6.62	LAPTM4B	8q22.1	lysosomal associated protein transmembrane 4 beta
214505_s_at	6.45	FHL1	Xq26	four and a half LIM domains 1
206030_at	6.41	ASPA	17pter-p13	aspartoacylase (Canavan disease)
221724_s_at	6.25	CLEC4A	12p13	C-type lectin domain family 4, member A
1552610_a_at	6.20	JAK1	1p32.3-p31.3	Janus kinase 1 (a protein tyrosine kinase)
243514_at	6.18	WDFY2	13q14.3	WD repeat and FYVE domain containing 2
235315_at	6.15	TSC22D1	13q14	TSC22 domain family, member 1
214455_at	6.09	HIST1H2BC	6p21.3	histone 1, H2bc
201242_s_at	12.2	ATP1B1	1q24	ATPase, Na+/K+ transporting, beta 1 polypeptide
204014_at	8.4	DUSP4	8p12-p11	dual specificity phosphatase 4
213350_at	7.1	RPS11	19q13.3	ribosomal protein S11
212097_at	7.08	CAV1	7q31.1	caveolin 1, caveolae protein, 22kDa
226022_at	6.68	SASH1	6q24.3	SAM and SH3 domain containing 1
209444_at	6.6	RAP1GDS1	4q23-q25	RAP1, GTP-GDP dissociation stimulator 1
201243_s_at	6.24	ATP1B1	1q24	ATPase, Na+/K+ transporting, beta 1 polypeptide
228802_at	6.16	RBPMS2	15q22.31	RNA binding protein with multiple splicing 2

Appendix 3: Expression array results for individual patients

Probe ID	fold change	gene.symbol	map	description
204015_s_at	6.15	DUSP4	8p12-p11	dual specificity phosphatase 4
224209_s_at	5.34	GDA	9q21.13	guanine deaminase
206102_at	5.11	GINS1	20p11.21	GINS complex subunit 1 (Psf1 homolog)
218910_at	5.1	TMEM16K	3p22.1-p21.33	transmembrane protein 16K
201890_at	5.07	RRM2	2p25-p24	ribonucleotide reductase M2 polypeptide
217996_at	5.05	PHLDA1	12q15	pleckstrin homology-like domain, family A, member 1
229420_at	4.85	RPL23A	17q11	ribosomal protein L23a
201426_s_at	4.76	VIM	10p13	vimentin
225660_at	4.6	SEMA6A	5q23.1	sema domain, transmembrane domain (TM), and cytoplasmic domain, (semaphorin) 6A
212044_s_at	4.52	RPL27A	11p15	ribosomal protein L27a
205203_at	4.48	PLD1	3q26	phospholipase D1, phosphatidylcholine-specific
1555826_at	4.47	BIRC5	17q25	baculoviral IAP repeat-containing 5 (survivin)

Appendix 3: Expression array results for individual patients